Electronic Supplementary Material (ESI) for ChemComm.

Supporting Information

Tandem double hydrophosphination of α,β,γ,δ-unsaturated-1,3-indandiones: diphosphine synthesis, mechanistic investigations and coordination chemistry.

László B. Balázs,[a] Jasmina B. Khalikuzzaman,[a] Yongxin Li,[a] Dániel Csókás,[b] Sumod A. Pullarkat*[a] and Pak-Hing Leung*[a]

*e-mail for Pullarkat, S.A.: sumod@ntu.edu.sg
*e-mail for Leung, P.-H.: pakhing@ntu.edu.sg

Table of content

1. General methods

1.1 General considerations

All air sensitive manipulations were carried out under positive pressure of nitrogen using Schlenk techniques. Chloroform (AR), acetonitrile (AR), methanol (AR), dichloromethane (HPLC), acetone (AR) and ethyl acetate (AR) was purchased from VWR; *n*-hexanes (AR) and toluene (AR) from Avantor. Solvents were degassed prior to use. All other reactants and reagents were used as supplied without further purification unless stated otherwise. NMR spectra were recorded on Bruker AV 300, AV 400, AV 500 and BBFO 400 spectrometers. Chemical shifts were reported in ppm and referenced to an internal $SiMe_4$ standard (0 ppm) in $CDCl_3$, acetone-*d* (2.09 ppm) in $(CD_3)_2CO$, dichloromethane-*d* (5.33 ppm) in CD_2Cl_2 for ^1H NMR; chloroform-*d* (77.22 ppm) in $CDCl_3$, acetone-*d* (205.87 ppm) in $(CD_3)_2CO$, dichloromethane-*d* (54.24 ppm) in CD_2Cl_2 for ^{13}C NMR and an external 85% H_3PO_4 for $^{31}P\{^1H\}$ NMR. Low Temp Pairstirrer PSL-1800 was used for low temperature reactions. Column chromatography was performed with Silica gel 60 (purchased from Merck). Melting points were measured using SRS Optimelt Automated Point System SRS MPA100. HRMS using electrospray ionization (ESI) method was performed on the Waters Q-Tof Premier spectrometer. Optical rotations were examined with JASCO P-1030 Polarimeter in DCM in a 0.1 dm cell at specified temperatures.

Compounds **2a**[1], **2b**[2], **2c**[2] and **15**[3] were prepared following reported procedures.

1.2 General procedures

1.2.1 Synthesis of α,β,γ,δ-unsaturated-1,3-indandiones

Compounds **1a**, **1b**, **1c**, **1f** and **1h** were synthesized according to reported procedure (the physical data of these compounds correlated to the literature values).[4]

Characterization data:

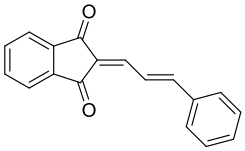

*(E)-2-(3-phenylallylidene)-1H-indene-1,3(2H)-dione (**1a**)*.

Appearance: yellow solid, Mp. (lit.)[4] = 160.4-162.0 °C.

NMR shifts in $CDCl_3$:

^1H NMR (400 MHz, $CDCl_3$) δ 8.46 (dd, *J* = 15.5, 11.9 Hz, 1H), 8.03 – 7.95 (m, 2H), 7.83 – 7.75 (m, 2H), 7.69 (d, *J* = 2.6 Hz, 2H), 7.66 (d, *J* = 11.9 Hz, 1H), 7.47 – 7.40 (m, 3H), 7.35 (d, *J* = 15.5 Hz, 1H).

^{13}C NMR (101 MHz, $CDCl_3$) δ 190.61, 190.17, 151.25, 144.75, 142.32, 141.01, 135.70, 135.27, 135.15, 131.06, 129.19, 128.84, 128.31, 128.28, 128.10, 123.80, 123.27, 123.11.

NMR shifts in acetone-d_6 (for mechanistic studies):

^1H NMR (400 MHz, Acetone-d_6) δ 8.50 (dd, *J* = 15.6, 11.8 Hz, 1H), 8.07 – 7.90 (m, 4H), 7.79 (dd, *J* = 7.6, 1.6 Hz, 2H), 7.67 (dd, *J* = 13.7, 5.0 Hz, 2H), 7.59 – 7.47 (m, 3H).

^{13}C NMR (101 MHz, Acetone-d_6) δ 190.53, 189.61, 151.49, 144.15, 142.74, 141.47, 136.48, 136.03, 135.96, 131.47, 129.81, 129.07, 128.76, 123.83, 123.37, 123.26.

NMR shifts in CD_2Cl_2 (for mechanistic studies):

^{1}H NMR (400 MHz, CD_2Cl_2) δ 8.45 (dd, *J* = 15.6, 11.9 Hz, 1H), 8.00 – 7.89 (m, 2H), 7.84 – 7.76 (m, 2H), 7.72 – 7.66 (m, 2H), 7.62 (d, *J* = 11.9 Hz, 1H), 7.50 – 7.41 (m, 3H), 7.38 (d, *J* = 15.6 Hz, 1H).

^{13}C NMR (101 MHz, CD_2Cl_2) δ 191.08, 190.52, 151.61, 144.87, 142.99, 141.68, 136.45, 135.94, 135.82, 131.64, 129.83, 129.39, 128.91, 124.33, 123.69, 123.58.

HRMS (+ESI) m/z calcd for $C_{18}H_{13}O_2$ $(M + H)^+$: 261.0916; found: 261.0912.

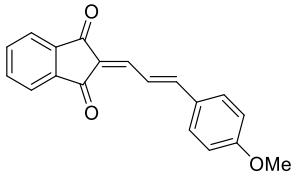

*(E)-2-(3-(4-methoxyphenyl)allylidene)-1H-indene-1,3(2H)-dione (**1b**)*.

Appearance: yellow solid, Mp. (lit)[4] = 220.8-222.5 °C.

^{1}H NMR (400 MHz, $CDCl_3$) δ 8.33 (dd, *J* = 15.4, 12.0 Hz, 1H), 8.00 – 7.90 (m, 2H), 7.82 – 7.72 (m, 2H), 7.69 – 7.59 (m, 3H), 7.31 (d, *J* = 15.4 Hz, 1H), 6.95 (d, *J* = 8.8 Hz, 2H), 3.87 (s, 3H).

^{13}C NMR (126 MHz, $CDCl_3$) δ 190.98, 190.54, 162.40, 151.67, 145.62, 142.33, 141.02, 135.12, 134.98, 130.90, 128.73, 126.92, 123.18, 122.99, 121.93, 114.82, 55.68.

HRMS (+ESI) m/z calcd for $C_{19}H_{15}O_3$ $(M + H)^+$: 291.1021; found: 291.1013.

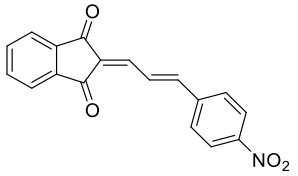

*(E)-2-(3-(4-nitrophenyl)allylidene)-1H-indene-1,3(2H)-dione (**1c**)*.

Appearance: yellow solid, Mp. (lit.)[4] = 248.8-250 °C.

^{1}H NMR (500 MHz, $CDCl_3$) δ 8.57 (dd, *J* = 15.6, 11.8 Hz, 1H), 8.29 (d, *J* = 8.7 Hz, 2H), 8.05 – 7.95 (m, 2H), 7.89 – 7.75 (m, 4H), 7.63 (d, *J* = 11.8 Hz, 1H), 7.34 (d, *J* = 15.6 Hz, 1H).

^{13}C NMR (126 MHz, $CDCl_3$) δ 190.39, 189.69, 148.71, 146.70, 142.63, 142.50, 141.73, 141.26, 135.78, 135.71, 130.36, 129.13, 127.49, 124.51, 123.65, 123.50.

HRMS (+ESI) m/z calcd for $C_{18}H_{12}NO_4$ $(M + H)^+$: 306.0766; found: 306.0770.

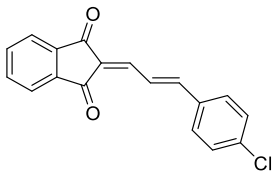

*(E)-2-(3-(4-chlorophenyl)allylidene)-1H-indene-1,3(2H)-dione (**1f**)*.

Appearance: yellow solid, Mp. (lit)[4] = 188.8-190.1 °C.

^{1}H NMR (400 MHz, $CDCl_3$) δ 8.39 (dd, *J* = 15.5, 11.9 Hz, 1H), 8.00 – 7.91 (m, 2H), 7.84 – 7.73 (m, 2H), 7.63 – 7.54 (m, 3H), 7.38 (d, *J* = 8.5 Hz, 2H), 7.25 (d, *J* = 15.5 Hz, 1H).

^{13}C NMR (101 MHz, $CDCl_3$) δ 190.62, 190.08, 149.35, 144.20, 142.36, 141.07, 136.99, 135.40, 135.29, 134.22, 129.90, 129.53, 128.52, 124.25, 123.37, 123.21.

HRMS (+ESI) m/z calcd for $C_{18}H_{12}ClO_2$ $(M + H)^+$: 295.0526; found: 295.0521.

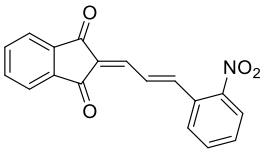

*(E)-2-(3-(2-nitrophenyl)allylidene)-1H-indene-1,3(2H)-dione (**1h**)*.

Appearance: yellow solid, Mp. (lit)[4] = 229.7-231.0 °C.

^{1}H NMR (500 MHz, $CDCl_3$) δ 8.42 (dd, *J* = 15.4, 11.8 Hz, 1H), 8.05 (dd, *J* = 8.2, 1.0 Hz, 1H), 8.03 – 7.96 (m, 2H), 7.93 (d, *J* = 7.5 Hz, 1H), 7.88 – 7.79 (m, 3H), 7.75 – 7.63 (m, 2H), 7.60 – 7.52 (m, 1H).

^{13}C NMR (126 MHz, $CDCl_3$) δ 190.30, 189.46, 148.37, 144.02, 143.02, 142.25, 141.04, 135.46, 133.49, 131.08, 130.49, 129.91, 129.20, 127.69, 125.11, 123.45, 123.23.

HRMS (+ESI) m/z calcd for $C_{18}H_{12}NO_4$ $(M + H)^+$: 306.0766; found: 306.0762.

General procedure A: Compounds **1d**, **1e** and **1g** were synthesized according to modified literature procedure:

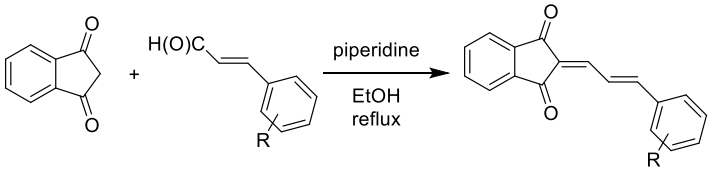

To a solution of 1,3-Indandione (3.42 mmol, 1 equiv) and cinnamaldehyde (3.42 mmol, 1 equiv) in ethanol (12 mL), 1 drop of piperidine was added under N_2 atmosphere. The reaction mixture was brought to reflux temperature and was stirred until all starting materials were consumed (the reaction was monitored by TLC). After completion of the reaction, the mixture was cooled down to room temperature, followed by the removal of the solvent under vacuum. Then the crude mixture was first pushed through a silica gel column eluted with *n*-hexanes/ethyl acetate 98:2 to 80:20. Then single re-crystallization was performed using DCM/*n*-hexanes solvent system to obtain the pure product. The chemical yields of the obtained compounds are listed below.

Characterization data:

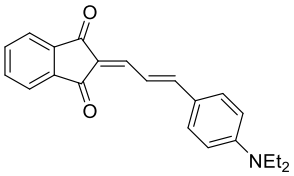

*(E)-2-(3-(4-(diethylamino)phenyl)allylidene)-1H-indene-1,3(2H)-dione (**1d**)*.

Appearance: yellow solid, Yield=45%, Mp. (lit)[5] = 184-186 °C.

^{1}H NMR (300 MHz, $CDCl_3$) δ 8.35 – 7.99 (m, 1H), 7.98 – 7.77 (m, 2H), 7.77 – 7.39 (m, 5H), 7.38 – 7.11 (m, 1H), 6.75 – 6.47 (m, 2H), 3.55 – 3.24 (m, 4H), 1.30 – 0.96 (m, 6H).

^{13}C NMR (75 MHz, $CDCl_3$) δ 191.26, 190.91, 153.96, 150.54, 146.73, 142.15, 140.83, 134.46, 134.29, 131.90, 124.07, 123.19, 122.61, 122.38, 118.99, 111.61, 44.78, 12.78.

HRMS (+ESI) m/z calcd for $C_{22}H_{22}NO_2$ $(M + H)^+$: 332.1651; found: 332.1652.

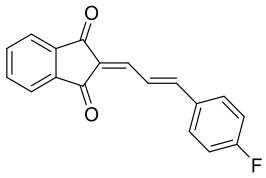

*(E)-2-(3-(4-fluorophenyl)allylidene)-1H-indene-1,3(2H)-dione (**1e**)*.

Appearance: yellow solid, Yield=56%, Mp. (dec.) = 188.5-190 °C.

^{1}H NMR (300 MHz, $CDCl_3$) δ 8.34 (dd, *J* = 15.3, 12.0 Hz, 1H), 8.02 – 7.88 (m, 2H), 7.84 – 7.72 (m, 2H), 7.71 – 7.50 (m, 3H), 7.34 – 7.19 (m, 1H), 7.10 (t, *J* = 8.4 Hz, 2H).

^{13}C NMR (75 MHz, $CDCl_3$) δ 190.63, 190.11, 166.08, 162.72, 149.63, 144.49, 142.31, 141.01, 135.30, 135.19, 132.07, 132.03, 130.82, 130.70, 128.14, 123.55, 123.52, 123.30, 123.13, 116.59, 116.29.

HRMS (+ESI) m/z calcd for $C_{18}H_{12}FO_2$ $(M + H)^+$: 279.0821; found: 279.0822.

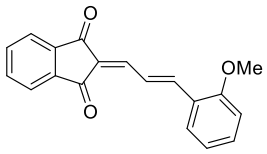

*(E)-2-(3-(2-methoxyphenyl)allylidene)-1H-indene-1,3(2H)-dione (**1g**)*.

Appearance: yellow solid, Yield=48%, Mp. (dec.) = 183.2-185 °C.

^{1}H NMR (500 MHz, $CDCl_3$) δ 8.45 (dd, *J* = 15.6, 12.1 Hz, 1H), 7.99 – 7.87 (m, 2H), 7.81 – 7.69 (m, 4H), 7.65 (d, *J* = 12.1 Hz, 1H), 7.36 (t, *J* = 7.7 Hz, 1H), 6.99 (t, *J* = 7.7 Hz, 1H), 6.90 (d, *J* = 8.3 Hz, 1H), 3.92 (s, 3H).

^{13}C NMR (126 MHz, $CDCl_3$) δ 190.74, 190.37, 158.63, 146.65, 146.03, 142.28, 140.95, 135.08, 134.94, 132.58, 128.84, 127.30, 124.70, 124.08, 123.11, 122.94, 121.09, 111.35, 55.76.

HRMS (+ESI) m/z calcd for $C_{19}H_{15}O_3$ $(M + H)^+$: 291.1021; found: 291.1018.

1.2.2 Optimization of diphosphine synthesis via double hydrophosphination

General procedure for the synthesis and reaction condition optimization of compound **4aa:**

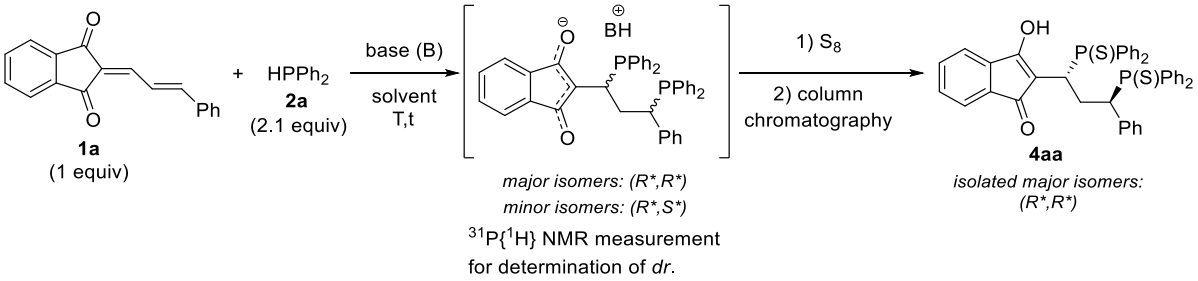

A nitrogen flushed 2-neck flask was charged with **1a** (19.7 mg, 75.7 µmol, 1 equiv) and base (*for the corresponding amount, see Table S1*) in de-gassed acetone (2.5 mL) at room temperature, followed by the addition of **2a** (29.6 mg, 159 µmol, 2.1 equiv). The setup was stirred and monitored by TLC. The conversion and the *dr* was determined by $^{31}P\{^{1}H\}$ NMR measurement of the crude mixture. Upon completion, sulphur (37.9 µmol, 0.5 equiv of S_8) was added into the flask and the mixture was stirred for another 5 mins. Evaporation of the solvent under reduced pressure provided the crude mixture, which was purified by silica gel column chromatography, eluted with *n*-hexane/EtOAc (97:3 to 70:30) eluent system.

Table S1 Reaction condition optimization of **4aa** diphosphine synthesis.

Entry	Base (equiv)	Solvent	T [°C]	t	Conv. [%]	*dr* [XX/XY]
1	-	acetone	RT	1.5 h	99	5.9 : 1
2	Et_3N (1)	acetone	RT	15 mins	99	11.5 : 1
3	Et_3N (2)	acetone	RT	10 mins	99	>20 : 1
4	Et_3N (5)	acetone	RT	<5 mins	99	16.7 : 1
5	NaOAc (1)	acetone	RT	1.5 h	99	9.1 : 1
6	K_2CO_3 (1)	acetone	RT	2.75 h	99	8.8 : 1
7	NaOMe (1)	acetone	RT	2.75 h	99	6 : 1
8	DABCO (1)	acetone	RT	15 mins	99	>20 : 1
9	DABCO (0.5)	acetone	RT	20 mins	99	14 : 2
10	DTBP (1)	acetone	RT	4 h	99	5.3 : 1
11	Pyridine (1)	acetone	RT	3 h	99	8 : 1
12	DMA (1)	acetone	RT	3.5 h	99	8 : 1
13	TMG (1)	acetone	RT	16 h	99	>20 : 1
14	-	DCM	RT	12 h	99	3.4 : 1
15	Et_3N (1)	DCM	RT	30 mins	99	13.2 : 1
16	Et_3N (2)	DCM	RT	10 mins	99	>20 : 1
17	TMG (1)	DCM	RT	16 h	99	>20 : 1
18	Et_3N (1)	MeOH	RT	10 h	99	5.3 :1
19	Et_3N (1)	Toluene	RT	4 h	99	4.8 : 1
20	Et_3N (1)	$CHCl_3$	RT	4.5 h	99	4.2 : 1
21	Et_3N (1)	MeCN	RT	20 mins	99	15.9 : 1
22	Et_3N (1)	hexanes	RT	24 h	0	-

DABCO: 1,4-diazabicyclo[2.2.2]octane; DTBP: 2,6-ditert-butyl piridine; DMA: N,N-dimethylaniline, TMG: 1,1,3,3,-tetramethylguanidine

Based on optimization, the selected reaction condition for the generation of **4aa** and for the substrate scope includes the usage of 2 equivalent amount of triethylamine and acetone as a solvent (Table S1, Entry 3). The product **4aa** was obtained as yellow solid material in 95% isolated yield.

Characterization data:

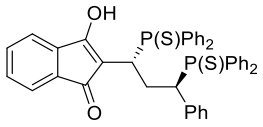

(R,R*)*-**4aa**

*2-(1,3-bis(diphenylphosphorothioyl)-3-phenylpropyl)-3-hydroxy-1H-inden-1-one (**4aa**)*.

Appearance: yellow solid, Yield=95%, Mp. (dec.) = 197.8-199 °C.

^{1}H NMR (400 MHz, $CDCl_3$) δ 11.06 (s, 1H, O*H*), 7.86 (dd, *J* = 11.7, 7.8 Hz, 2H, Ar*H*), 7.70 (dd, *J* = 12.6, 7.4 Hz, 2H, Ar*H*), 7.52 (dd, *J* = 12.7, 7.7 Hz, 2H, Ar*H*), 7.48 – 7.37 (m, 4H, Ar*H*), 7.37 – 7.26 (m, 7H, Ar*H*), 7.24 – 7.14 (m, 6H, Ar*H*), 7.13 – 7.03 (m, 4H, Ar*H*), 7.03 – 6.96 (m, 2H, Ar*H*), 3.98 (t, *J* = 10.8 Hz, 1H, $CH_2C\underline{H}$Ph), 3.66 (t, *J* = 10.5 Hz, 1 H, C(O)C$\underline{C}H_2$), 2.48 – 2.29 (m, 2H, C*H*$_2$).

^{13}C NMR (101 MHz, $CDCl_3$) δ 194.18 (d, $^{3}J_{PC}$ = 6.7 Hz, 1C, *C*(O)), 175.90 (d, $^{3}J_{PC}$ = 5.1 Hz, 1C, C=$\underline{C}$-OH), 141.25 – 101.50 (37C, Ar and $\underline{C}$=C-OH), 45.14 (dd, $^{1}J_{PC}$ = 51.4, $^{3}J_{PC}$ = 13.7 Hz, 1C, $CH_2\underline{C}$HPh), 33.74 (dd, $^{1}J_{PC}$ = 56.3, $^{3}J_{PC}$ = 15.1 Hz, 1C, C$\underline{C}$HCH$_2$), 30.38 (t, $^{2}J_{PC}$ = 4.4 Hz, 1C, *C*H$_2$).

^{31}P{^{1}H} NMR (162 MHz, $CDCl_3$) δ 49.22 (d, $^{4}J_{PP}$ = 5.4 Hz, 1P), 47.10 (d, $^{4}J_{PP}$ = 5.8 Hz, 1P).

HRMS (+ESI) m/z calcd for $C_{42}H_{35}O_2P_2S_2$ $(M + H)^+$: 697.1554; found: 697.1544.

1.2.3 Determination of diastereomeric ratio (*dr)* in double hydrophosphination:

In the double hydrophosphination reaction, 4 possible non-superimposable isomers can be produced theoretically with the *(R*,R*)* and *(R*,S*)* relative configurations. According to our investigations (X-Ray analysis of isolated major isomers, **4aa**), it turned out that the major product is the racemic *(R*,R*)* isomer. The amount of the diastereomeric *(R*,S*)* isomers produced in the reaction can be decreased by addition of appropriate bases. The *dr* values were determined by the $^{31}P\{^{1}H\}$ NMR analysis of the crude mixture **before sulfurization**. As an example, herein we present the corresponding $^{31}P\{^{1}H\}$ NMR crude spectra (Figure S1 and S2) of the non-optimized hydrophosphination (Table S1, Entry 1) and that of the optimized reaction (Table S1, Entry 3) measured in acetone. The $^{31}P\{^{1}H\}$ NMR peaks belong to the isomers of compound **13** (produced in the base-free reaction) and **3aa** (in the presence of triethylamine).

Figure S1 Crude $^{31}P\{^{1}H\}$ NMR spectrum of the non-optimized double hydrophosphination.

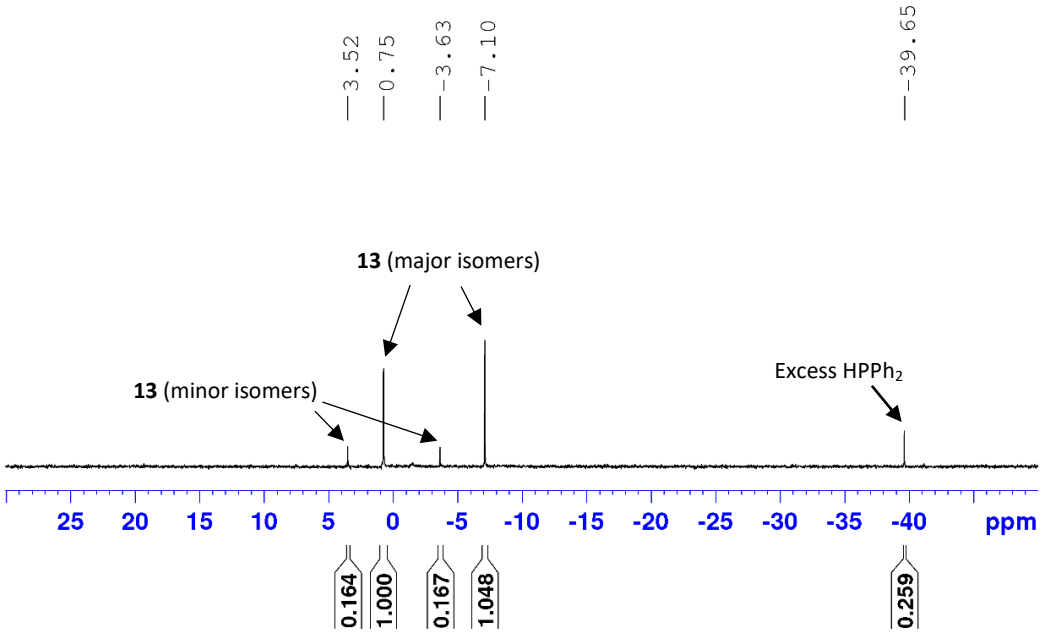

Figure S2 Crude $^{31}P\{^{1}H\}$ NMR spectrum of the optimized double hydrophosphination.

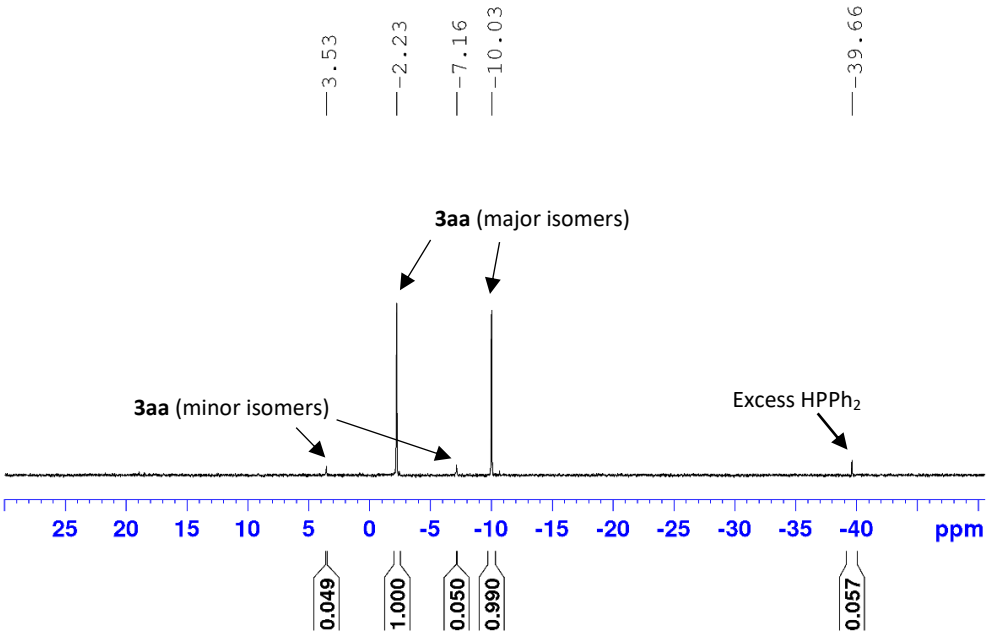

1.2.4 General procedure of diphosphine synthesis via double hydrophosphination

General Procedure B: Compounds **4ab**-**4ha** were synthesized according to the following procedure:

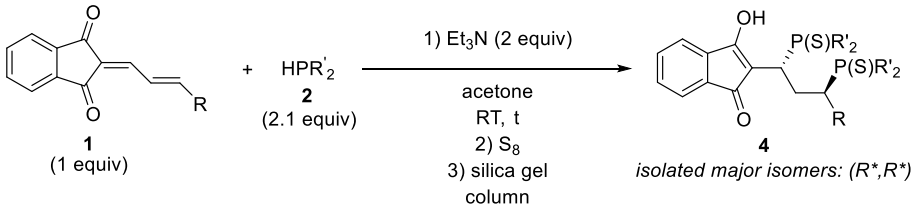

A nitrogen flushed 2-neck flask was charged with α,β,γ,δ-unsaturated-1,3-indandione (**1**) (75.7 µmol, 1 equiv) and triethylamine (15.3 mg, 151.4 µmol, 2 equiv) in de-gassed acetone (2.5 mL) at room temperature, followed by the addition of diarylphosphine (**2**) (159 µmol, 2.1 equiv). The setup was stirred and monitored by TLC. Upon completion, sulphur (37.9 µmol, 0.5 equiv of S_8) was added into the flask and the mixture was stirred for another 5 mins. Evaporation of the solvent under reduced pressure provided the crude mixture, which was purified by silica gel column chromatography, eluted with *n*-hexane/EtOAc (97:3 to 70:30) eluent system. The chemical yields of the corresponding diphosphine syntheses are listed below.

Characterization data:

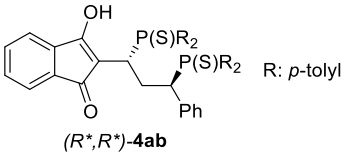

(R,R*)*-**4ab**

*2-(1,3-bis(di-p-tolylphosphorothioyl)-3-phenylpropyl)-3-hydroxy-1H-inden-1-one (**4ab**)*.

Appearance: yellow solid, Yield=95%, Mp. (dec.) = 196.1-198 °C.

^{1}H NMR (300 MHz, $CDCl_3$) δ 11.13 (s, 1H, O*H*), 7.71 (dd, *J* = 11.8, 8.1 Hz, 2H, Ar*H*), 7.56 (dd, *J* = 12.6, 8.2 Hz, 2H, Ar*H*), 7.47 – 7.29 (m, 5H, Ar*H*), 7.20 – 7.10 (m, 4H, Ar*H*), 7.10 – 6.99 (m, 8H, Ar*H*), 6.97 – 6.82 (m, 4H, Ar*H*), 4.02 – 3.81 (m, 1H, $CH_2C\underline{H}$Ph), 3.68 – 3.52 (m, 1H, C(O)C$\underline{C}H$$CH_2$), 2.36 (s, 3H, C*H*$_3$), 2.35 – 2.31 (m, 2H, C*H*$_2$), 2.30 (s, 3H, C*H*$_3$), 2.21 (s, 3H, C*H*$_3$), 2.18 (s, 3H, C*H*$_3$).

^{13}C NMR (75 MHz, $CDCl_3$) δ 194.33 (d, $^3J_{PC}$ = 6.8 Hz, 1C, *C*(O)), 175.85 (d, $^3J_{PC}$ = 5.1 Hz, 1C, C=$\underline{C}$-OH), 143.12 – 103.39 (37C, Ar and $\underline{C}$=C-OH), 45.37 (dd, $^1J_{PC}$ = 51.7, $^3J_{PC}$ = 13.6 Hz, 1C, $CH_2\underline{C}$HPh), 33.88 (dd, $^1J_{PC}$ = 56.3, $^3J_{PC}$ = 15.1 Hz, 1C, C$\underline{C}$HCH_2), 30.66 (t, $^2J_{PC}$ = 4.4 Hz, 1C, *C*H_2), 21.65 (t, *J* = 1.4 Hz, 2C, *C*H_3), 21.54 (d, *J* = 1.3 Hz, 1C, *C*H_3), 21.44 (d, *J* = 1.3 Hz, 1C, *C*H_3).

^{31}P{^{1}H} NMR (202 MHz, $CDCl_3$) δ 48.75 (d, $^4J_{PP}$ = 5.6 Hz, 1P), 46.60 (d, $^4J_{PP}$ = 5.5 Hz, 1P).

HRMS (+ESI) m/z calcd for $C_{46}H_{43}O_2P_2S_2$ $(M + H)^+$: 753.2180; found: 753.2181.

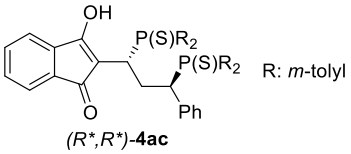

(R,R*)*-**4ac**

*2-(1,3-bis(di-m-tolylphosphorothioyl)-3-phenylpropyl)-3-hydroxy-1H-inden-1-one (**4ac**)*.

Appearance: yellow solid, Yield=94%, Mp. (dec.) = 168.7-169 °C.

^{1}H NMR (400 MHz, $CDCl_3$) δ 11.09 (s, 1H, O*H*), 7.75 (d, *J* = 13.0 Hz, 1H, Ar*H*), 7.60 – 7.51 (m, 2H, Ar*H*), 7.47 – 7.27 (m, 7H, Ar*H*), 7.24 – 7.08 (m, 7H, Ar*H*), 7.08 – 6.93 (m, 7H, Ar*H*), 6.90 (d, *J* = 7.7 Hz, 2H, Ar*H*), 3.91 (t, *J* = 10.3 Hz, 1H, $CH_2C\underline{H}$Ph), 3.61 (t, *J* = 10.3 Hz, 1H, C(O)CC$\underline{H}CH_2$), 2.46 – 2.38 (m, 2H, CH_2), 2.30 (s, 3H, CH_3), 2.25 (s, 3H, CH_3), 2.21 (s, 3H, CH_3), 2.07 (s, 3H, CH_3).

^{13}C NMR (101 MHz, $CDCl_3$) δ 194.04 (d, $^{3}J_{PC}$ = 6.4 Hz, 1C, *C*(O)), 175.70 (d, $^{3}J_{PC}$ = 5.3 Hz, 1C, C=$\underline{C}$-OH), 140.21 – 103.60 (37C, Ar and $\underline{C}$=C-OH), 45.19 (dd, $^{1}J_{PC}$ = 50.9, $^{3}J_{PC}$ = 13.7 Hz, 1C, $CH_2\underline{C}$HPh), 33.77 (dd, $^{1}J_{PC}$ = 55.7, $^{3}J_{PC}$ = 15.2 Hz, 1C, C$\underline{C}HCH_2$), 29.95 (t, $^{2}J_{PC}$ = 3.9 Hz, 1C, *C*H_2), 21.73 (s, 1C, *C*H_3), 21.62 (s, 1C, *C*H_3), 21.49 (s, 1C, *C*H_3), 21.37 (s, 1C, *C*H_3).

^{31}P{^{1}H} NMR (162 MHz, $CDCl_3$) δ 50.50 (d, $^{4}J_{PP}$ = 5.1 Hz, 1P), 48.30 (d, $^{4}J_{PP}$ = 5.2 Hz, 1P).

HRMS (+ESI) m/z calcd for $C_{46}H_{43}O_2P_2S_2$ $(M + H)^+$: 753.2180; found: 753.2178.

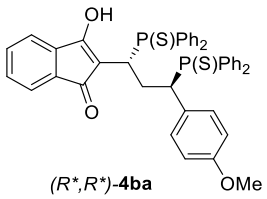

(R,R*)*-**4ba**

*2-(1,3-bis(diphenylphosphorothioyl)-3-(4-methoxyphenyl)propyl)-3-hydroxy-1H-inden-1-one (**4ba**).*
Appearance: yellow solid, Yield=95%, Mp. (dec.) = 201.8-203 °C.

^{1}H NMR (400 MHz, $CDCl_3$) δ 11.05 (s, 1H, O*H*), 7.89 – 7.79 (m, 2H, Ar*H*), 7.77 – 7.66 (m, 2H, Ar*H*), 7.60 – 7.50 (m, 2H, Ar*H*), 7.50 – 7.35 (m, 4H, Ar*H*), 7.35 – 7.26 (m, 7H, Ar*H*), 7.25 – 7.14 (m, 5H, Ar*H*), 7.10 (td, *J* = 7.6, 3.1 Hz, 2H, Ar*H*), 6.91 (dd, *J* = 8.7, 1.8 Hz, 2H, Ar*H*), 6.60 (d, *J* = 8.6 Hz, 2H, Ar*H*), 3.99 (t, *J* = 10.7 Hz, 1H, $CH_2C\underline{H}$Ar), 3.78 (s, 3H, OCH_3), 3.61 (t, *J* = 10.3 Hz, 1H, C(O)CC$\underline{H}CH_2$), 2.45 – 2.20 (m, 2H, CH_2).

^{13}C NMR (101 MHz, $CDCl_3$) δ 194.22 (d, $^{3}J_{PC}$ = 6.7 Hz, 1C, *C*(O)), 175.86 (d, $^{3}J_{PC}$ = 5.2 Hz, 1C, C=$\underline{C}$-OH), 160.39 – 102.45 (37C, Ar and $\underline{C}$=C-OH), 55.34 (s, 1C, O*C*H_3), 44.29 (dd, $^{1}J_{PC}$ = 52.0, $^{3}J_{PC}$ = 13.7 Hz, 1C, $CH_2\underline{C}$HAr), 33.67 (dd, $^{1}J_{PC}$ = 56.3, $^{3}J_{PC}$ = 15.1 Hz, 1C, C$\underline{C}HCH_2$), 30.45 (t, $^{2}J_{PC}$ = 4.8 Hz, 1C, *C*H_2).

^{31}P{^{1}H} NMR (162 MHz, $CDCl_3$) δ 49.13 (d, $^{4}J_{PP}$ = 5.5 Hz, 1P), 47.31 (d, $^{4}J_{PP}$ = 5.6 Hz, 1P).

HRMS (+ESI) m/z calcd for $C_{43}H_{37}O_3P_2S_2$ $(M + H)^+$: 727.1659; found: 727.1667.

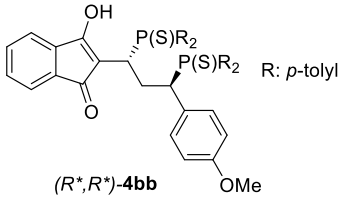

(R,R*)*-**4bb**

*2-(1,3-bis(di-p-tolylphosphorothioyl)-3-(4-methoxyphenyl)propyl)-3-hydroxy-1H-inden-1-one (**4bb**).*
Appearance: yellow solid, Yield=94%, Mp. (dec.) = 179.0-181 °C.

^{1}H NMR (400 MHz, $CDCl_3$) δ 11.12 (s, 1H, O*H*), 7.69 (dd, *J* = 11.8, 8.1 Hz, 2H, Ar*H*), 7.57 (dd, *J* = 12.5, 8.1 Hz, 2H, Ar*H*), 7.45 – 7.30 (m, 5H, Ar*H*), 7.21 – 7.12 (m, 3H, Ar*H*), 7.07 (d, *J* = 7.9 Hz, 4H, Ar*H*), 6.99 (dd, *J* = 8.7, 1.8 Hz, 2H, Ar*H*), 6.91 (d, *J* = 7.8 Hz, 4H, Ar*H*), 6.60 (d, *J* = 8.6 Hz, 2H, Ar*H*), 3.92 (t, *J* = 11.1 Hz, 1H, $CH_2C\underline{H}$Ar), 3.80 (s, 3H OCH_3), 3.55 (t, *J* = 10.6 Hz, 1H, C(O)CC$\underline{H}CH_2$), 2.37 (s, 3H, CH_3), 2.30 (s, 3H, CH_3), 2.29 – 2.22 (m, 2H, CH_2), 2.21 (s, 3H, CH_3), 2.20 (s, 3H, CH_3).

^{13}C NMR (126 MHz, $CDCl_3$) δ 194.41 (d, $^{3}J_{PC}$ = 6.9 Hz, 1C, *C*(O)), 175.85 (d, $^{3}J_{PC}$ = 5.1 Hz, 1C, C=$\underline{C}$-OH), 143.56 – 102.84 (37C, Ar and $\underline{C}$=C-OH), 55.32 (s, 1C, O*C*H_3), 44.51 (dd, $^{1}J_{PC}$ = 52.5, $^{3}J_{PC}$ = 13.6 Hz, 1C, $CH_2\underline{C}$HAr), 33.82 (dd, $^{1}J_{PC}$ = 56.4, $^{3}J_{PC}$ = 15.0 Hz, 1C, C$\underline{C}HCH_2$), 30.77 (t, $^{2}J_{PC}$ = 4.7 Hz, 1C, *C*H_2), 21.67 (s, 2C, *C*H_3), 21.55 (d, *J* = 1.2 Hz, 1C, *C*H_3), 21.46 (d, *J* = 0.9 Hz, 1C, *C*H_3).

$^{31}P\{^{1}H\}$ NMR (162 MHz, $CDCl_3$) δ 48.56 (d, $^{4}J_{PP}$ = 6.0 Hz, 1P), 46.57 (d, $^{4}J_{PP}$ = 5.7 Hz, 1P).

HRMS (+ESI) m/z calcd for $C_{47}H_{45}O_3P_2S_2$ $(M + H)^+$: 783.2285; found: 783.2278.

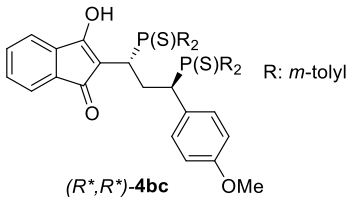

*2-(1,3-bis(di-m-tolylphosphorothioyl)-3-(4-methoxyphenyl)propyl)-3-hydroxy-1H-inden-1-one (**4bc**).*
Appearance: yellow solid, Yield=93%, Mp. (dec.) = 165.4-167 °C.

^{1}H NMR (500 MHz, $CDCl_3$) δ 11.09 (s, 1H, O*H*), 7.74 (d, *J* = 12.9 Hz, 1H, Ar*H*), 7.60 – 7.49 (m, 2H, Ar*H*), 7.47 – 7.27 (m, 7H, Ar*H*), 7.25 – 7.18 (m, 3H, Ar*H*), 7.17 – 7.09 (m, 2H, Ar*H*), 7.05 – 6.96 (m, 5H, Ar*H*), 6.82 (dd, *J* = 8.6, 1.8 Hz, 2H, Ar*H*), 6.59 (d, *J* = 8.6 Hz, 2H, Ar*H*), 3.93 (t, *J* = 10.9 Hz, 1H, $CH_2C\underline{H}Ar$), 3.78 (s, 3H, OCH_3), 3.58 (t, *J* = 10.5 Hz, 1H, $C(O)CC\underline{H}CH_2$), 2.44 – 2.32 (m, 2H, CH_2), 2.30 (s, 3H, CH_3), 2.23 (s, 3H, CH_3), 2.20 (s, 3H, CH_3), 2.09 (s, 3H, CH_3).

^{13}C NMR (126 MHz, $CDCl_3$) δ 194.10 (d, *J* = 6.6 Hz, 1C, *C*(O)), 175.67 (d, *J* = 5.2 Hz, C=*C*-OH), 159.60 – 103.42 (37C, Ar and *C*=C-OH), 55.30 (s, 1C, OCH_3), 44.31 (dd, $^{1}J_{PC}$ = 51.4, $^{3}J_{PC}$ = 13.7 Hz, 1C, $CH_2\underline{C}HAr$), 33.69 (dd, $^{1}J_{PC}$ = 56.0, $^{3}J_{PC}$ = 15.1 Hz, 1C, $C\underline{C}HCH_2$), 30.01 (t, $^{2}J_{PC}$ = 4.5 Hz, 1C, CH_2), 21.64 (s, 1C, CH_3), 21.58 (s, 1C, CH_3), 21.47 (s, 1C, CH_3), 21.39 (s, 1C, CH_3).

$^{31}P\{^{1}H\}$ NMR (162 MHz, $CDCl_3$) δ 49.69 (d, $^{4}J_{PP}$ = 5.6 Hz, 1P), 47.61 (d, $^{4}J_{PP}$ = 5.7 Hz, 1P).

HRMS (+ESI) m/z calcd for $C_{47}H_{45}O_3P_2S_2$ $(M + H)^+$: 783.2285; found: 783.2283.

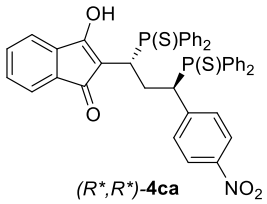

*2-(1,3-bis(diphenylphosphorothioyl)-3-(4-nitrophenyl)propyl)-3-hydroxy-1H-inden-1-one (**4ca**).*
Appearance: yellow solid, Yield=75%, Mp. (dec.) = 190.0-192 °C.

^{1}H NMR (300 MHz, $CDCl_3$) δ 11.04 (s, 1H, O*H*), 7.86 – 7.69 (m, 4H, Ar*H*), 7.63 (dd, *J* = 12.7, 7.7 Hz, 2H, Ar*H*), 7.55 – 7.42 (m, 3H, Ar*H*), 7.41 – 7.28 (m, 5H, Ar*H*), 7.26 – 7.15 (m, 8H, Ar*H*), 7.15 – 6.94 (m, 6H, Ar*H*), 3.80 – 3.63 (m, 2H, $CH_2C\underline{H}Ar$ and $C(O)CC\underline{H}CH_2$), 2.46 – 2.16 (m, 2H, CH_2).

^{13}C NMR (75 MHz, $CDCl_3$) δ 194.55 (d, $^{3}J_{PC}$ = 6.9 Hz, 1C, *C*(O)), 176.04 (d, $^{3}J_{PC}$ = 5.1 Hz, 1C, C=*C*-OH), 148.47 – 102.10 (37C, Ar and *C*=C-OH), 45.21 (dd, $^{1}J_{PC}$ = 49.9, $^{3}J_{PC}$ = 13.4 Hz, 1C, $CH_2\underline{C}HAr$), 34.21 (dd, $^{1}J_{PC}$ = 56.1, $^{3}J_{PC}$ = 14.5 Hz, 1C, $C\underline{C}HCH_2$), 30.59 (dd, $^{2}J_{PC}$ = 5.2, $^{2}J_{PC}$ = 3.1 Hz, 1C, CH_2).

$^{31}P\{^{1}H\}$ NMR (162 MHz, $CDCl_3$) δ 49.23 (d, $^{4}J_{PP}$ = 4.9 Hz, 1P), 46.94 (d, $^{4}J_{PP}$ = 4.9 Hz, 1P).

HRMS (+ESI) m/z calcd for $C_{42}H_{34}NO_4P_2S_2$ $(M + H)^+$: 742.1405; found: 742.1414.

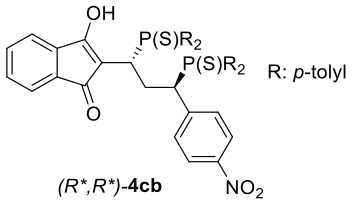

(*R*,R**)-**4cb**

*2-(1,3-bis(di-p-tolylphosphorothioyl)-3-(4-nitrophenyl)propyl)-3-hydroxy-1H-inden-1-one (**4cb**).* Appearance: yellow solid, Yield=74%, Mp. (dec.) = 182.2-184 °C.

^{1}H NMR (400 MHz, $CDCl_3$) δ 11.18 (s, 1H, O*H*), 7.83 (d, *J* = 8.5 Hz, 2H, Ar*H*), 7.69 (dd, *J* = 12.0, 8.0 Hz, 2H, Ar*H*), 7.56 (dd, *J* = 12.5, 8.1 Hz, 2H, Ar*H*), 7.50 – 7.32 (m, 5H, Ar*H*), 7.25 – 7.15 (m, 5H, Ar*H*), 7.13 – 7.02 (m, 4H, Ar*H*), 6.99 – 6.89 (m, 4H, Ar*H*), 3.83 – 3.64 (m, 2H, $CH_2C\underline{H}$Ar and C(O)CC$\underline{H}CH_2$), 2.40 (s, 3H, CH_3), 2.37 – 2.30 (m, 2H, CH_2), 2.29 (s, 3H, CH_3), 2.23 (s, 3H, CH_3), 2.21 (s, 3H, CH_3).

^{13}C NMR (75 MHz, $CDCl_3$) δ 194.78 (d, $^{3}J_{PC}$ = 7.1 Hz, 1C, *C*(O)), 176.01 (d, $^{3}J_{PC}$ = 5.1 Hz, 1C, C=$\underline{C}$-OH), 148.46 – 102.78 (37C, Ar and $\underline{C}$=C-OH), 45.43 (dd, $^{1}J_{PC}$ = 50.3, $^{3}J_{PC}$ = 13.2 Hz, 1C, $CH_2\underline{C}$HAr), 34.32 (dd, $^{1}J_{PC}$ = 56.2, $^{3}J_{PC}$ = 14.3 Hz, 1C, C$\underline{C}HCH_2$), 31.11 (dd, $^{2}J_{PC}$ = 4.8, $^{2}J_{PC}$ = 3.1 Hz, 1C, *C*H_2), 21.66 (d, *J* = 1.1 Hz, 1C, *C*H_3), 21.58 (d, *J* = 1.1 Hz, 2C, *C*H_3), 21.48 (d, *J* = 1.2 Hz, 1C, *C*H_3).

^{31}P{^{1}H} NMR (162 MHz, $CDCl_3$) δ 48.52 (d, $^{4}J_{PP}$ = 5.1 Hz, 1P), 46.15 (d, $^{4}J_{PP}$ = 5.4 Hz, 1P).

HRMS (+ESI) m/z calcd for $C_{46}H_{42}NO_4P_2S_2$ $(M + H)^+$: 798.2031; found:798.2033.

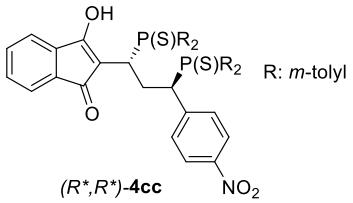

(*R*,R**)-**4cc**

*2-(1,3-bis(di-m-tolylphosphorothioyl)-3-(4-nitrophenyl)propyl)-3-hydroxy-1H-inden-1-one (**4cc**).* Appearance: yellow solid, Yield=76%, Mp. (dec.) = 201.6-203 °C.

^{1}H NMR (400 MHz, $CDCl_3$) δ 11.16 (s, 1H, O*H*), 7.83 (d, *J* = 8.6 Hz, 2H, Ar*H*), 7.72 (d, *J* = 13.2 Hz, 1H, Ar*H*), 7.59 – 7.48 (m, 2H, Ar*H*), 7.45 – 7.32 (m, 6H, Ar*H*), 7.27 – 7.13 (m, 6H, Ar*H*), 7.11 – 7.00 (m, 5H, Ar*H*), 7.00 – 6.93 (m, 2H, Ar*H*), 3.84 – 3.62 (m, 2H, $CH_2C\underline{H}$Ar and C(O)CC$\underline{H}CH_2$), 2.53 – 2.34 (m, 2H, CH_2), 2.31 (s, 3H, CH_3), 2.25 (s, 3H, CH_3), 2.23 (s, 3H, CH_3), 2.10 (s, 3H, CH_3).

^{13}C NMR (101 MHz, $CDCl_3$) δ 194.43 (d, $^{3}J_{PC}$ = 6.8 Hz, 1C, *C*(O)), 175.86 (d, $^{3}J_{PC}$ = 5.2 Hz, 1C, C=$\underline{C}$-OH), 148.56 – 102.55 (37C, Ar and $\underline{C}$=C-OH), 45.21 (dd, $^{1}J_{PC}$ = 49.2, $^{3}J_{PC}$ =13.3 Hz, 1C, $CH_2\underline{C}$HAr), 34.21 (dd, $^{1}J_{PC}$ = 55.8, $^{3}J_{PC}$ = 14.5 Hz, 1C, C$\underline{C}HCH_2$), 30.30 – 30.09 (m, 1C, *C*H_2), 21.61 (s, 2C, *C*H_3), 21.52 (s, 1C, *C*H_3), 21.43 (s, 1C, *C*H_3).

^{31}P{^{1}H} NMR (162 MHz, $CDCl_3$) δ 49.75 (d, $^{4}J_{PP}$ = 4.7 Hz, 1P), 47.33 (d, $^{4}J_{PP}$ = 4.5 Hz, 1P).

HRMS (+ESI) m/z calcd for $C_{46}H_{42}NO_4P_2S_2$ $(M + H)^+$: 798.2031; found: 798.2012.

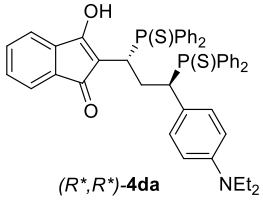

(*R*,R**)-**4da**

*2-(3-(4-(diethylamino)phenyl)-1,3-bis(diphenylphosphorothioyl)propyl)-3-hydroxy-1H-inden-1-one (**4da**).* Appearance: red solid, Yield=94%, Mp. (dec.) = 185.2-187 °C.

^{1}H NMR (400 MHz, $CDCl_3$) δ 11.01 (s, 1H, O*H*), 7.83 (dd, *J* = 11.8, 7.4 Hz, 2H, Ar*H*), 7.76 – 7.66 (m, 2H, Ar*H*), 7.56 (dd, *J* = 12.8, 7.4 Hz, 2H, Ar*H*), 7.48 – 7.26 (m, 11H, Ar*H*), 7.25 – 7.03 (m, 7H, Ar*H*), 6.87 (dd, *J* = 8.6, 1.6 Hz, 2H, Ar*H*), 6.40 (d, *J* = 8.7 Hz, 2H, Ar*H*), 4.15 – 4.06 (m, 1H, $CH_2C\underline{H}Ar$), 3.53 (td, *J* = 10.3, 1.9 Hz, 1H, $C(O)CC\underline{H}CH_2$), 3.43 – 3.22 (m, 4H, $N(C\underline{H_2}CH_3)_2$), 2.42 – 2.20 (m, 2H, $CHC\underline{H_2}CH$), 1.16 (t, *J* = 7.0 Hz, 6H, $N(CH_2C\underline{H_3})_2$).

^{13}C NMR (101 MHz, $CDCl_3$) δ 194.16 (d, $^{3}J_{PC}$ = 6.7 Hz, 1C, *C*(O)), 175.78 (d, $^{3}J_{PC}$ = 5.1 Hz, 1C, C=$\underline{C}$-OH), 148.39 – 101.87 (37C, Ar and $\underline{C}$=C-OH), 44.50 (s, 2C, $N(\underline{C}H_2CH_3)_2$), 44.33 (dd, $^{1}J_{PC}$ = 52.3, $^{3}J_{PC}$ = 14.0 Hz, 1C, $CH_2\underline{C}HAr$), 33.53 (dd, $^{1}J_{PC}$ = 56.3, $^{3}J_{PC}$ = 15.3 Hz, 1C, $C\underline{C}HCH_2$), 30.46 (t, $^{2}J_{PC}$ = 5.1 Hz, 1C, $CH\underline{C}H_2CH$), 12.78 (s, 2C, $N(CH_2\underline{C}H_3)_2$).

^{31}P{^{1}H} NMR (162 MHz, $CDCl_3$) δ 48.86 (d, $^{4}J_{PP}$ = 6.4 Hz, 1P), 47.14 (d, $^{4}J_{PP}$ = 6.3 Hz, 1P).

HRMS (+ESI) m/z calcd for $C_{46}H_{44}NO_2P_2S_2$ $(M + H)^+$: 768.2289; found: 768.2278.

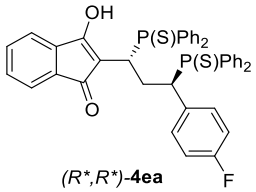

(R,R*)*-**4ea**

*2-(1,3-bis(diphenylphosphorothioyl)-3-(4-fluorophenyl)propyl)-3-hydroxy-1H-inden-1-one (**4ea**).*
Appearance: yellow solid, Yield=93%, Mp. (dec.) = 176.1-178 °C.

^{1}H NMR (500 MHz, $CDCl_3$) δ 11.08 (s, 1H, O*H*), 7.87 – 7.81 (m, 2H, Ar*H*), 7.75 – 7.68 (m, 2H, Ar*H*), 7.59 – 7.54 (m, 2H, Ar*H*), 7.52 – 7.47 (m, 1H, Ar*H*), 7.46 – 7.27 (m, 11H, Ar*H*), 7.25 – 7.22 (m, 2H, Ar*H*), 7.18 (td, *J* = 7.9, 3.0 Hz, 2H, Ar*H*), 7.12 (td, *J* = 7.9, 3.1 Hz, 2H, Ar*H*), 6.98 – 6.91 (m, 2H, Ar*H*), 6.73 (t, *J* = 8.6 Hz, 2H, Ar*H*), 3.92 (t, *J* = 11.0 Hz, 1H, $CH_2C\underline{H}Ar$), 3.64 (t, *J* = 10.5 Hz, 1H, $C(O)CC\underline{H}CH_2$), 2.44 – 2.32 (m, 1H, CH_2), 2.32 – 2.21 (m, 1H, CH_2).

^{13}C NMR (126 MHz, $CDCl_3$) δ 194.41 (d, $^{3}J_{PC}$ = 6.7 Hz, 1C, *C*(O)), 175.99 (d, $^{3}J_{PC}$ = 5.2 Hz, 1C, C=$\underline{C}$-OH), 164.08 – 102.48 (37C, Ar and $\underline{C}$=C-OH), 44.31 (dd, $^{1}J_{PC}$ = 51.8, $^{3}J_{PC}$ = 13.7 Hz, 1C, $CH_2\underline{C}HAr$), 33.83 (dd, $^{1}J_{PC}$ = 56.3, $^{3}J_{PC}$ = 14.9 Hz, 1C, $C\underline{C}HCH_2$), 30.58 (t, $^{2}J_{PC}$ = 4.5 Hz, 1C, CH_2).

^{31}P{^{1}H} NMR (202 MHz, $CDCl_3$) δ 49.23 (d, $^{4}J_{PC}$ = 4.5 Hz, 1P), 47.04 (d, $^{4}J_{PC}$ = 5.2 Hz, 1P).

HRMS (+ESI) m/z calcd for $C_{42}H_{34}FO_2P_2S_2$ $(M + H)^+$: 715.1460; found: 715.1462.

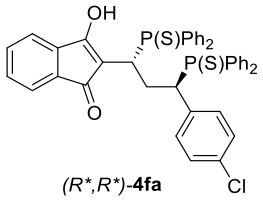

(R,R*)*-**4fa**

*2-(3-(4-chlorophenyl)-1,3-bis(diphenylphosphorothioyl)propyl)-3-hydroxy-1H-inden-1-one (**4fa**).*
Appearance: yellow solid, Yield=93%, Mp. (dec.) = 179.7-181 °C.

^{1}H NMR (500 MHz, $CDCl_3$) δ 11.08 (s, 1H, O*H*), 7.87 – 7.79 (m, 2H, Ar*H*), 7.76 – 7.67 (m, 2H, Ar*H*), 7.58 – 7.51 (m, 2H, Ar*H*), 7.51 – 7.47 (m, 1H, Ar*H*), 7.45 – 7.28 (m, 11H, Ar*H*), 7.25 – 7.22 (m, 1H, Ar*H*), 7.20 (d, *J* = 7.0 Hz, 1H, Ar*H*), 7.19 – 7.10 (m, 4H, Ar*H*), 7.02 – 6.97 (m, 2H, Ar*H*), 6.97 – 6.92 (m, 2H, Ar*H*), 3.90 (t, *J* = 11.1 Hz, 1H, $CH_2C\underline{H}Ar$), 3.64 (t, *J* = 10.6 Hz, 1H, $C(O)CC\underline{H}CH_2$), 2.40 – 2.30 (m, 1H, CH_2), 2.30 – 2.19 (m, 1H, CH_2).

^{13}C NMR (126 MHz, $CDCl_3$) δ 194.46 (d, $^{3}J_{PC}$ = 6.8 Hz, 1C, *C*(O)), 175.99 (d, $^{3}J_{PC}$ = 5.0 Hz, 1C, C=$\underline{C}$-OH), 141.24 – 102.84 (37C, Ar and $\underline{C}$=C-OH), 44.49 (dd, $^{1}J_{PC}$ = 51.5, $^{3}J_{PC}$ = 13.6 Hz, 1C, $CH_2\underline{C}HAr$), 33.83 (dd, $^{1}J_{PC}$ = 56.2, $^{3}J_{PC}$ = 14.8 Hz, 1C, $C\underline{C}HCH_2$), 30.74 (t, $^{2}J_{PC}$ = 4.6 Hz, 1C, CH_2).

^{31}P{^{1}H} NMR (202 MHz, $CDCl_3$) δ 48.90 (d, $^{4}J_{PP}$ = 5.3 Hz, 1P), 46.86 (d, $^{4}J_{PP}$ = 5.5 Hz, 1P).

HRMS (+ESI) m/z calcd for $C_{42}H_{34}ClO_2P_2S_2$ $(M + H)^+$: 731.1164; found: 731.1159.

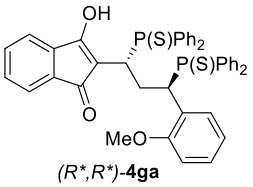

(R,R*)*-**4ga**

*2-(1,3-bis(diphenylphosphorothioyl)-3-(2-methoxyphenyl)propyl)-3-hydroxy-1H-inden-1-one (**4ga**).*
Appearance: yellow solid, Yield=94%, Mp. (dec.) = 202.4-205 °C.

^{1}H NMR (500 MHz, $CDCl_3$) δ 10.78 (s, 1H, O*H*), 7.98 (dd, *J* = 11.8, 7.3 Hz, 2H, Ar*H*), 7.79 – 7.70 (m, 4H, Ar*H*), 7.58 – 7.50 (m, 2H, Ar*H*), 7.48 – 7.43 (m, 4H, Ar*H*), 7.42 – 7.36 (m, 1H, Ar*H*), 7.32 – 7.27 (m, 4H, Ar*H*), 7.25 – 7.08 (m, 7H, Ar*H*), 6.98 (td, *J* = 7.9, 3.0 Hz, 2H, Ar*H*), 6.82 (t, *J* = 7.5 Hz, 1H, Ar*H*), 6.44 (d, *J* = 8.2 Hz, 1H, Ar*H*), 4.67 (t, *J* = 10.8 Hz, 1H, $CH_2C\underline{H}Ar$), 3.88 (td, *J* = 11.6, 2.3 Hz, 1H, $C(O)CC\underline{H}CH_2$), 3.08 (s, 3H, OCH_3), 2.66 – 2.48 (m, 1H, CH_2), 2.45 – 2.32 (m, 1H, CH_2).

^{13}C NMR (126 MHz, $CDCl_3$) δ 192.31 (d, $^{3}J_{PC}$ = 6.1 Hz, 1C, *C*(O)), 174.82 (d, $^{3}J_{PC}$ = 5.4 Hz, 1C, C=$\underline{C}$-OH), 158.08 – 102.82 (37C, Ar and $\underline{C}$=C-OH), 54.28 (s, 1C, OCH_3), 34.20 (dd, $^{1}J_{PC}$ = 51.5, $^{3}J_{PC}$ = 13.3 Hz, 1C, $CH_2\underline{C}HAr$), 33.80 (dd, $^{1}J_{PC}$ = 55.8, $^{3}J_{PC}$ = 15.7 Hz, 1C, $C\underline{C}HCH_2$), 27.79 (t, $^{2}J_{PC}$ = 5.2 Hz, 1C, CH_2).

^{31}P{^{1}H} NMR (202 MHz, $CDCl_3$) δ 50.83 (s, 1P), 48.45 (s, 1P).

HRMS (+ESI) m/z calcd for $C_{43}H_{37}O_3P_2S_2$ $(M + H)^+$: 727.1659; found: 727.1656.

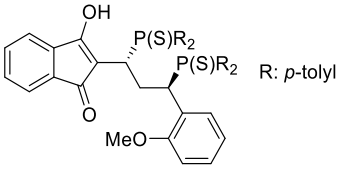

(R,R*)*-**4gb**

*2-(1,3-bis(di-p-tolylphosphorothioyl)-3-(2-methoxyphenyl)propyl)-3-hydroxy-1H-inden-1-one (**4gb**).*
Appearance: yellow solid, Yield=81%, Mp. (dec.) = 210.9-212 °C.

^{1}H NMR (400 MHz, $CDCl_3$) δ 10.85 (s, 1H, O*H*), 7.83 (dd, *J* = 11.7, 8.0 Hz, 2H, Ar*H*), 7.67 – 7.53 (m, 4H, Ar*H*), 7.45 – 7.34 (m, 1H, Ar*H*), 7.31 – 7.26 (m, 3H, Ar*H*), 7.25 – 7.12 (m, 6H, Ar*H*), 7.10 – 6.98 (m, 4H, Ar*H*), 6.85 – 6.74 (m, 3H, Ar*H*), 6.45 (d, *J* = 8.2 Hz, 1H, Ar*H*), 4.61 (t, *J* = 10.8 Hz, 1H, $CH_2C\underline{H}Ar$), 3.83 (t, *J* = 10.4 Hz, 1H, $C(O)CC\underline{H}CH_2$), 3.09 (s, 3H, OCH_3), 2.64 – 2.49 (m, 1H, CH_2), 2.43 (s, 3H, CH_3), 2.42 (s, 3H, CH_3), 2.39 – 2.29 (m, 1H, CH_2), 2.20 (s, 3H, CH_3), 2.15 (s, 3H, CH_3).

^{13}C NMR (101 MHz, $CDCl_3$) δ 192.40 (d, $^{3}J_{PC}$ = 6.2 Hz, 1C, *C*(O)), 174.80 (d, $^{3}J_{PC}$ = 5.3 Hz, 1C, C=$\underline{C}$-OH), 158.79 – 102.49 (37C, Ar and $\underline{C}$=C-OH), 54.28 (s, 1C, OCH_3), 34.37 (dd, $^{1}J_{PC}$ = 52.3, $^{3}J_{PC}$ = 13.4 Hz, 1C, $CH_2\underline{C}HAr$), 33.90 (dd, $^{1}J_{PC}$ = 56.2, $^{3}J_{PC}$ = 15.3 Hz, 1C, $C\underline{C}HCH_2$), 27.91 (t, $^{2}J_{PC}$ = 4.9 Hz, 1C, CH_2), 21.75 (s, 2C, CH_3), 21.55 (s, 1C, CH_3), 21.39 (s, 1C, CH_3).

^{31}P{^{1}H} NMR (162 MHz, $CDCl_3$) δ 50.49 (s, 1P), 48.18 (s, 1P).

HRMS (+ESI) m/z calcd for $C_{47}H_{45}O_3P_2S_2$ $(M + H)^+$: 783.2285; found: 783.2281.

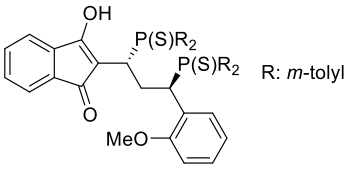

(R,R*)*-**4gc**

*2-(1,3-bis(di-m-tolylphosphorothioyl)-3-(2-methoxyphenyl)propyl)-3-hydroxy-1H-inden-1-one (**4gc**).*
Appearance: yellow solid, Yield=92%, Mp. (dec.) = 183.9-185 °C.

^{1}H NMR (500 MHz, $CDCl_3$) δ 10.85 (s, 1H, O*H*), 7.82 (d, *J* = 12.4 Hz, 1H, Ar*H*), 7.74 – 7.68 (m, 1H, Ar*H*), 7.59 (dd, *J* = 13.4, 7.6 Hz, 2H, Ar*H*), 7.55 – 7.44 (m, 2H, Ar*H*), 7.41 – 7.27 (m, 8H, Ar*H*), 7.19 (t, *J* = 7.8 Hz, 1H, Ar*H*), 7.14 – 7.08 (m, 3H, Ar*H*), 6.96 – 6.81 (m, 5H, Ar*H*), 6.46 (d, *J* = 8.3 Hz, 1H, Ar*H*), 4.64 (t, *J* = 10.7 Hz, 1H, $CH_2C\underline{H}$Ar), 3.86 (t, *J* = 10.5 Hz, 1H, C(O)C$C\underline{H}CH_2$), 3.07 (s, 3H, OCH_3), 2.69 – 2.54 (m, 1H, CH_2), 2.42 (s, 3H, CH_3), 2.41 (s, 3H, CH_3), 2.40 – 2.34 (m, 1H, CH_2), 2.19 (s, 3H, CH_3), 2.03 (s, 3H, CH_3).

^{13}C NMR (126 MHz, $CDCl_3$) δ 192.34 (d, $^{3}J_{PC}$ = 6.1 Hz, 1C, *C*(O)), 174.70 (d, $^{3}J_{PC}$ = 5.4 Hz, 1C, C=$\underline{C}$-OH), 158.12 – 102.49 (37C, Ar and $\underline{C}$=C-OH), 54.30 (s, 1C, OCH_3), 34.06 (dd, $^{1}J_{PC}$ = 51.4, $^{3}J_{PC}$ = 13.4 Hz, 1C, $CH_2\underline{C}$HAr), 33.72 (dd, $^{1}J_{PC}$ = 55.7, $^{3}J_{PC}$ = 15.3 Hz, 1C, C$\underline{C}HCH_2$), 27.69 (t, $^{2}J_{PC}$ = 5.1 Hz, 1C, CH_2), 21.81 (s, 1C, CH_3), 21.74 (s, 1C, CH_3), 21.47 (s, 1C, CH_3), 21.27 (s, 1C, CH_3).

^{31}P{^{1}H} NMR (202 MHz, $CDCl_3$) δ 51.08 (s, 1P), 48.62 (s, 1P).

HRMS (+ESI) m/z calcd for $C_{47}H_{45}O_3P_2S_2$ $(M + H)^+$: 783.2285; found: 783.2288.

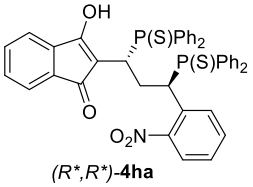

(R,R*)*-**4ha**

*2-(1,3-bis(diphenylphosphorothioyl)-3-(2-nitrophenyl)propyl)-3-hydroxy-1H-inden-1-one (**4ha**).*

Appearance: yellow solid, Yield=82% (mixture of diastereomers in 1 : 0.17 ratio, based on ^{31}P{H} NMR spectrum. The two isomers were not separable.), Mp. (dec.) = 185.9-188 °C.

NMR characterization data of the major diastereomer:

^{1}H NMR (500 MHz, $CDCl_3$, mixture) δ 10.73 (s, 1H, O*H*), 8.09 – 8.01 (m, 2H, Ar*H*), 7.89 – 7.84 (m, 1H, Ar*H*), 7.78 – 7.71 (m, 4H, Ar*H*), 7.64 – 7.57 (m, 2H, Ar*H*), 7.51 – 7.43 (m, 4H, Ar*H*), 7.42 – 7.38 (m, 3H, Ar*H*), 7.36 – 7.30 (m, 3H, Ar*H*), 7.30 – 7.26 (m, 3H, Ar*H*), 7.25 – 7.23 (m, 1H, Ar*H*), 7.19 – 7.15 (m, 1H, Ar*H*), 7.02 – 6.94 (m, 4H, Ar*H*), 5.62 – 5.53 (m, 1H, $CH_2C\underline{H}$Ar), 3.82 – 3.68 (m, 1H, C(O)C$C\underline{H}CH_2$), 2.52 – 2.43 (m, 2H, CH_2).

^{13}C NMR (126 MHz, $CDCl_3$, mixture) δ 193.61 (d, $^{3}J_{PC}$ = 6.3 Hz, 1C, *C*(O)), 175.34 (d, $^{3}J_{PC}$ = 5.3 Hz, 1C, C=$\underline{C}$-OH), 150.22 – 101.82 (37C, Ar and $\underline{C}$=C-OH), 37.41 (dd, $^{1}J_{PC}$ = 48.2, $^{3}J_{PC}$ = 13.4 Hz, 1C, $CH_2\underline{C}$HAr), 34.19 (dd, $^{1}J_{PC}$ = 56.2, $^{3}J_{PC}$ = 14.8 Hz, 1C, C$\underline{C}HCH_2$), 28.89 (dd, $^{2}J_{PC}$ = 5.3, $^{2}J_{PC}$ = 4.1 Hz, 1C, CH_2).

^{31}P{^{1}H} NMR (202 MHz, $CDCl_3$, mixture) δ 52.68 (s, 1P), 47.75 (s, 1P).

HRMS (+ESI) m/z calcd for $C_{42}H_{34}NO_4P_2S_2$ $(M + H)^+$: 742.1405; found: 742.1409.

1.2.5 Synthesis of optically pure bimetallic complexes:

General Procedure C: Compounds **16** were synthesized according to the following procedure:

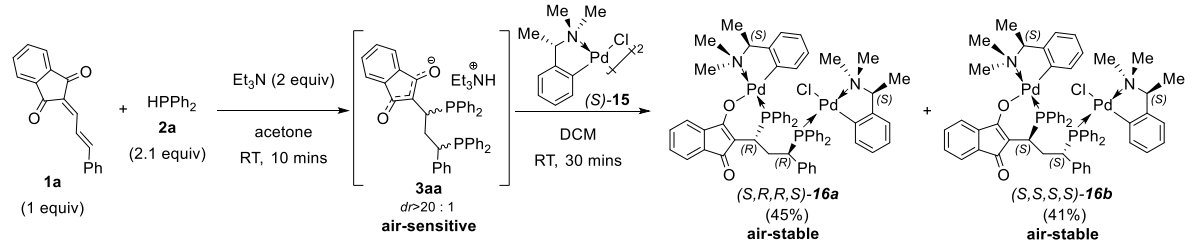

A nitrogen flushed 2-neck flask was charged with **1a** (19.7 mg, 75.7 µmol, 1 equiv) and triethylamine (15.3 mg, 151.4 µmol, 2 equiv) in de-gassed acetone (2.5 mL) at room temperature, followed by the addition of **2a** (29.6 mg, 159 µmol, 2.1 equiv). The setup was stirred for 10 mins, then the solvent was removed with vacuum distillation. The generated phosphine salt was dissolved in 2 mL de-gassed DCM, then complex **15** (46.1 mg, 79.5 µmol, 1.05 equiv) was added to the solution. The mixture was stirred at room temperature for another 30 mins. Upon completion of coordination, the generated diastereomers were separated via multiple silica gel column chromatography, using DCM/ ethyl acetate (100:0 to 50:50) eluent system. The chemical yields of the isolated bimetallic complexes are listed below.

Characterization data:

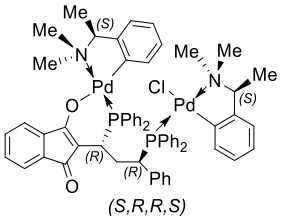

*Bimetallic Complex (S,R,R,S)-**16a**.*

Appearance: yellow solid, Yield=45% (after separation of the diastereomers), Mp. (dec.) = 194-196 °C, $[\alpha]_D^{20}$ = −17.4 (c 0.5, CH_2Cl_2)

^{1}H NMR (400 MHz, $CDCl_3$) δ 7.91 – 7.80 (m, 2H, Ar*H*), 7.78 – 7.68 (m, 2H, Ar*H*), 7.35 – 7.19 (m, 10H, Ar*H*), 7.15 – 7.07 (m, 3H, Ar*H*), 7.04 – 6.98 (m, 3H, Ar*H*), 6.97 – 6.87 (m, 3H, Ar*H*), 6.85 – 6.73 (m, 6H, Ar*H*), 6.72 – 6.61 (m, 3H, Ar*H*), 6.58 – 6.47 (m, 2H, Ar*H*), 6.46 – 6.39 (m, 1H, Ar*H*), 6.06 (t, *J* = 7.1 Hz, 1H, Ar*H*), 5.84 (t, *J* = 7.0 Hz, 1H, Ar*H*), 4.58 (q, *J* = 6.3 Hz, 1H, C*H*), 3.71 – 3.55 (m, 1H, C*H*), 3.50 – 3.37 (m, 1H, C*H*), 2.93 – 2.80 (m, 1H, C*H*), 2.76 – 2.70 (m, 1H, C*H*$_2$), 2.68 (d, *J* = 2.8 Hz, 3H, NC*H*$_3$), 2.58 (d, *J* = 1.5 Hz, 3H, NC*H*$_3$), 2.53 (d, *J* = 2.8 Hz, 3H, NC*H*$_3$), 2.52 – 2.48 (m, 1H, C*H*$_2$), 2.46 (d, *J* = 1.6 Hz, 3H, NC*H*$_3$), 1.48 (d, *J* = 6.5 Hz, 3H, NCHC*H*$_3$), 1.37 (d, *J* = 6.7 Hz, 3H, NCHC*H*$_3$).

^{13}C NMR (101 MHz, $CDCl_3$) δ 192.48 (d, $^3J_{PC}$ = 7.3 Hz, 1C, *C*(O)), 186.42 (d, $^3J_{PC}$ = 5.0 Hz, 1C, *C*OPd), 155.82 – 101.53 (49C, Ar and *C*=C-OPd), 75.98 (d, $^3J_{PC}$ = 2.6 Hz, 1C, *C*NMe$_2$), 71.26 (d, $^3J_{PC}$ = 2.7 Hz, 1C, *C*NMe$_2$), 50.09 (s, 1C, N*C*H$_3$), 46.64 (s, 2C, N*C*H$_3$), 46.16 – 45.20 (m, 1C, C*C*HCH$_2$), 41.30 (s, 1C, N*C*H$_3$), 35.80 (d, $^1J_{PC}$ = 15.8 Hz, 1C, CH$_2$*C*HPh), 28.18 (dd, $^2J_{PC}$ = 29.6, $^2J_{P'C}$ = 11.8 Hz, 1C, *C*H$_2$), 22.01 (s, 1C, NCH*C*H$_3$), 11.80 (s, 1C, NCH*C*H$_3$).

^{31}P{^{1}H} NMR (162 MHz, $CDCl_3$) δ 52.06 (s, 1P), 45.06 (s, 1P).

HRMS (+ESI) m/z calcd for $C_{62}H_{62}ClN_2O_2P_2{}^{106}Pd{}^{108}Pd$ $(M + H)^+$: 1177.2049; found: 1177.2041.

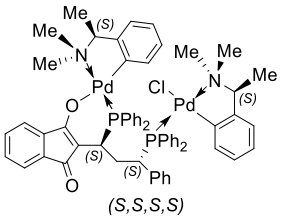

(S,S,S,S)

*Bimetallic Complex (S,S,S,S)-**16b**.*

Appearance: yellow solid, Yield=41% (after separation of the diastereomers), Mp. (dec.) = 185-186 °C, $[\alpha]_D^{20}$ = +53.1 (c 0.5, CH_2Cl_2)

^{1}H NMR (400 MHz, $CDCl_3$) δ 7.80 – 7.70 (m, 2H, Ar*H*), 7.50 – 7.38 (m, 2H, Ar*H*), 7.34 – 7.19 (m, 9H, Ar*H*), 7.18 – 7.09 (m, 5H, Ar*H*), 7.08 – 6.90 (m, 9H, Ar*H*), 6.88 – 6.73 (m, 4H, Ar*H*), 6.64 – 6.48 (m, 3H, Ar*H*), 6.41 (td, *J* = 7.5, 1.2 Hz, 1H, Ar*H*), 6.10 (t, *J* = 6.9 Hz, 1H, Ar*H*), 5.86 (t, *J* = 7.0 Hz, 1H, Ar*H*), 4.34 – 4.19 (m, 1H, C*H*), 3.63 – 3.49 (m, 2H, 2XC*H*), 2.95 – 2.83 (m, 1H, C*H*), 2.69 (s, 3H, NC*H*$_3$), 2.59 (s, 3H, NC*H*$_3$), 2.51 (d, *J* = 2.6 Hz, 3H, NC*H*$_3$), 2.48 – 2.43 (m, 1H, C*H*$_2$), 2.39 (d, *J* = 3.2 Hz, 3H, NC*H*$_3$), 2.22 – 2.09 (m, 1H, C*H*$_2$), 1.74 (d, *J* = 6.4 Hz, 3H, CHC*H*$_3$), 1.36 (d, *J* = 6.5 Hz, 3H, CHC*H*$_3$).

^{13}C NMR (101 MHz, $CDCl_3$) δ 192.62 (d, $^3J_{PC}$ = 6.7 Hz, 1C, *C*(O)), 186.04 (d, $^3J_{PC}$ = 4.8 Hz, 1C, *C*OPd), 157.82 – 101.82 (49C, Ar and *C*=C-OPd), 74.87 (s, 1C, *C*NMe_2), 65.77 (s, 1C, *C*NMe_2), 50.58 (s, 1C, NCH_3), 49.68 (s, 1C, NCH_3), 45.16 (s, 1C, NCH_3), 44.98 (s, 1C, NCH_3), 42.69 – 42.13 (m, 1C, C*C*HCH_2), 33.41 (d, $^1J_{PC}$ = 19.5 Hz, 1C, CH_2*C*HAr), 27.59 (dd, $^2J_{PC}$ = 29.9, $^2J_{P'C}$ = 10.5 Hz, 1C, *C*H_2), 25.32 (s, 1C, NCH*C*H_3), 18.96 (s, 1C, NCH*C*H_3).

^{31}P{^{1}H} NMR (162 MHz, $CDCl_3$) δ 52.41 (s, 1P), 46.26 (s, 1P).

HRMS (+ESI) m/z calcd for $C_{62}H_{62}N_2O_2P_2{}^{104}Pd^{110}Pd$ $(M + H - Cl)^+$: 1142.2379; found: 1142.2384.

1.2.6 Synthesis of monometallic complex:

General Procedure D: Compound **18** was synthesized according to the following procedure:

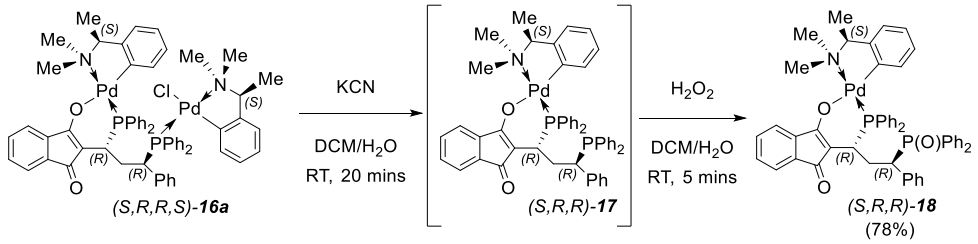

A nitrogen flushed 2-neck flask was charged with bimetallic complex *(S,R,R,S)*-**16a** (20 mg, 17 µmol, 1 equiv) in de-gassed DCM (2 mL) at room temperature, followed by the addition of KCN solution (50 mg dissolved in 1 mL de-gassed H_2O). The solution was stirred vigorously for 20 mins. The organic layer was separated and washed with de-gassed water until all the excess amount of KCN was removed. Then 0.1 mL hydrogen peroxide solution (30% H_2O_2 solution in water) was introduced into the flask and the mixture was stirred for 5 mins at room temperature. After completion of the reaction, the organic phase was separated, and the solvent was removed under reduced pressure. The crude mixture was purified on silica gel column chromatography using DCM/ ethyl acetate (80:20 to 20:80) eluent system. The monometallic complex was obtained as yellow solid in 78% yield.

Characterization data:

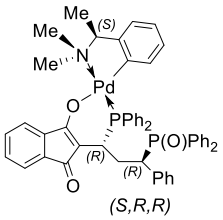

*Monometallic Complex (S,R,R)-**18**.*

Appearance: yellow solid, Yield=78%, Mp. (dec.) = 173-175 °C, $[\alpha]_D^{20}$ = -18.4 (c 1.0, CH_2Cl_2)

^{1}H NMR (400 MHz, $CDCl_3$) δ 7.87 – 7.74 (m, 2H, Ar*H*), 7.72 – 7.62 (m, 2H, Ar*H*), 7.43 – 7.26 (m, 11H, Ar*H*), 7.26 – 6.98 (m, 14H, Ar*H*), 6.97 – 6.87 (m, 2H, Ar*H*), 6.63 – 6.47 (m, 2H, Ar*H*), 4.51 (q, *J* = 7.0 Hz, 1H, C*H*), 3.52 (dd, *J* = 10.7, 6.9 Hz, 1H, C*H*), 3.22 (dd, *J* = 17.1, 11.1 Hz, 1H, C*H*), 2.68 (d, *J* = 2.9 Hz, 3H, NC*H*$_3$), 2.51 (s, 3H, NC*H*$_3$), 2.33 (dd, *J* = 22.8, 10.9 Hz, 1H, C*H*$_2$), 2.22 – 2.11 (m, 1H, C*H*$_2$), 1.48 (d, *J* = 6.6 Hz, 3H, CHC*H*$_3$).

^{13}C NMR (101 MHz, $CDCl_3$) δ 193.25 (d, *J* = 7.3 Hz, 1C, *C*(O)), 186.92 (d, *J* = 4.9 Hz, 1C, *C*OPd), 153.93 – 102.54 (43C, Ar and *C*=C-OPd), 71.59 (d, $^3J_{PC}$ = 2.8 Hz, 1C, *C*NMe$_2$), 46.44 (d, $^3J_{PC}$ = 2.3 Hz, 1C, NCH$_3$), 44.56 (dd, $^1J_{PC}$ = 68.0, $^3J_{PC}$ = 13.9 Hz, 1C, C*C*HCH$_2$), 41.40 (d, $^3J_{PC}$ = 2.6 Hz, 1C, NCH$_3$), 32.68 (d, $^1J_{PC}$ = 15.4 Hz, 1C, CH$_2$*C*HAr), 28.53 (dd, $^2J_{PC}$ = 29.3, $^2J_{P'C}$ = 14.9 Hz, 1C, *C*H$_2$), 11.68 (s, 1C, NCH*C*H$_3$).

^{31}P{^{1}H} NMR (162 MHz, $CDCl_3$) δ 52.96 (s), 34.17 (s).

HRMS (+ESI) m/z calcd for $C_{52}H_{48}NO_3P_2Pd$ $(M + H)^+$: 902.2144; found: 902.2132.

2. Mechanistic investigations

Plausible mechanism:

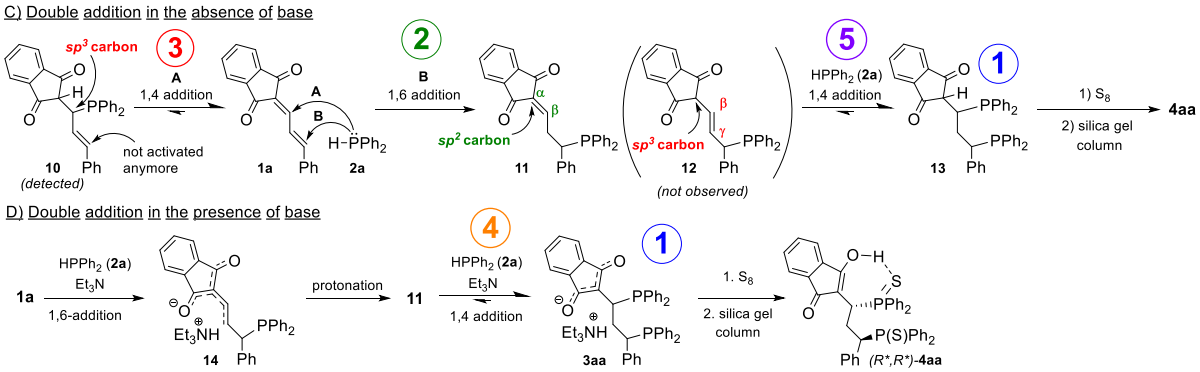

Experimental Investigations:

2.1: Confirmation of the formation of diketo diphosphine (**13**) and diphosphine salt (**3aa**). (1)

2.2: Investigation on the consecutive manner of the reaction and determination of the order of the double-addition. (2)

2.3: Investigation on 1,4-retro-Michael addition of compound **10**. (3)

2.4: Investigation on 1,4-retro-Michael addition of compound **3aa**. (4)

2.5: Investigation on 1,4-retro-Michael addition of compound **13**. (5)

2.1) Confirmation of the formation of diketo product (13) and phosphine salt (3aa). (1)

The product of the double hydrophosphination is the enol diphosphine sulphide (**4aa**), which can be obtained after the purification step on silica gel. This is the final compound, regardless if the reaction is set up in the presence or the absence of base. However, during our mechanistic investigations, we have realized that the intermediate compounds have various structures during the reactions. In many cases, these intermediates could not be isolated because either these compounds are air-sensitive or they undergo further structural transformations during purification (e.g. tautomerization). Despite the challenge, our aim was to gain as much information about these structures as possible.

2.1.1 Structural confirmation of **13**: Upon completion of the base-free dihydrophosphination, the observed diphosphine in the crude mixture turned out to be the diketo diphosphine (**13**). Later this compound was converted to **4aa** by sulfurization and tautomerization on silica gel.

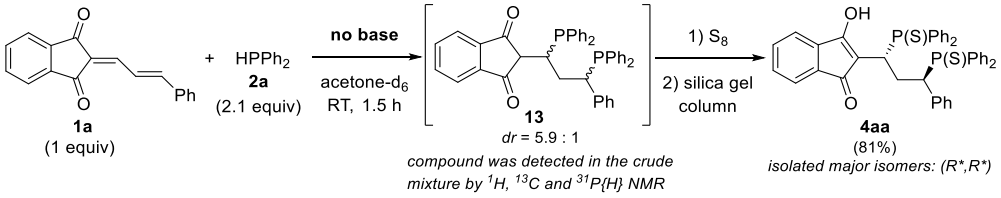

Procedure:

For details, see "1.2.2 Optimization of diphosphine synthesis via double hydrophosphination" chapter in this document.

After the reaction was completed, NMR sample was prepared under nitrogen and the crude reaction mixture was measured by ^{1}H, ^{13}C and $^{31}P\{H\}$ NMR (Figures S3 to S5).

Figure S3 Crude ^{1}H NMR spectrum of the base-free dihydrophosphination before sulfurization in acetone-d_6.

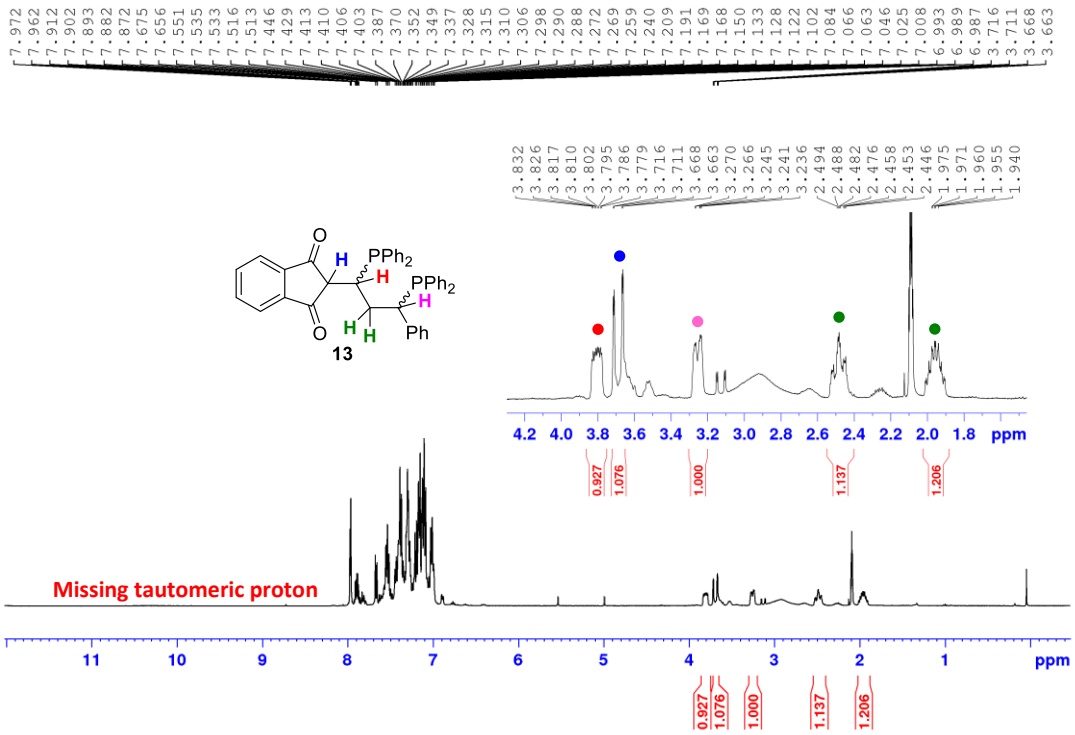

Figure S4 Crude ^{13}C NMR spectrum of the base-free dihydrophosphination before sulfurization in acetone-d_6.

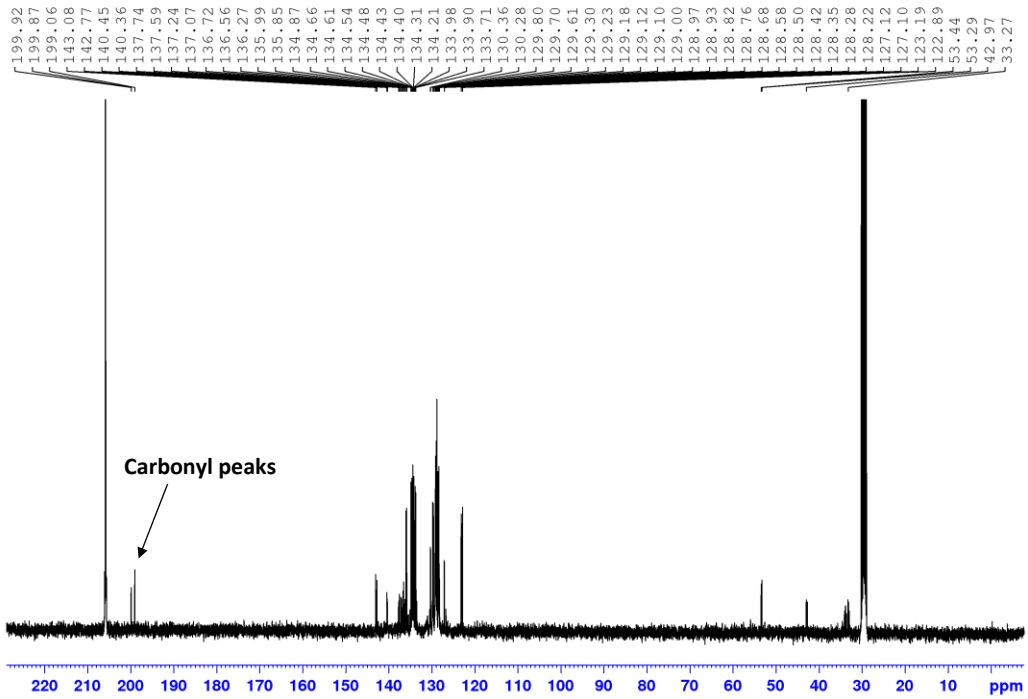

Figure S5 Crude $^{31}P\{^1H\}$ NMR spectrum of the base-free dihydrophosphination before sulfurization in acetone-d_6.

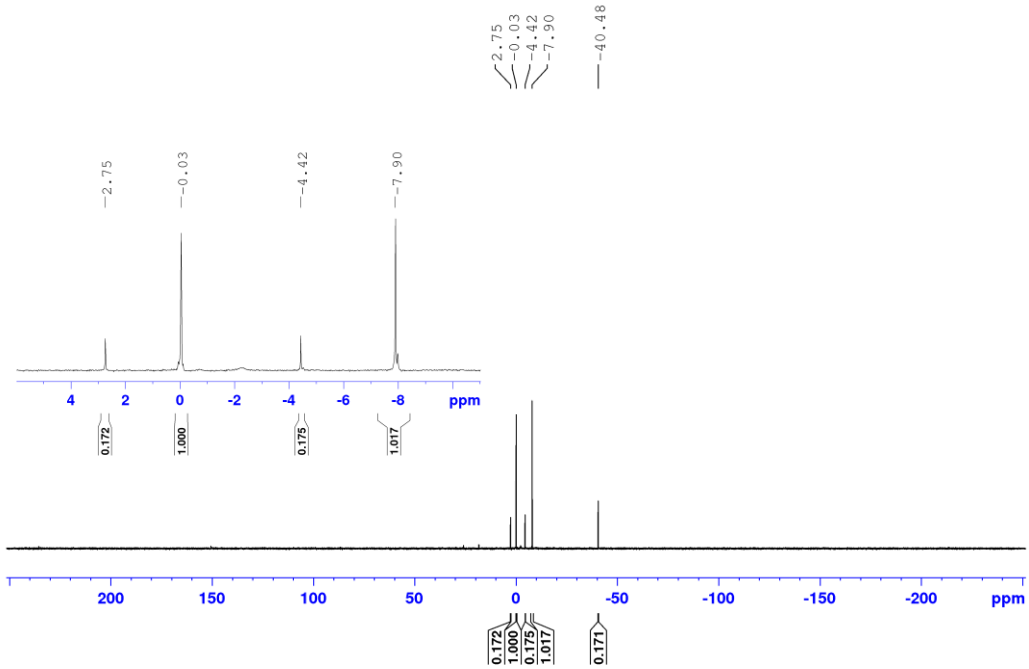

Analysing the crude NMR spectra, a few statements were made, which supports our proposed structure of the diketo diphosphine (**13**):

a) The $^{31}P\{^{1}H\}$ NMR clearly shows the formation of a diphosphine product. The diastereomeric ratio is relatively low, which can be explained by the base-free (=non-optimized) conditions.
b) The tautomeric proton (=proton of the enol OH) is missing from the ^{1}H NMR spectrum.
c) In the ^{13}C NMR, the two carbonyl peaks can be clearly detected. This statement together with b) are strong evidences that the diphosphine is presented in its diketo form in the crude mixture.
d) At the aliphatic region of the ^{1}H NMR, five protons could be detected with the same integration ratios. These protons belong to the five aliphatic protons, presented in the structure of **13**.

*Remark: The undefined aliphatic protons might belong to the minor diastereomer of **13**. The aromatic protons were not identified in the crude ^{1}H NMR spectrum, due to the presence of the minor diastereomers and the excess diphenylphosphine.*

Characterization data of **13**:

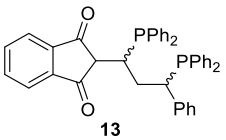

13

^{1}H NMR (400 MHz, Acetone-d_6, mixture) δ 8.01 – 6.95 (m, 29H, Ar*H*), 3.85 – 3.75 (m, 1H, C(O)CHC*H*P), 3.69 (dd, J_{HH} = 2.1, J_{PH} = 19.2 Hz, 1H, C(O)C*H*CHP), 3.31 – 3.20 (m, 1H, PC*H*Ph), 2.56 – 2.40 (m, 1H, CH_2), 2.03 – 1.88 (m, 1H, CH_2).

^{13}C NMR (101 MHz, Acetone-d_6, mixture) δ 199.89 (d, *J* = 5.0 Hz, 1C, *C*(O)), 199.06 (s, 1C, *C*(O)), 145.09 – 121.05 (36C, Ar), 53.36 (d, $^{2}J_{PC}$ = 14.0 Hz, (C(O))$_2$*C*H), 42.85 (dd, *J* = 13.9, 10.6 Hz, 1C), 33.85 (dd, *J* = 24.1, 21.2 Hz, 1C), 33.14 (dd, *J* = 16.2, 10.8 Hz, 1C).

$^{31}P\{^{1}H\}$ NMR (162 MHz, Acetone-d_6, mixture) δ -0.03 (s, 1P), -7.90 (s, 1P).

2.1.2 Structural confirmation of **3aa**: If the dihydrophosphination is set up in the presence of triethylamine, the observed product in the crude mixture is **3aa**, which can be converted to **4aa** after sulfurization and silica gel purification. For structural confirmation, the dihydrophosphination was set up in deuterated acetone and multi-nuclei NMR spectra were recorded.

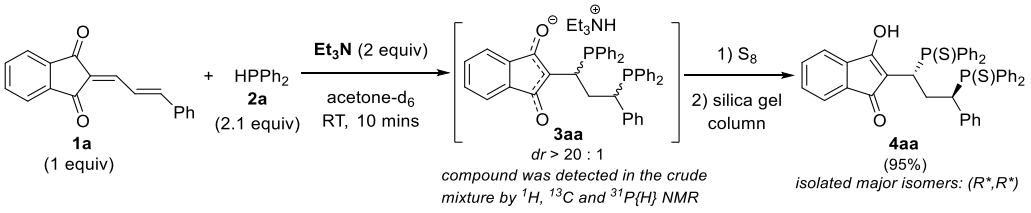

Procedure:

For details, see "1.2.2 Optimization of diphosphine synthesis via double hydrophosphination" chapter in this document.

After the first step of the reaction was completed, NMR sample was prepared under nitrogen and the crude reaction mixture was measured by ^{1}H, ^{13}C and $^{31}P\{H\}$ NMR (Figures S6 to S9).

Figure S6 Crude ^{1}H NMR spectrum of the dihydrophosphination with triethylamine before sulfurization in acetone-d_6.

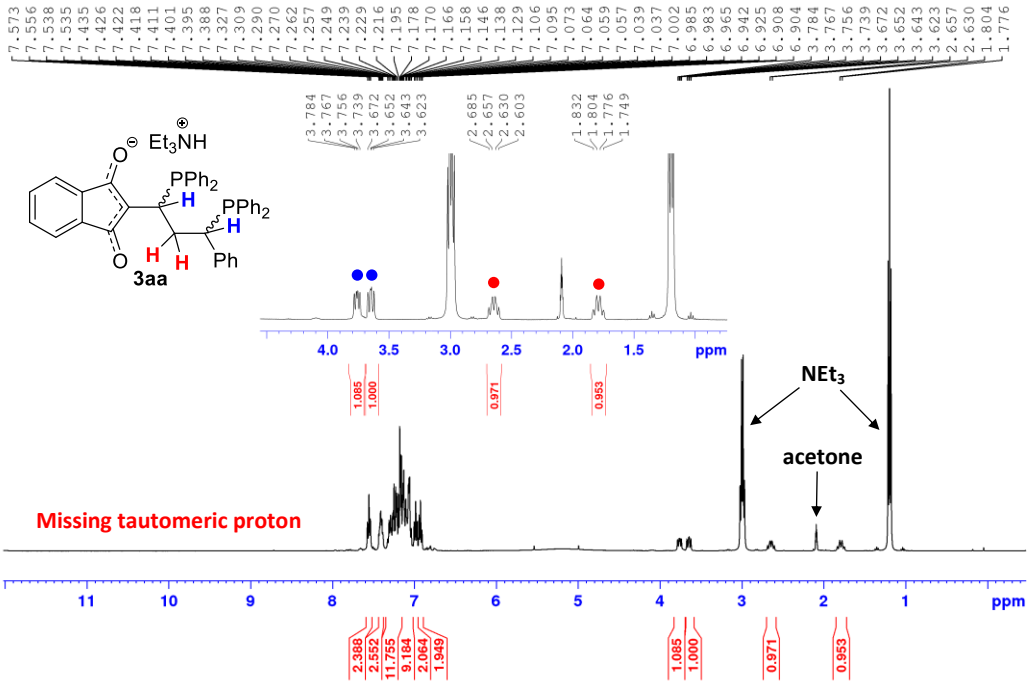

Figure S7 Crude ^{13}C NMR spectrum of the dihydrophosphination with triethylamine before sulfurization in acetone-d_6.

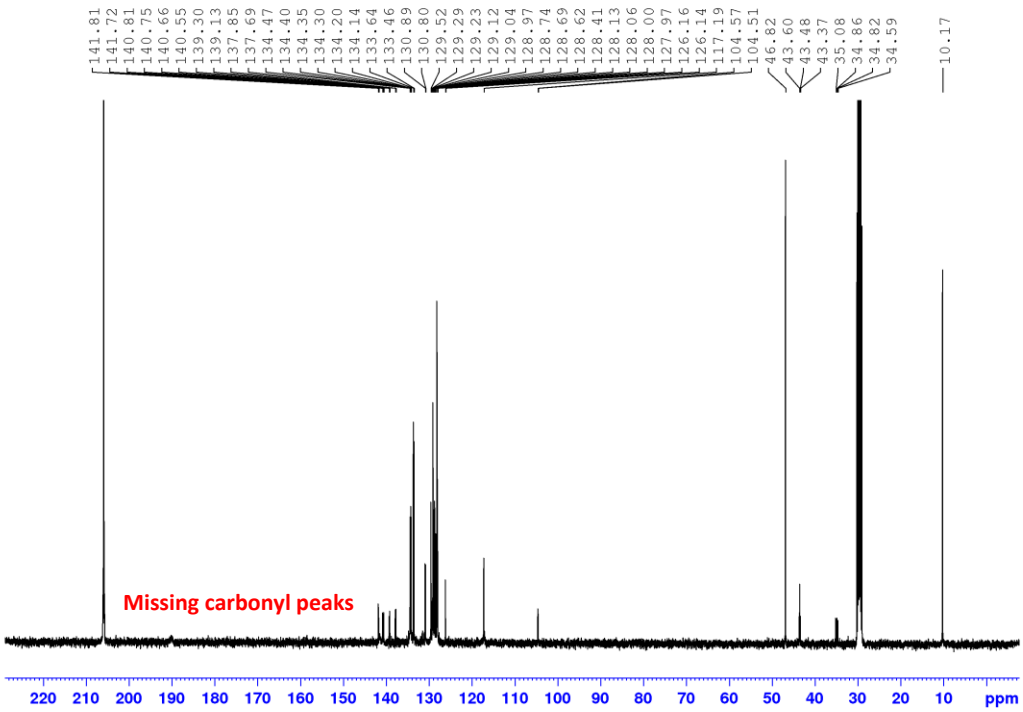

Figure S8 Crude ^{13}C NMR spectrum of the dihydrophosphination with triethylamine before sulfurization in CD_2Cl_2.

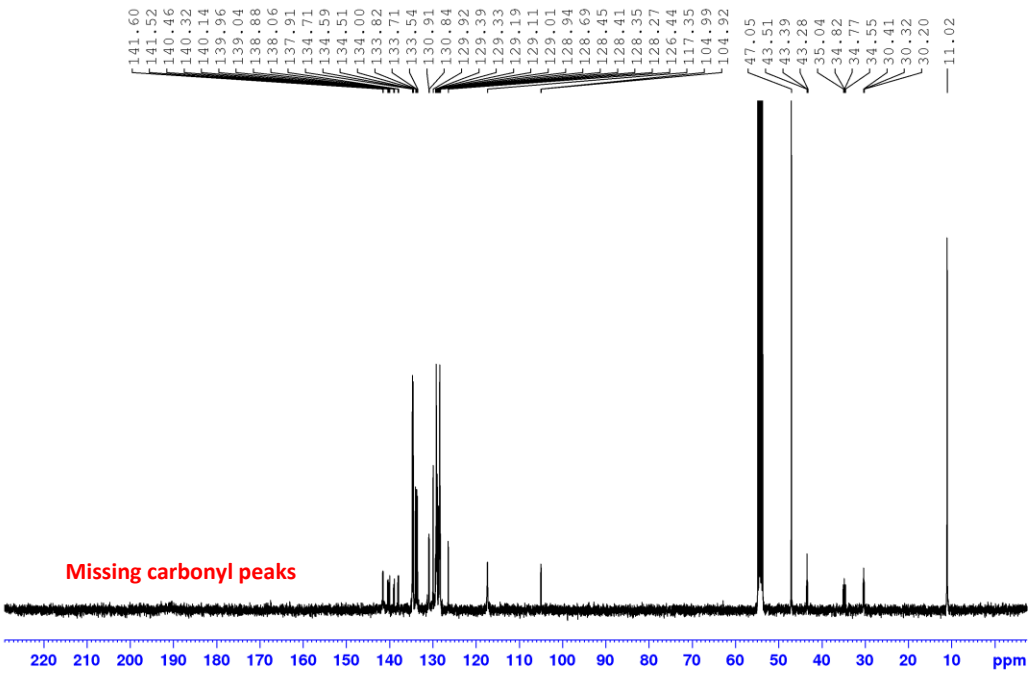

Figure S9 Crude $^{31}P\{^1H\}$ NMR spectrum of the dihydrophosphination with triethylamine before sulfurization in acetone-d_6.

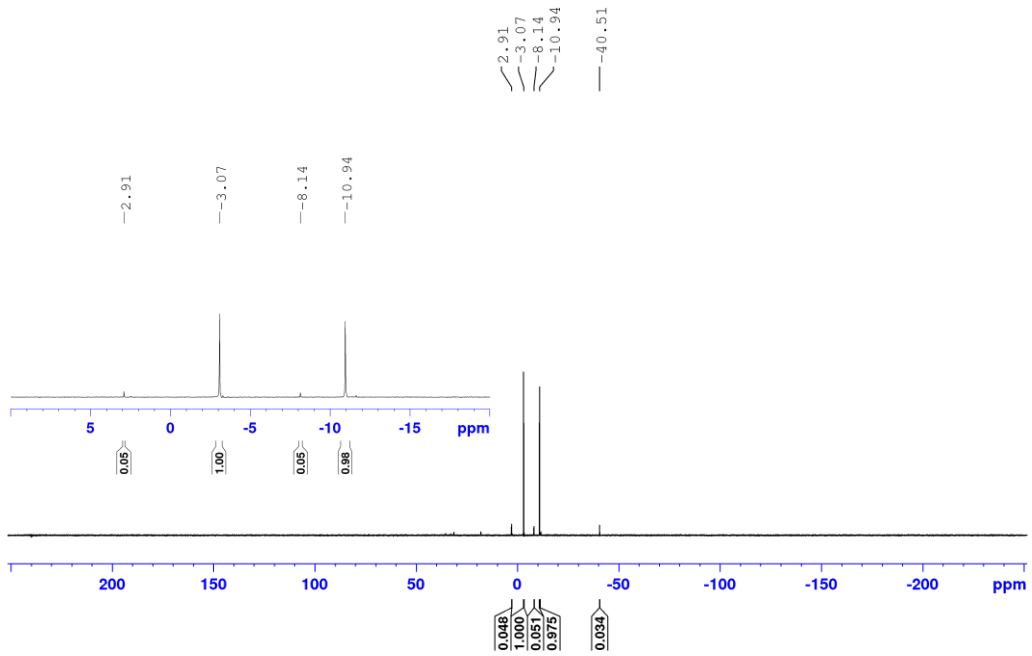

Analysing the crude NMR spectra, a few statements were made, which supports our proposed structure of the diphosphine salt (**3aa**):

a) The $^{31}P\{^{1}H\}$ NMR clearly shows the formation of a diphosphine product. The diastereomeric ratio is excellent, due to the optimized conditions.
b) The tautomeric proton (=proton of the enol OH) is missing from the ^{1}H NMR spectrum.
c) In the ^{13}C NMR, the carbonyl peaks are missing, which evidence together with statement b) supports the anionic structure of the indandione moiety.
d) At the aliphatic region of the ^{1}H NMR, four protons can be detected with the same integration ratios. These protons belong to the four aliphatic protons, presented in the structure of **3aa**.

Characterization data of **3aa**:

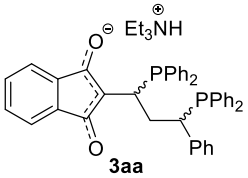

3aa

^{1}H NMR (400 MHz, Acetone-d_6, mixture) δ 7.59 – 7.53 (m, 2H, Ar*H*), 7.45 – 7.37 (m, 2H, 2H, Ar*H*), 7.35 – 7.15 (m, 12H, 2H, Ar*H*), 7.15 – 7.02 (m, 9H, 2H, Ar*H*), 7.01 – 6.95 (m, 2H, 2H, Ar*H*), 6.95 – 6.90 (m, 2H, 2H, ArH), 3.76 (dd, J_{HH} = 10.9 Hz, J_{PH} = 7.0 Hz, 1H, C*H*), 3.65 (dd, J_{HH} = 10.9 Hz, J_{PH} = 8.0 Hz, 1H, C*H*), 2.64 (q, *J* = 10.9 Hz, 1H, C$\underline{H}_2$), 1.79 (q, *J* = 10.9 Hz, 1H, CH_2).

^{13}C NMR (101 MHz, Acetone-d_6, mixture) δ 143.32 – 101.93 (39C, Ar), 46.82 (s, 3C, N$\underline{C}H_2CH_3$), 43.49 (t, *J* = 11.6 Hz, 1C), 34.84 (dd, *J* = 27.3, 22.3 Hz, 1C), 30.99 – 28.57 (m, 1C, overlapping peak), 10.17 (s, 3C, $NCH_2\underline{C}H_3$).

^{13}C NMR (101 MHz, CD_2Cl_2, mixture) δ 142.85 – 103.11 (39C, Ar), 47.05 (s, 3C, N$\underline{C}H_2CH_3$), 43.39 (t, *J* = 11.5 Hz, 1C), 34.80 (dd, *J* = 27.1, 22.9 Hz, 1C), 30.73 – 29.96 (m, 1C), 11.02 (s, 3C, $NCH_2\underline{C}H_3$).

$^{31}P\{1H\}$ NMR (162 MHz, Acetone-d_6, mixture) δ -3.07 (s, 1P), -10.94 (s, 1P).

2.1.3 Converting **13** to **3aa**:

After careful examination of the NMR spectra, we proposed the possible structures of **13** and **3aa**. If we look at these two compounds carefully, we can see that the only difference between them is the presence of a highly acidic proton at the α-position. We expected, that triethylamine should be strong enough for the removal of this proton. In order to get final confirmation to our hypothesis and to the proposed structures, we tried out if we could convert **13** to **3aa**, by treating the crude mixture of **13** with excess amount of triethylamine.

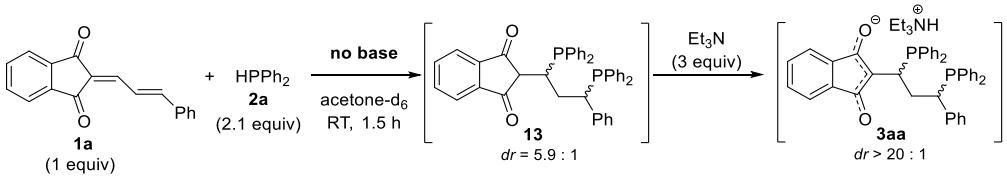

Procedure:

For details, see "1.2.2 Optimization of diphosphine synthesis via double hydrophosphination" chapter in this document. After the first step was completed, excess amount of triethylamine (3 equiv) was introduced to the reaction mixture. NMR sample was prepared and multi nuclei NMR spectra were recorded (Figures S10 to S14).

Identity of the presented spectra in the comparison:

A: Spectrum of the starting material (**1a**) measured in acetone-d_6.

B: Spectrum of the crude mixture for base-free dihydrophosphination measured in acetone-d_6 (for details see 2.1.1).

C: Spectrum of the crude mixture after introducing 3 equivavlent amount of triethylamine to the mixture of the base-free dihydrophosphination measured in acetone-d_6 (second step of 2.1.3).

D: Spectrum of the crude mixture for dihydrophosphination in the presence of triethylamine measured in acetone-d_6 (for details see 2.1.2).

Figure S10 Comparison of the ^{1}H NMR spectra of **1a**, 2.1.1, 2.1.2 and 2.1.3 measured in acetone-d_6.

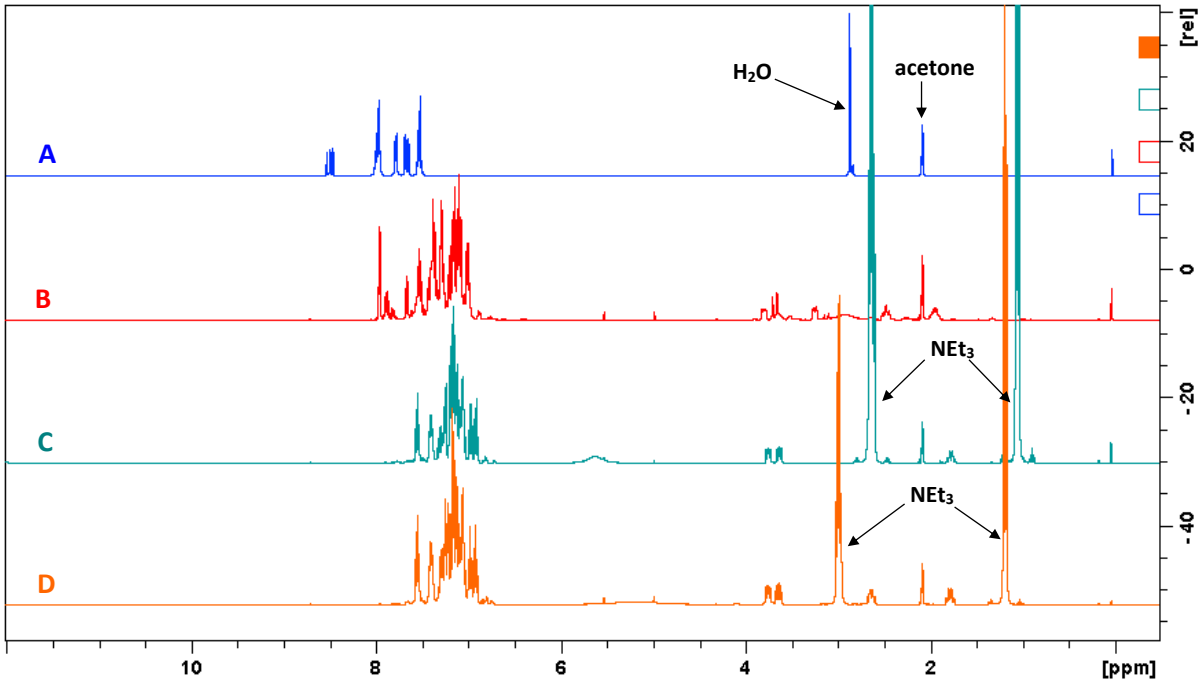

Figure S11 Comparison of the ^{1}H NMR spectra of **1a**, 2.1.1, 2.1.2 and 2.1.3 measured in acetone-d_6.

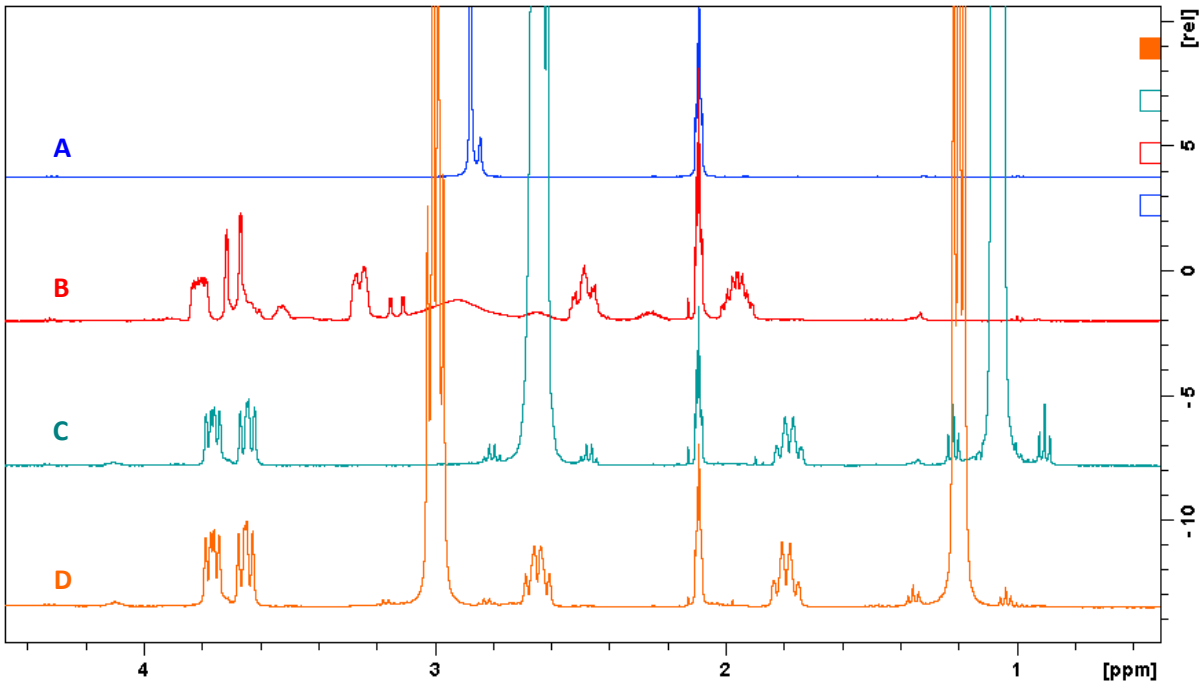

Figure S12 Comparison of the ^{1}H NMR spectra of **1a**, 2.1.1, 2.1.2 and 2.1.3 measured in acetone-d_6.

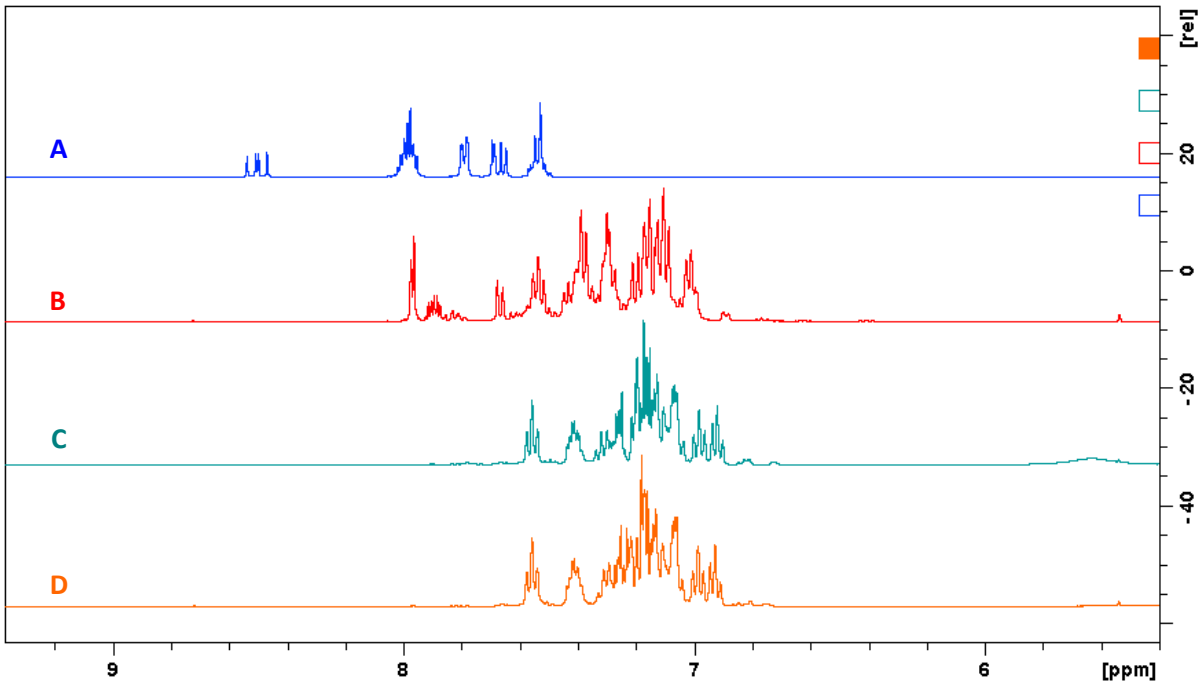

Figure S13 Comparison of the ^{13}C NMR spectra of **1a**, 2.1.1, 2.1.2 and 2.1.3 measured in acetone-d_6.

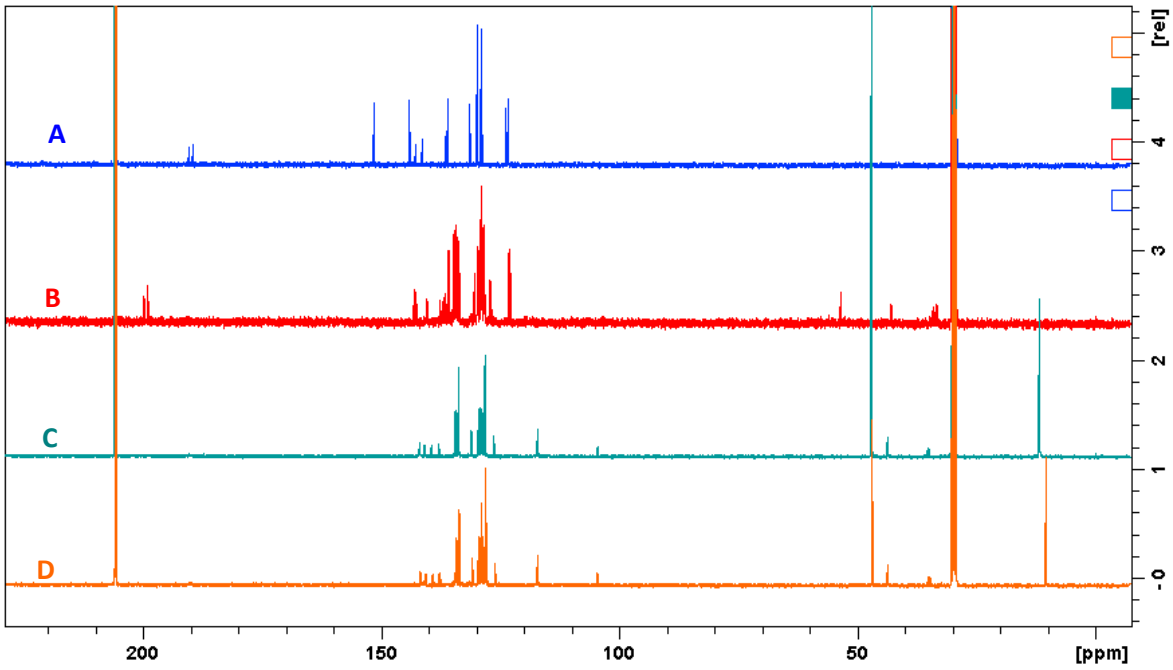

Figure S14 Comparison of the $^{31}P\{^1H\}$ NMR spectra of **1a**, 2.1.1, 2.1.2 and 2.1.3 measured in acetone-d_6.

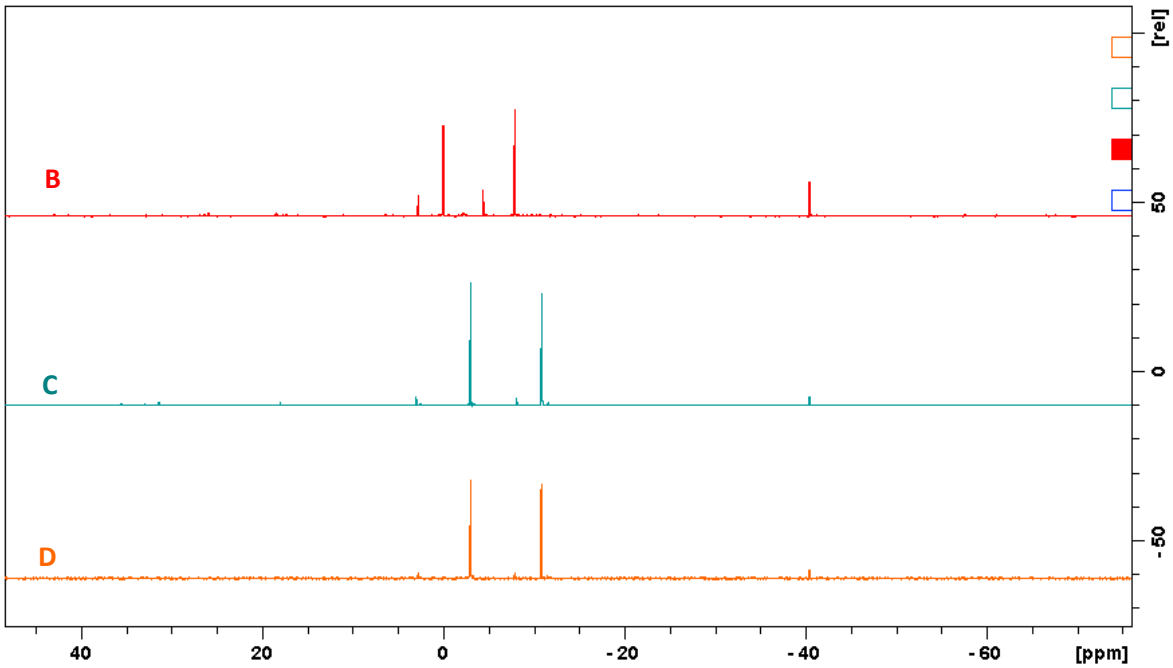

The chemical peaks of the compounds obtained in experiment C and D are identical in both the ^1H, ^{13}C and $^{31}P\{^1H\}$ NMR spectra. Based on these comparisons, it can be clearly seen, that compound **13** can be easily converted to **3aa**, by introducing excess amount of triethylamine to the crude mixture. These findings support the proposed structures of **13** and **3aa**. An interesting result was the observed changes in the diastereoselectivity, by the addition of the triethylamine. This was a hint for a possible retro-Michael addition at the 1,4-position, which altered the chirality at the α position. For more details see 2.3, 2.4 and 2.5 chapters.

2.2) Investigation on the consecutive manner of the reaction and determination of the order of the double-addition. (2)

To gain more information of the possible intermediates, the reaction was set up in a 1 to 1 ratio calculated to **1a** and **2a** starting materials. In this setup, the diphenylphosphine was presented as a limiting reagent, thus we hoped that an intermediate monophosphine can be detected and/or isolated. After a short preliminary screening, it was found that the consumption of **2a** is too fast to detect any intermediates in the presence of base, hence all amount of **2a** was converted to **3aa**. In order to slow down the transformation, the reaction was set up in the absence of base. Unfortunately, the formation of the diphosphines could not be avoided even using base-free conditions and furthermore, the absence of base resulted lower diastereoselectivity. After 24 hours reaction time in toluene, the crude mixture was sulfurized, transferred to $CDCl_3$, followed by ^1H and $^{31}P\{^1H\}$ NMR measurements of the crude mixture (Figures S15 and S17 to S20). In the $^{31}P\{^1H\}$ crude NMR spectrum, the formation of a monophosphine intermediate (**6**) was clearly seen. After isolation of it by column chromatography, the structure of compound **6** was confirmed.

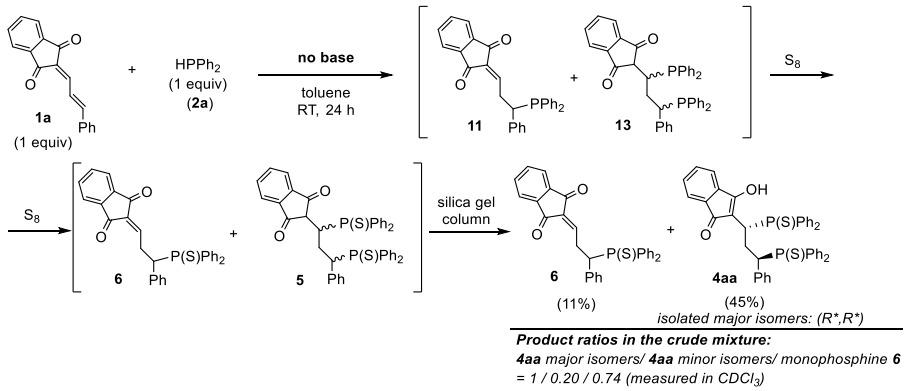

Procedure:

A nitrogen flushed 2-neck flask was charged with **1a** (19.7 mg, 75.7 µmol, 1 equiv) and **2a** (14.1 mg, 75.7 µmol, 1 equiv) in de-gassed toluene (2.5 mL) at room temperature. The setup was stirred for 24 hous, followed by the addition of sulphur (37.9 µmol, 0.5 equiv of S_8). Then the mixture was stirred for another 5 mins. Evaporation of the solvent under reduced pressure provided the crude mixture, which was purified by silica gel column chromatography, eluted with *n*-hexane/EtOAc (97:3 to 70:30) eluent system. In order to increase the formation of the 1,6-monophosphine product in the hydrophosphination reaction, a short optimization was performed:

Table S2 Optimization of the monophosphine formation.

Entry	Base	Solvent	T [°C]	t	Major isomers [ratio][a]	Minor isomers [ratio][a]	Monophosphine [ratio][a]	Unreacted $HPPh_2$ [ratio][a]
1	Et_3N (5)	acetone	RT	5 mins	1	0.05	0	-
2	-	acetone	-40	7 h	1	0.33	0	1.36
3	-	acetone	RT	1 h	1	0.14	0.23	-
4	-	toluene	RT	24 h	1	0.20	0.74	-
5	-	$CHCl_3$	RT	4.5 h	1	0.31	0.51	-
6	-	DCM	RT	4.5 h	1	0.31	-	0.52
7	-	Hexanes	RT	24 h	-	-	-	-
8	-	MeOH	RT	4 h	1	0.27	0.55	-

[a]The ratios of the corresponding compounds produced in the reaction were determined by the $^{31}P\{^1H\}$ NMR spectrum of the crude mixture.

Figure S15 Crude $^{31}P\{^{1}H\}$ NMR spectrum of the optimized monophosphine formation (Table S2, Entry 4), before silica gel purification measured in $CDCl_3$.

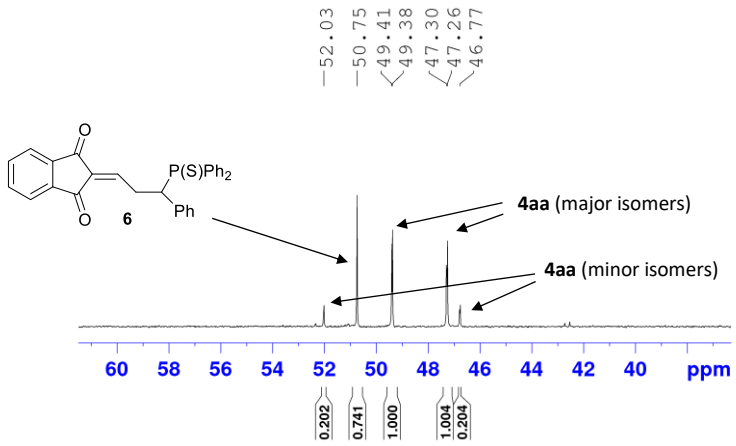

*Remark: based on the ^{1}H ($CDCl_3$) spectrum of the crude mixture (Figure S17 to S19), the produced diphosphines were found to be the major and minor isomers of **4aa** instead of the expected diketo phosphine (**13**). This can be explained, as during the solvent exchange of the crude mixture (toluene to $CDCl_3$), the diketo diphosphines (**13**) underwent tautomerization.*

Based on the integration values, presented in the $^{31}P\{^{1}H\}$ NMR crude spectrum, the monophosphine was generated in 23.6% conversion. However, the polarity of the monophosphine (**6**) was found to be significantly similar to that of **4aa** (major and minor isomers). Because of this reason, the effectiveness of the column separation was quite modest. Due to significant overlapping, the pure monophosphine (**6**) was obtained in only 11% isolated yield.

To determine the structure of the isolated monophosphine, we analysed the ^{1}H NMR spectrum of the compound and compared the result with the possible monophosphine structures proposed by us:

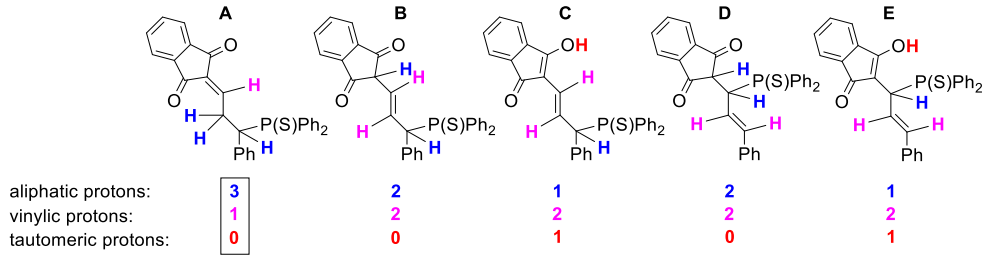

In the ^{1}H NMR spectrum, we have clearly determined 3 protons at the aliphatic region (Figure S16). Comparing this finding with the possible structures, only the structure of compound A has the same pattern that we observed. The tautomeric proton is missing from our spectrum, hence compound C and E can be clearly excluded. Moreover, the position of the vinylic proton is expected to be located at a relatively higher ppm value, due to the highly electron-withdrawing indandione moiety nearby. This was also confirmed in the recorded spectrum, as we observed, the vinylic proton was overlapping with the aromatic protons.

Figure S16 The ^{1}H spectrum of the isolated monophosphine (**6**).

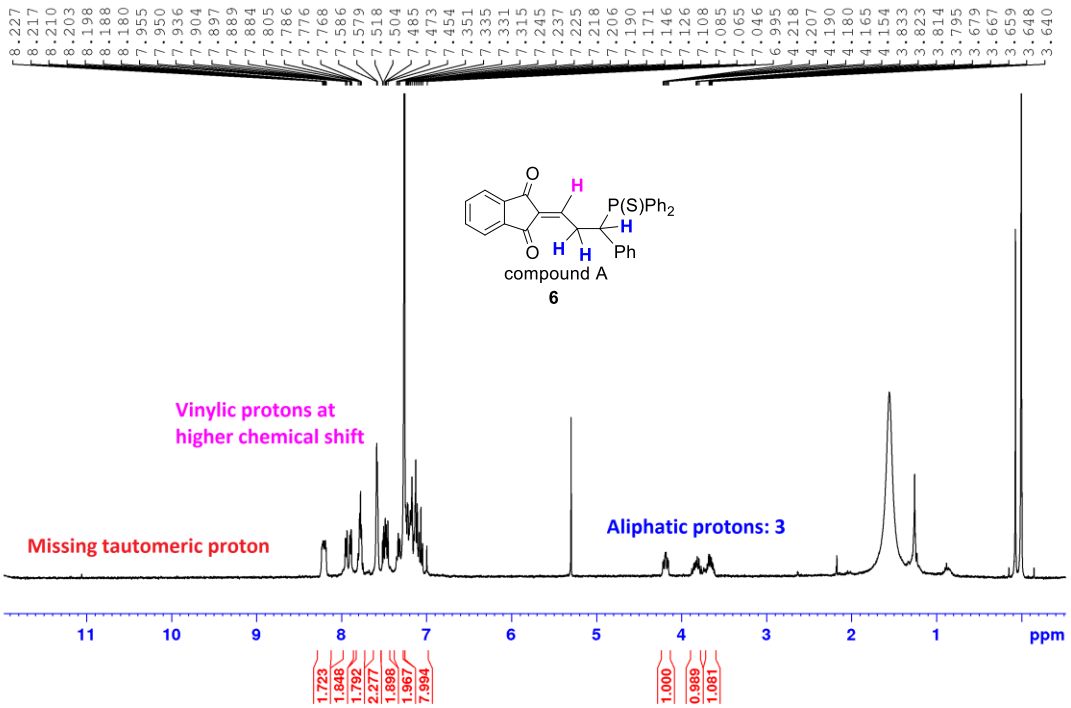

Characterization data:

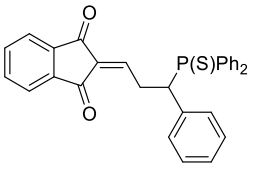

*2-(3-(diphenylphosphorothioyl)-3-phenylpropylidene)-1H-indene-1,3(2H)-dione (**6**).*

Appearance: white solid, Yield=11%.

^{1}H NMR (400 MHz, $CDCl_3$) δ 8.27 – 8.14 (m, 2H, Ar*H*), 8.00 – 7.85 (m, 2H, Ar*H*), 7.82 – 7.72 (m, 2H, Ar*H*), 7.65 – 7.54 (m, 2H, Ar*H*), 7.52 – 7.43 (m, 2H, Ar*H*), 7.37 – 7.30 (m, 2H, Ar*H*), 7.26 – 6.97 (m, 8H, Ar*H* and C=C*H*), 4.18 (td, *J* = 10.6, 4.3 Hz, 1H, CH_2CHPh), 3.88 – 3.59 (m, 2H, CH_2).

^{13}C NMR (101 MHz, $CDCl_3$) δ 190.07 (s, 1C, *C*(O)), 188.58 (s, 1C, *C*(O)), 152.41 – 122.63 (26C, Ar and C=C), 47.07 (d, $^{1}J_{PC}$ = 49.4 Hz, 1C, CH_2CHPh), 28.78 (d, $^{2}J_{PC}$ = 3.0 Hz, 1C, CH_2).

$^{31}P\{^{1}H\}$ NMR (162 MHz, $CDCl_3$) δ 50.72 (s, 1P).

HRMS (+ESI) m/z calcd for $C_{30}H_{24}O_2PS$ $(M + H)^+$: 479.1235; found: 479.1230.

In order to fully rule out the formation of other possible monophosphine compounds (compound B to E), herein we present a comparison between the ^{1}H and $^{31}P\{^{1}H\}$ NMR spectra of the isolated compounds and that of the crude mixture. All the presented spectra were measured in $CDCl_3$:

Figure S17 Comparison of ^{1}H spectra of the isolated compounds and the crude mixture.

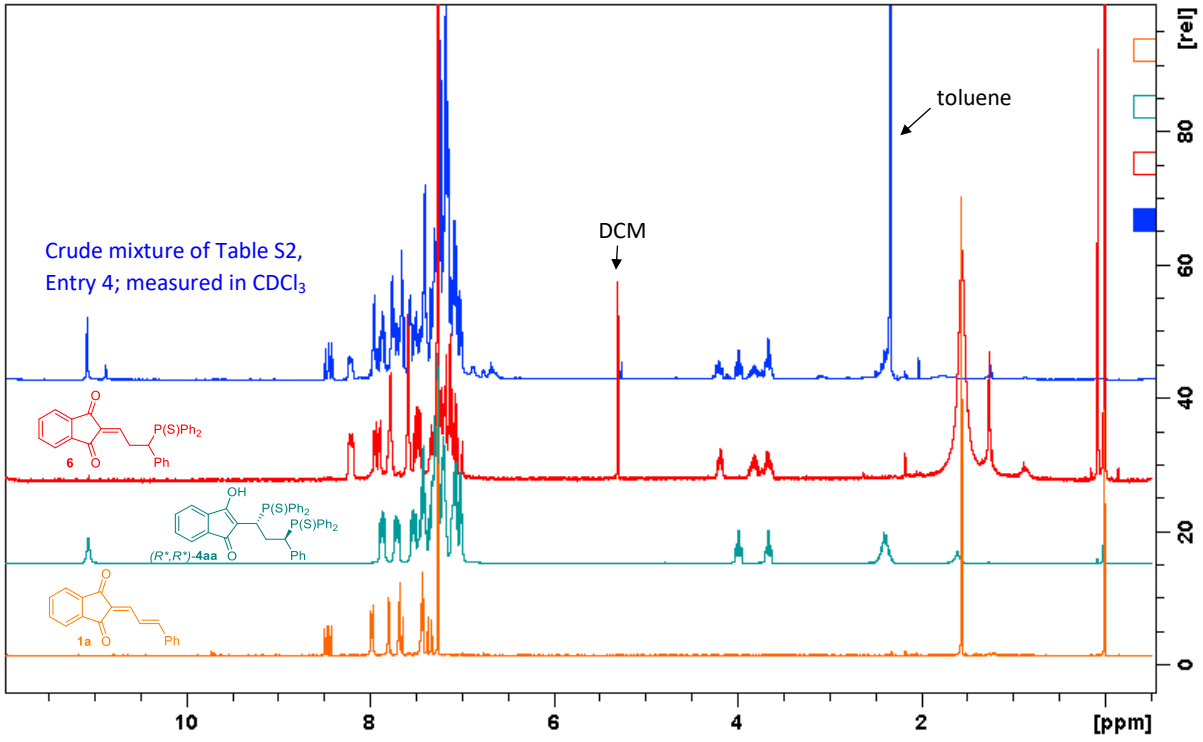

Figure S18 Comparison of ^{1}H spectra of the isolated compounds and the crude mixture.

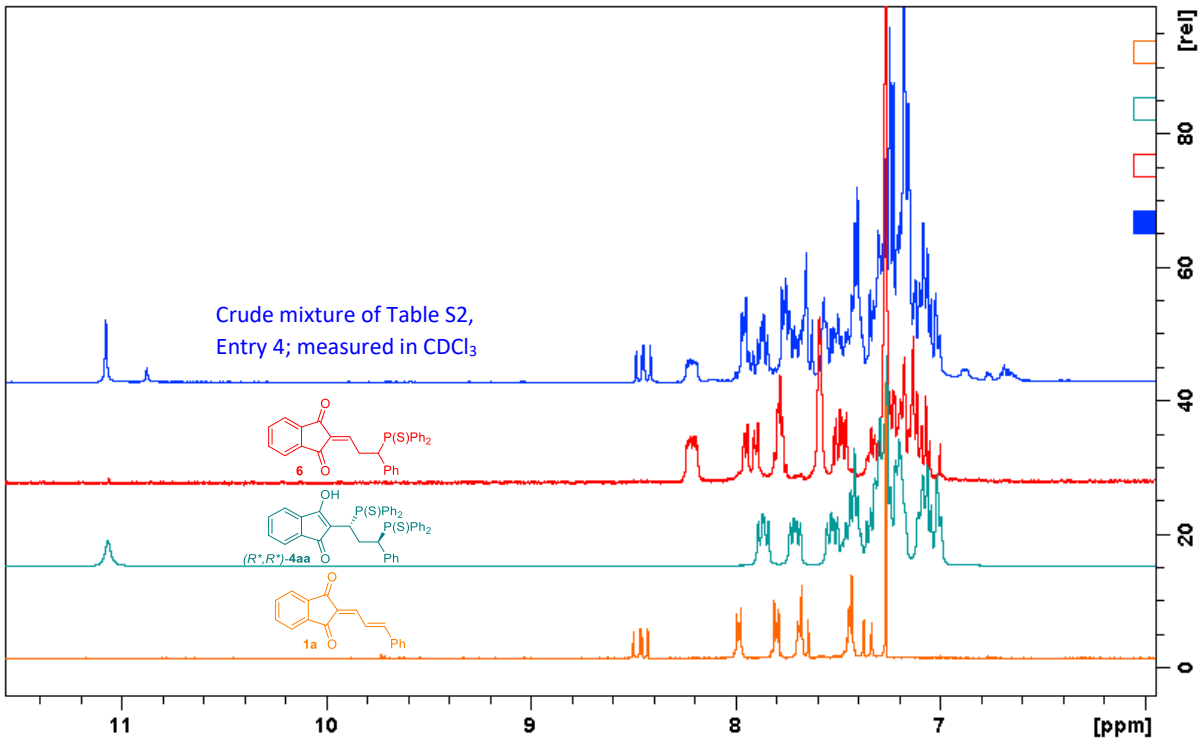

Figure S19 Comparison of ^{1}H spectra of the isolated compounds and the crude mixture.

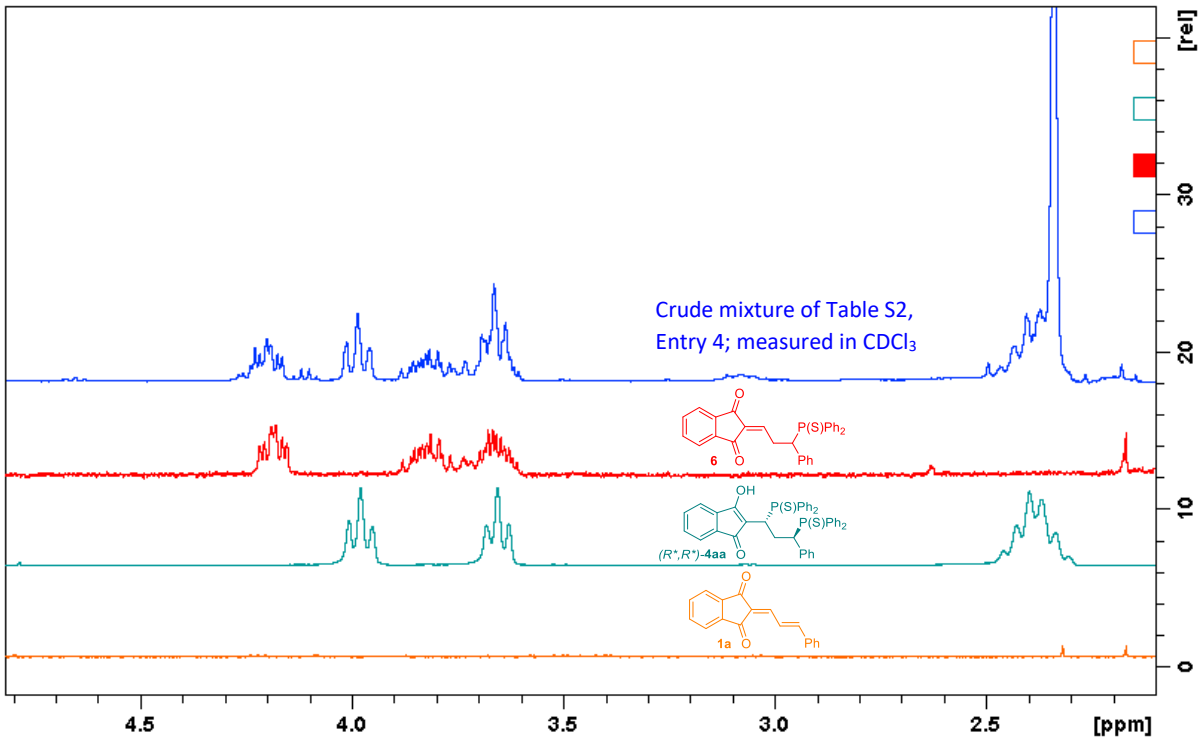

Figure S20 Comparison of $^{31}P\{^{1}H\}$ spectra of the isolated compounds and the crude mixture.

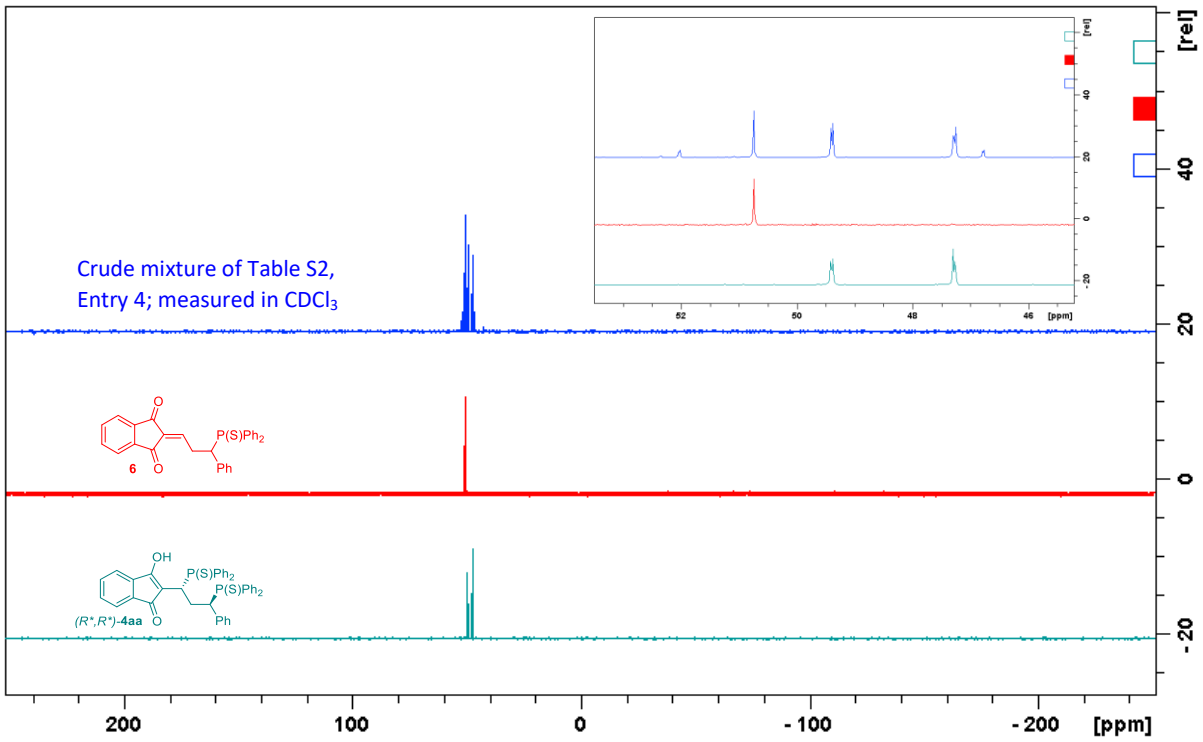

From this comparison, it can clearly seen that the crude mixture contains one monophosphine intermediate (**6**), the formation of any other proposed monophosphine (compound B to E) was not observed.

2.3) Investigation on 1,4-retro-Michael addition of compound 10. ③

In order to gain more information of the possible retro-addition, the double hydrophosphination was set up in the absence of base in deuterated acetone at room temperature and the reaction was monitored by ^{1}H and $^{31}P\{^{1}H\}$ NMR measurements.

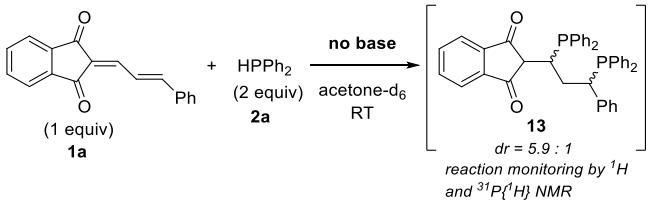

Procedure:

A nitrogen flushed 2-neck flask was charged with **1a** (19.7 mg, 75.7 µmol, 1 equiv) in deuterated acetone (2.5 mL) at room temperature, followed by the addition of **2a** (28.2 mg, 151.4 µmol, 2.0 equiv). NMR sample was prepared under nitrogen and the reaction was monitored by ^{1}H and $^{31}P\{^{1}H\}$ NMR measurements (Figures S21 to S27).

By analysing the $^{31}P\{^{1}H\}$ NMR spectra, it can be seen that in the first 30 minutes of the reaction, a monophosphine intermediate was produced; however, as the starting materials were consumed in the transformation, the compound was slowly disappearing. At the aliphatic and the vinylic region of the ^{1}H NMR spectrum, four protons can be clearly identified (two aliphatic- and two vinylic protons). Herein we present all the proposed structures of the possible 1,4- and 1,6-adducts:

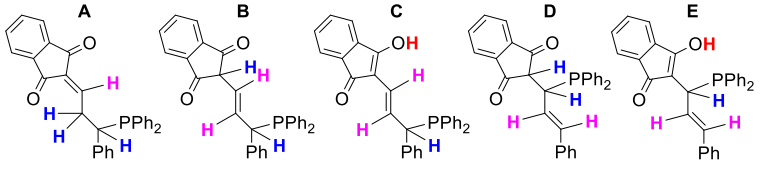

	A	B	C	D	E
aliphatic protons:	3	2	1	2	1
vinylic protons:	1	2	2	2	2
tautomeric protons:	0	0	1	0	1

Among these structures, only **B** and **D** have the same pattern that we observed in the ^{1}H NMR spectrum. In order to determine if we have the 1,4- or the 1,6-adduct, we compared the coupling patterns of the detected protons in the ^{1}H spectra and compared them with other spectra of 1,4- and 1,6-adducts from the literature. Based on our comparison, the observed intermediate is more likely compound **D**, which is strongly supported by the coupling pattern of the vinylic protons:

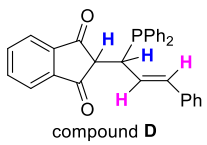
compound **D**

^{1}H NMR (400 MHz, Acetone-d_6) δ 8.05 – 6.94 (19 ArH), **6.39** (**dd**, J_{HH} = 15.8, J_{PH} = 3.0 Hz, 1H, CH=C*H*Ph), **6.16** (**ddd**, J_{HH} = 15.8, 10.0, J_{PH} = 5.6 Hz, 1H, C*H*=CHPh), **4.17** (ddd, J_{HH} = 10.0, 2.7, J_{PH} = 4.9, 1H, PC*H*), **3.33** (dd, J_{HH} = 2.7 Hz, J_{PH} = 12.3, 1H, $(C(O))_2C\underline{H}$). $^{31}P\{^{1}H\}$ NMR (162 MHz, Acetone-d_6) δ -9.89 (s, 1P).

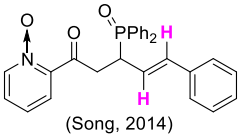
(Song, 2014)

^{1}H NMR (400 MHz, $CDCl_3$, lit.[6]): δ 8.14 (d, J_{HH} = 6.3 Hz, 1H), 7.94–7.89 (m, 2H), 7.79–7.74 (m, 2H), 7.53–7.41 (m, 7H), 7.33–7.29 (m, 1H), 7.24–7.13 (m, 6H), **6.30** (**dd**, J = 4.3, 15.9 Hz, 1H), **6.08** (**ddd**, J_{HH} = 14.9 and 9.1 Hz, J_{HP} = 5.7 Hz, 1H), **4.20–4.12** (m, 1H, PC*H*CH_2), **3.76** (ddd, J_{HH} = 17.7 and 10.0 Hz, J_{HP} = 8.0 Hz, 1H, PCHC*H*H), **3.61** (ddd, J_{HH} = 17.5 and 4.0 Hz, J_{HP} = 9.8 Hz, 1H, PCHCH*H*).

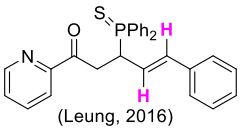

(Leung, 2016)

^{1}H NMR ($CDCl_3$, 400 MHz, lit.[7]): *δ* 8.66 (d, 1H, ^{3}J = 4.2 Hz, Ar), 8.13-8.07 (m, 2H, Ar), 7.93-7.89 (m, 3H, Ar), 7.78-7.74 (m, 1H, Ar), 7.50-7.38 (m, 7H, Ar), 7.21-7.12 (m, 5H, Ar), **6.29** (**dd**, 1H, ^{3}J = 15.9 Hz, $^{4}J_{HP}$= 4.6 Hz, PhC*H*=CH), **6.16** (**ddd**, 1H, ^{3}J = 15.8 Hz, $^{3}J_{HP}$ = 8.7 Hz, ^{3}J = 6.5 Hz, PhCH=C*H*), **4.50-4.42** (m, 1H, PC*H*CH_2), **4.11** (ddd, 1H, ^{2}J = 17.7 Hz, $^{3}J_{PH}$ = 10.5 Hz, ^{3}J =5.6 Hz, O=CCH_2), **3.35** (ddd, 1H, ^{2}J = 17.6 Hz, $^{3}J_{PH}$ = 12.5 Hz, ^{3}J = 2.3 Hz, O=CCH_2);

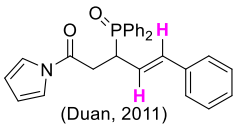

(Duan, 2011)

^{1}H NMR ($CDCl_3$, lit.[8]): δ 7.91 (t, J_{HH} = 8.8 Hz, 2H), 7.79 (dd, *J* = 10.0 and 8.0 Hz, 2H), 7.57-7.16 (m, 13H), **6.45** (**dd**, *J* = 15.6 and 3.6 Hz, 1H), 6.25 (s, 2H), **6.13** (**ddd**, *J* = 15.6, 8.8 and 2.4 Hz, 1H), **4.06** (q, *J* = 8.8 Hz, 1H), **3.41** (ddd, J_{HH} = 17.2 and 10.0 Hz, J_{HP} = 4.4 Hz, 1H), **3.21** (ddd, J_{HH} = 16.8 and 2.0 Hz, J_{HP} = 10.8 Hz, 1H).

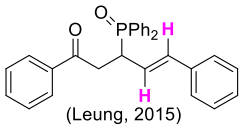

(Leung, 2015)

^{1}H NMR ($CDCl_3$, 300 MHz, lit.[9]): δ 7.95-7.88 (m, 4H, Ar), 7.85-7.78 (m, 2H, Ar), 7.55-7.38 (m, 9H, Ar), 7.23-7.12 (m, 5H, Ar), **6.41** (**dd**, 1H, $^{4}J_{HP}$ = 4.2 Hz, $^{3}J_{HH}$ = 15.9 Hz, PhC*H*=CH), **6.12** (**ddd**, 1H, $^{3}J_{HH}$ = 15.9 Hz, $^{3}J_{HP}$ = 9.1 Hz, $^{3}J_{HH}$ = 6.4 Hz, PhCH=C*H*), **4.22-4.11** (m, 1H, PC*H*), **3.67** (ddd, 1H, $^{2}J_{HH}$ = 17.7 Hz, $^{3}J_{HP}$ = 10.2 Hz, $^{3}J_{HH}$ = 4.5 Hz, PCHC*H*H), **3.29** (ddd, 1H, $^{2}J_{HH}$ = 17.7 Hz, $^{3}J_{HP}$ = 11.4 Hz, $^{3}J_{HH}$ = 2.4 Hz, PCHCH*H*)

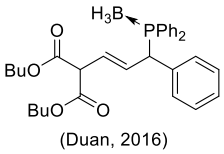

(Duan, 2016)

^{1}H NMR (400 MHz, $CDCl_3$, lit.[10]): δ = 7.90–7.80 (m, 2 H), 7.55–7.16 (m, 9 H), 7.14 (d, J_{HH} = 6.8 Hz, 2 H), 7.06 (d, J_{HH} = 6.4 Hz, 2 H), **6.11** (ddd, *J* = 14.8, 9.2, 6.8 Hz, 1 H), **5.73** (ddd, *J* = 14.8, 8.0, 2.8 Hz, 1 H), 4.44 (dd, *J* = 15.2, 8.8 Hz, 1 H), 3.77 (d, *J* = 8.4 Hz, 1 H), 1.37 (s, 9 H), 1.36 (s, 9 H), 0.88 (br,3 H).

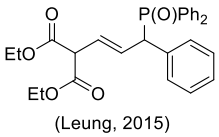

(Leung, 2015)

^{1}H NMR ($CDCl_3$, 400 MHz, lit.[11]): *δ* 7.86-7.81 (m, 2H, Ar), 7.53-7.47 (m, 5H, Ar), 7.37-7.35 (m, 2H, Ar), 7.30-7.24 (m, 3H, Ar), 7.20-7.17 (m, 3H, Ar), **6.14** (ddd, 1H, ^{3}J = 15.3 Hz, 9.28 Hz, 6.64 Hz, PhCHPC*H*=CH), **5.72** (ddd, 1H, ^{3}J = 15.4 Hz, 9.04 Hz, 3.80 Hz, PhCHPCH=C*H*), 4.29-4.24 (m, 1H, PhC*H*P), 4.10 (q, 2H, ^{3}J = 7.08 Hz, $CO_2C\underline{H_2}CH_3$), 4.03-3.99 (m, 2H, $CO_2C\underline{H_2}CH_3$), 3.93 (d, 1H, ^{3}J = 9.08 Hz, $(CO_2)_2C\underline{H}$), 1.19-1.14 (m, 6H, $CO_2CH_2C\underline{H_3}$);

Figure S21 The ^{1}H NMR spectra of base-free double hydrophosphination measured in acetone-d_6.

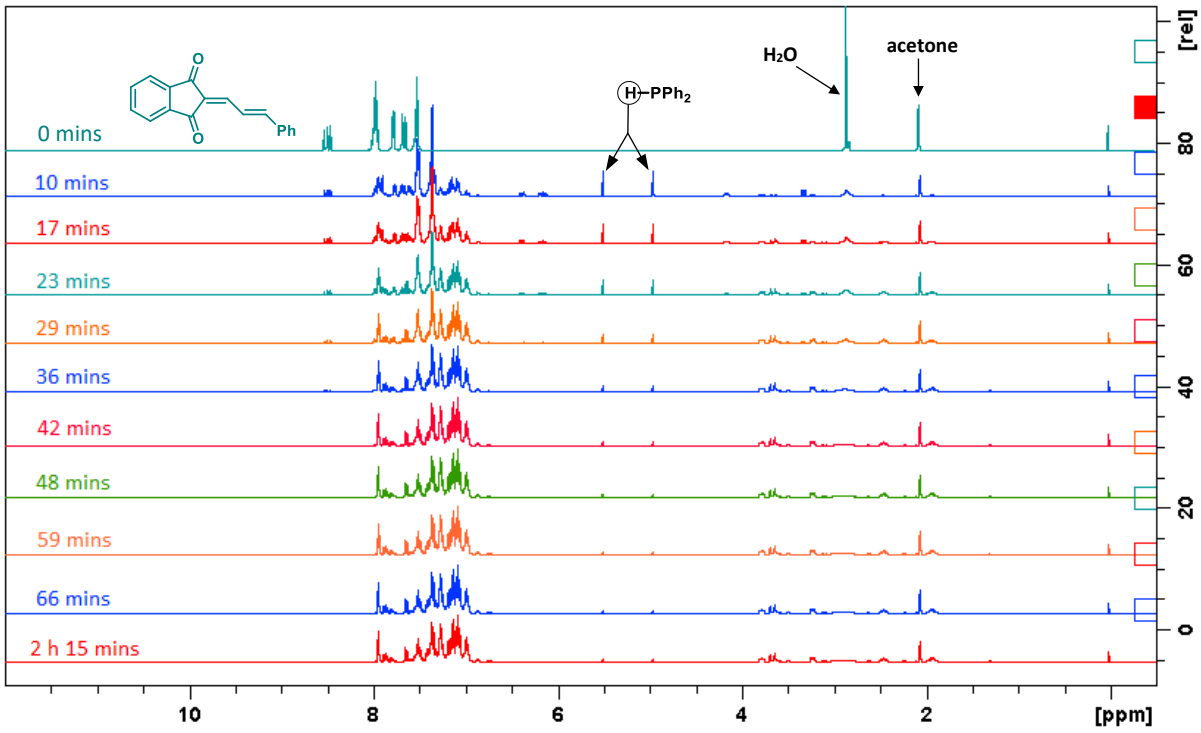

Figure S22 The ^{1}H NMR spectra of base-free double hydrophosphination measured in acetone-d_6.

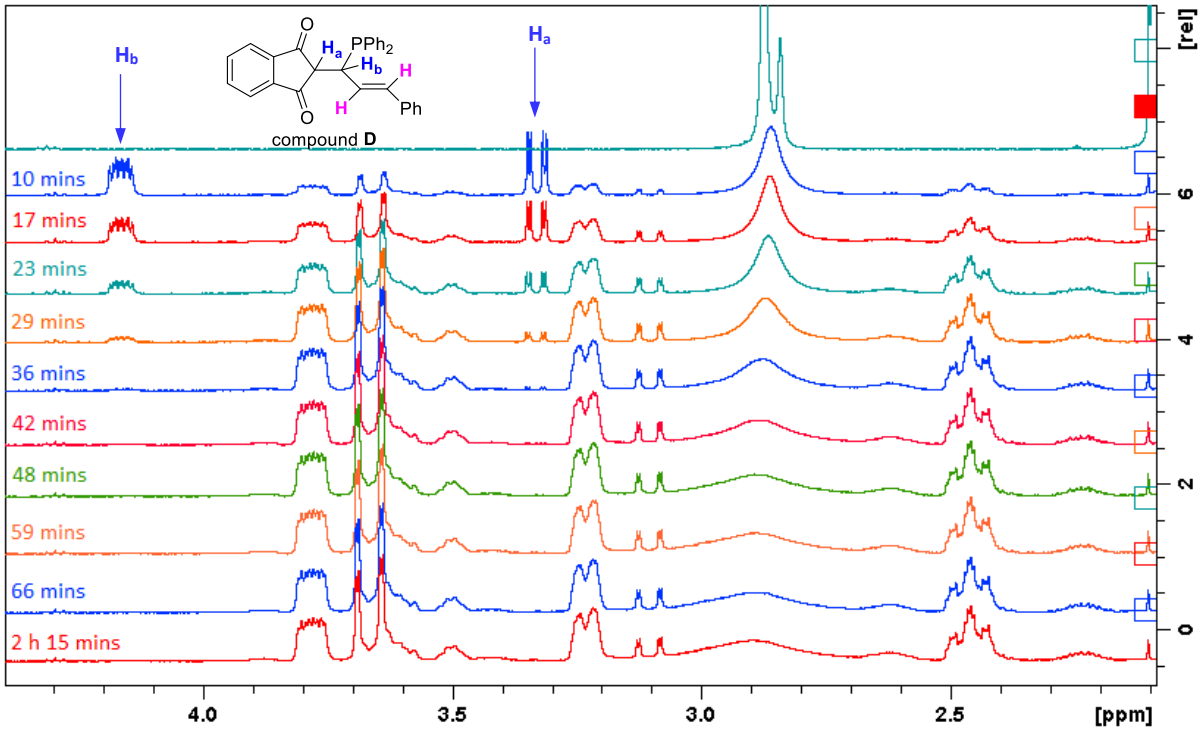

Figure S23 The ^{1}H NMR spectra of base-free double hydrophosphination measured in acetone-d_6.

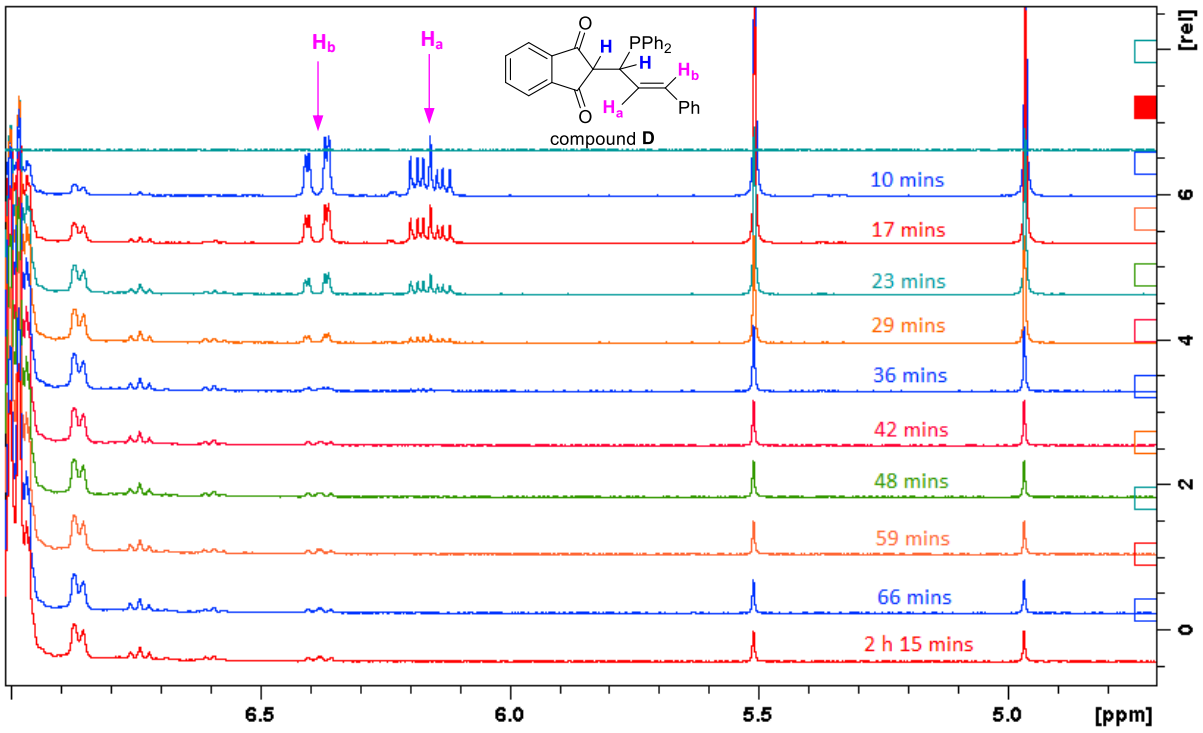

Figure S24 The ^{1}H NMR spectrum of double hydrophosphination in the absence of base after 10 mins reaction time measured in acetone-d_6.

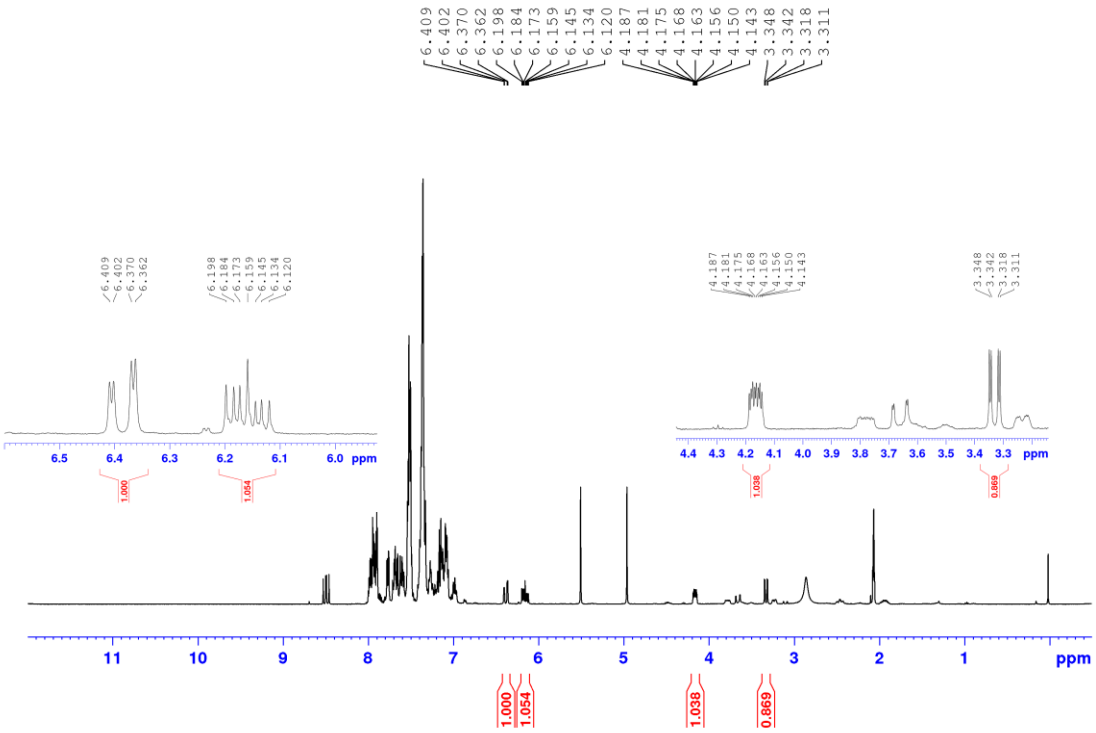

Figure S25 The $^{31}P\{^{1}H\}$ NMR spectra of base-free double hydrophosphination measured in acetone-d_6.

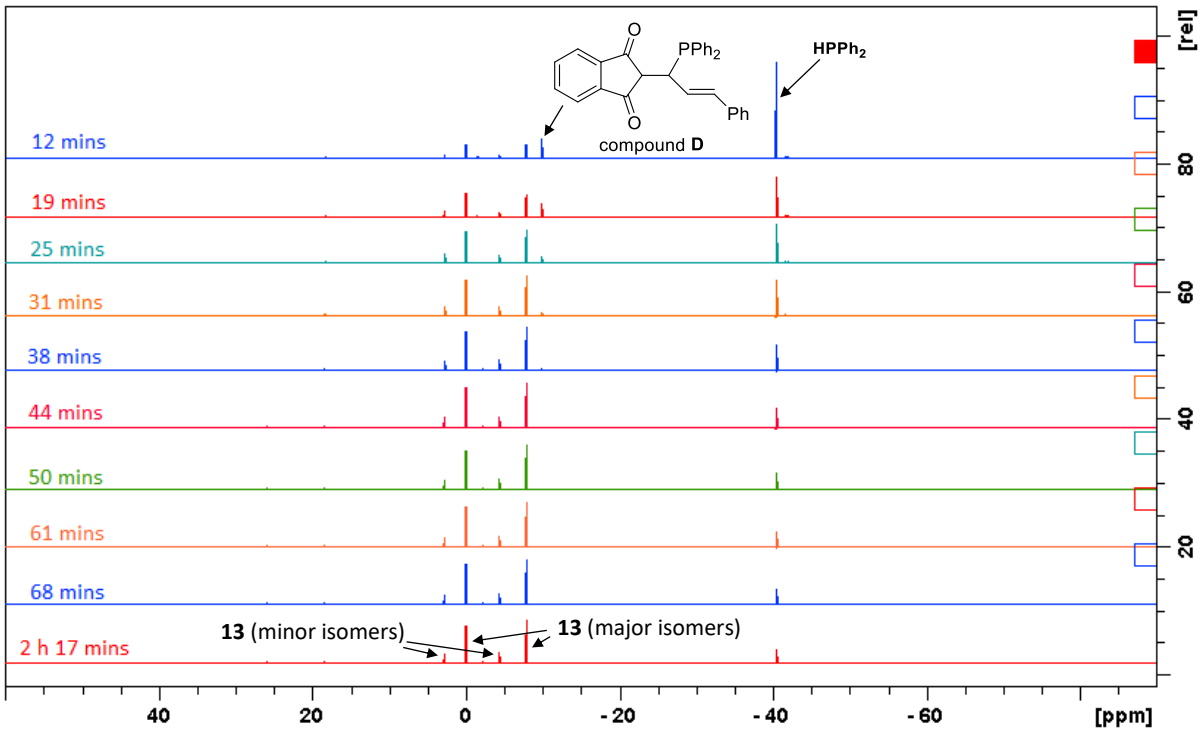

Figure S26 The $^{31}P\{^{1}H\}$ NMR spectra of base-free double hydrophosphination measured in acetone-d_6.

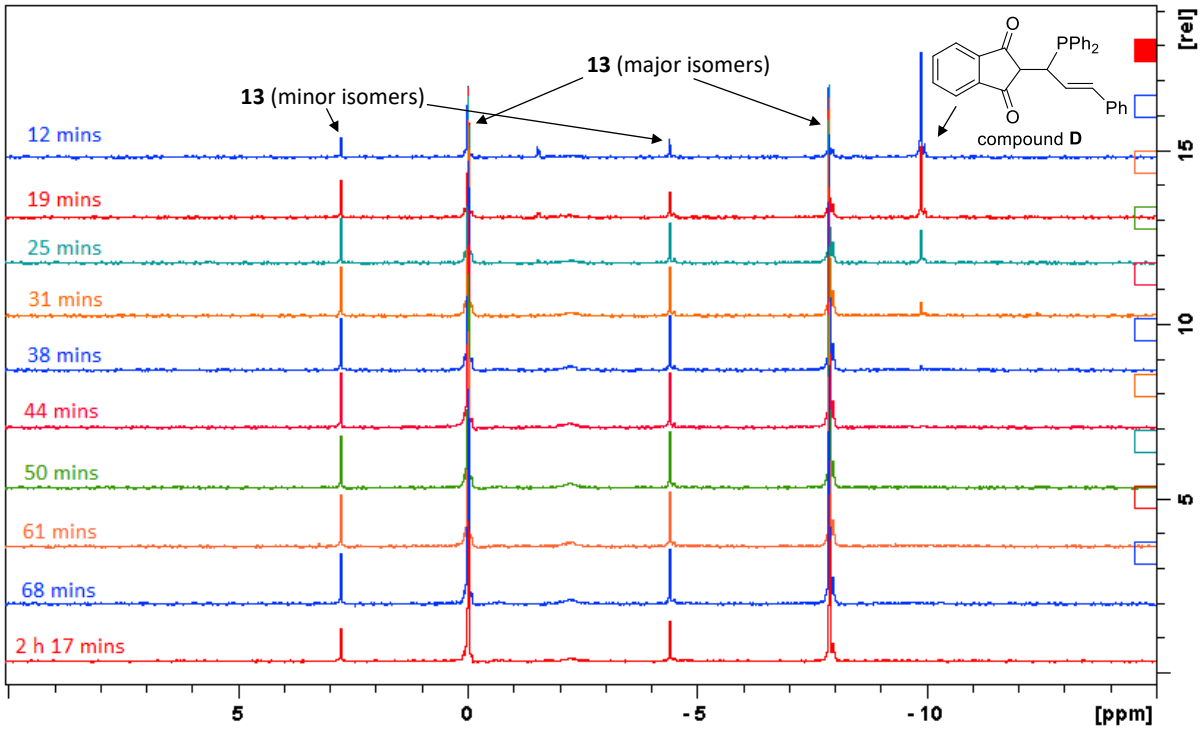

Figure S27 The $^{31}P\{^{1}H\}$ NMR spectrum of double hydrophosphination in the absence of base after 12 mins measured in acetone-d_6.

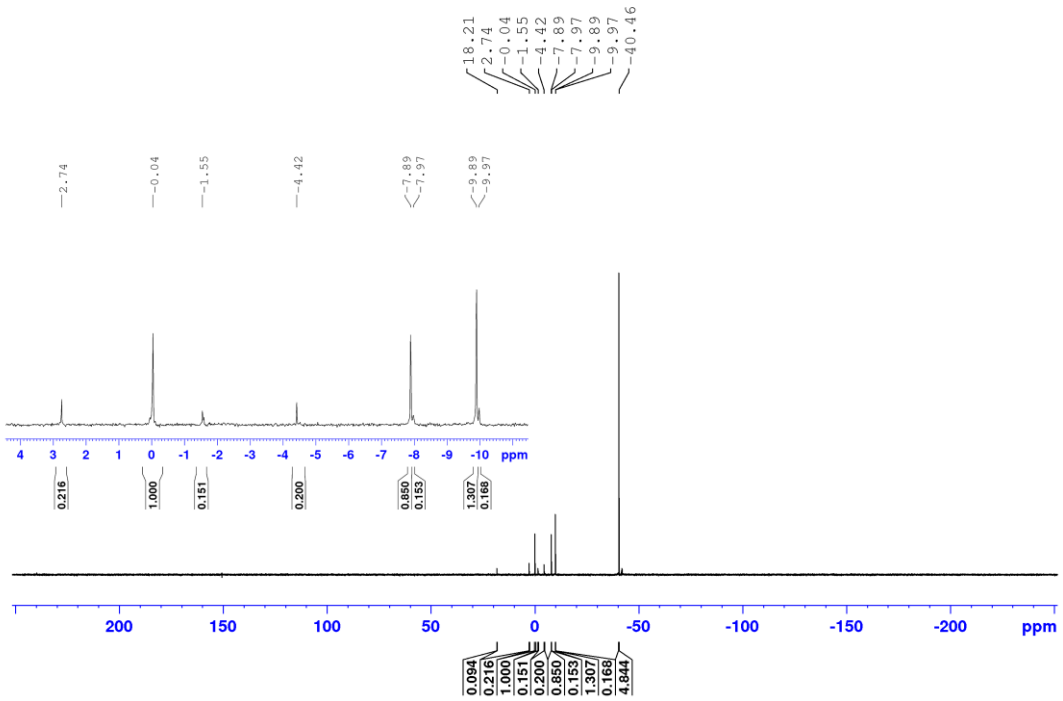

Due to the sp^3 carbons at the α- and β-positions in compound **D**, the remaining double bond (between γ and δ) is not activated anymore in this intermediate, thus the second 1,6-addition cannot occur on this compound. However, since this compound can be only detected in the beginning of the transformation, we suggest that the PPh_2 moiety of compound **D** (**10**) was eliminated from the molecule and the starting materials (**1a** and **2a**) are generated back via a 1,4-retro-Michael addition.

2.4) Investigation on 1,4-retro-Michael addition of compound 3aa. (4)

As a further test of the possible 1,4-retro-Michael addition, we have planned a two-steps synthesis, which may provide an even clearer evidence for our hypothesis. Firstly, the double hydrophosphination was set up under the optimized conditions to generate **3aa**. Then, in the second step, another primary phosphine (di-p-tolylphosphine, **2b**) was introduced to the reaction mixture. The reaction was monitored by $^{31}P\{^{1}H\}$ NMR (Figures S28 to S30).

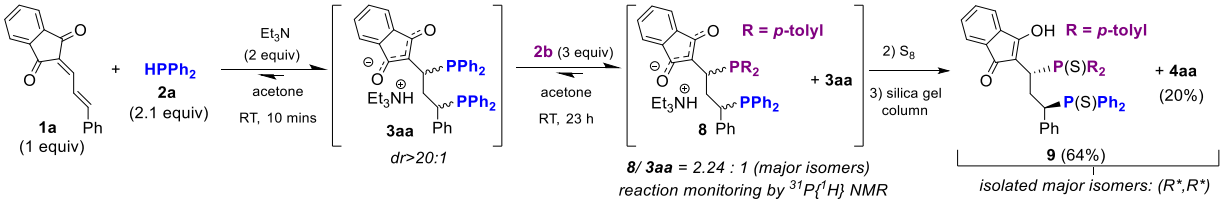

Procedure:

A nitrogen flushed 2-neck flask was charged with **1a** (19.7 mg, 75.7 µmol, 1 equiv) in degassed acetone (2.5 mL) at room temperature, followed by the addition of triethylamine (15.3 mg, 151.4 µmol, 2 equiv) and **2a** (29.6 mg, 159 µmol, 2.1 equiv). The reaction was stirred for 10 mins, then **2b** (48.6 mg, 151.4 µmol, 3 equiv) was introduced to the mixture. After stirring for 23 hours, the reaction was treated with sulphur (37.9 µmol, 0.5 equiv of S_8) and the crude mixture was purified on column chromatography by using *n*-hexanes/EtOAc (98:2 to 70:30) eluent systems. Compound **9** was isolated as yellow solids in 64% yield and **4aa**, yellow solids, in 20% yield.

*(Remark: the reaction was monitored by $^{31}P\{^{1}H\}$ NMR measurements after the addition of **2b** and before sulfurization.)*

After **3aa** was generated according to the above-mentioned procedure, we introduced 3 equivalent amount of **2b** and then the mixture was monitored $^{31}P\{^{1}H\}$ NMR measurements to detect any possible changes. After the first measurement was completed (after 20 mins reaction time), the formation of a new diphosphine species (**8**) could be detected and at the same time, the regeneration of **2a** primary phosphine was observed. The reaction was ongoing for 23 hours, then the phosphines were sulfurized and purified on silica gel. After the column chromatography, two phosphines were isolated, **9** and **4aa** in 64% and 20% isolated yields respectively. Compound **9** was confirmed to have P(*p*-tolyl)$_2$ moiety at the 1,4- and PPh_2 unit at the 1,6-position *(for X-ray crystallographic data, see chapter 6 in this document)*. This investigation became a clear evidence of the 1,4-retro addition, which is happening not only in case of the diketo 1,4-monophosphine (**10**), but also of diphosphine salt **3aa**.

Figure S28 The $^{31}P\{^{1}H\}$ NMR spectra of the generation of mixed phosphine **8**, measured in acetone.

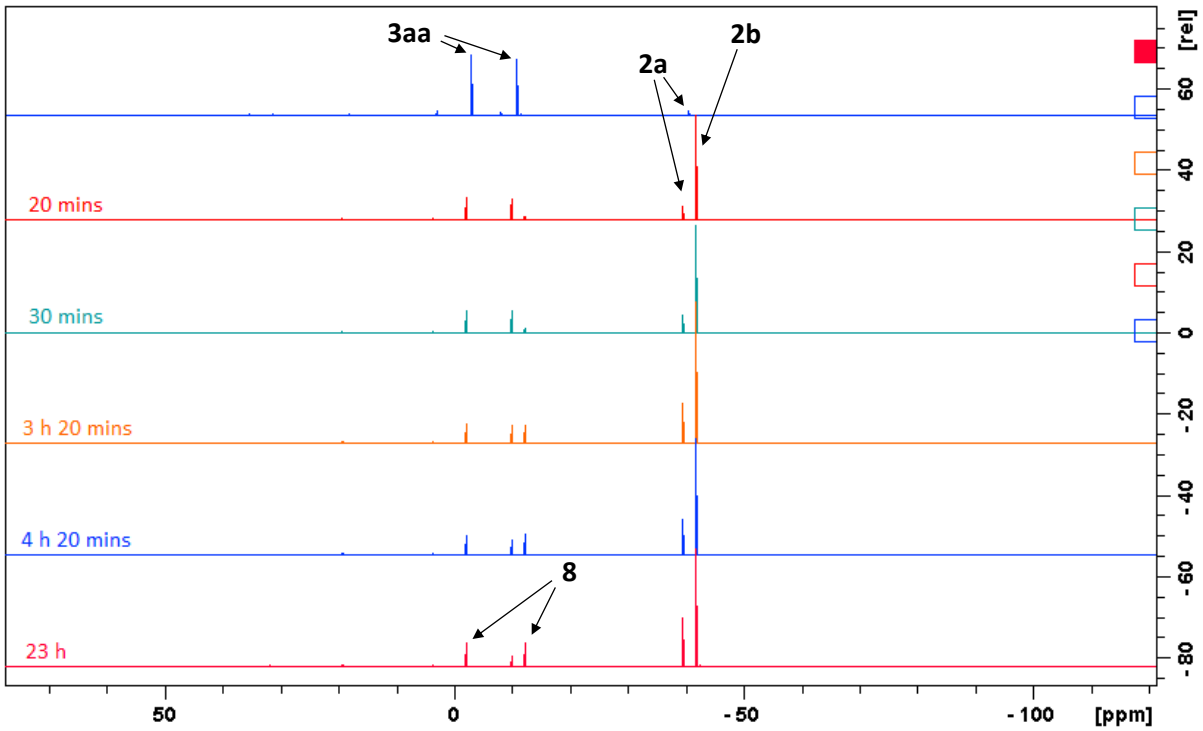

Figure S29 The $^{31}P\{^{1}H\}$ NMR spectra of the generation of mixed phosphine **8**, measured in acetone.

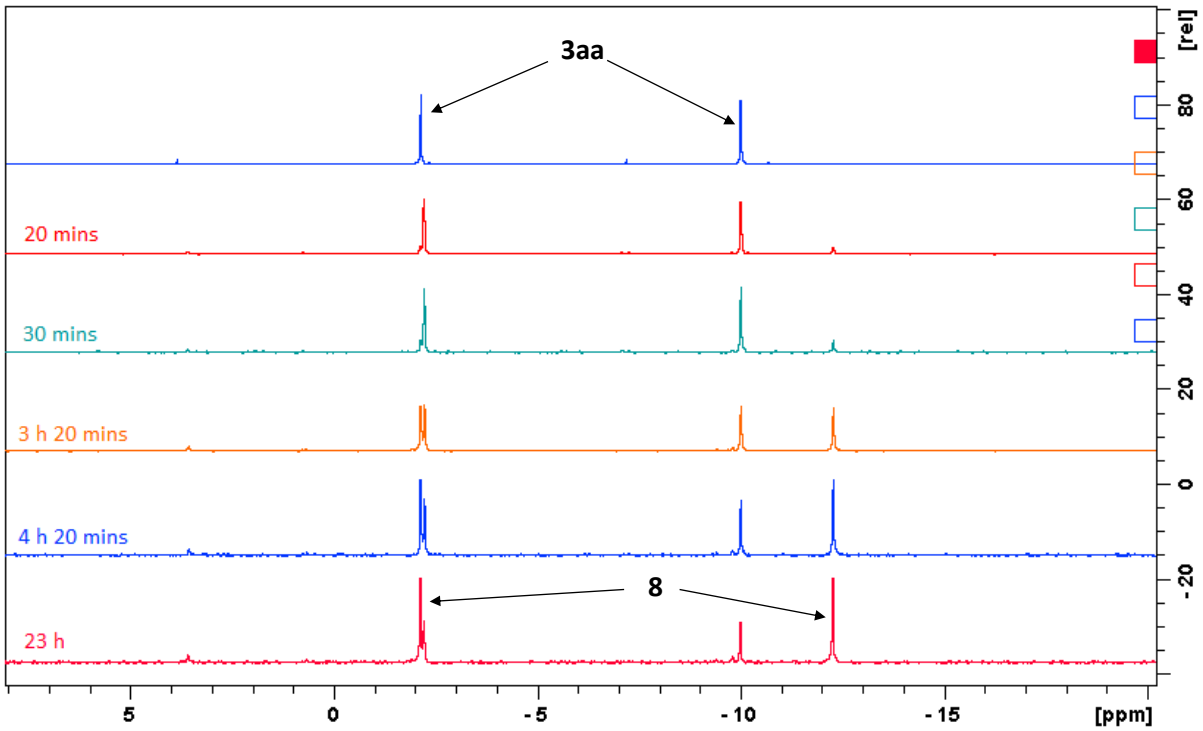

Figure S30 The $^{31}P\{^{1}H\}$ NMR spectrum of the generation of mixed phosphine **8**, measured in acetone after 24 hours reaction time.

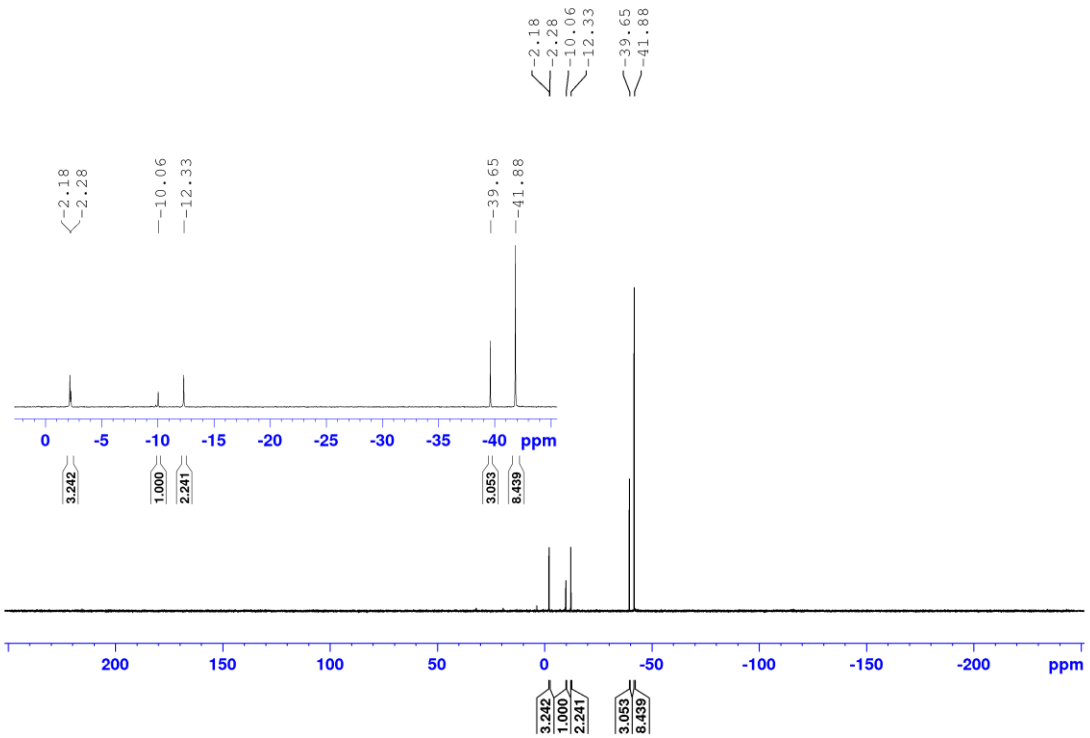

Characterization data of **9**:

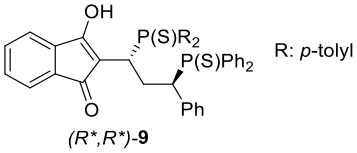

(R,R*)*-**9**

*2-(1-(di-p-tolylphosphaneyl)-3-(diphenylphosphaneyl)-3-phenylpropyl)-3-hydroxy-1H-inden-1-one (**9**).*

Appearance: yellow solid, Yield=64%, Mp.= 177.9-180

^{1}H NMR (500 MHz, $CDCl_3$) δ 11.16 (s, 1H, O*H*), 7.86 (dd, *J* = 11.9, 7.3 Hz, 2H, Ar*H*), 7.57 (dd, *J* = 12.6, 8.2 Hz, 2H, Ar*H*), 7.44 – 7.36 (m, 5H, Ar*H*), 7.36 – 7.31 (m, 1H, Ar*H*), 7.29 – 7.26 (m, 1H, Ar*H*), 7.25 – 7.22 (m, 1H, Ar*H*), 7.22 – 7.14 (m, 5H, Ar*H*), 7.11 – 7.02 (m, 8H, Ar*H*), 7.02 – 6.97 (m, 2H, Ar*H*), 3.97 – 3.87 (m, 1H, $CH_2C\underline{H}Ph$), 3.65 (td, *J* = 10.4, 2.6 Hz, 1H, C(O)CC$\underline{H}CH_2$), 2.38 (s, 3H), 2.38 – 2.33 (m, 2H, CH_2), 2.21 (s, 3H).

^{13}C NMR (126 MHz, $CDCl_3$) δ 194.30 (d, $^{3}J_{PC}$ = 6.8 Hz, 1C, *C*(O)), 175.87 (d, $^{3}J_{PC}$ = 5.1 Hz, 1C, C=$\underline{C}$-OH), 143.21 – 103.38 (37C, Ar and $\underline{C}$=C-OH), 45.15 (dd, $^{1}J_{PC}$ = 51.4, $^{3}J_{PC}$ = 13.7 Hz, 1C, $CH_2\underline{C}HPh$), 33.89 (dd, $^{1}J_{PC}$ = 56.3, $^{3}J_{PC}$ = 15.1 Hz, 1C, C$\underline{C}HCH_2$), 30.34 (t, $^{2}J_{PC}$ = 4.3 Hz, 1C, CH_2), 21.68 (s, 1C, CH_3), 21.57 (s, 1C, CH_3).

$^{31}P\{^{1}H\}$ NMR (202 MHz, $CDCl_3$) δ 49.38 (d, $^{4}J_{PP}$ = 5.7 Hz, 1P), 46.71 (d, $^{4}J_{PP}$ = 5.3 Hz, 1P).

HRMS (+ESI) m/z calcd for $C_{44}H_{39}O_2P_2S_2$ $(M + H)^+$: 725.1867; found: 725.1892.

2.5) Investigation on 1,4-retro-Michael addition of compound 13. (5)

The 1,4-retro-Michael addition was confirmed to take place in compound **10** and **3aa**. We also intended to study, if compound **13**, the diketo diphosphine, is also able to go through this transformation or not. Similar test reaction to experiment 2.4 was investigated by us starting under base-free conditions:

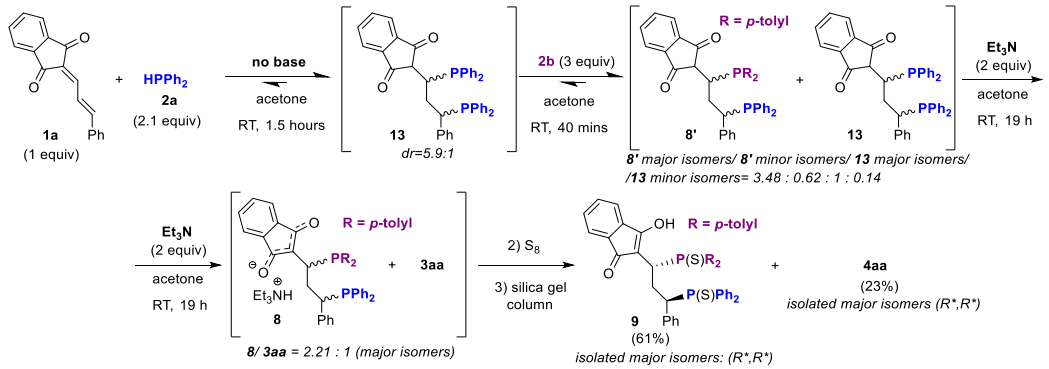

Procedure:

A nitrogen flushed 2-neck flask was charged with **1a** (19.7 mg, 75.7 µmol, 1 equiv) in degassed acetone (2.5 mL) at room temperature, followed by the addition of **2a** (29.6 mg, 159 µmol, 2.1 equiv). The reaction was stirred for 1.5 hours, then **2b** (48.6 mg, 151.4 µmol, 3 equiv) was introduced to the mixture. The solution was stirred for 40 minutes then triethylamine (15.3 mg, 151.4 µmol, 2 equiv) was introduced to the mixture. After stirring for another 19 hours, the mixture was treated with sulphur (37.9 µmol, 0.5 equiv of S_8) and the crude mixture was purified on column chromatography by using *n*-hexanes/EtOAc (98:2 to 70:30) eluent systems. Compound **9** was isolated as yellow solids in 61% yield and **4aa**, yellow solids, in 23% yield.

*(Remark: the reaction was monitored by $^{31}P\{^1H\}$ NMR measurements after the addition of **2b** and before sulfurization. See Figures S31 to S34)*

In this test experiment, compound **13** was generated first in a base-free transformation, followed by the addition of 3 equivalent amount of HP(*p*-tolyl)$_2$ (**2b**). After 20 minutes, the first $^{31}P\{^1H\}$ NMR spectrum was recorded and the new peaks already indicated the formation of the mixed diphosphine **8'**. After 40 mins, the ratio between **8'** major isomers/ **8'** minor isomers/ **13** major isomers/ **13** minor isomers was obtained as 3.48 : 0.62 : 1 : 0.14 respectively. The reason of the low diastereomeric ratio is the absence of base (=non-optimized contidion). In order to enhance the diastereoselectivity, 2 equivalent triethylamine was introduced to the reaction mixture. In experiment 2.1.3, it was already confirmed, that the transformation of the diketo diphosphines (**13**) to the corresponding diphosphine salt (**3aa**) provides the improvement of the diastereomeric ratio (due to the 1,4-retro-Michael addition). After the base addition, the reaction mixture was stirred for another 19 hours, until the observed peaks of the minor isomers in the $^{31}P\{^1H\}$ NMR disappeared. Before sulfurization, approximately the same **8**/ **3aa** ratio was developed like it was obtained in experiment 2.4 (when the whole process was ongoing in the presence of base). This experiment was a clear evidence, that the 1,4-retro-Michael addition can also occur in case of the diketo diphosphine (**13**).

Figure S31 The $^{31}P\{^{1}H\}$ NMR spectra of experiment 2.5, measured in acetone.

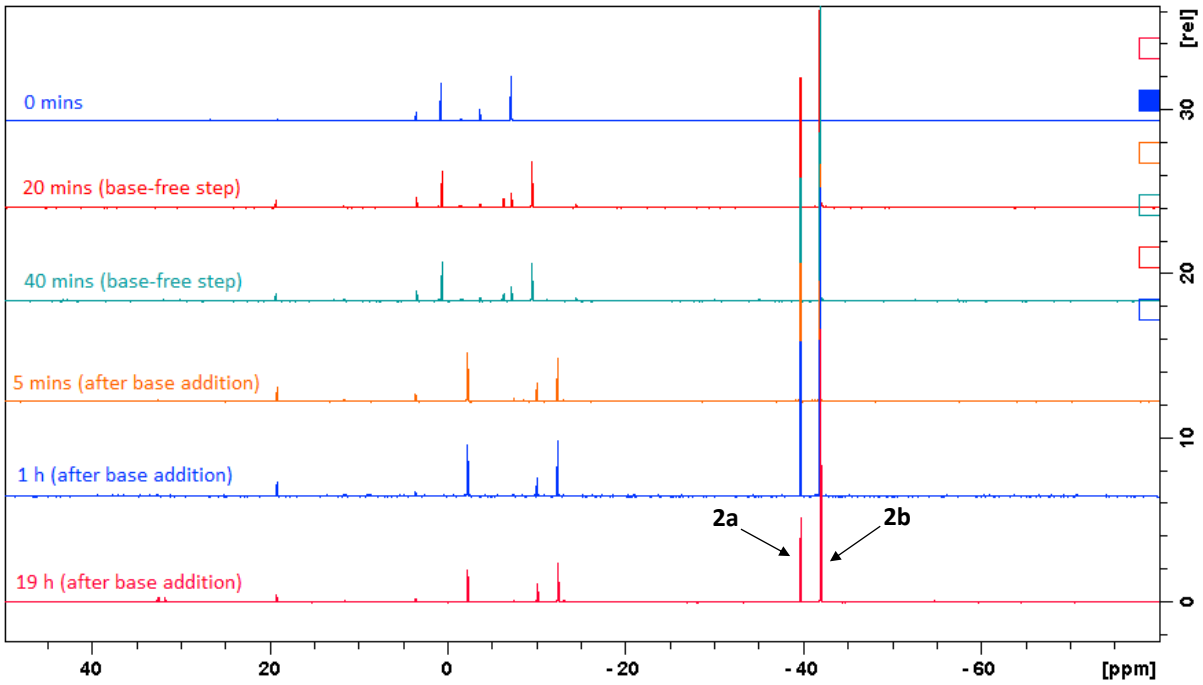

Figure S32 The $^{31}P\{^{1}H\}$ NMR spectra of experiment 2.5, measured in acetone.

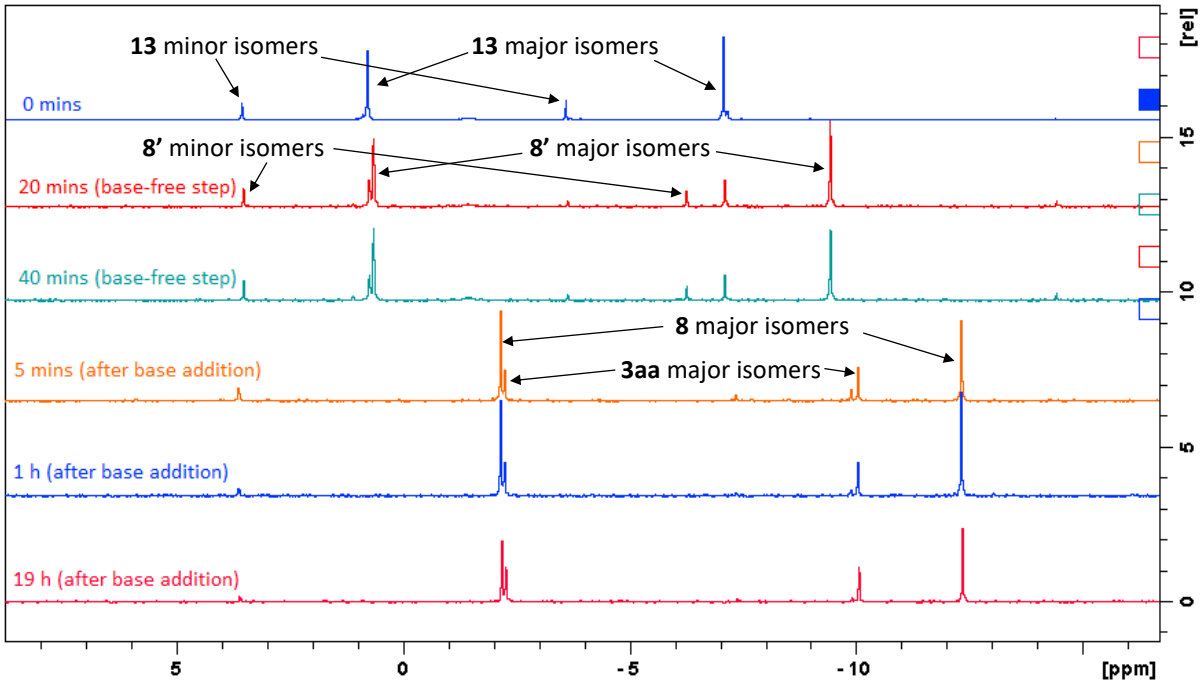

Figure S33 The $^{31}P\{^{1}H\}$ NMR spectrum of the base-free step of exp. 2.5, after 40 minutes reaction time, measured in acetone.

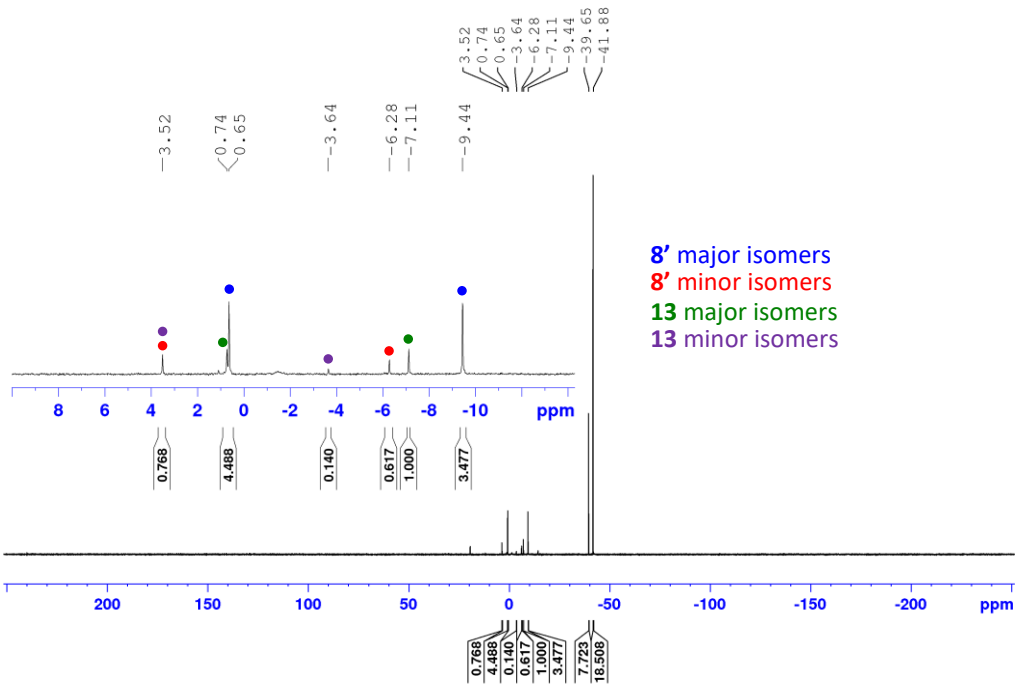

Figure S34 The $^{31}P\{^{1}H\}$ NMR spectrum of the second step of exp. 2.5 after triethylamine addition and 19 hours reaction time, measured in acetone.

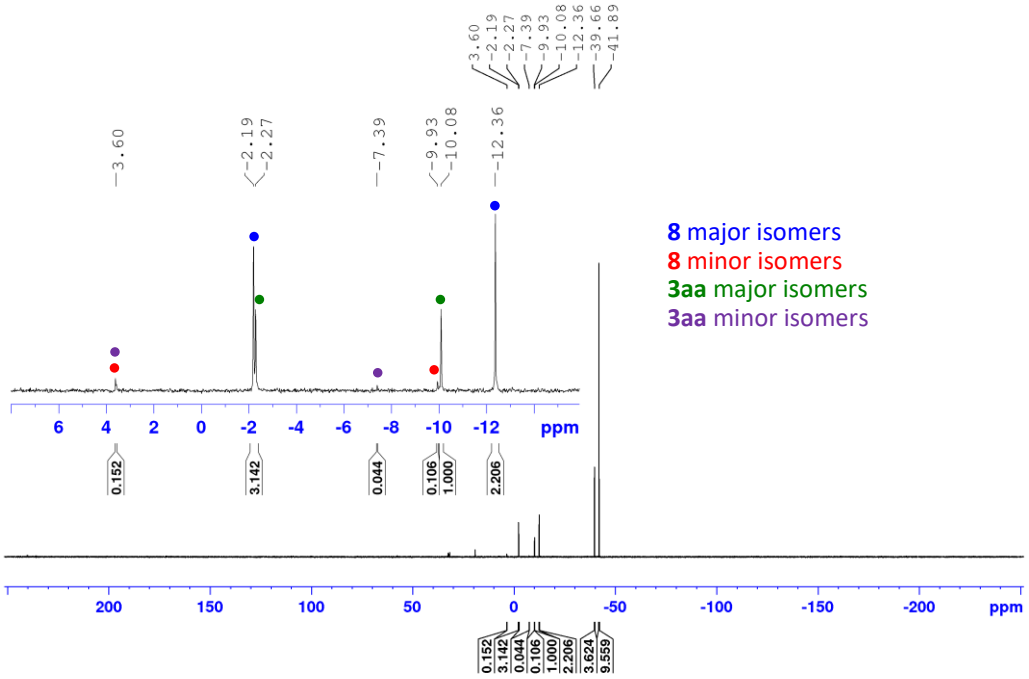

3. NMR spectra

Figure S35 ^{1}H NMR (400 MHz, $CDCl_3$) spectrum of **1a**.

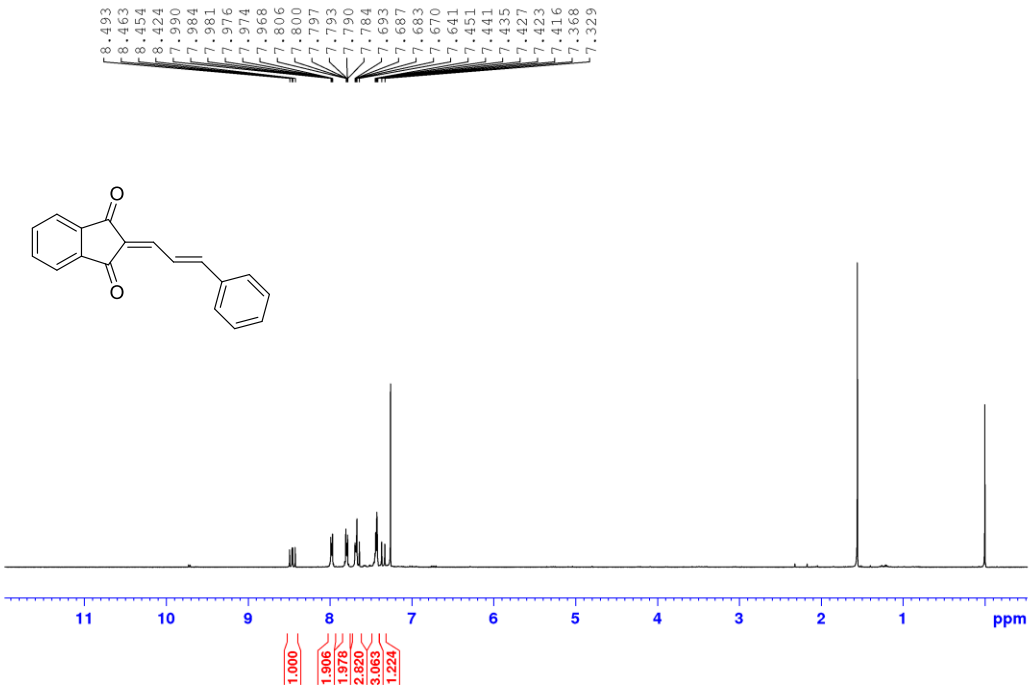

Figure S36 ^{13}C NMR (101 MHz, $CDCl_3$) spectrum of **1a**.

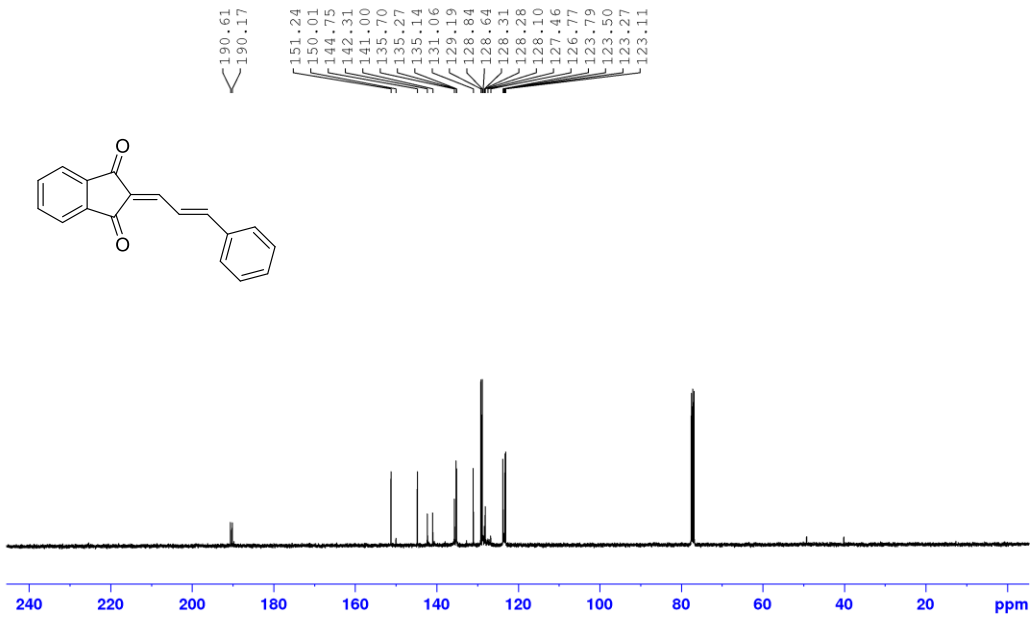

Figure S37 ^{1}H NMR (400 MHz, CD_2Cl_2) spectrum of **1a**.

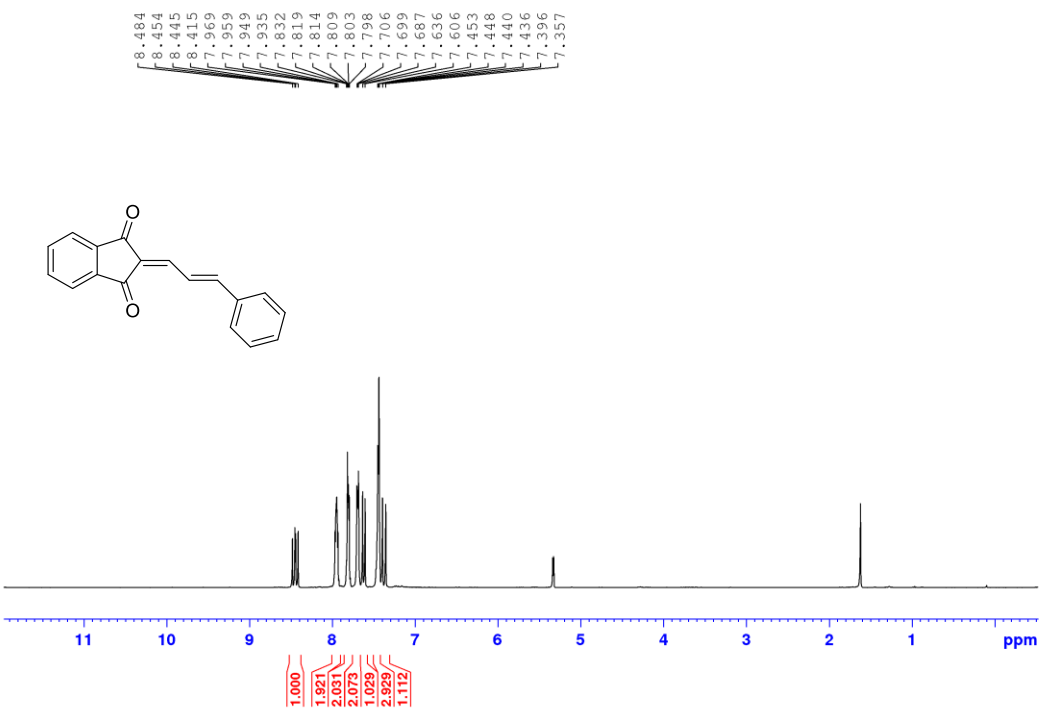

Figure S38 ^{13}C NMR (101 MHz, CD_2Cl_2) spectrum of **1a**.

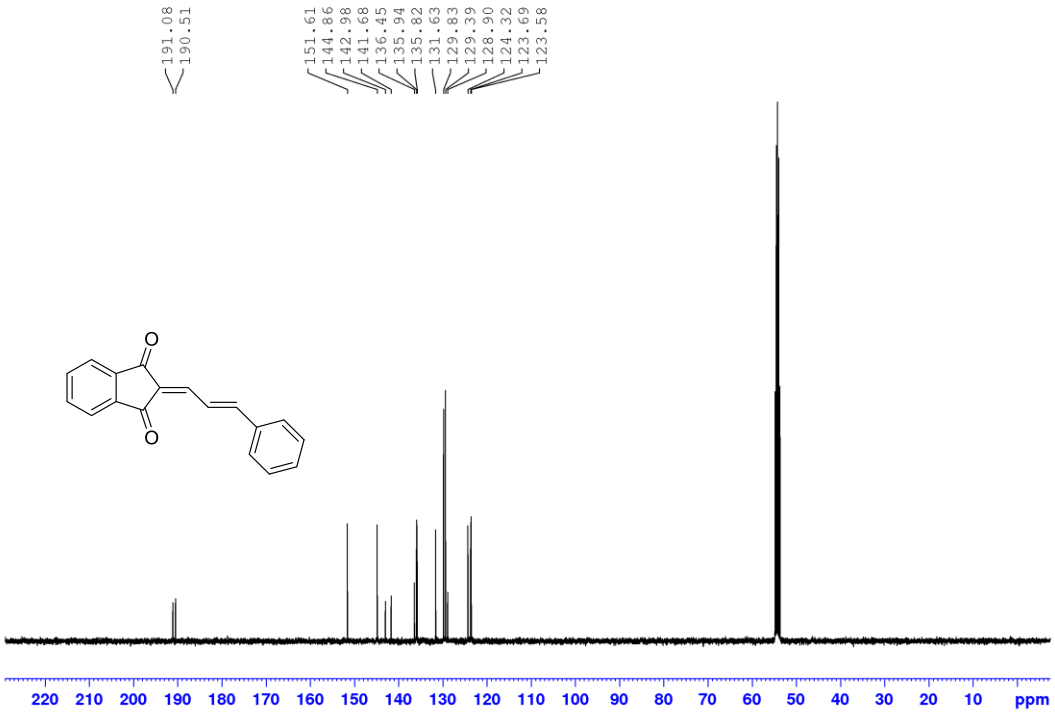

Figure S39 ^{1}H NMR (400 MHz, Acetone-d_6) spectrum of **1a**.

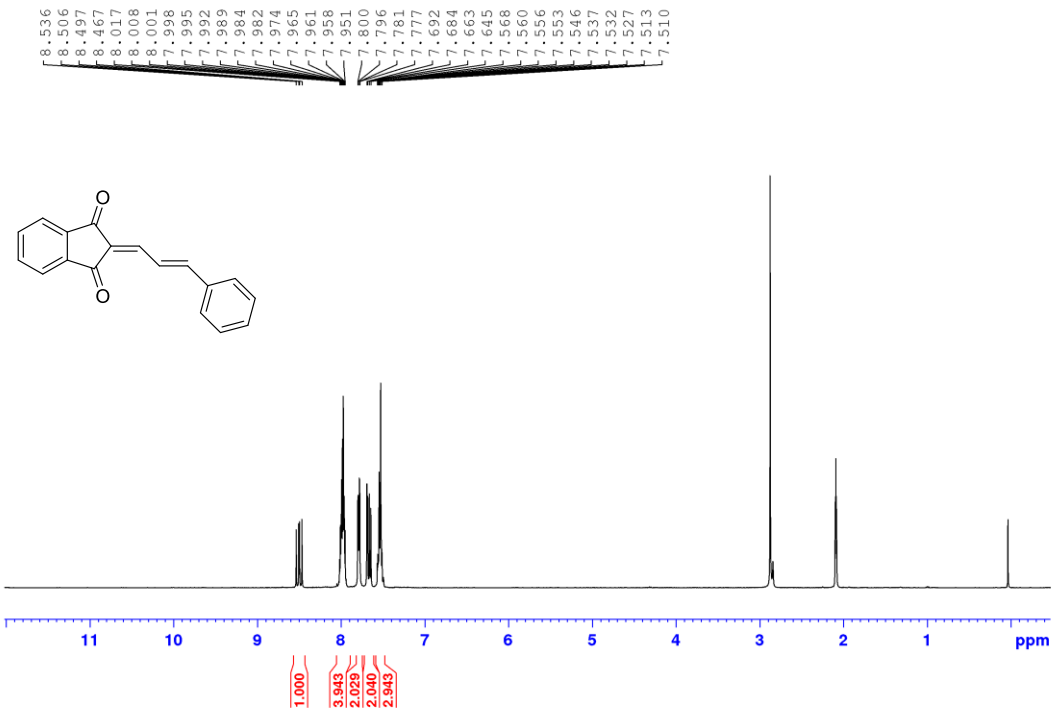

Figure S40 ^{13}C (101 MHz, Acetone-d_6) NMR spectrum of **1a**.

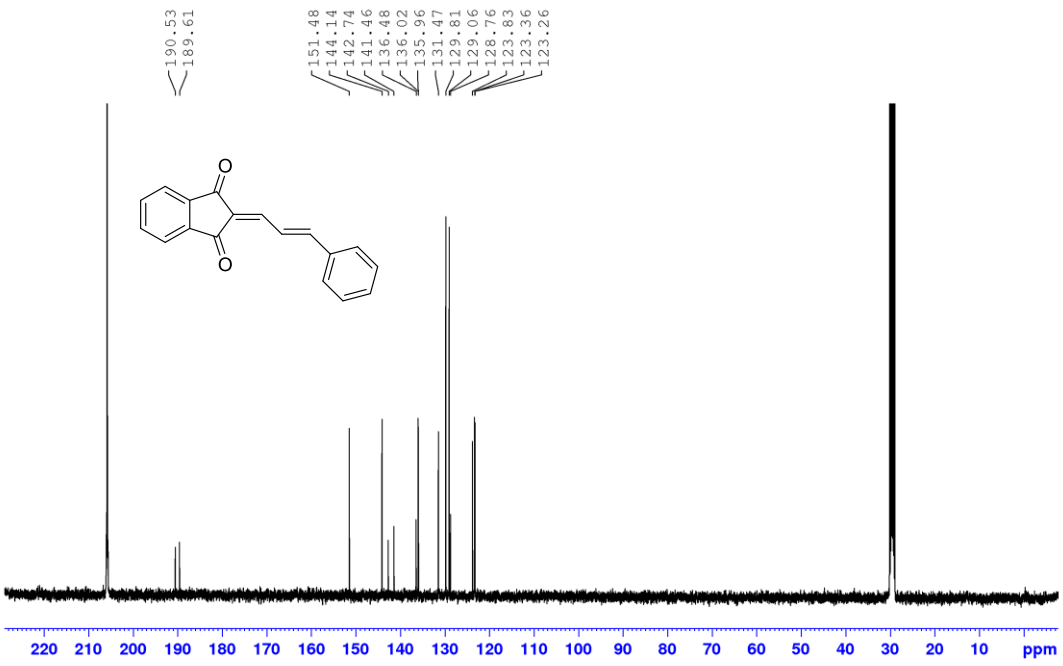

Figure S41 ^{1}H NMR (400 MHz, $CDCl_3$) spectrum of **1b**.

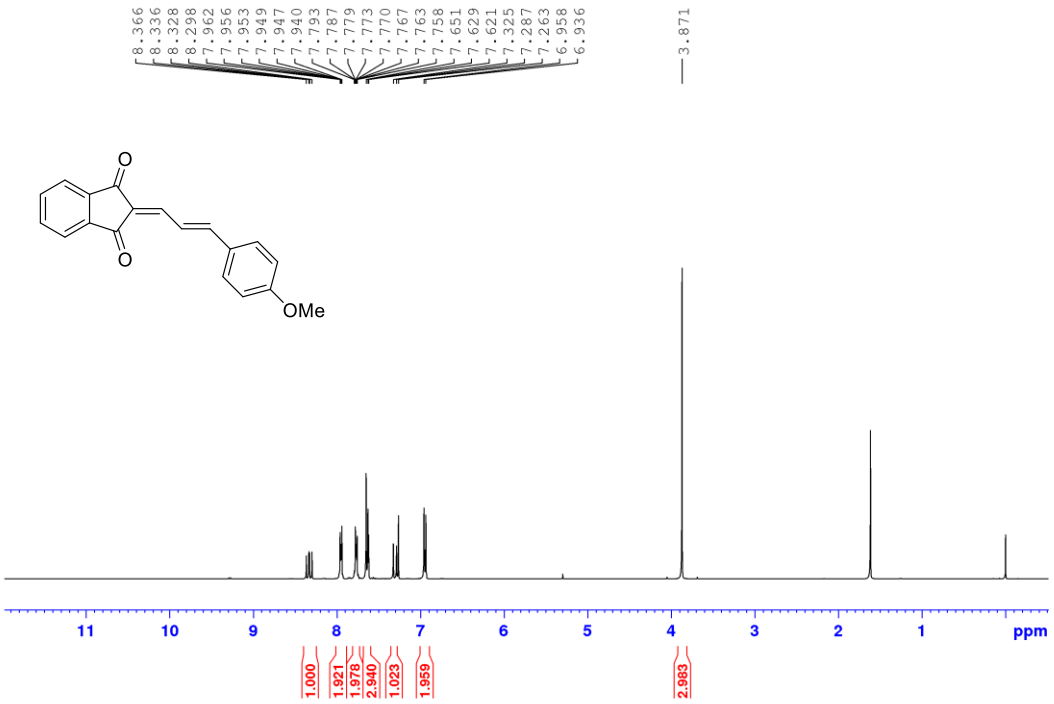

Figure S42 ^{13}C NMR (126 MHz, $CDCl_3$) spectrum of **1b**.

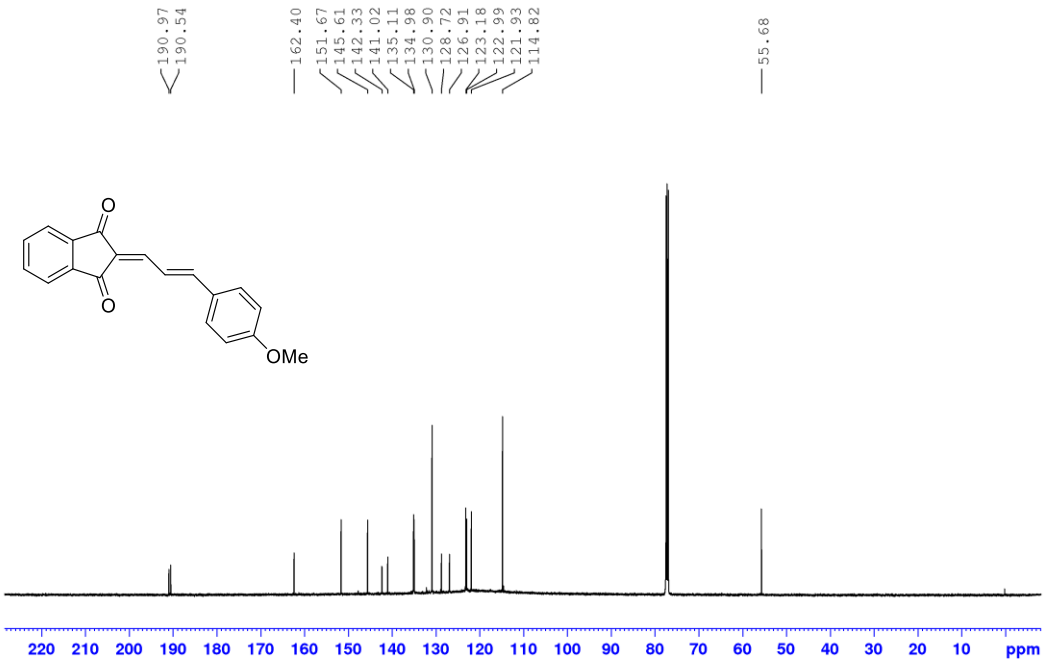

Figure S43 ^{1}H NMR (500 MHz, $CDCl_3$) spectrum of **1c**.

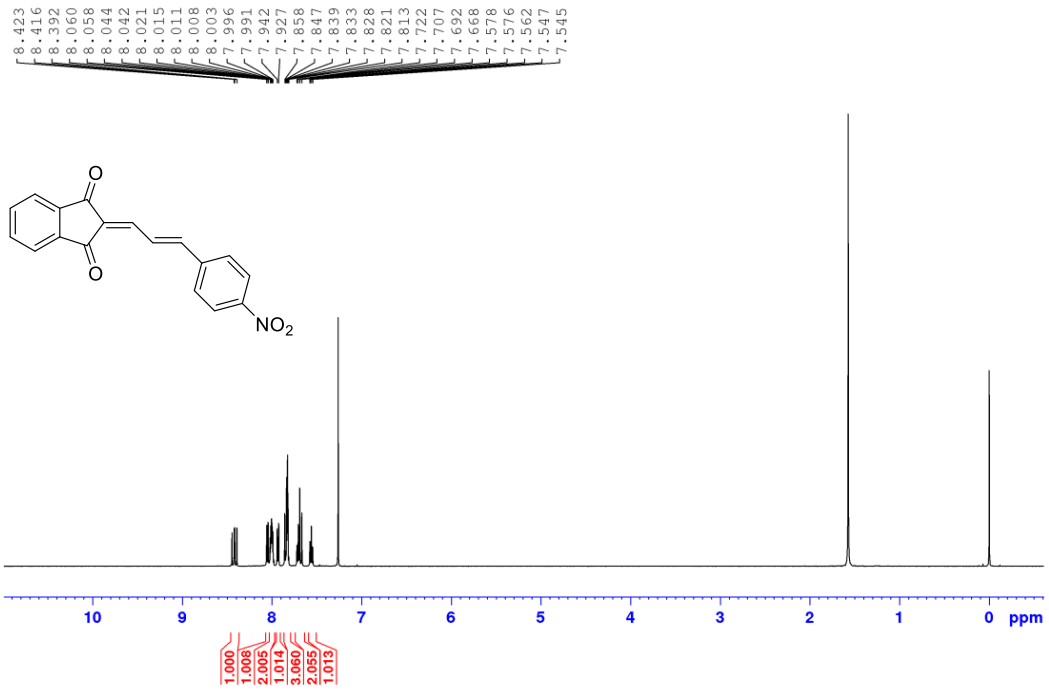

Figure S44 ^{13}C NMR (126 MHz, $CDCl_3$) spectrum of **1c**.

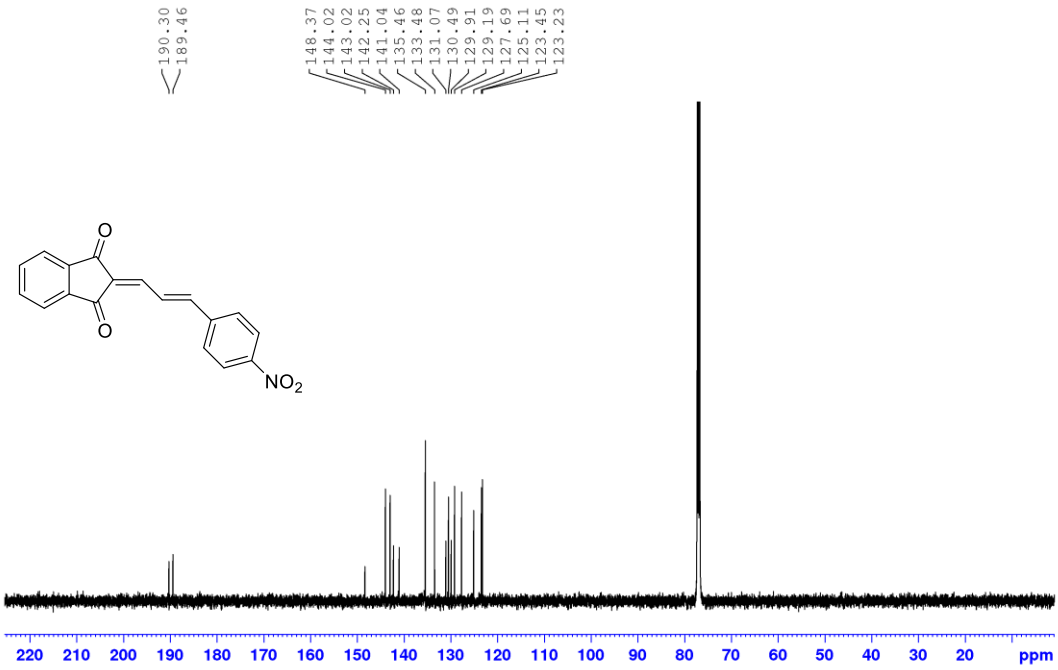

Figure S45 ^{1}H NMR (300 MHz, $CDCl_3$) spectrum of **1d**.

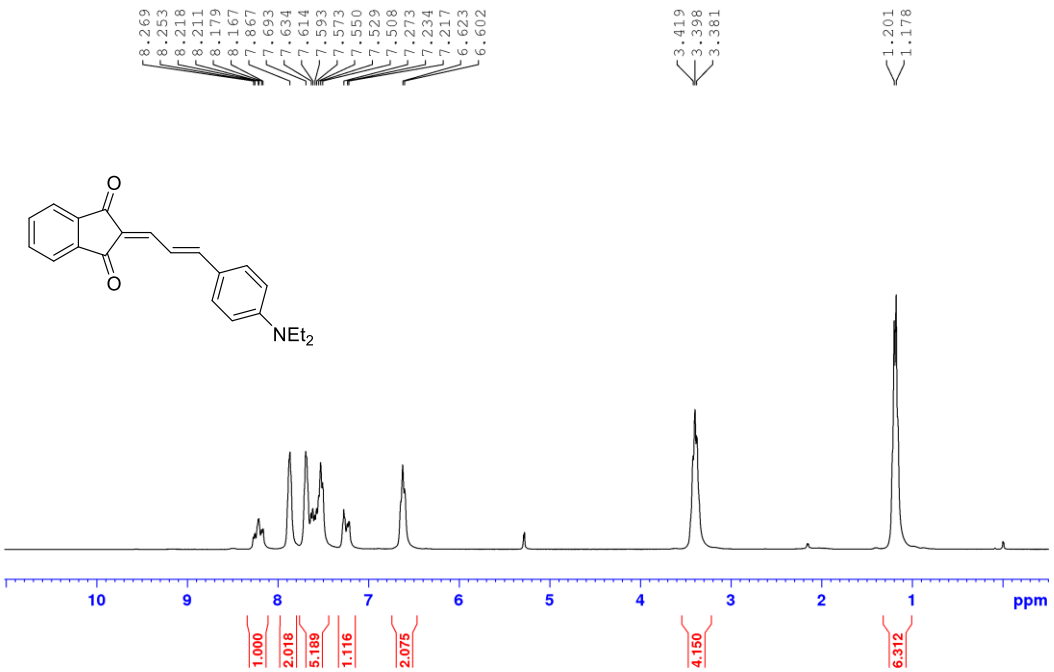

Figure S46 ^{13}C NMR (75 MHz, $CDCl_3$) spectrum of **1d**.

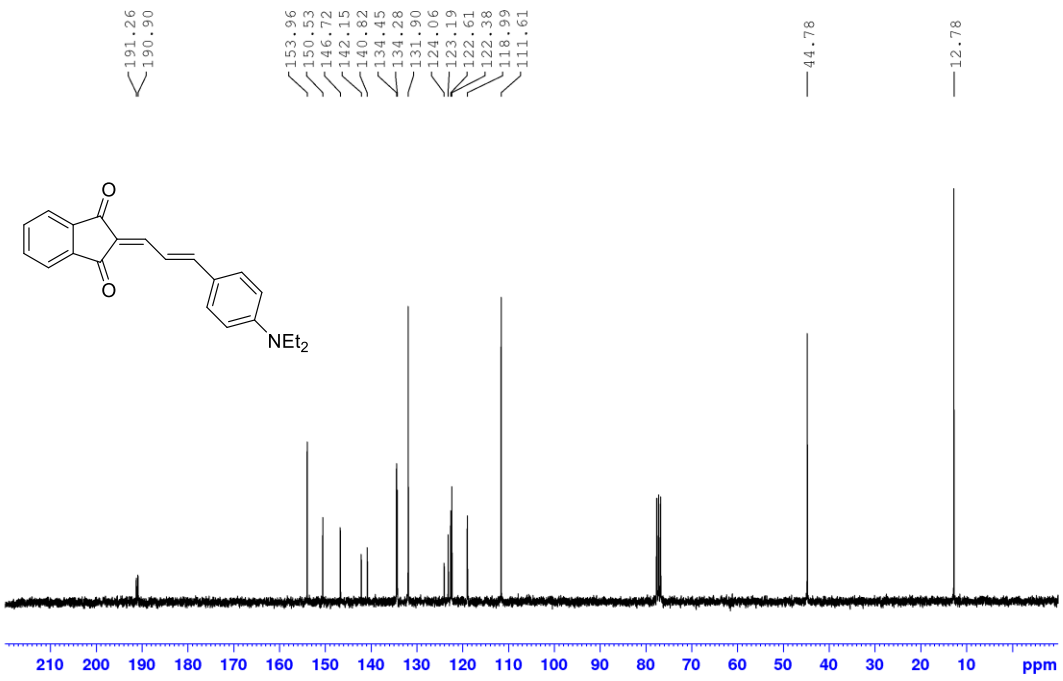

Figure S47 ^{1}H NMR (300 MHz, $CDCl_3$) spectrum of **1e**.

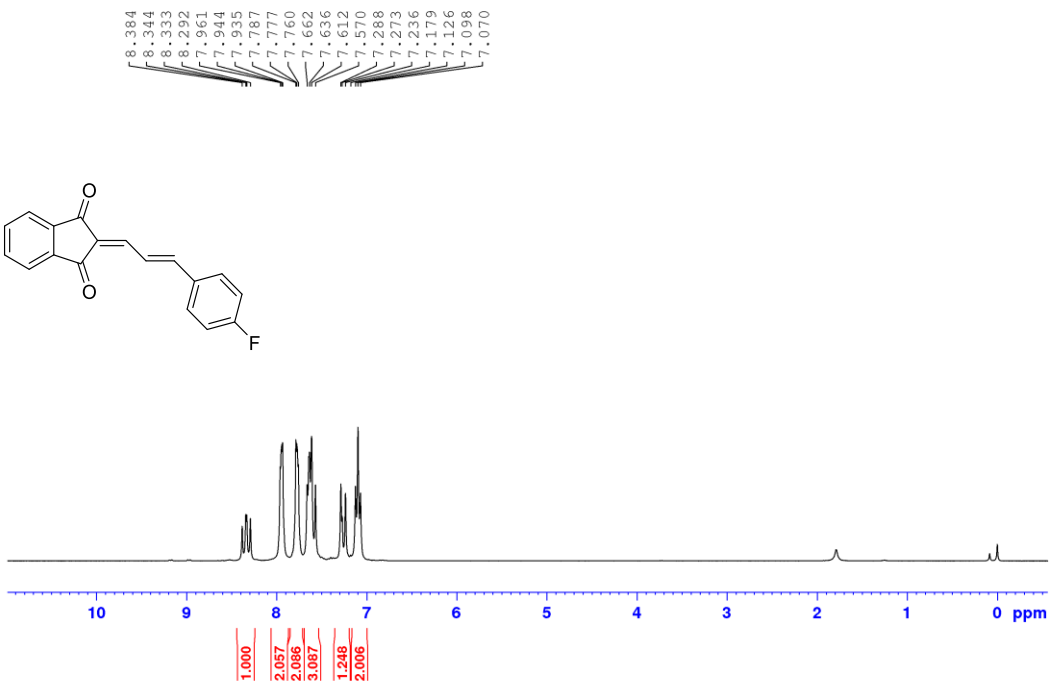

Figure S48 ^{13}C NMR (75 MHz, $CDCl_3$) spectrum of **1e**.

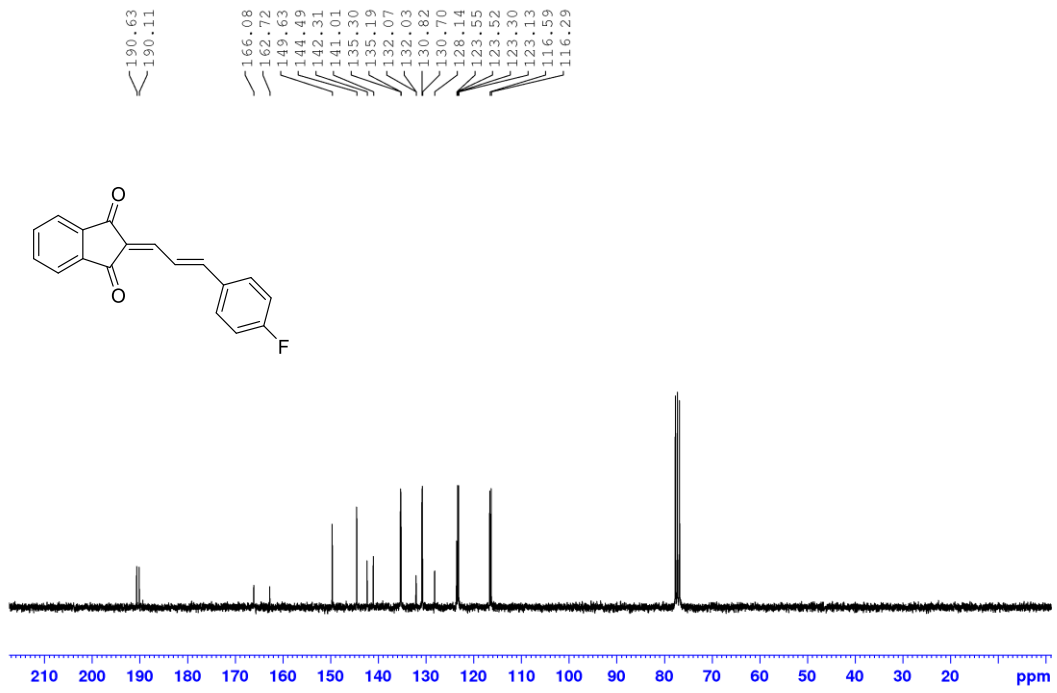

Figure S49 ^{1}H NMR (400 MHz, $CDCl_3$) spectrum of **1f**.

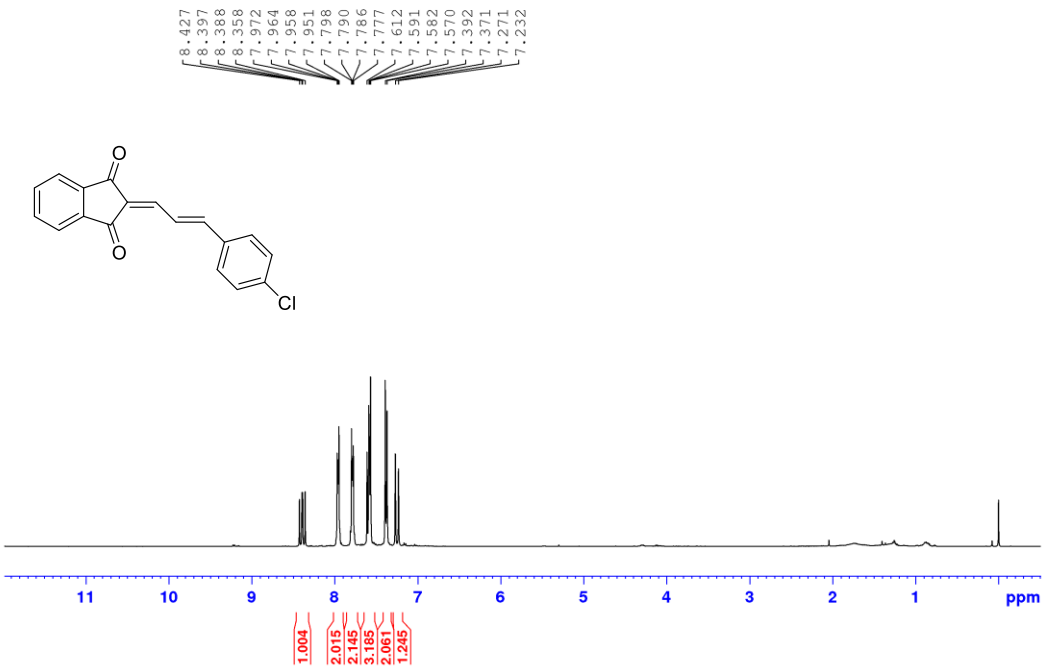

Figure S50 ^{13}C NMR (101 MHz, $CDCl_3$) spectrum of **1f**.

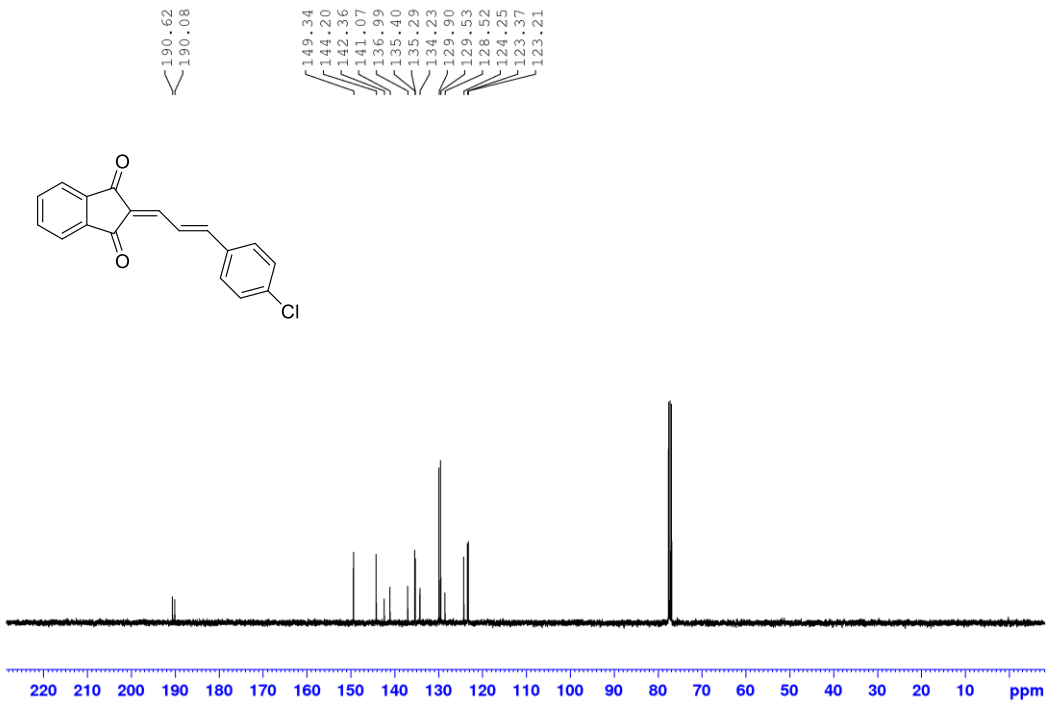

Figure S51 ^{1}H NMR (500 MHz, $CDCl_3$) spectrum of **1g**.

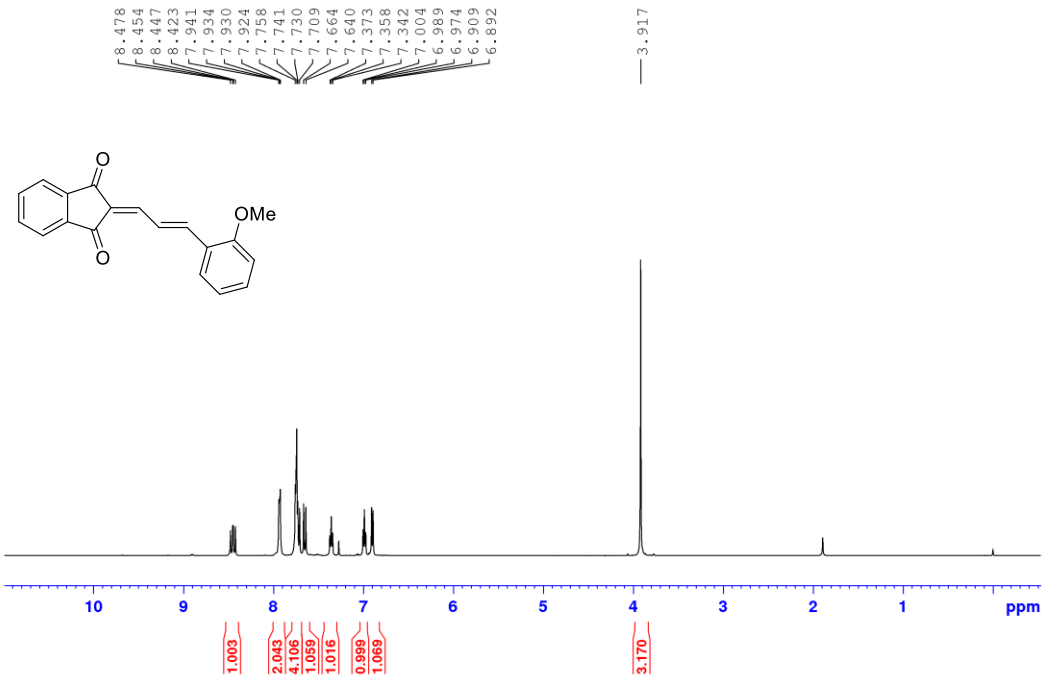

Figure S52 ^{13}C NMR (126 MHz, $CDCl_3$) spectrum of **1g**.

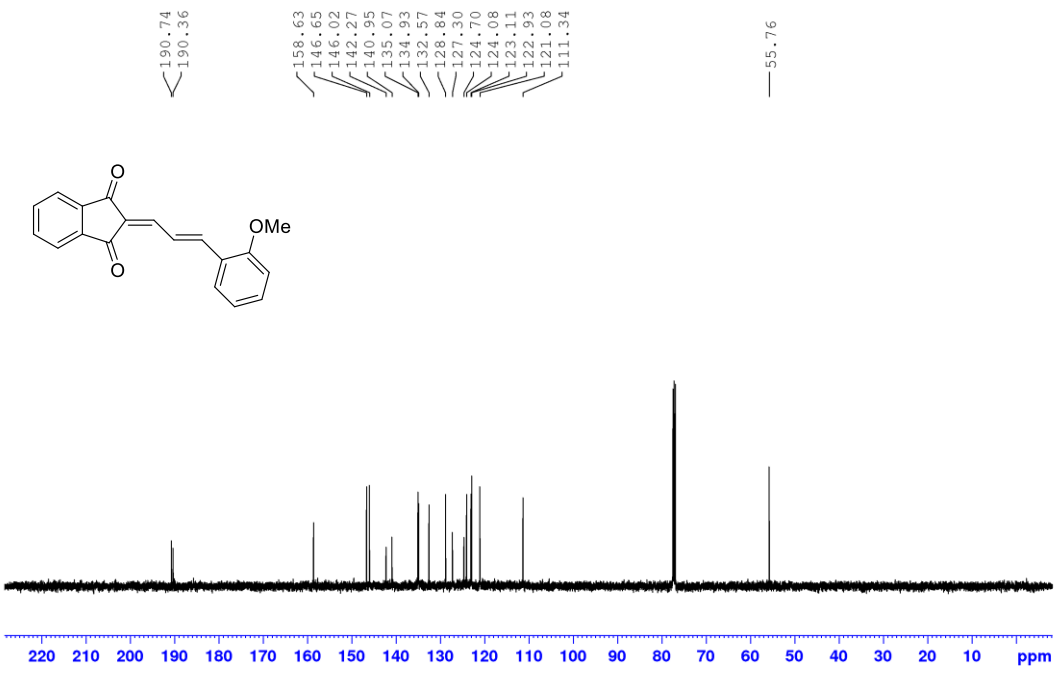

Figure S53 ^{1}H NMR (500 MHz, $CDCl_3$) spectrum of **1h**.

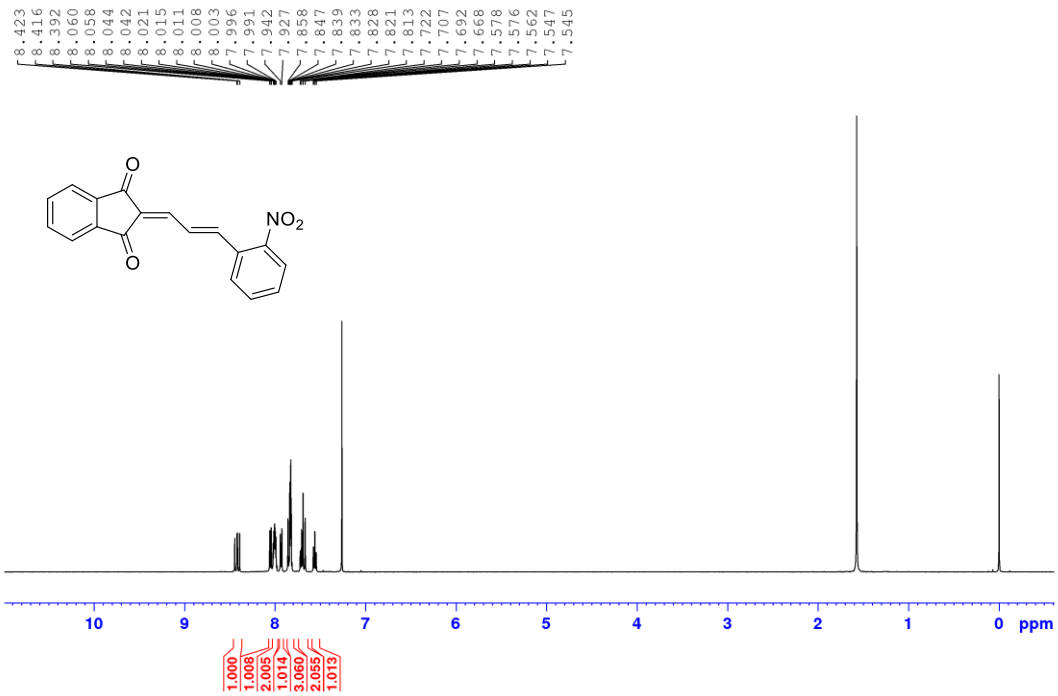

Figure S54 ^{13}C NMR (126 MHz, $CDCl_3$) spectrum of **1h**.

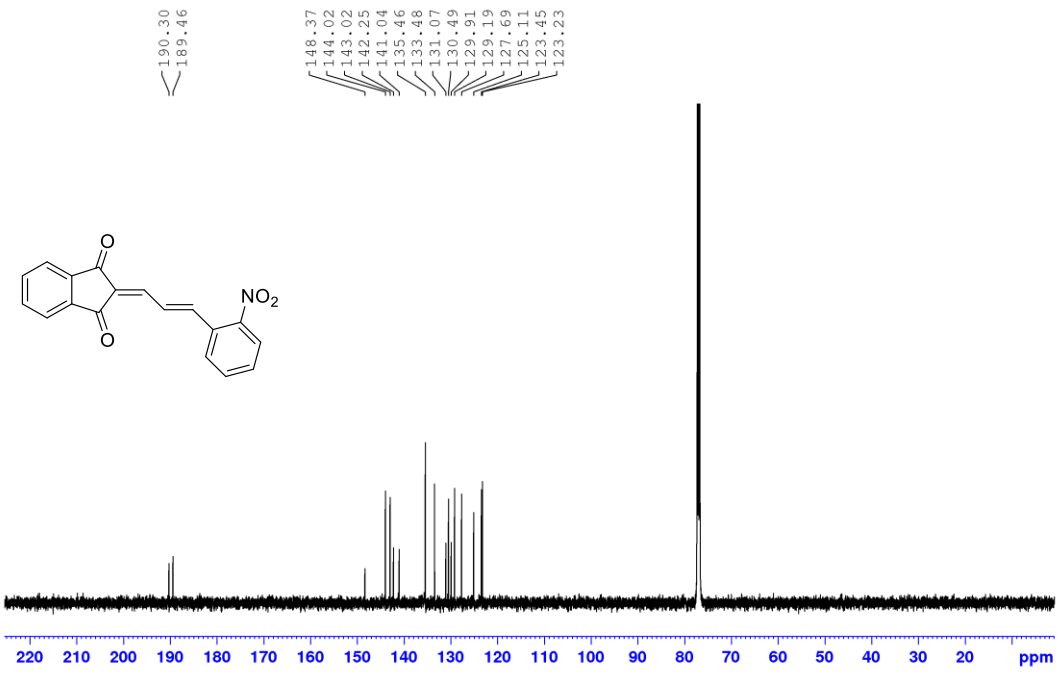

Figure S55 ^{1}H NMR (400 MHz, $CDCl_3$) spectrum of **4aa**.

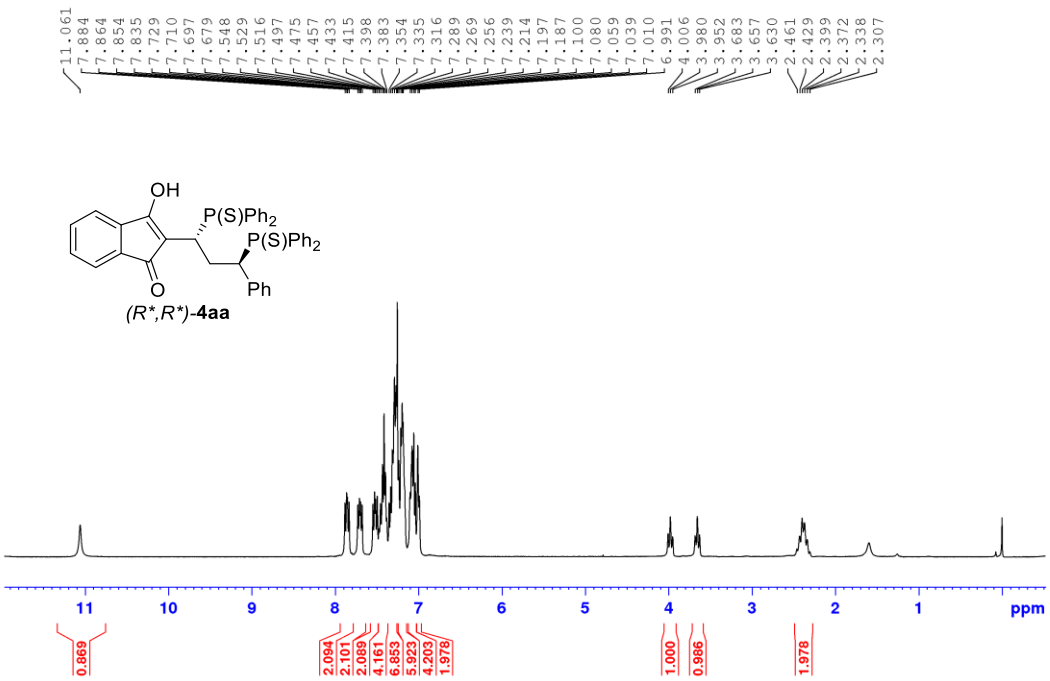

Figure S56 ^{13}C NMR (101 MHz, $CDCl_3$) spectrum of **4aa**.

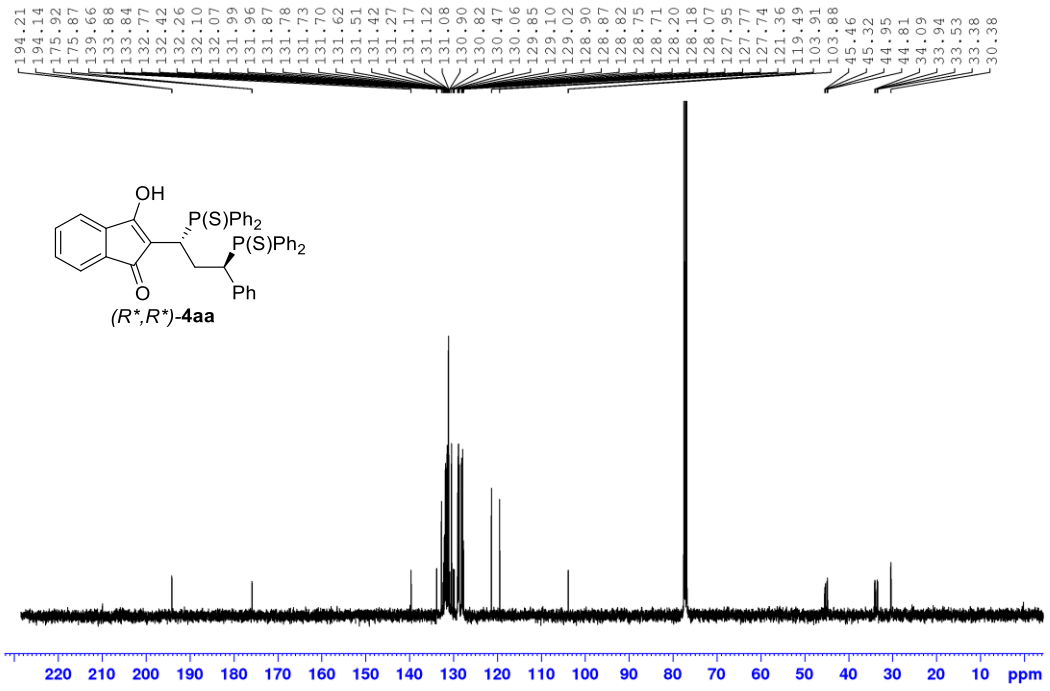

Figure S57 $^{31}P\{^{1}H\}$ NMR (162 MHz, $CDCl_3$) spectrum of **4aa**.

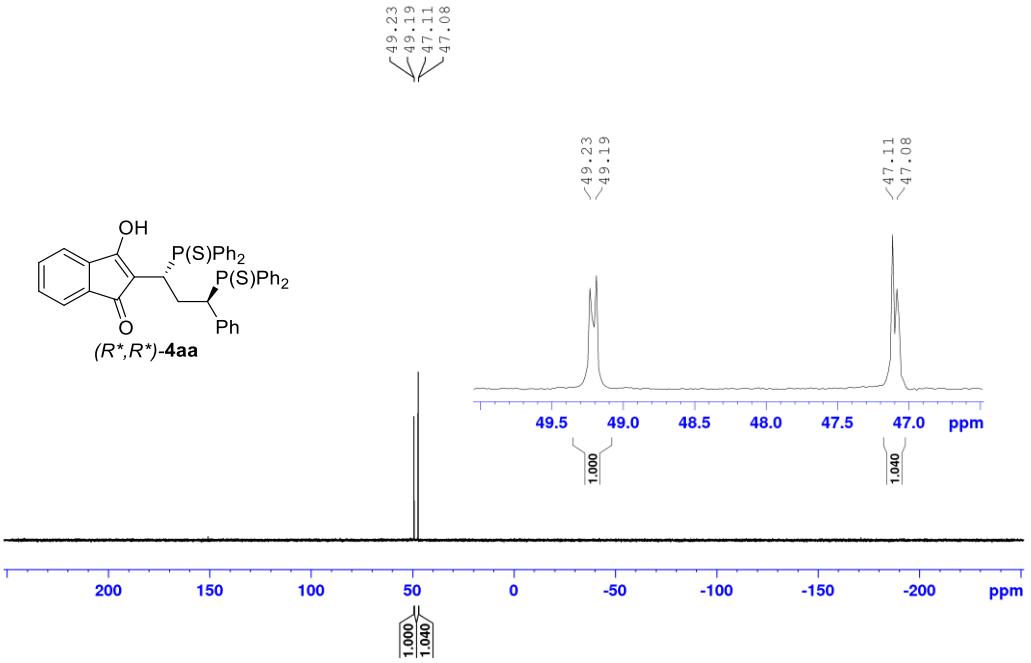

Figure S58 ^{1}H NMR (300 MHz, $CDCl_3$) spectrum of **4ab**.

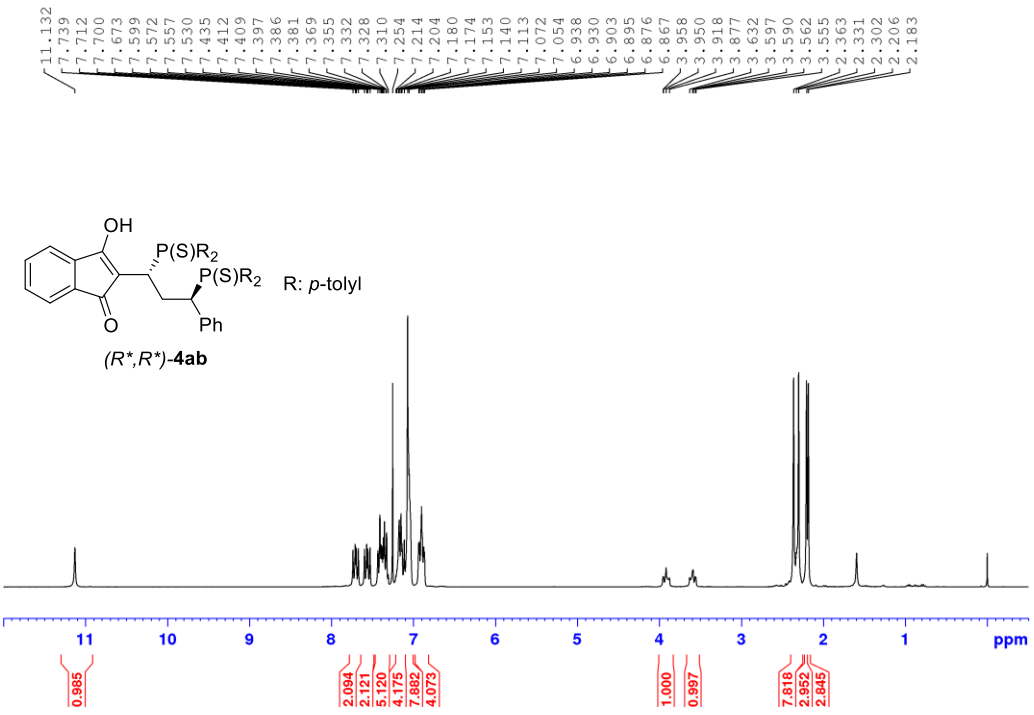

Figure S59 ^{13}C NMR (75 MHz, $CDCl_3$) spectrum of **4ab**.

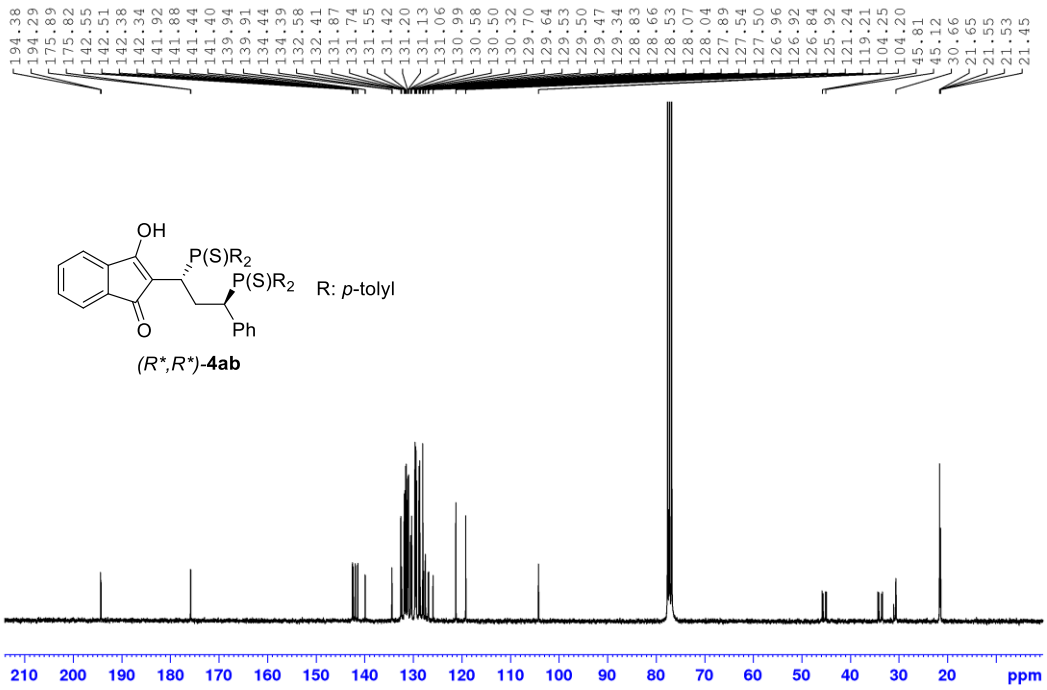

Figure S60 $^{31}P\{^1H\}$ NMR (202 MHz, $CDCl_3$) spectrum of **4ab**.

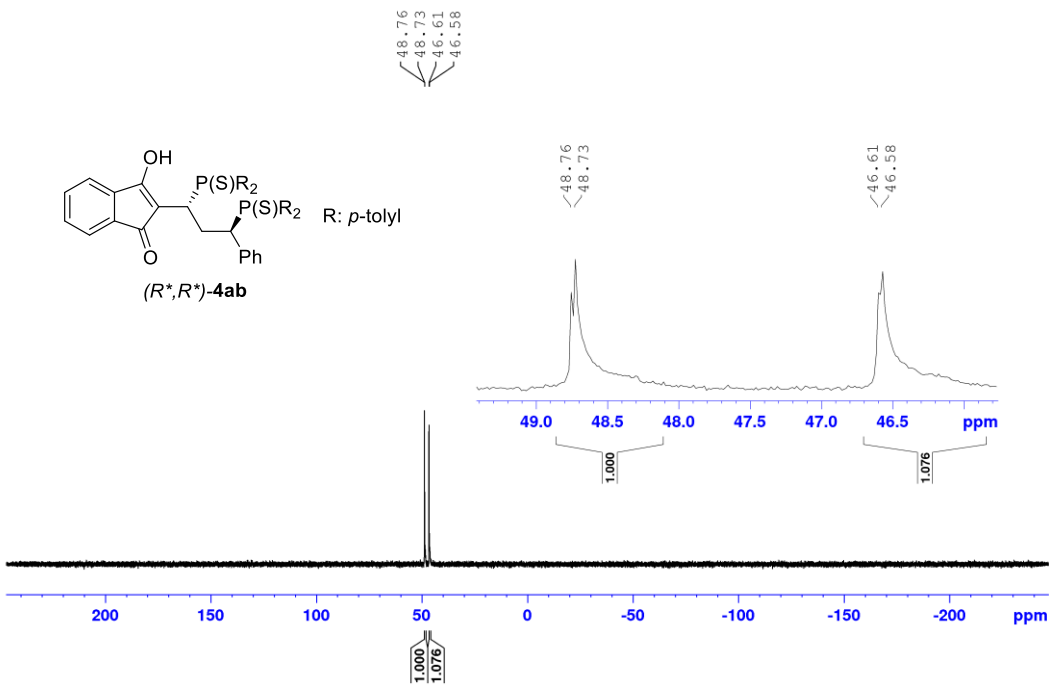

Figure S61 ^{1}H NMR (400 MHz, $CDCl_3$) spectrum of **4ac**.

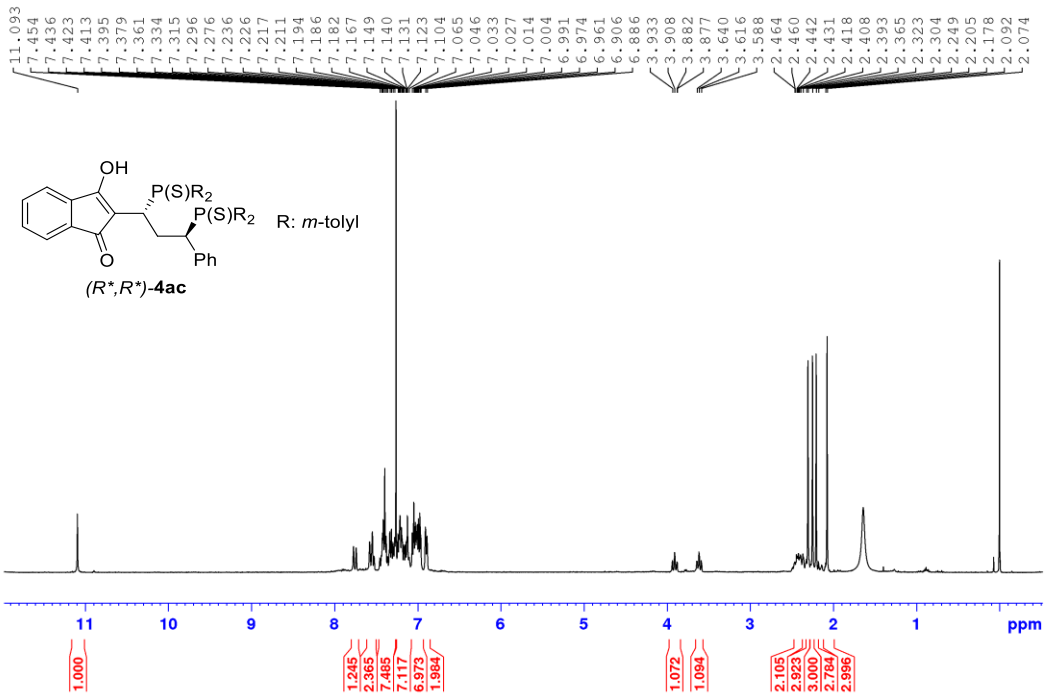

Figure S62 ^{13}C NMR (101 MHz, $CDCl_3$) spectrum of **4ac**.

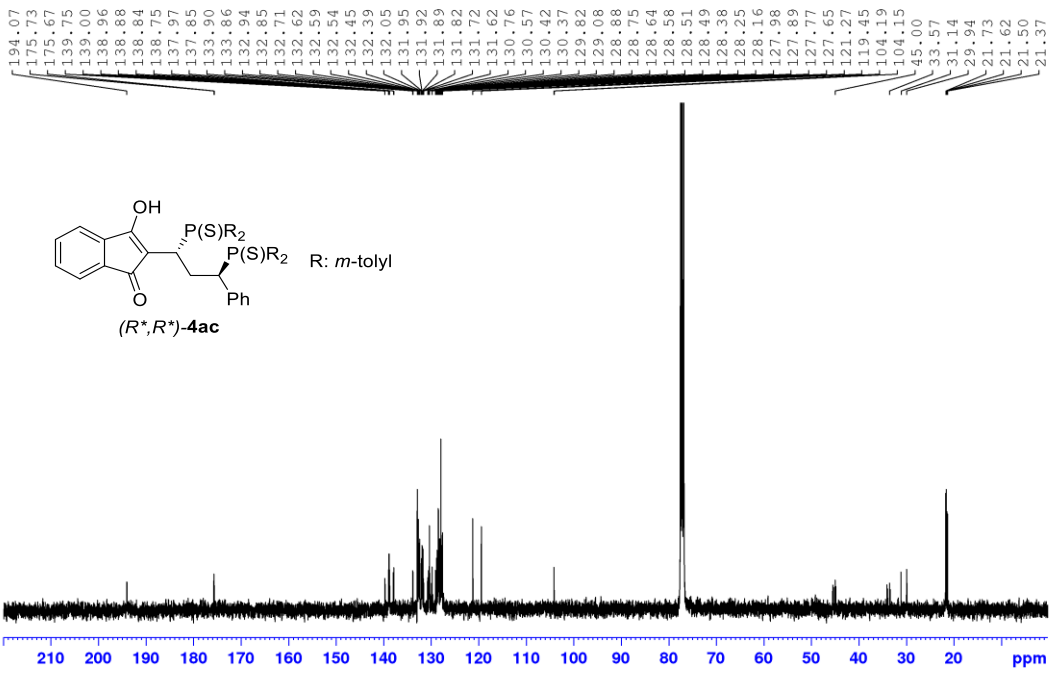

Figure S63 $^{31}P\{^{1}H\}$ NMR (162 MHz, $CDCl_3$) spectrum of **4ac**.

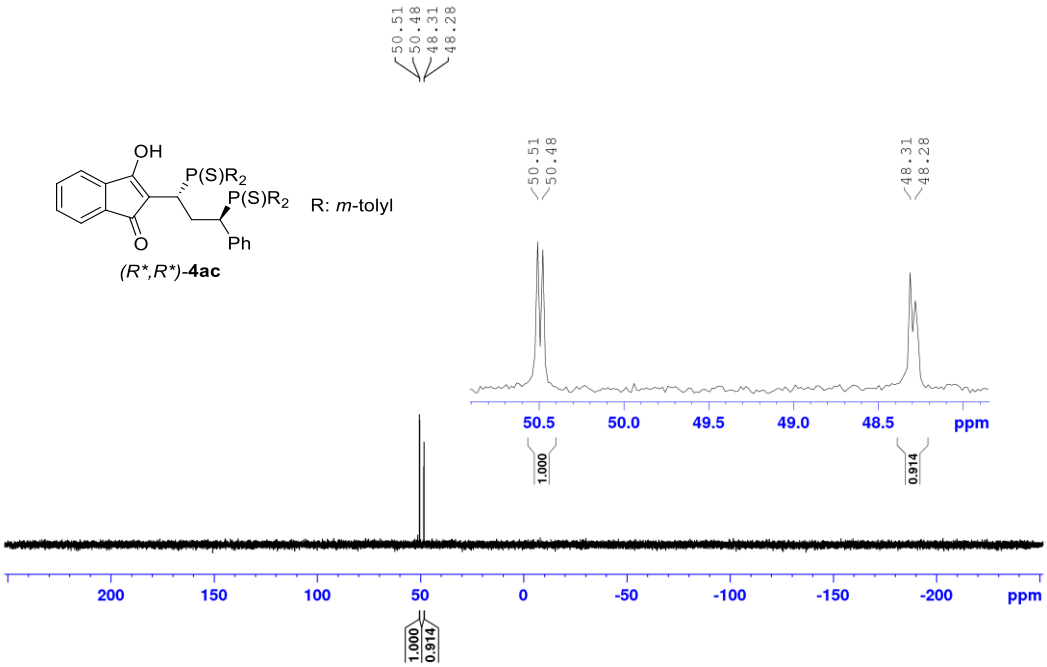

Figure S64 ^{1}H NMR (400 MHz, $CDCl_3$) spectrum of **4ba**.

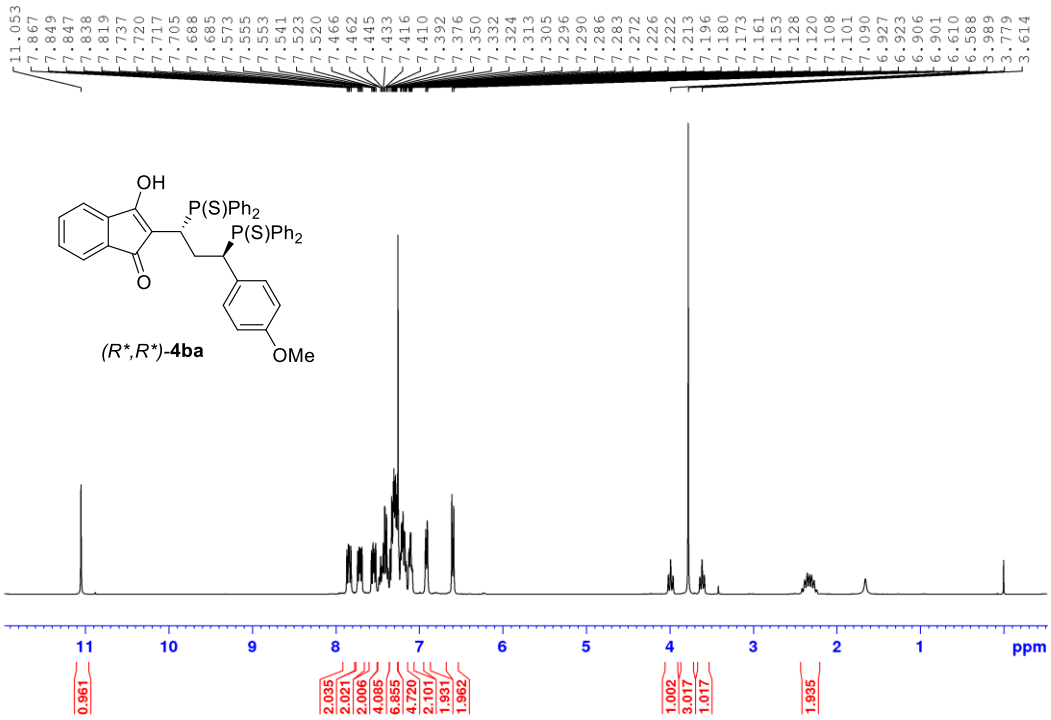

Figure S65 ^{13}C NMR (101 MHz, $CDCl_3$) spectrum of **4ba**.

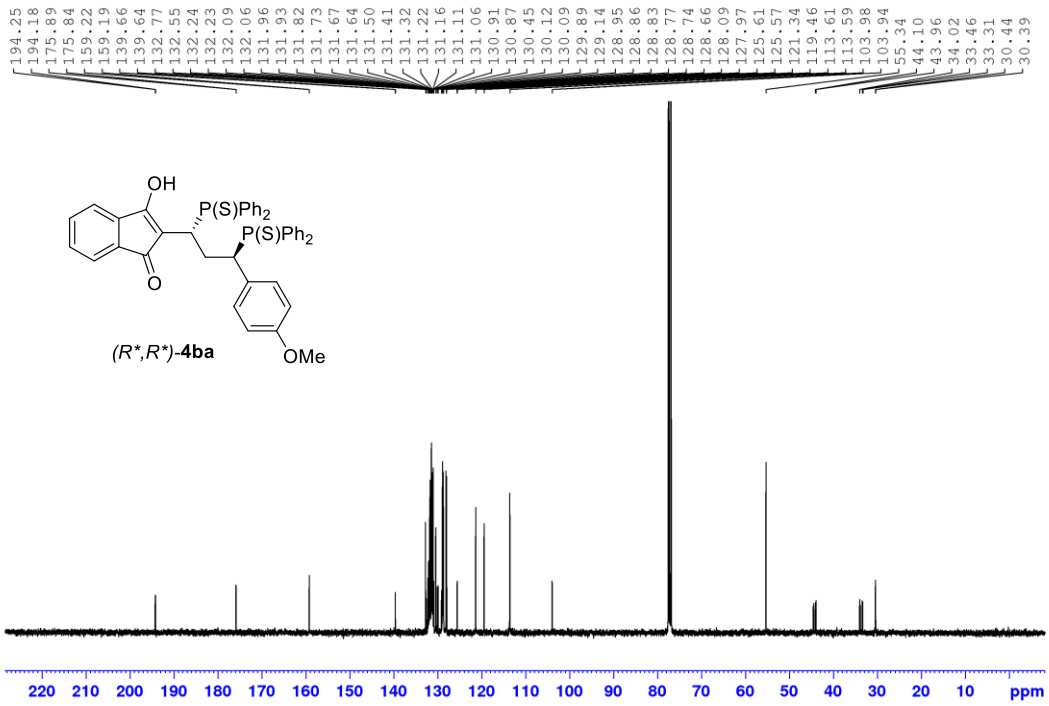

Figure S66 $^{31}P\{^1H\}$ NMR (162 MHz, $CDCl_3$) spectrum of **4ba**.

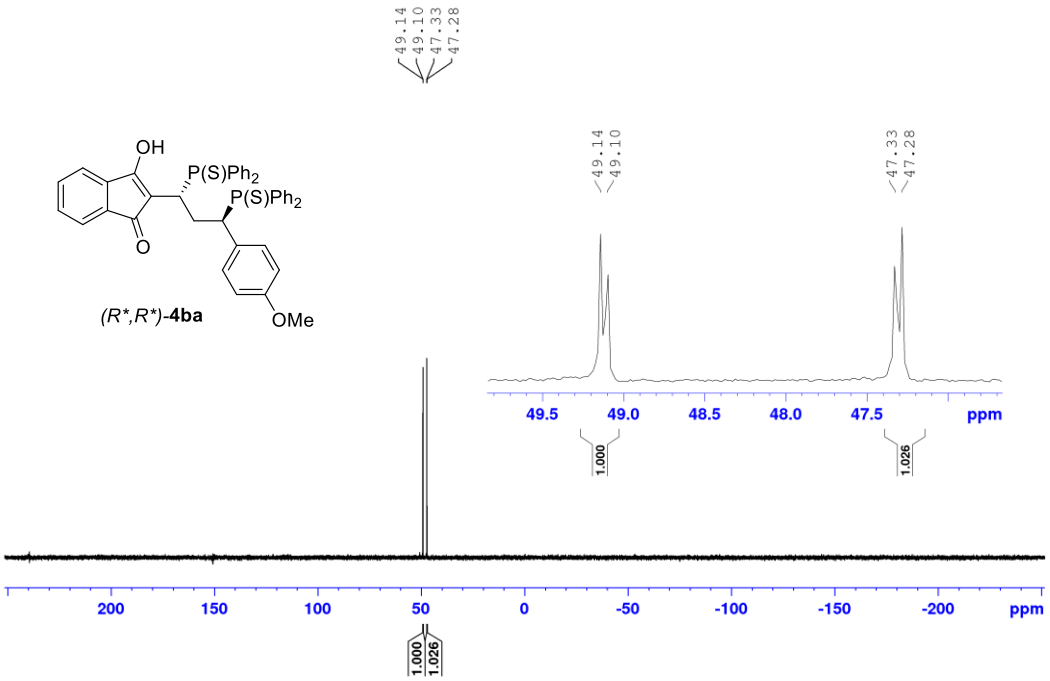

Figure S67 ^{1}H NMR (400 MHz, $CDCl_3$) spectrum of **4bb**.

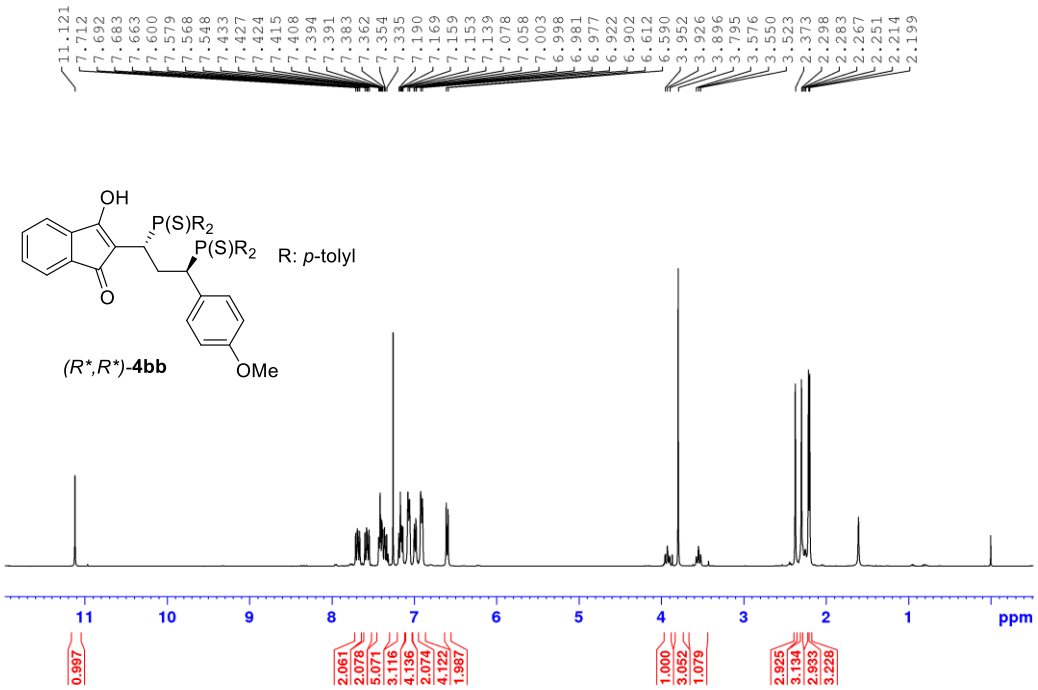

Figure S68 ^{13}C NMR (126 MHz, $CDCl_3$) spectrum of **4bb**.

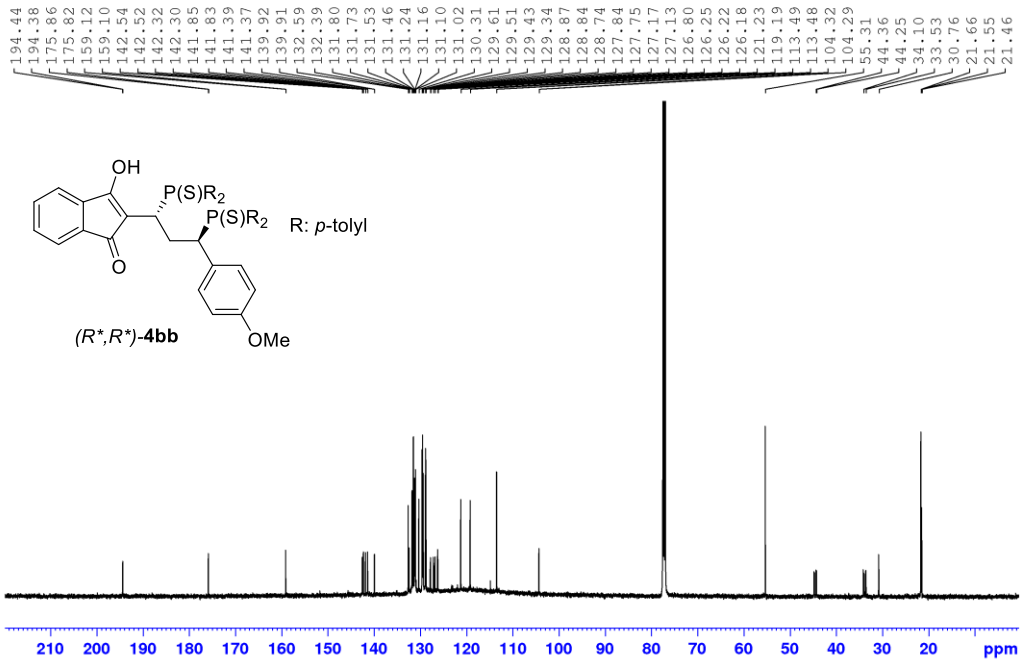

Figure S69 $^{31}P\{^{1}H\}$ NMR (162 MHz, $CDCl_3$) spectrum of **4bb**.

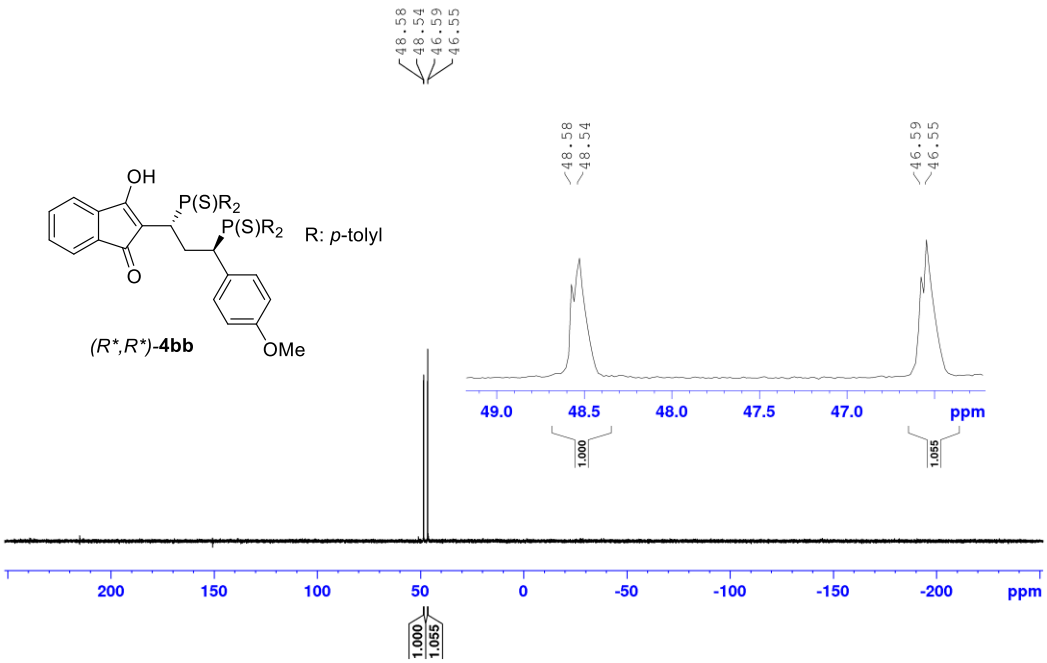

Figure S70 ^{1}H NMR (500 MHz, $CDCl_3$) spectrum of **4bc**.

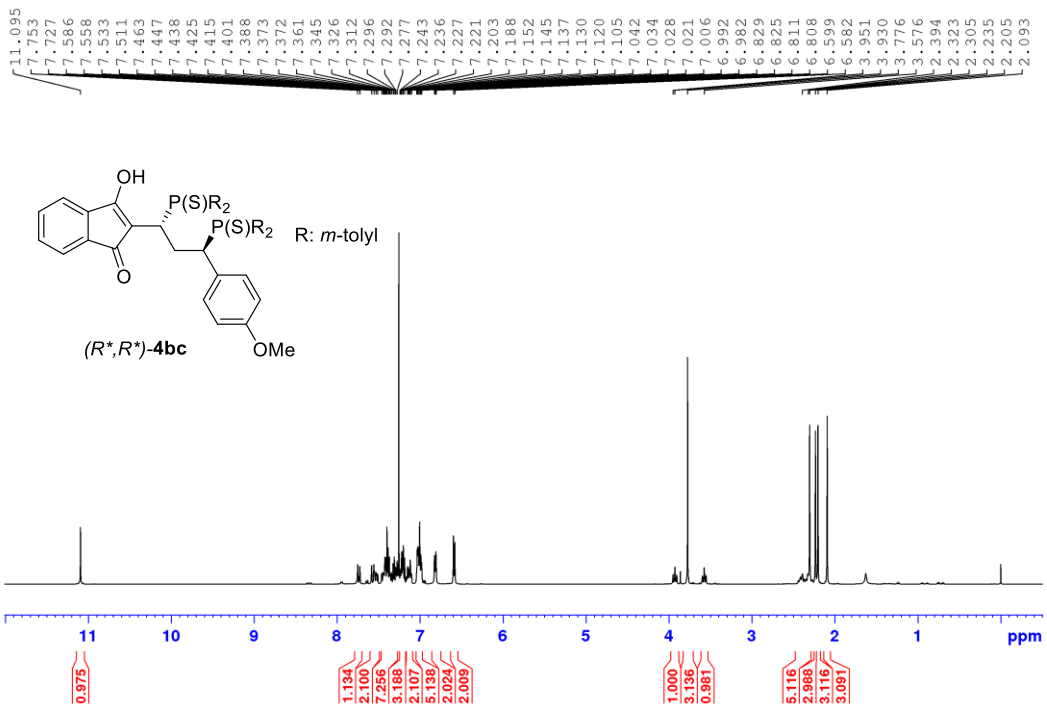

Figure S71 ^{13}C NMR (126 MHz, $CDCl_3$) spectrum of **4bc**.

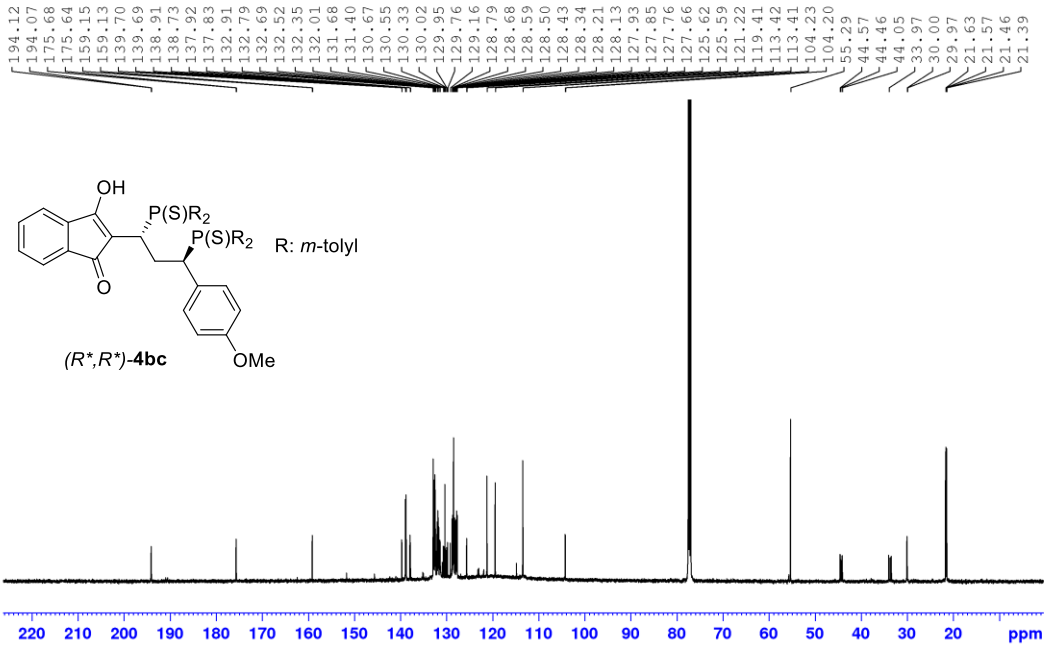

Figure S72 $^{31}P\{^1H\}$ NMR (162 MHz, $CDCl_3$) spectrum of **4bc**.

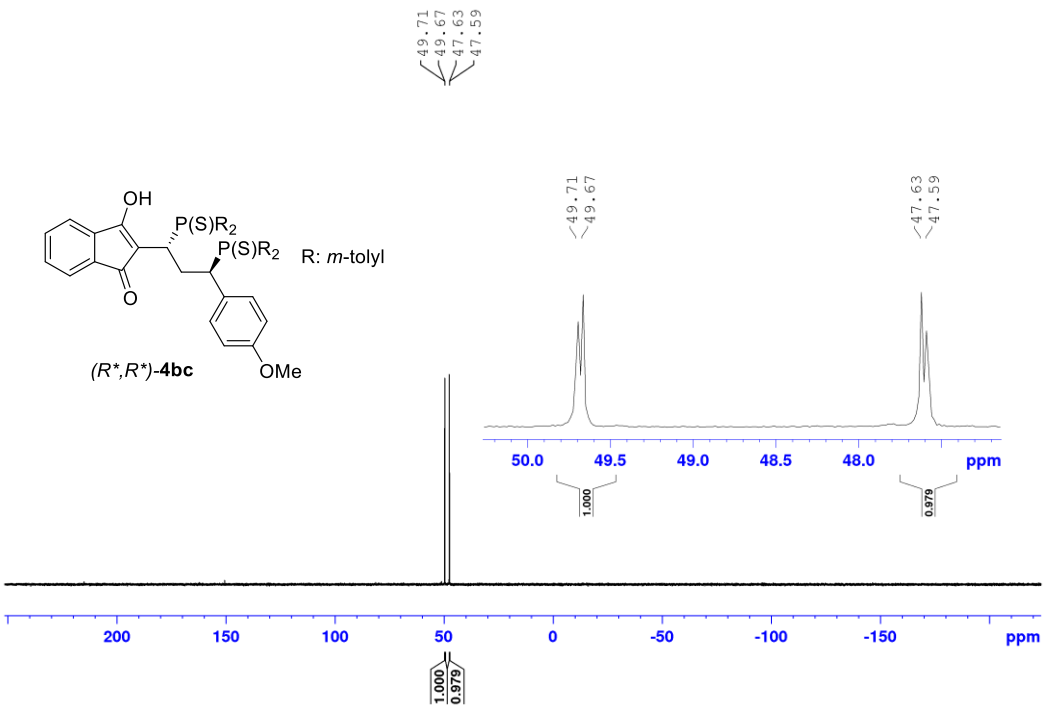

Figure S73 ^{1}H NMR (300 MHz, $CDCl_3$) spectrum of **4ca**.

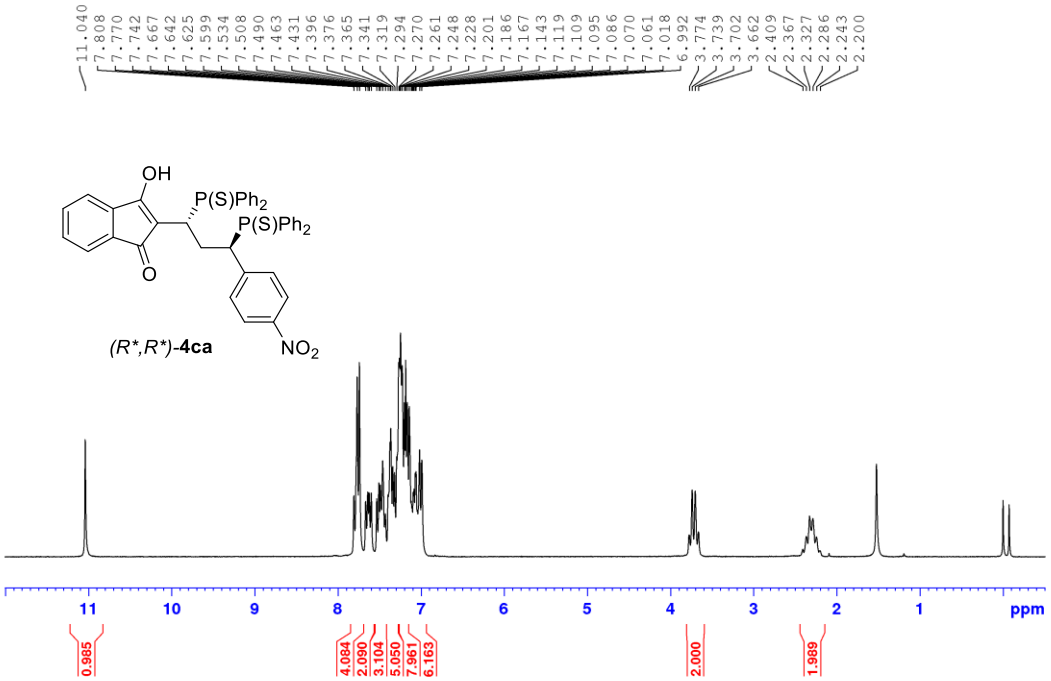

Figure S74 ^{13}C NMR (75 MHz, $CDCl_3$) spectrum of **4ca**.

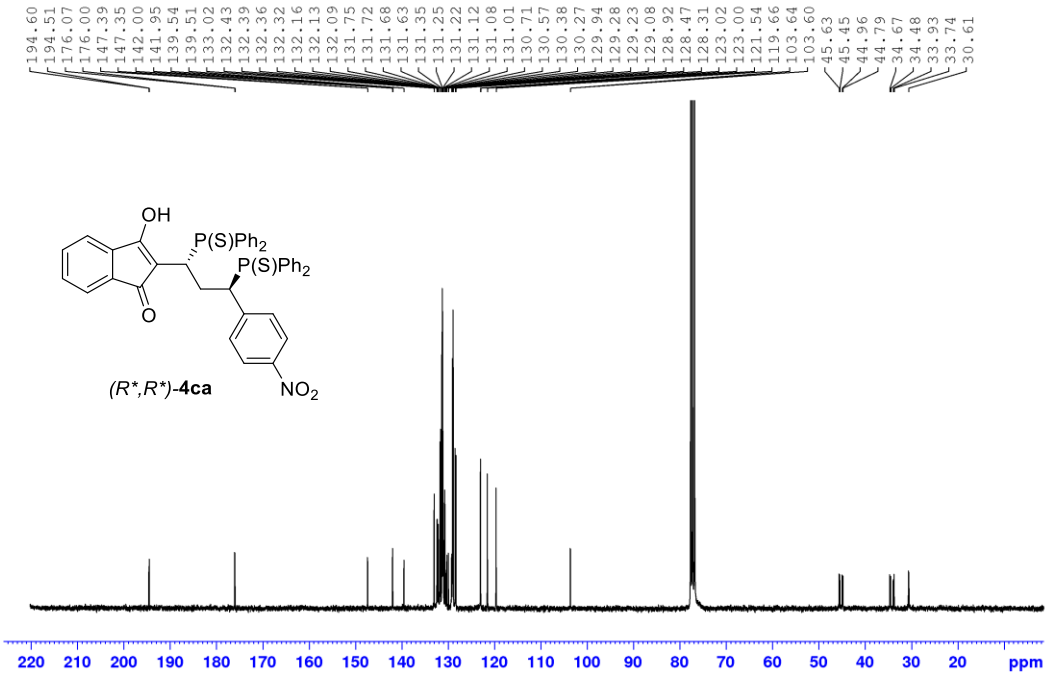

Figure S75 $^{31}P\{^{1}H\}$ NMR (162 MHz, $CDCl_3$) spectrum of **4ca**.

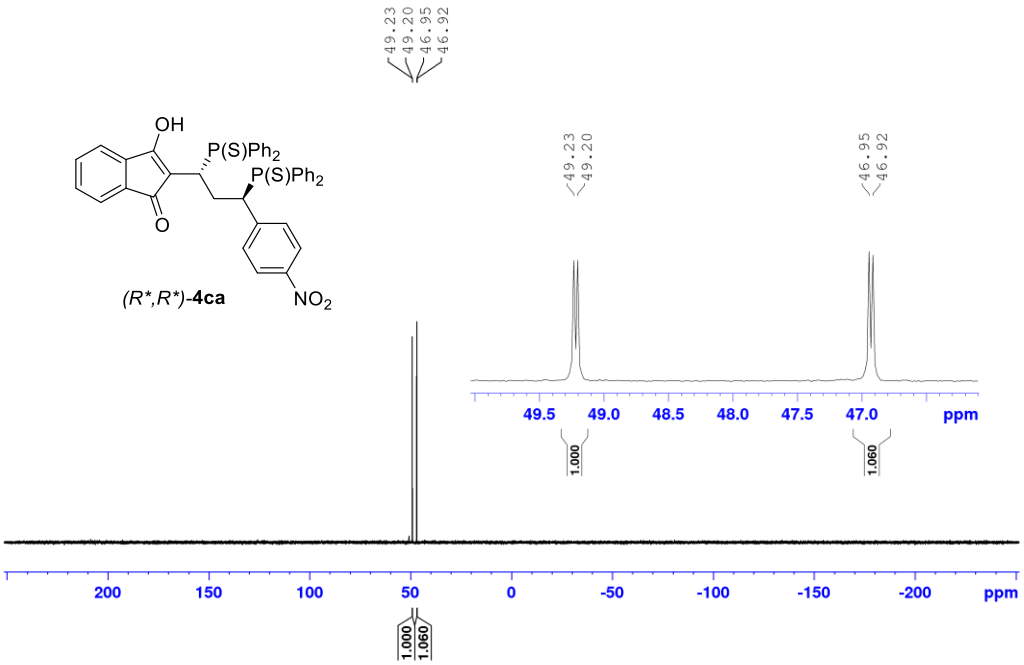

Figure S76 ^{1}H NMR (400 MHz, $CDCl_3$) spectrum of **4cb**.

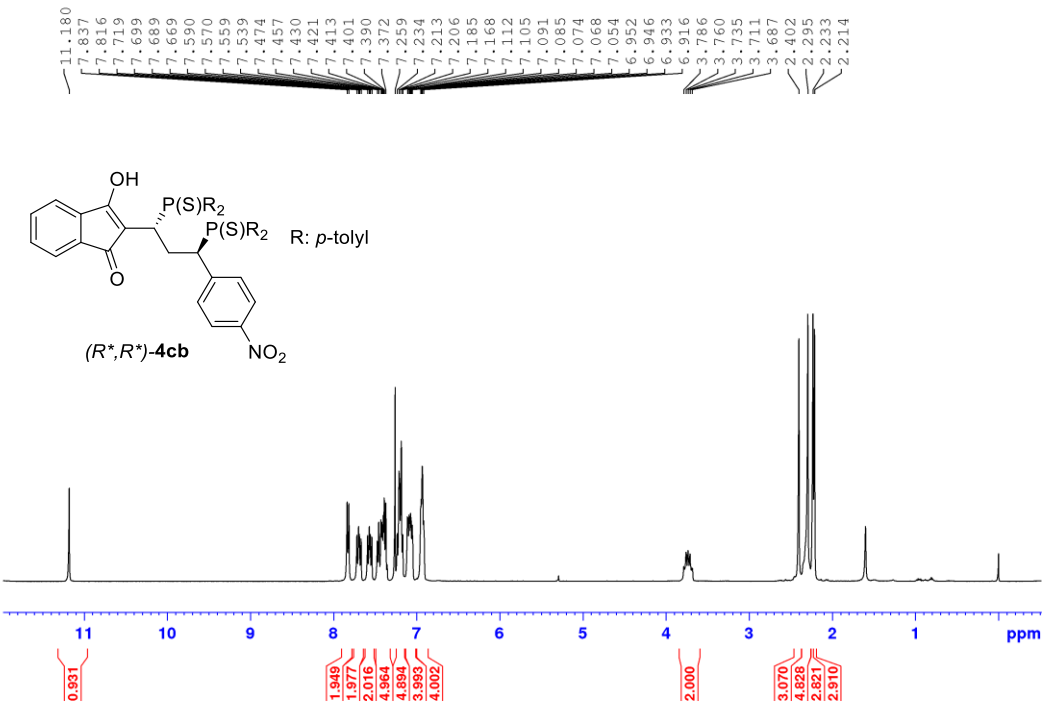

Figure S77 ^{13}C NMR (75 MHz, $CDCl_3$) spectrum of **4cb**.

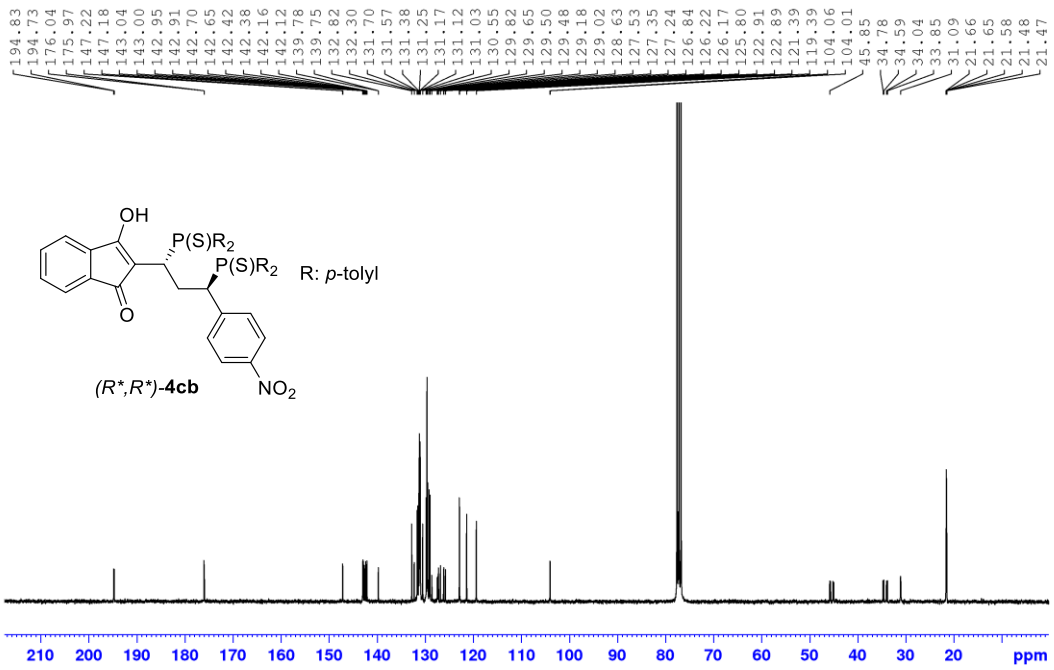

Figure S78 $^{31}P\{^1H\}$ NMR (162 MHz, $CDCl_3$) spectrum of **4cb**.

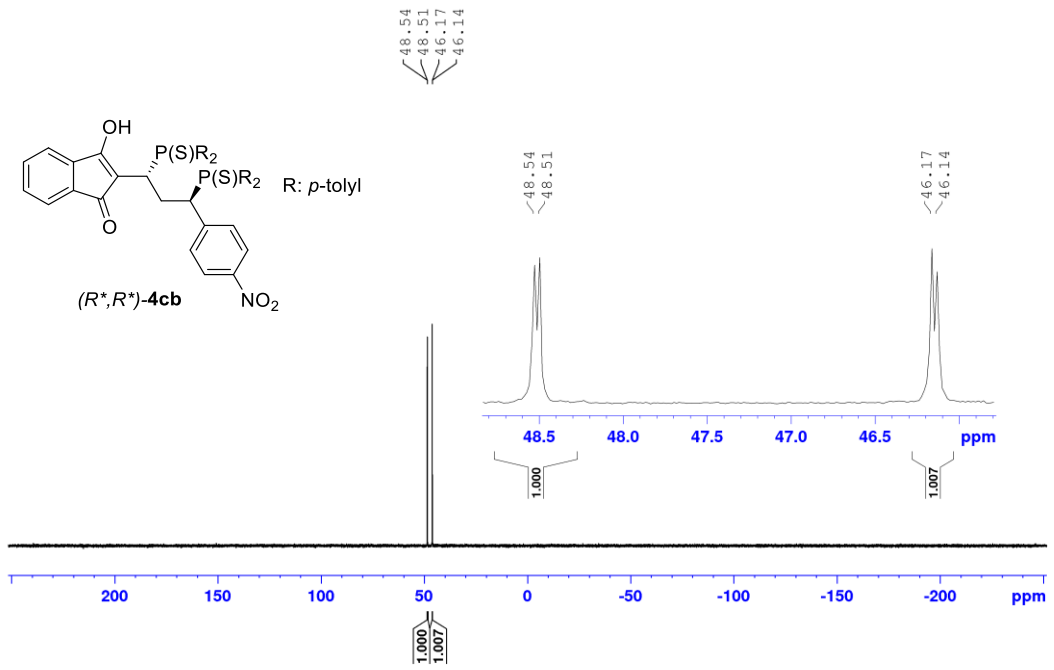

Figure S79 ^{1}H NMR (400 MHz, $CDCl_3$) spectrum of **4cc**.

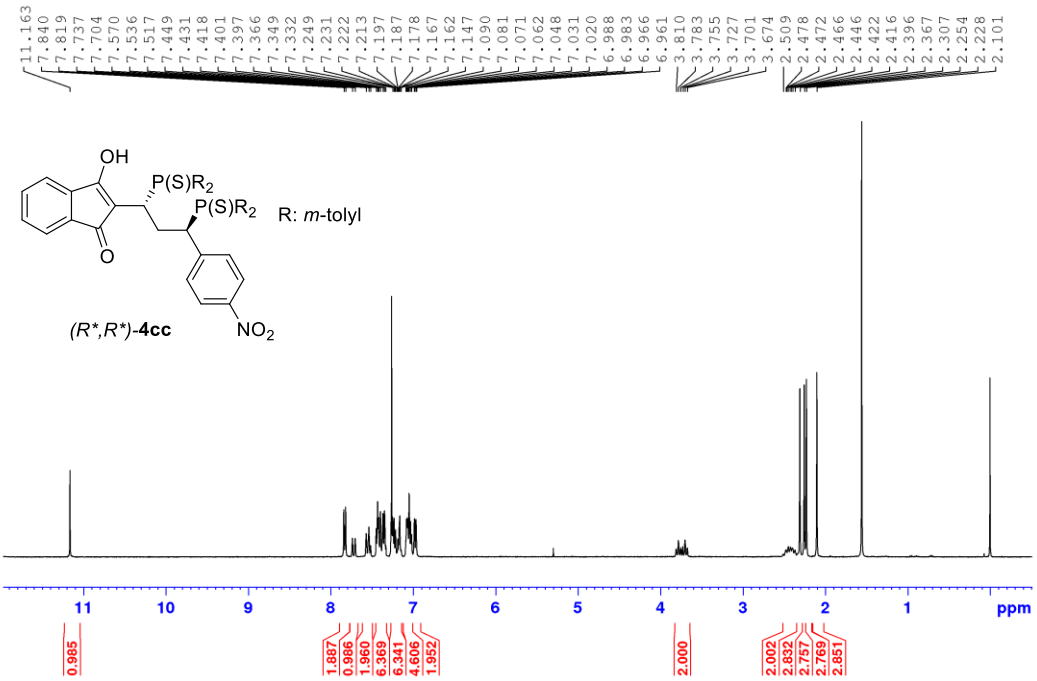

Figure S80 ^{13}C NMR (101 MHz, $CDCl_3$) spectrum of **4cc**.

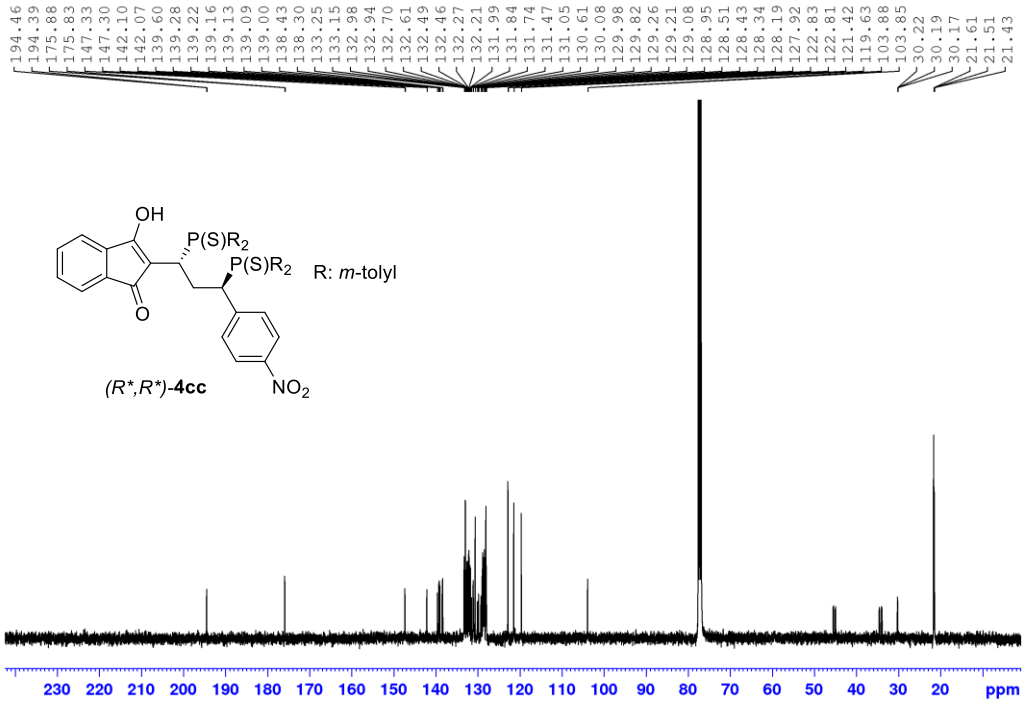

Figure S81 $^{31}P\{^{1}H\}$ NMR (162 MHz, $CDCl_3$) spectrum of **4cc**.

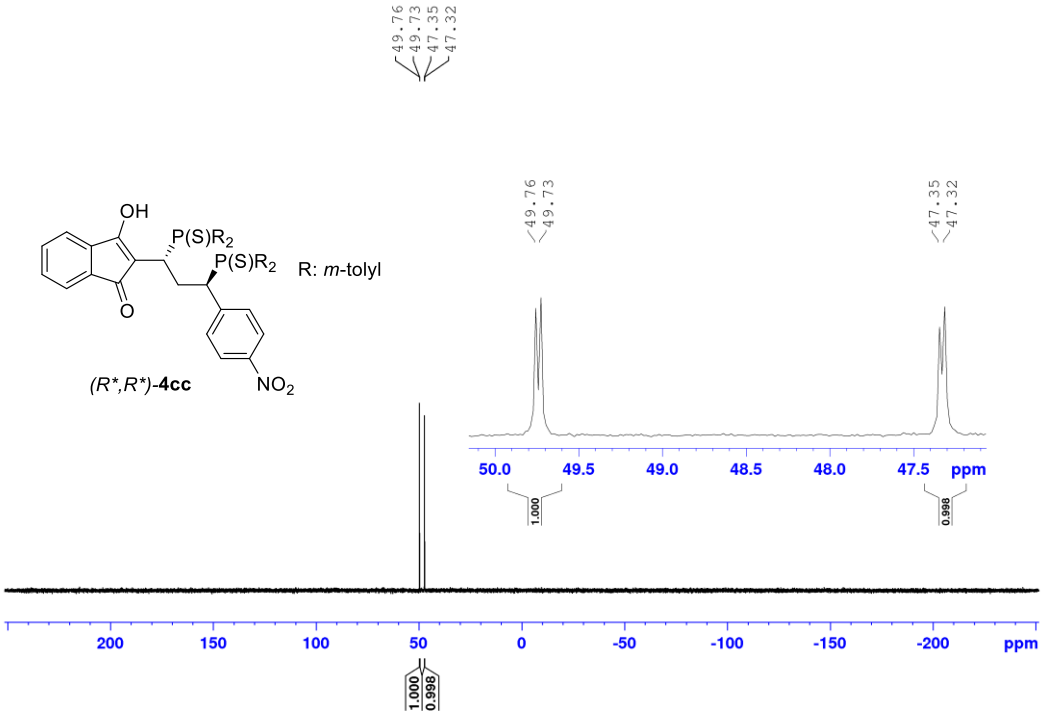

Figure S82 ^{1}H NMR (400 MHz, $CDCl_3$) spectrum of **4da**.

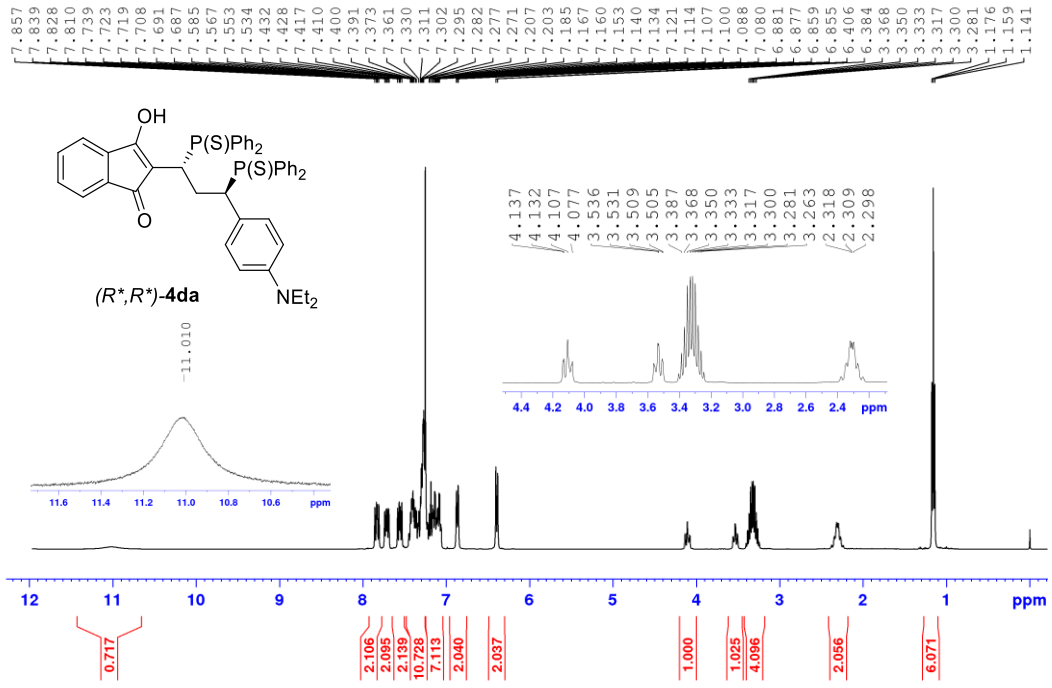

Figure S83 ^{13}C NMR (101 MHz, $CDCl_3$) spectrum of **4da**.

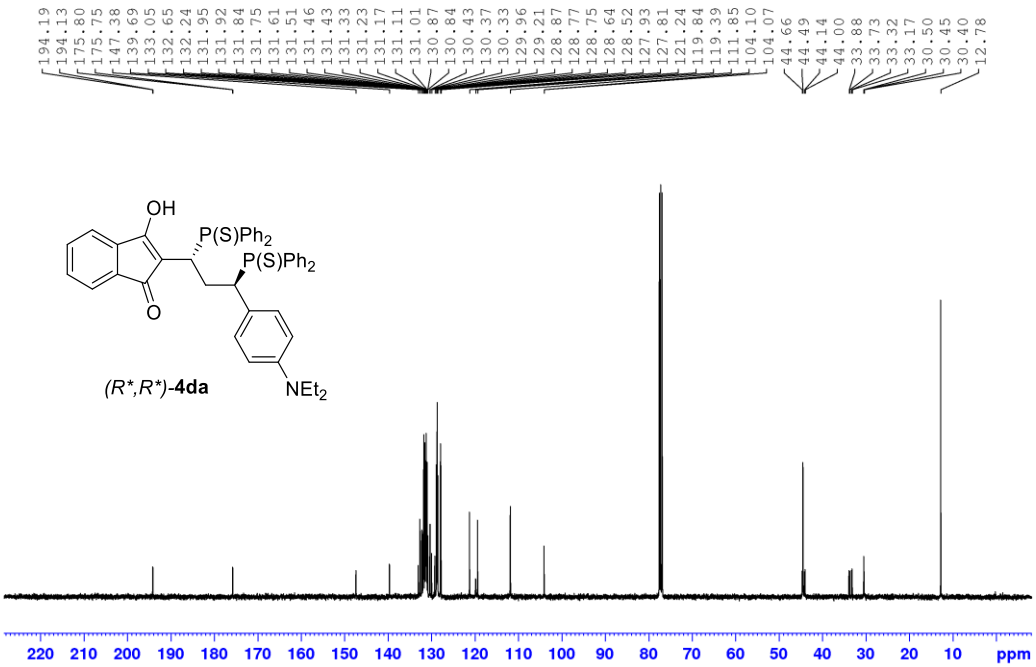

Figure S84 $^{31}P\{^1H\}$ NMR (162 MHz, $CDCl_3$) spectrum of **4da**.

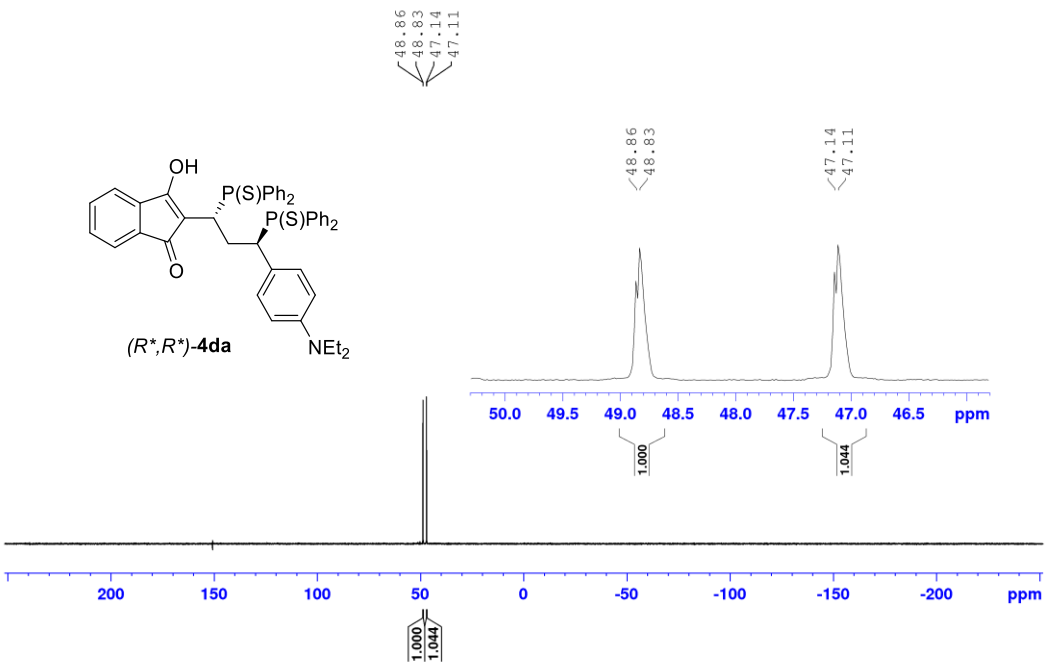

Figure S85 ^{1}H NMR (500 MHz, $CDCl_3$) spectrum of **4ea**.

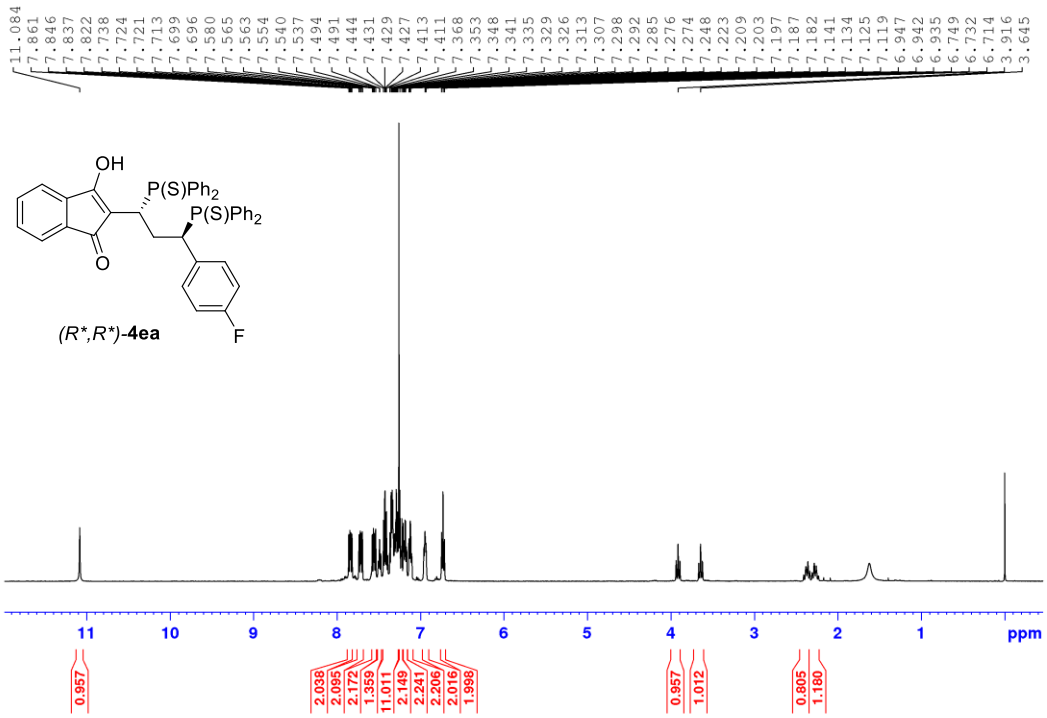

Figure S86 ^{13}C NMR (126 MHz, $CDCl_3$) spectrum of **4ea**.

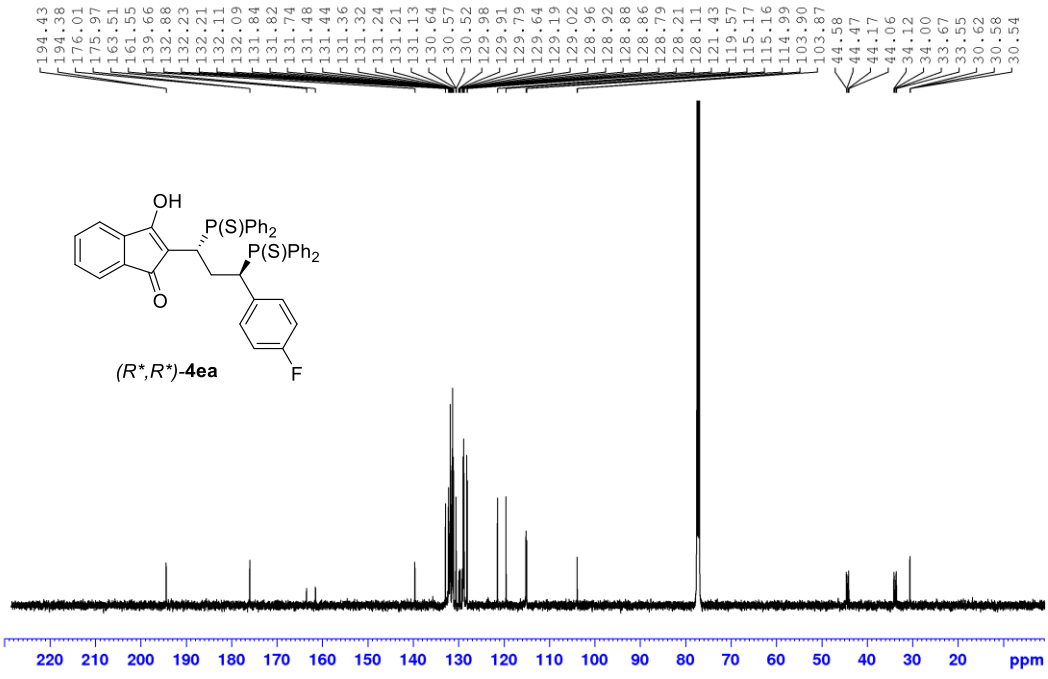

Figure S87 $^{31}P\{^{1}H\}$ NMR (202 MHz, $CDCl_3$) spectrum of **4ea**.

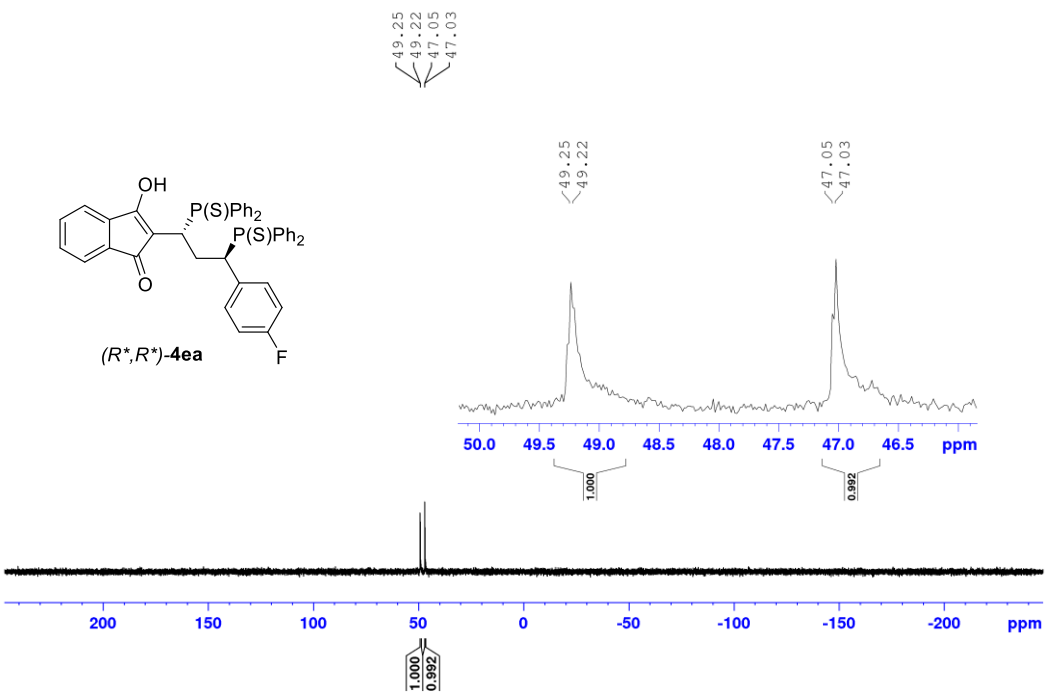

Figure S88 ^{1}H NMR (500 MHz, $CDCl_3$) spectrum of **4fa**.

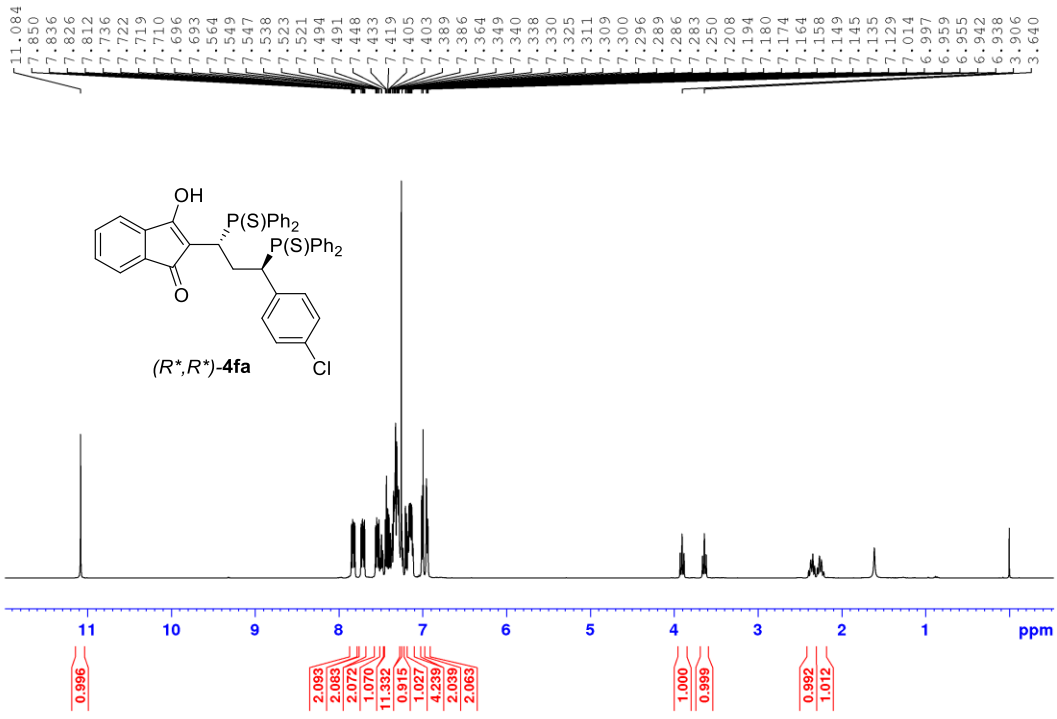

Figure S89 ^{13}C NMR (126 MHz, $CDCl_3$) spectrum of **4fa**.

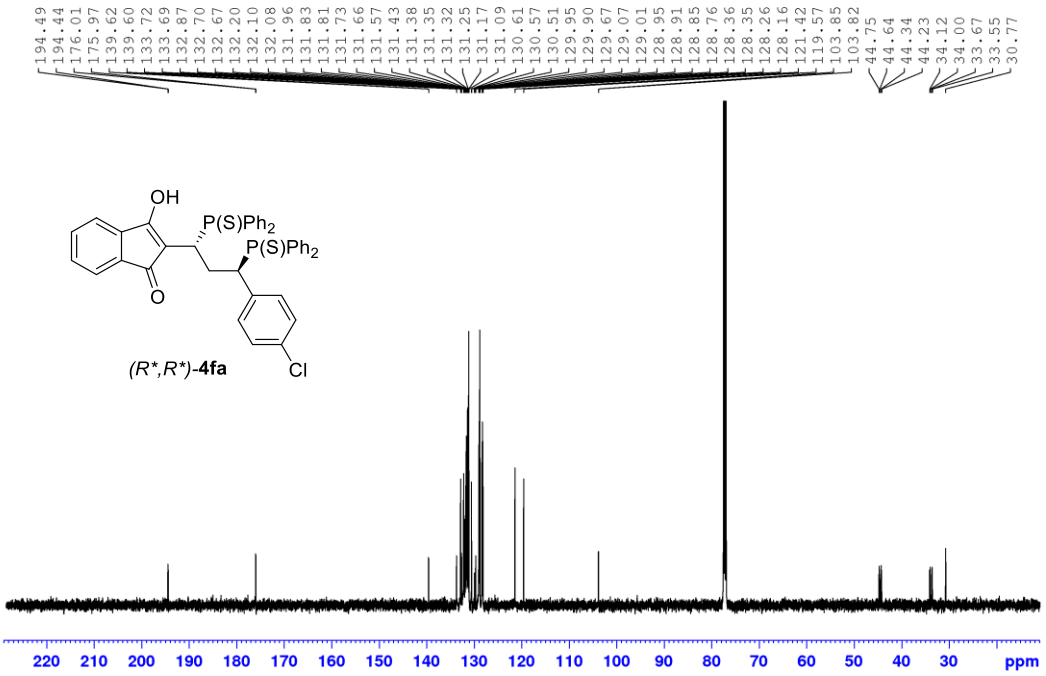

Figure S90 $^{31}P\{^1H\}$ NMR (202 MHz, $CDCl_3$) spectrum of **4fa**.

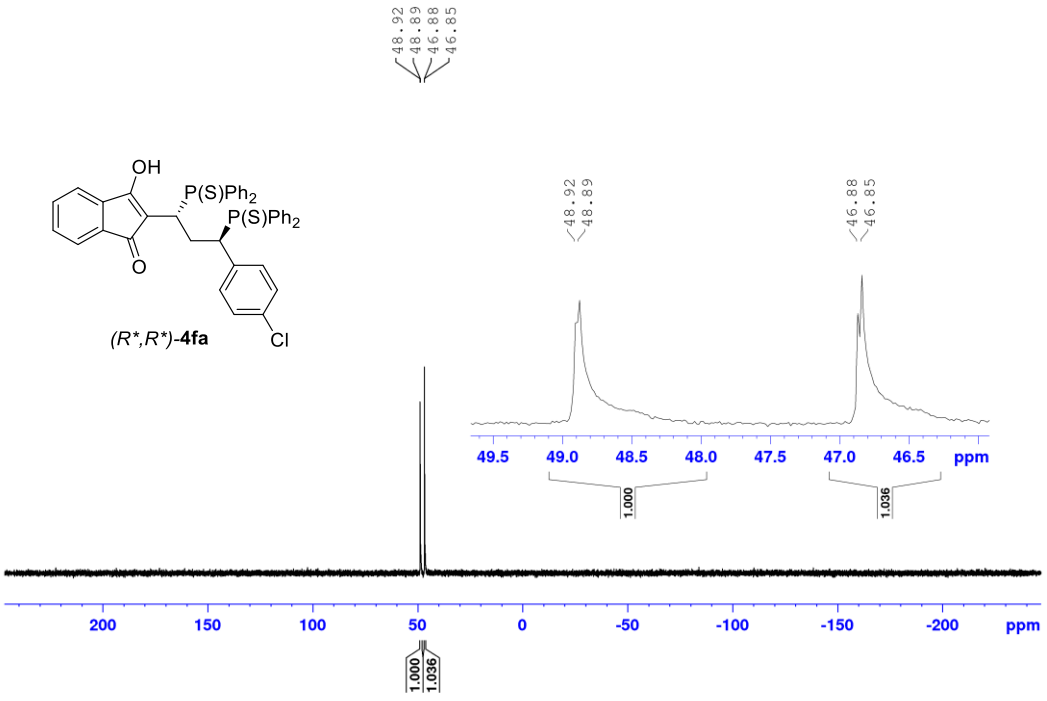

Figure S91 ^{1}H NMR (500 MHz, $CDCl_3$) spectrum of **4ga**.

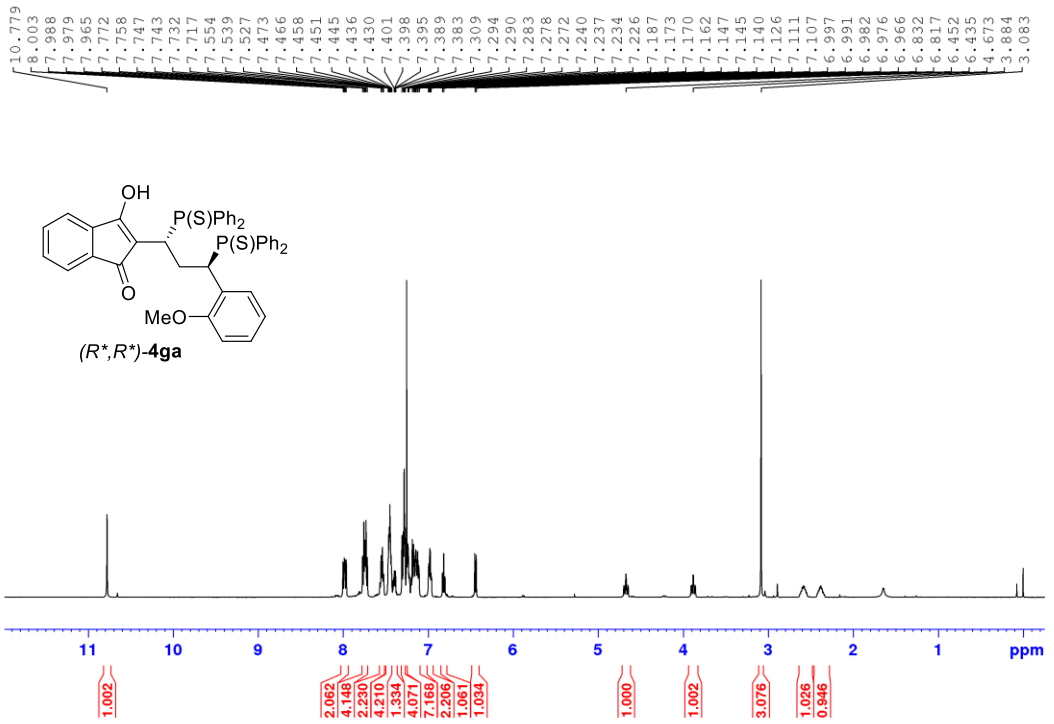

Figure S92 ^{13}C NMR (126 MHz, $CDCl_3$) spectrum of **4ga**.

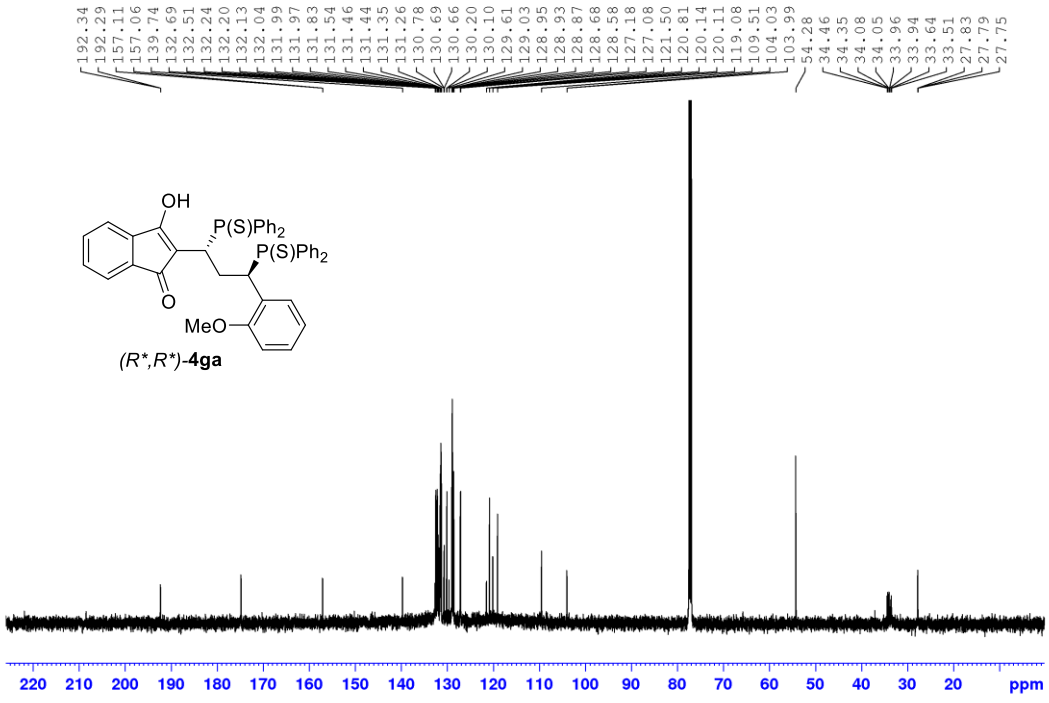

Figure S93 $^{31}P\{^{1}H\}$ NMR (202 MHz, $CDCl_3$) spectrum of **4ga**.

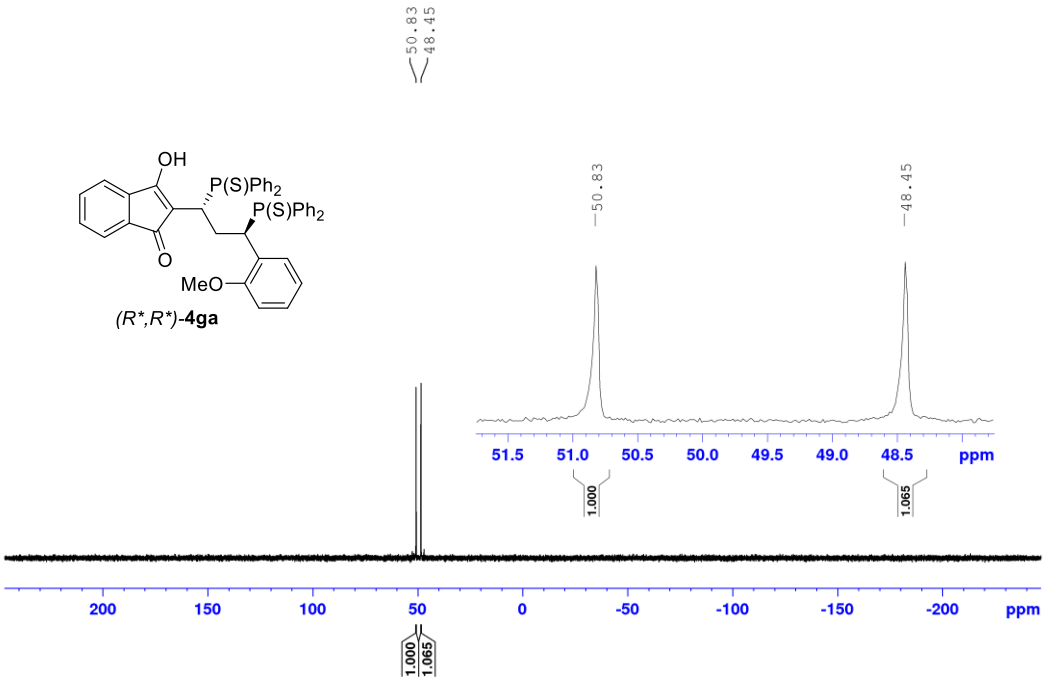

Figure S94 ^{1}H NMR (400 MHz, $CDCl_3$) spectrum of **4gb**.

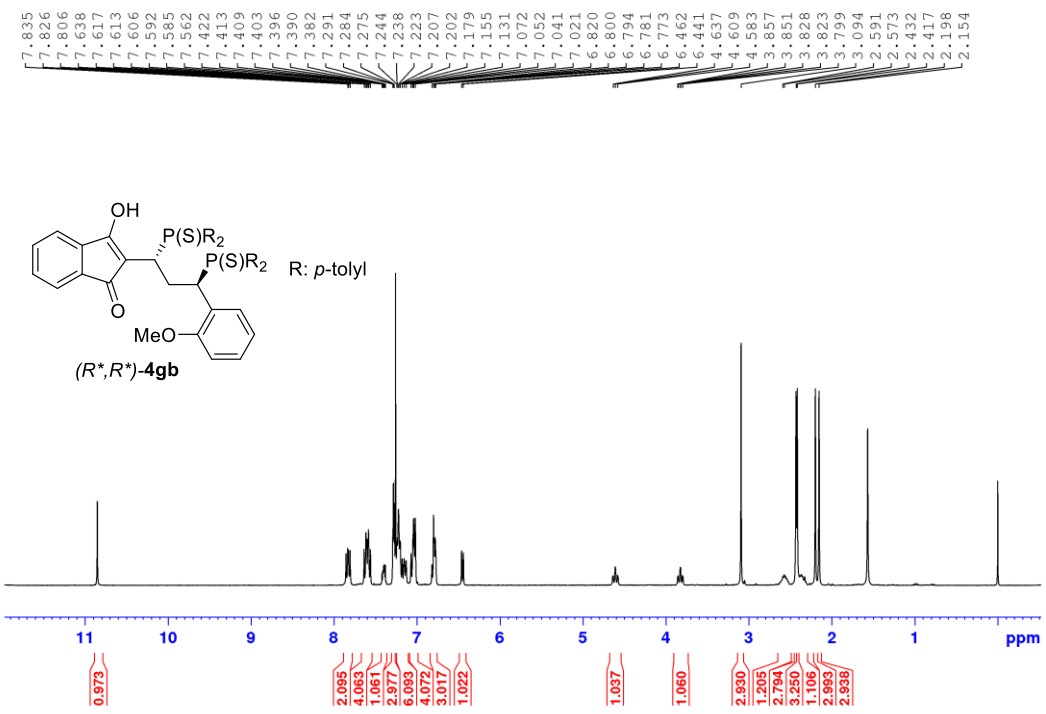

Figure S95 ^{13}C NMR (101 MHz, $CDCl_3$) spectrum of **4gb**.

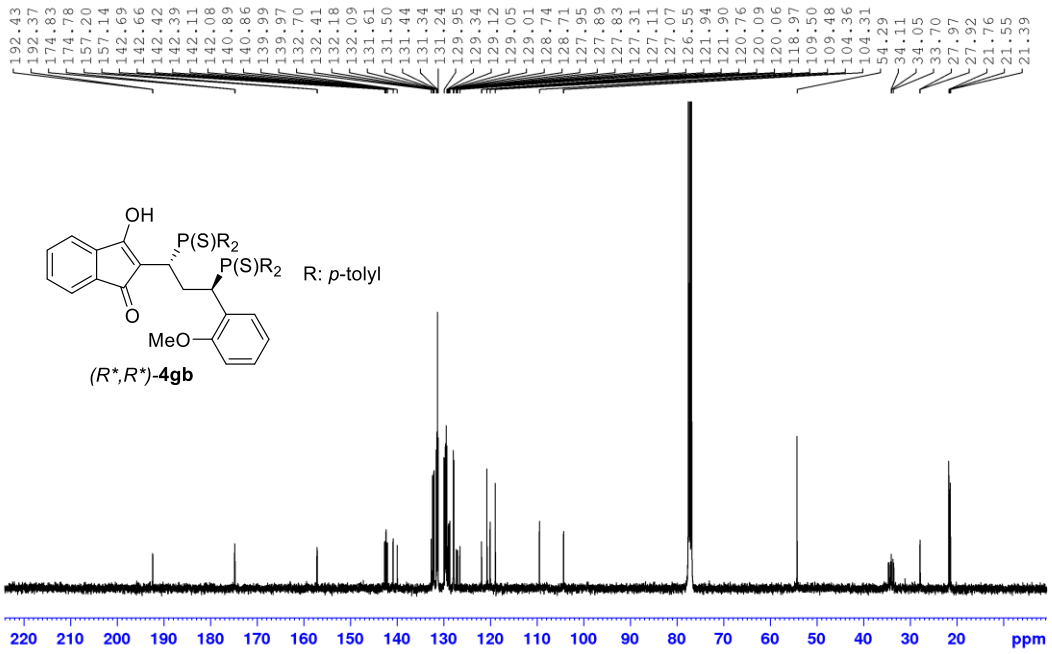

Figure S96 $^{31}P\{^1H\}$ NMR (162 MHz, $CDCl_3$) spectrum of **4gb**.

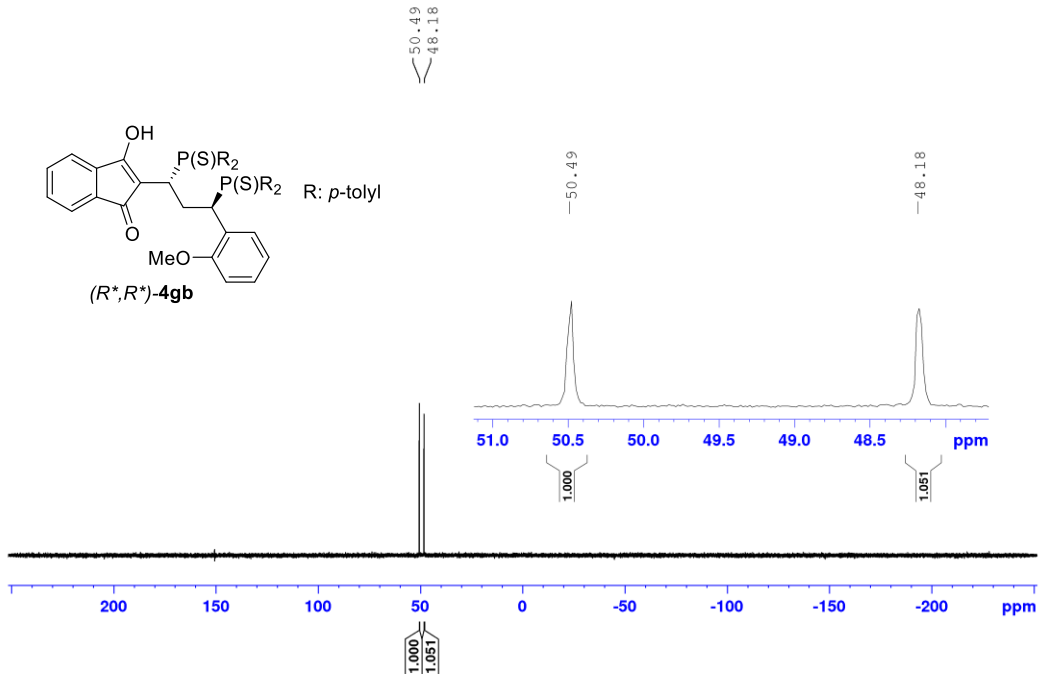

Figure S97 ^{1}H NMR (500 MHz, $CDCl_3$) spectrum of **4gc**.

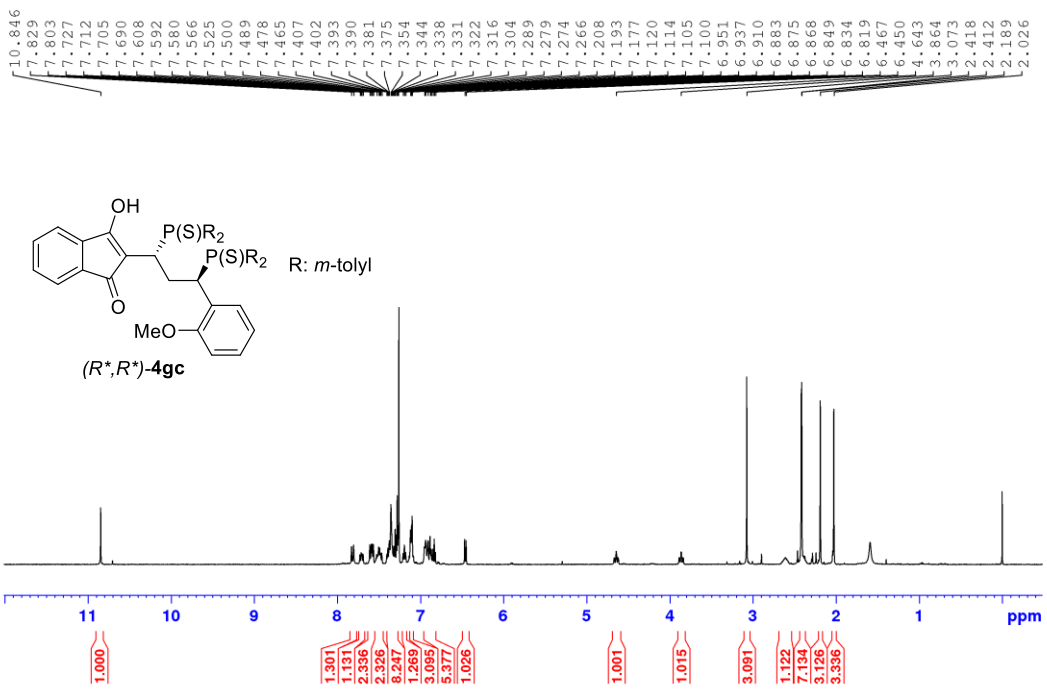

Figure S98 ^{13}C NMR (126 MHz, $CDCl_3$) spectrum of **4gc**.

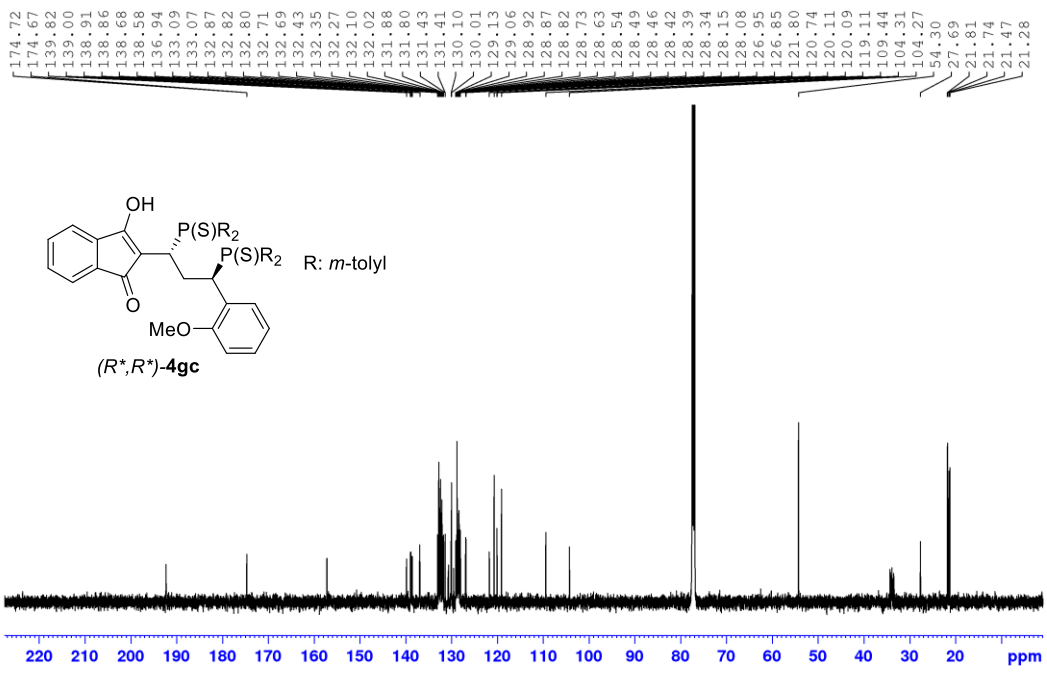

Figure S99 $^{31}P\{^{1}H\}$ NMR (202 MHz, $CDCl_3$) spectrum of **4gc**.

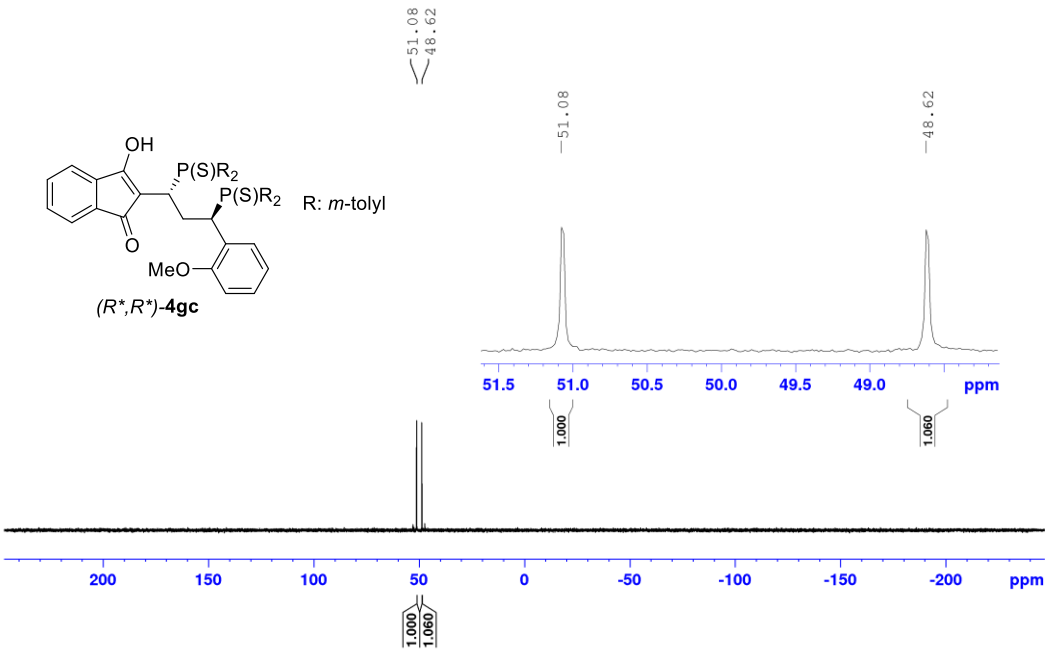

Figure S100 ^{1}H NMR (500 MHz, $CDCl_3$, mixture) spectrum of **4ha**.

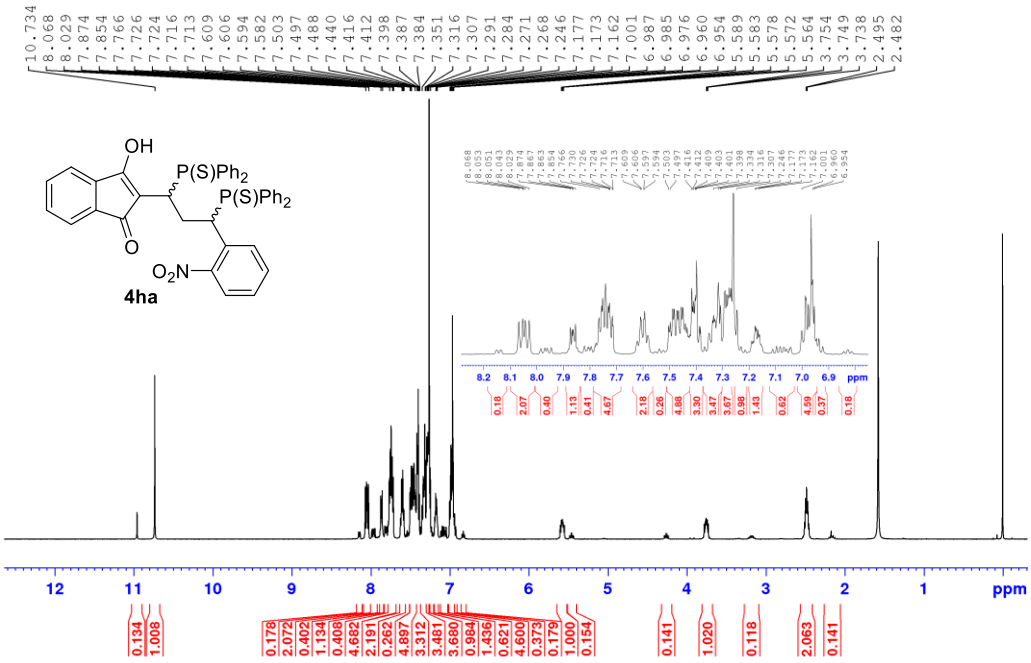

Figure S101 ^{13}C NMR (126 MHz, $CDCl_3$, mixture) spectrum of **4ha**.

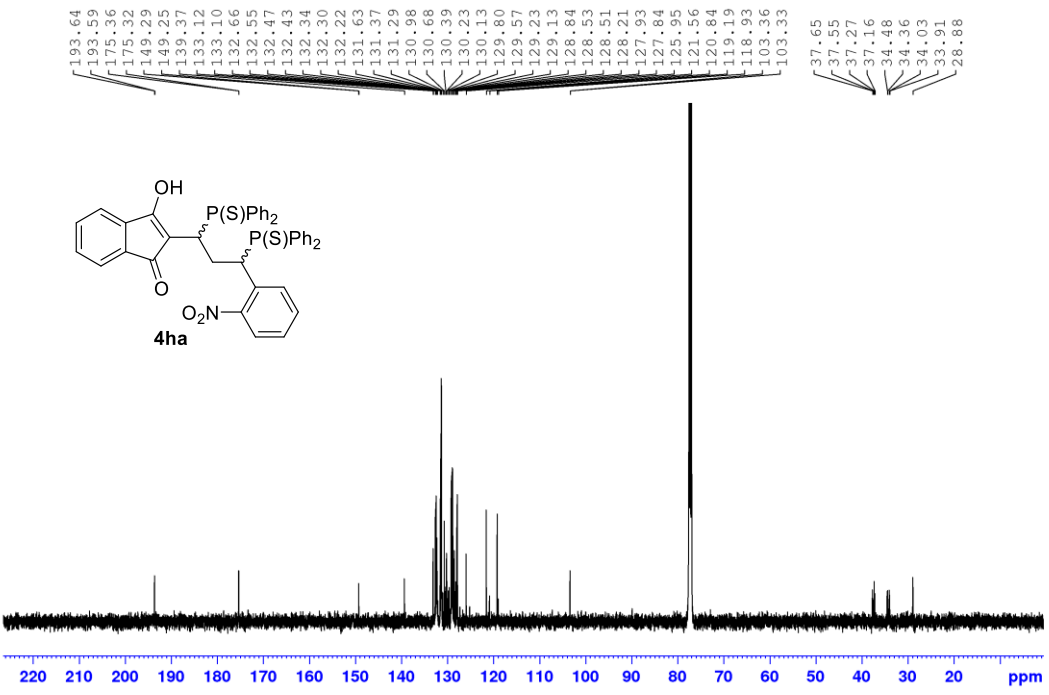

Figure S102 $^{31}P\{^{1}H\}$ NMR (202 MHz, $CDCl_3$, mixture) spectrum of **4ha**.

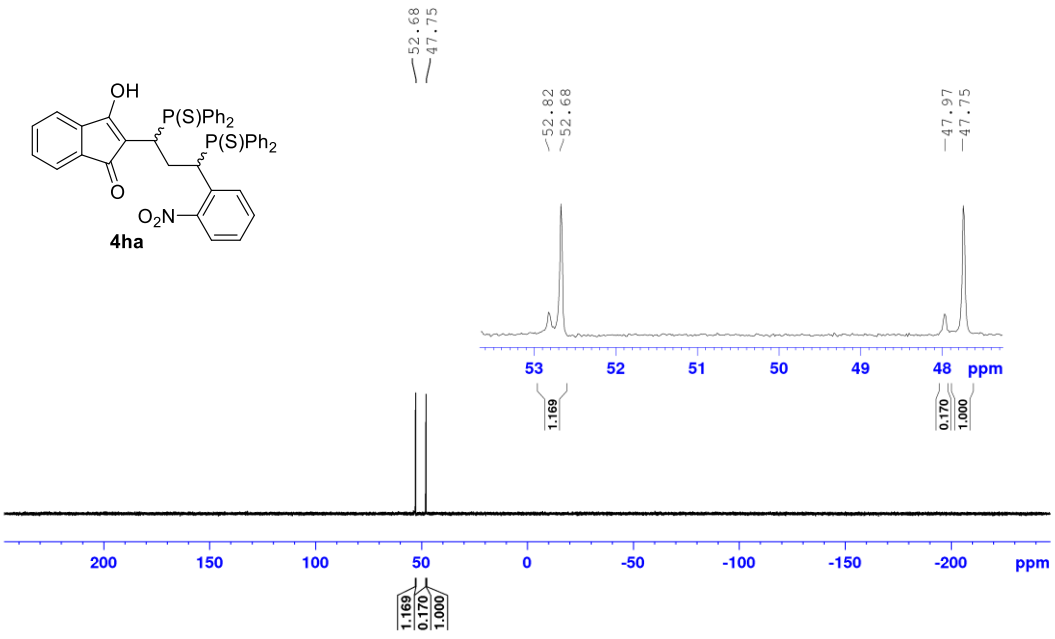

Figure S103 ^{1}H NMR (500 MHz, $CDCl_3$) spectrum of **9**.

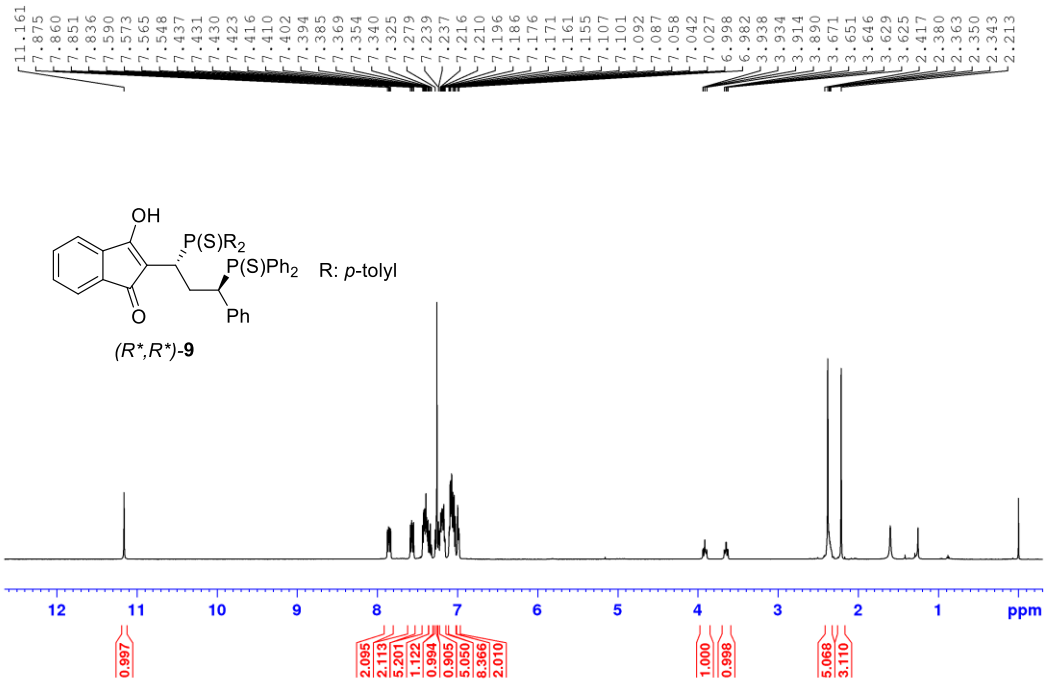

Figure S104 ^{13}C NMR (126 MHz, $CDCl_3$) spectrum of **9**.

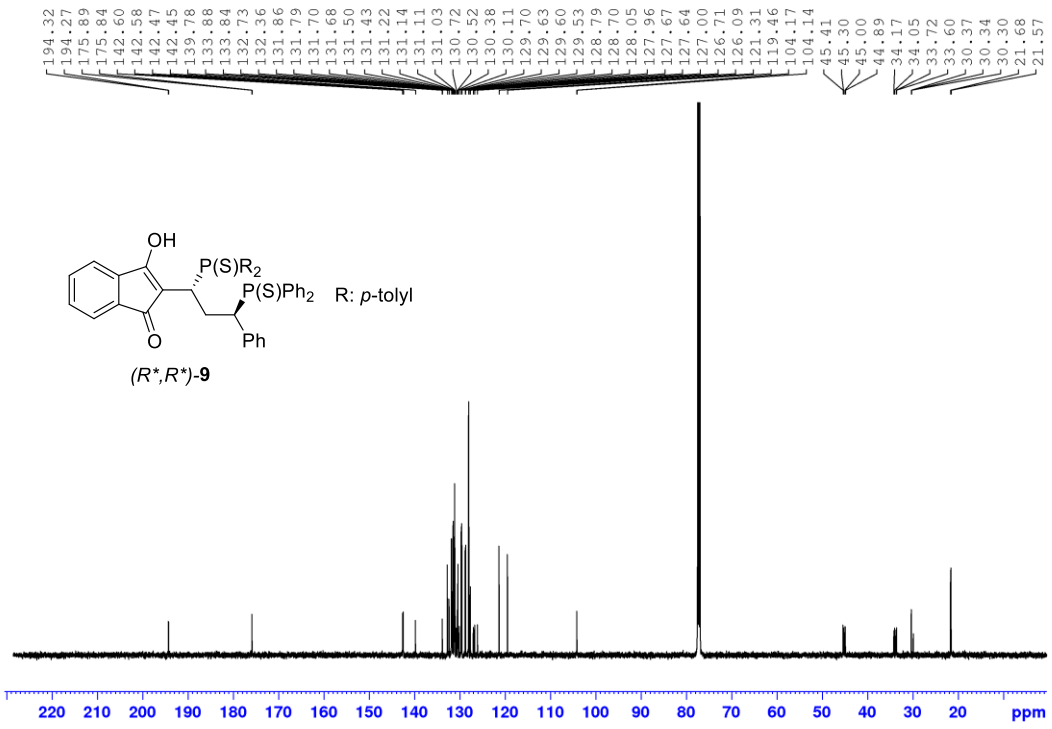

Figure S105 $^{31}P\{^{1}H\}$ NMR (202 MHz, $CDCl_3$, mixture) spectrum of **9**.

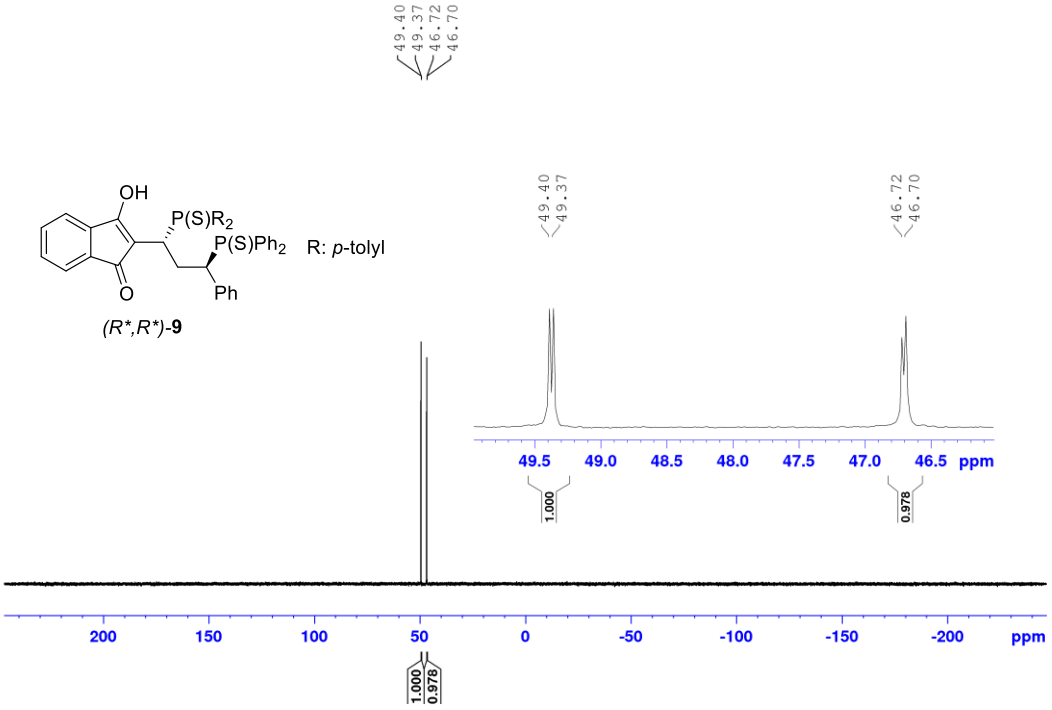

Figure S106 ^{1}H NMR (400 MHz, $CDCl_3$) spectrum of **6**.

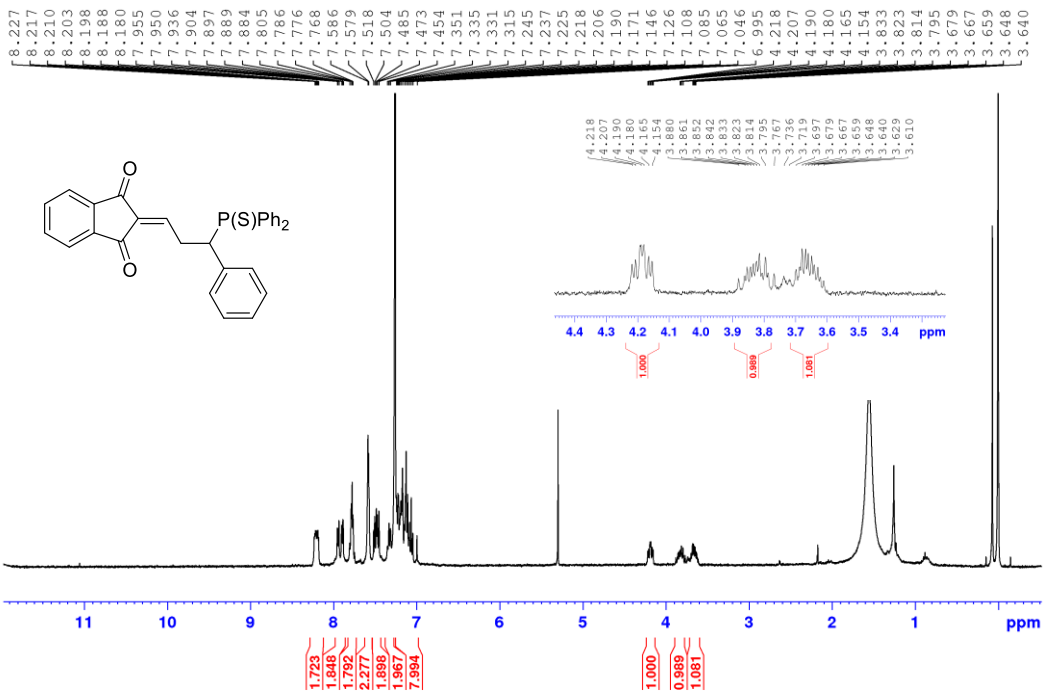

Figure S107 ^{13}C NMR (101 MHz, $CDCl_3$) spectrum of **6**.

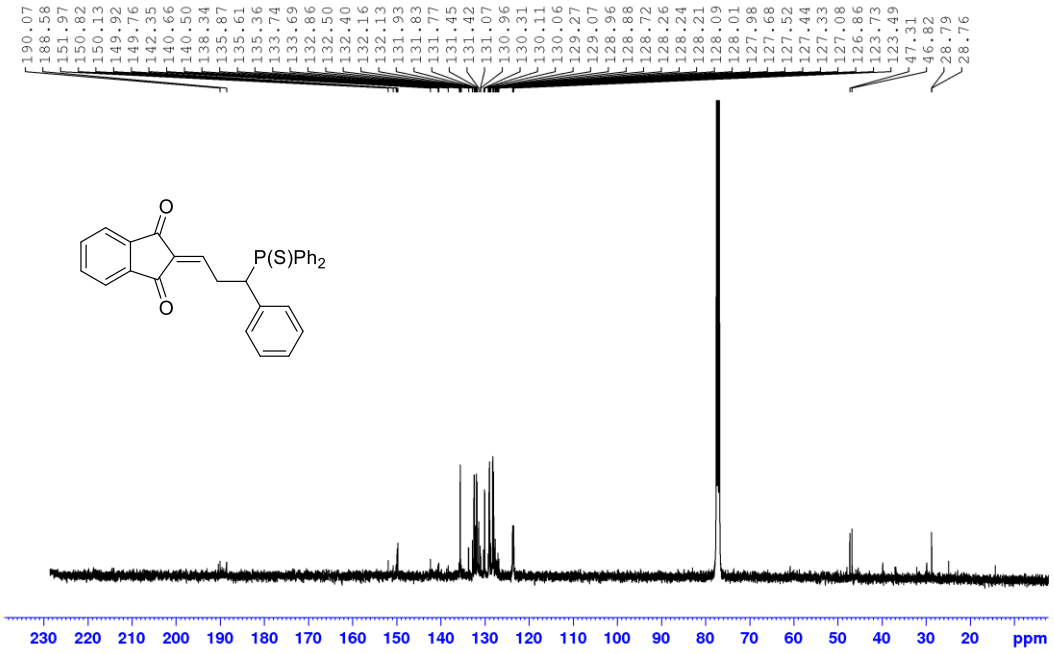

Figure S108 $^{31}P\{^1H\}$ NMR (162 MHz, $CDCl_3$) spectrum of **6**.

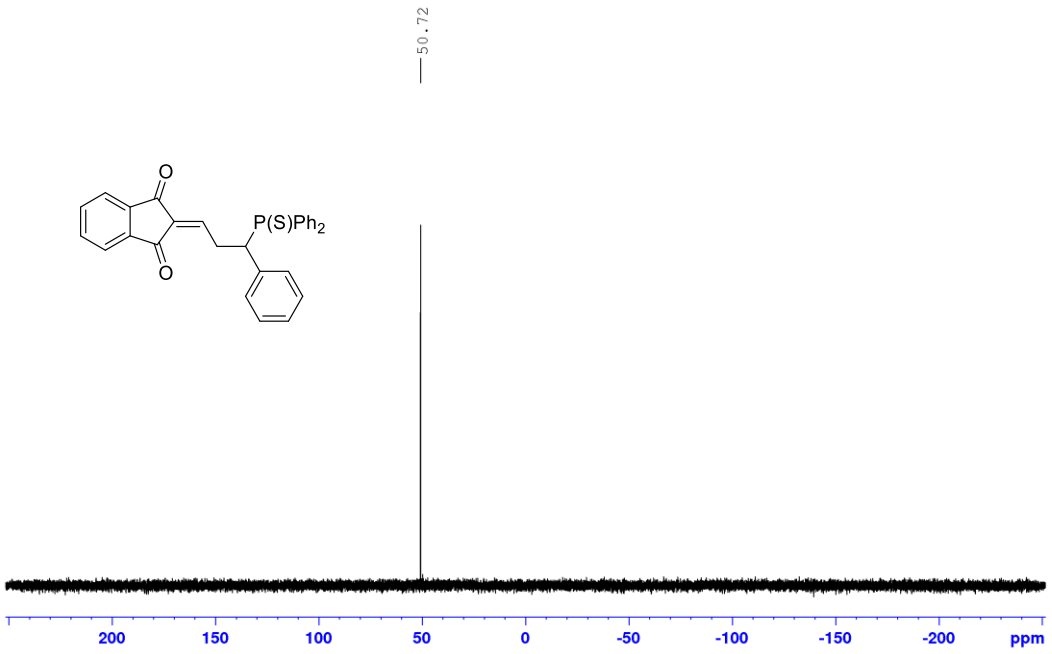

Figure S109 ^{1}H NMR (400 MHz, $CDCl_3$) spectrum of *(S,R,R,S)*-**16a**.

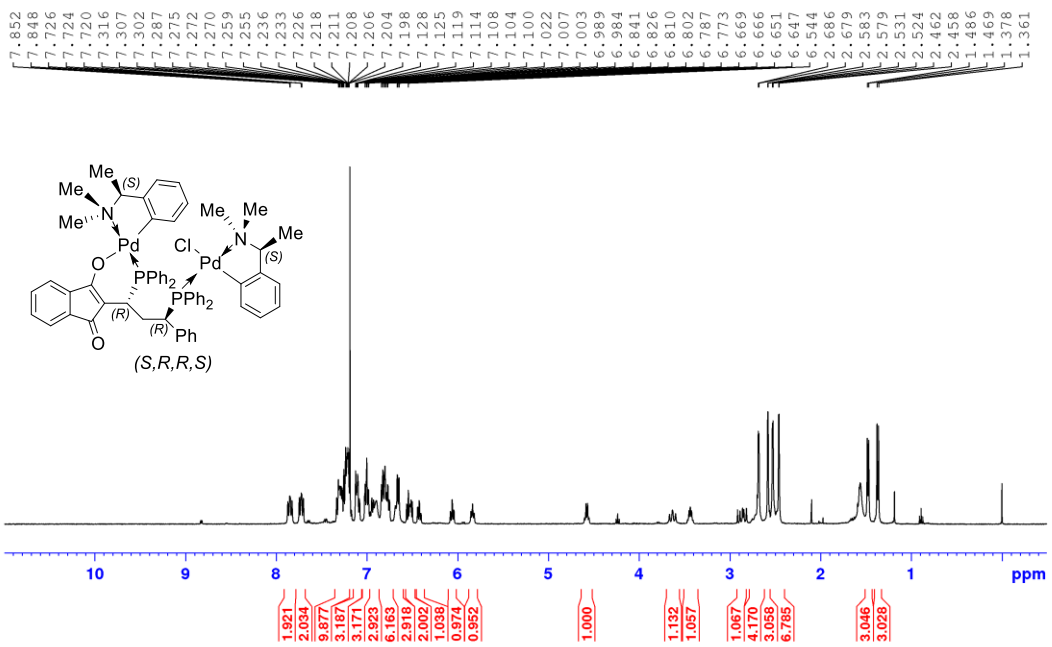

Figure S110 ^{13}C NMR (101 MHz, $CDCl_3$) spectrum of *(S,R,R,S)*-**16a**.

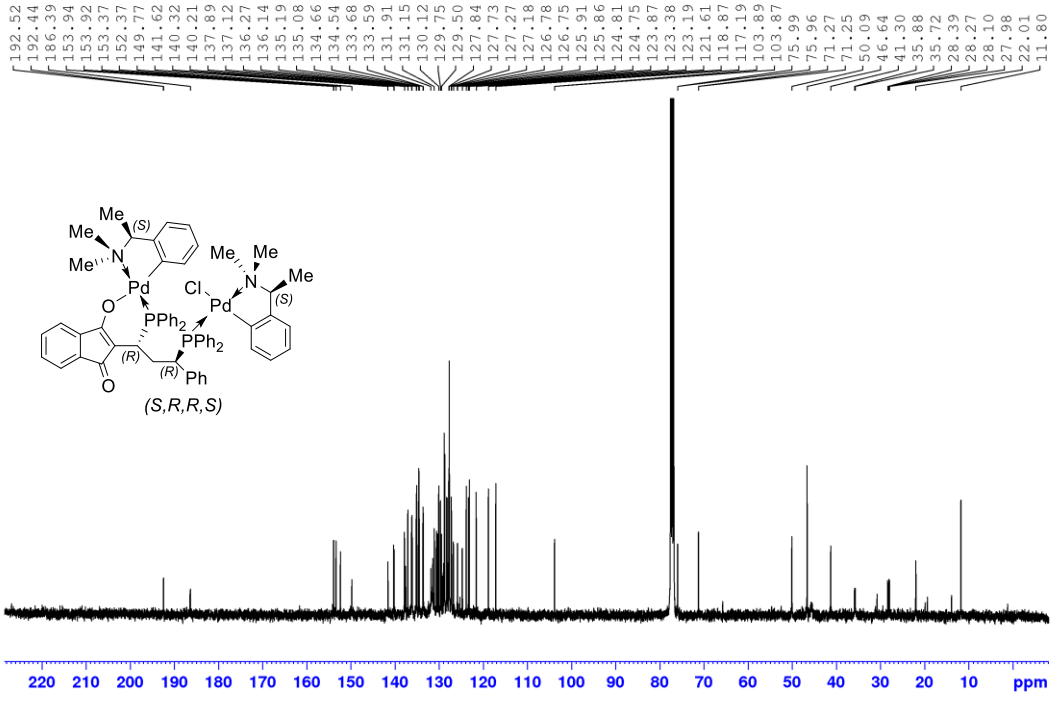

Figure S111 $^{31}P\{^{1}H\}$ NMR (162 MHz, $CDCl_3$) spectrum of *(S,R,R,S)*-**16a**.

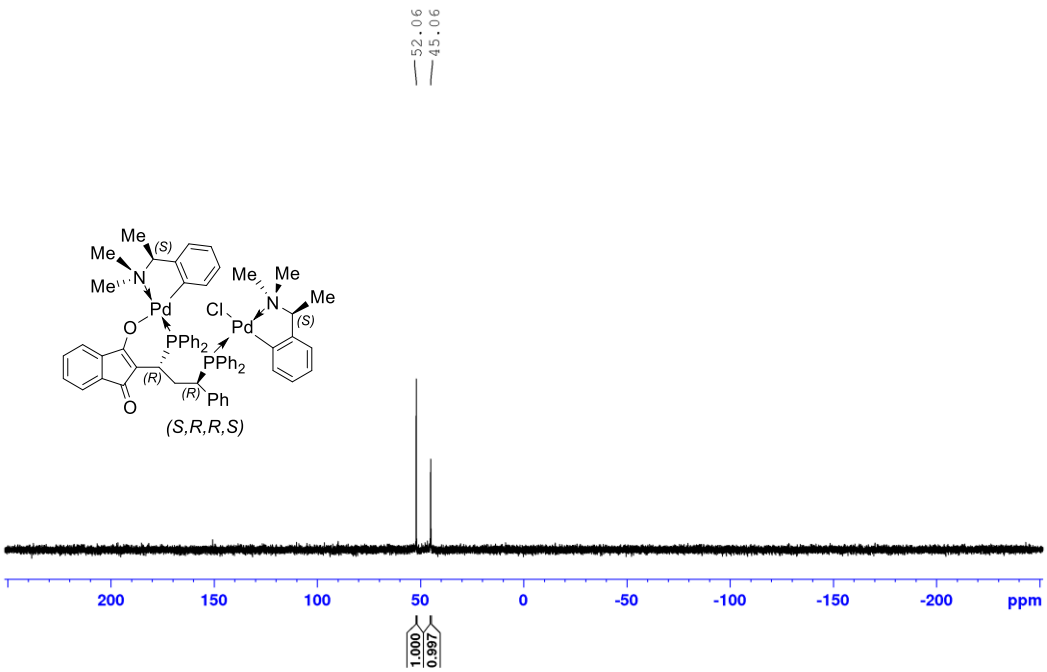

Figure S112 ^{1}H NMR (400 MHz, $CDCl_3$) spectrum of *(S,S,S,S)*-**16b**.

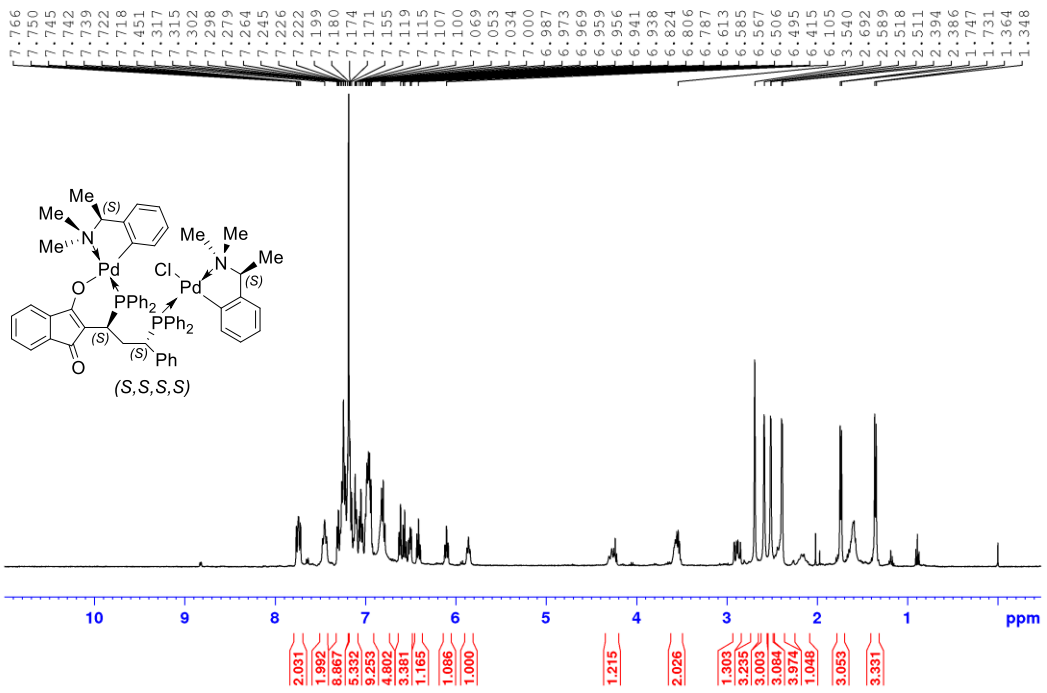

Figure S113 ^{13}C NMR (101 MHz, $CDCl_3$) spectrum of *(S,S,S,S)*-**16b**.

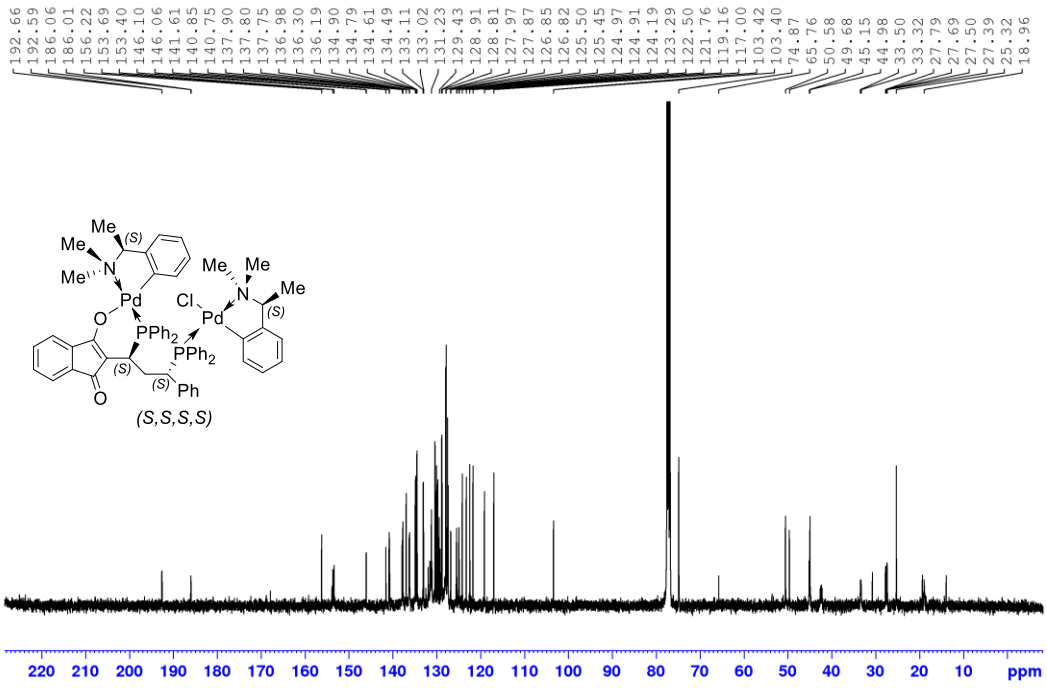

Figure S114 $^{31}P\{^1H\}$ NMR (162 MHz, $CDCl_3$) spectrum of *(S,S,S,S)*-**16b**.

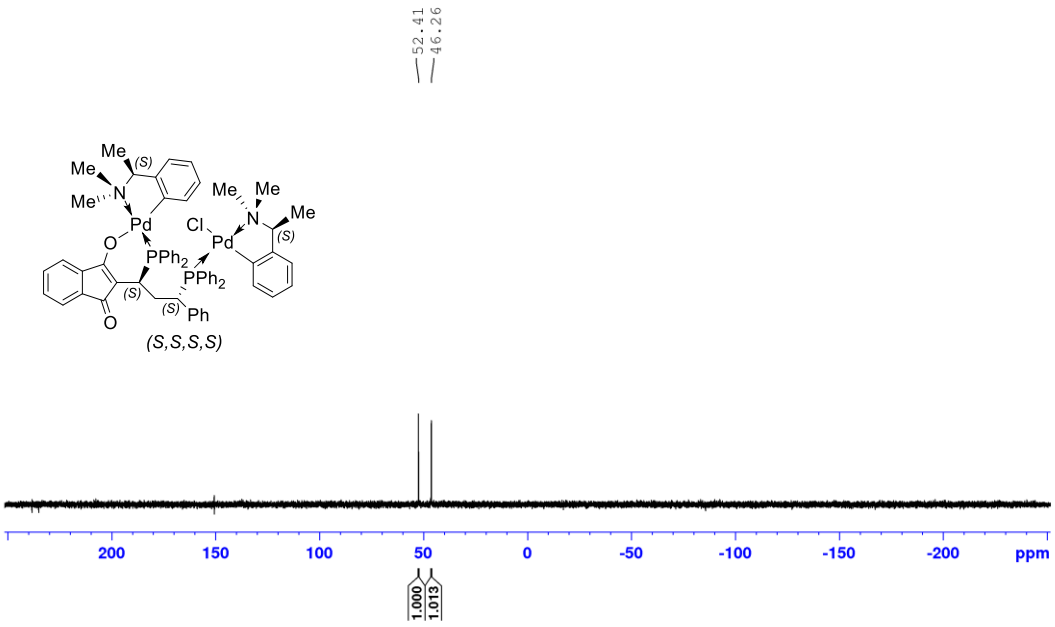

Figure S115 ^{1}H NMR (400 MHz, $CDCl_3$) spectrum of *(S,R,R)*-**18**.

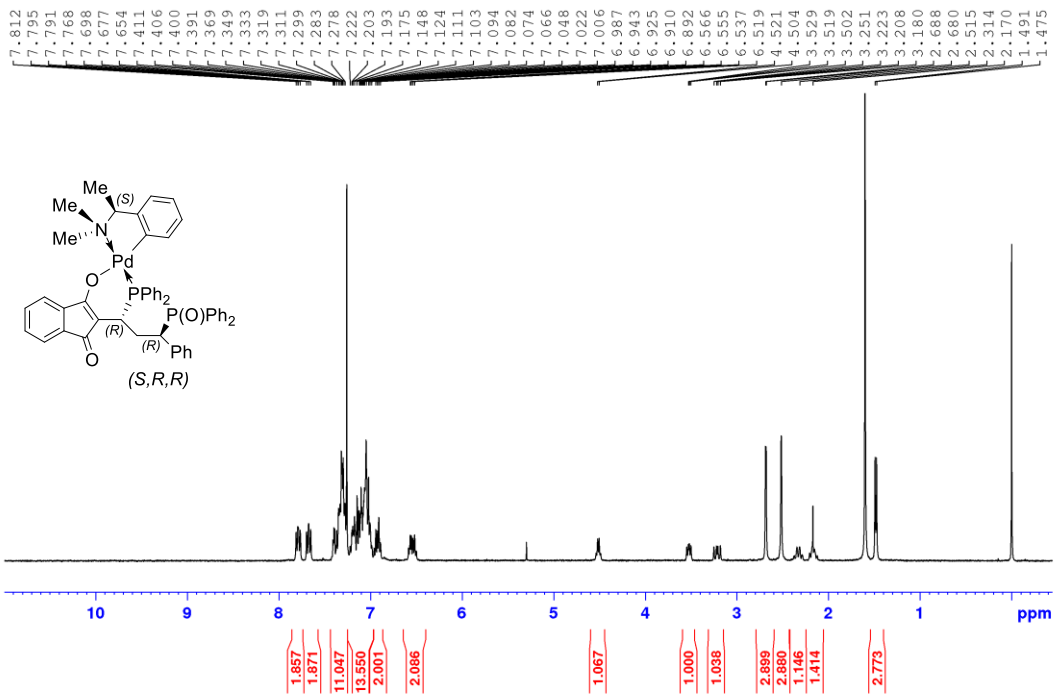

Figure S116 ^{13}C NMR (101 MHz, $CDCl_3$) spectrum of *(S,R,R)*-**18**.

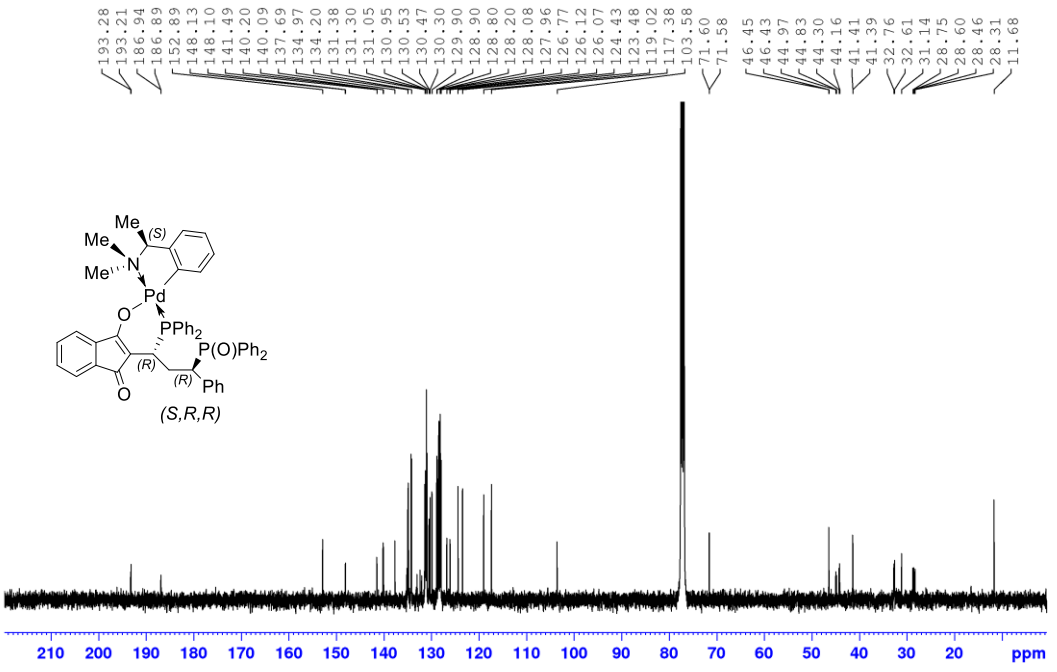

Figure S117 $^{31}P\{^{1}H\}$ NMR (162 MHz, $CDCl_3$) spectrum of *(S,R,R)*-**18**.

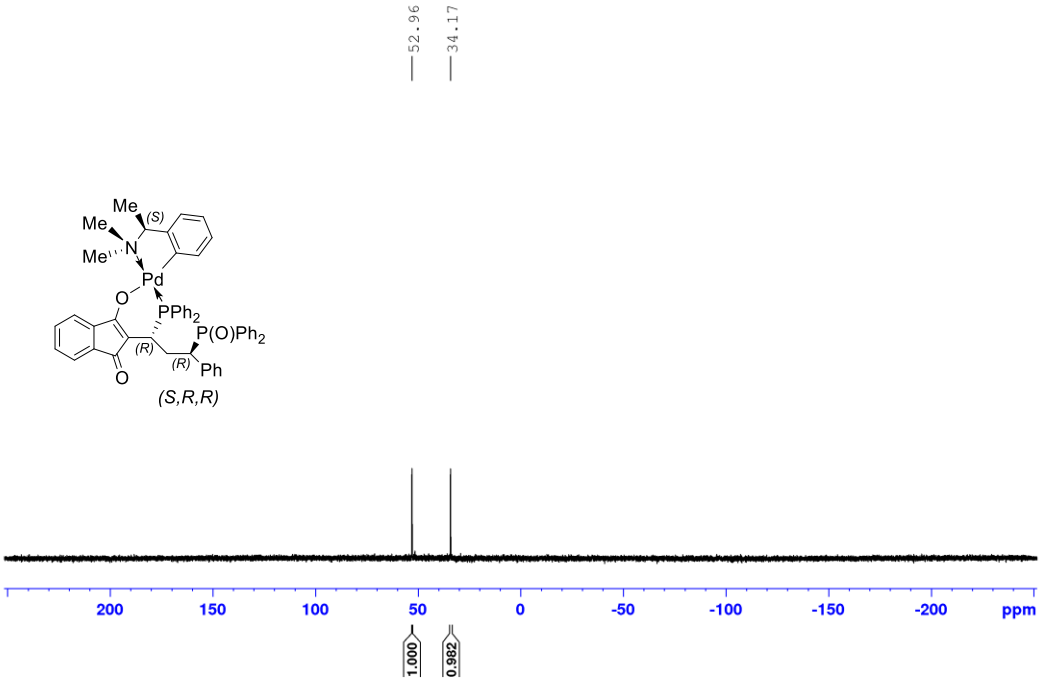

4. Calculation studies

4.1 Computational details

In the present computational investigation, we performed DFT calculations with the *Gaussian 16* suite of programs (Revision A.03).[12] The calculations were carried out with dispersion-corrected ωB97X-D exchange-correlation functional.[13] The SMD implicit solvation model was employed to take into account the global solvation effects.[14] The solvents used in our calculations were dichloromethane (ε = 8.93). The ultrafine integration was applied to increase the accuracy of the numerical integration in all the DFT calculations. The reported Gibbs free energies were obtained from ωB97X-D/Def2TZVPP electronic energies and all the additional terms computed at the ωB97X-D/Def2SVP level according to the following formula:

$$G = E_0' + (G_0 - E_0) + (G_{sol} - E_0) + \Delta G_{conc}.$$

In this formula, E_0' and E_0 are electronic energies obtained using Def2TZVPP and Def2SVP basis sets[15], respectively, G_0 and G_{sol} are gas-phase and solution-phase Gibbs free energies obtained from ωB97X-D/Def2SVP calculations (T = 298.15 K). The value of ΔG_{conc} (0.003019 Hartree ≈ 1.89 kcal/mol) corresponds to concentration correction to the Gibbs free energy when switching from ideal gas standard state (p = 1 atm) to the standard concentration in solution phase (c = 1 mol/dm3). Harmonic vibrational frequency calculations were used to corroborate the nature of the obtained structures. No imaginary frequencies were obtained for all the minima reported.

The presented molecular structures were rendered using *CYLview* and the majority of H atoms were omitted for clarity.[16]

4.2 Computational investigation

4.2.1 Overlay of the X-ray crystal and the optimized structures

We started our computational investigation by examining to what extent the computationally optimized and the crystal structures overlap with one another. The initial structure that was subjected to optimization at the ωB97X-D/Def2SVP level of theory was adopted from the X-ray crystal structure. As can be seen in Figure S118, the structure (in red) optimized in gas-phase showed good agreement with the X-ray crystal structure (in blue). The subtle changes in the conformation of the Ph-groups can be attributed to the crystal forces.

Figure S118 Overlay of the X-ray crystal structure (in blue) and the optimized structure (in red) at the ωB97X-D/Def2SVP level of theory.

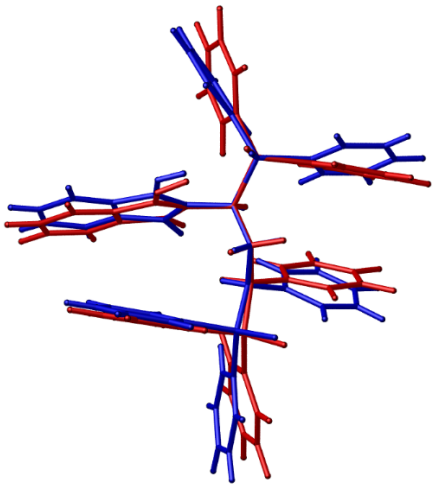

4.2.2 Computational examination of H-bonding in compound 4aa

Based on our investigations on the reaction mechanism, it was found that the base-free transformation results in the generation of a keto-diphosphine (**13**) and the presence of triethylamine leads to the formation of a diphosphine salt (**3aa**) in the double hydrophosphination process (for details see chapter 2 in this document). Upon sulfurization and purification on silica gel, compound **4aa** was isolated in both transformations. The X-ray crystallography clearly showed that **4aa** was in enol tautomeric form. In addition, the enol proton of **4aa** was observed as a sharp signal at 11.06 ppm in the ^{1}H-NMR spectrum measured in $CDCl_3$ (see Figure S55). In case of the formation of **3aa**, we assume that the tautomerization is induced by the triethylamine and the protonation occurs on the acidic silica gel. However, under base-free conditions, the produced diphosphine was presented in diketo form (**13**) in the crude reaction mixture and the tautomerization took place on silica gel. In order to find out the reason of the higher enol stability over the keto form, theoretical investigations were performed by us.

Inspection of the X-ray crystal structure reveals that the OH-group of the enol moiety is oriented towards the sulphur atom of the neighbouring phosphine sulphide fragment. To examine the reason of a stabilizing H-bond between the enol moiety and the sulphur atom, we applied three simple computational approaches.

First, the enol moiety was forced to move away from the sulphur atom in two separate relaxed scans (Figure S119). In the first attempt (I.), the dihedral angle of C1-C2-P-S was being gradually altered, while in the second attempts (II) the dihedral angle of C3-C4-O-H was subjected to systematic alteration. By doing so, the electronic energy continuously increased upon alteration in both cases. Besides, the relaxed scan provided further conformers, all of which were calculated to be higher in energy. This was indicative of an intramolecular H-bond with the sulphur atom.

Figure S119 Relaxed scan experiments to probe the stabilizing H-bond.

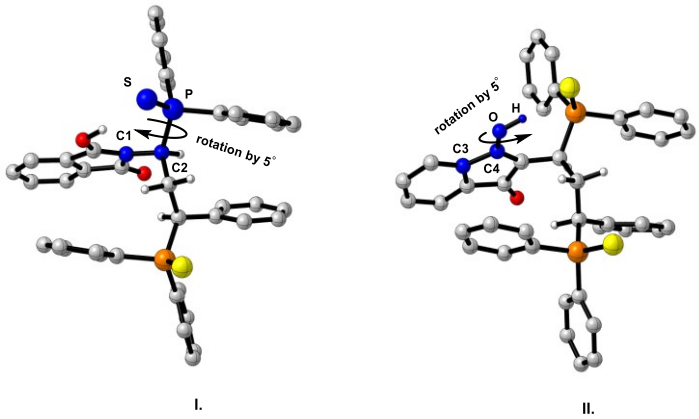

The corresponding dihedral angle (defined by atoms in blue) was varied with a step size of 5° and constrained optimization was performed for each dihedral angle at ωB97X-D/Def2SVP level.

In parallel, we arbitrary dislocated the enol moiety in such a way that OH-group was pointing to the center of the neighbouring phenyl ring in the altered structure, and then it was optimized (Figure S120, B). Also, the OH-group was rotated by 180° followed by optimization (Figure S120, C). The resultant structures B and C were found to be high-energy conformers in comparison with A in all energy terms (gas-phase electronic energy, gas-phase Gibbs free energy, solvent corrected Gibbs free energy).

Lastly, the computationally optimized enol product was manually modified to its keto form (Figure S120, D) and its optimization was carried out. The obtained structure was found to be less stable than the enol tautomer, again, in all energy terms.

Figure S120 Relative stability of different enol-conformations (A, B, C) and the diketone form (D) in kcal/mol.

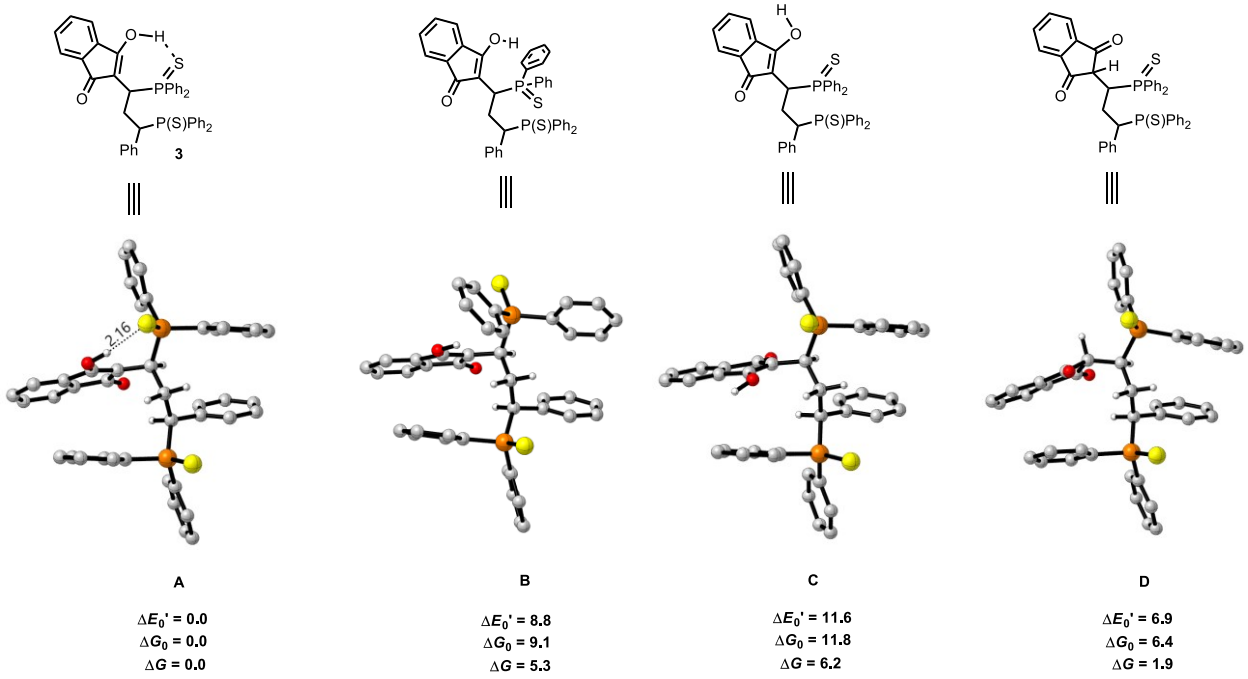

Notation of the indicated energy terms: E_0' electronic energies computed at ωB97X-D/Def2TZVPP level of theory, G_0 gas-phase Gibbs free energies computed at ωB97X D/Def2SVP level of theory, G solvation corrected (dcm) Gibbs free energies using the reevaluated E_0' electronic energies (see 4.3 *Computational details*).

Based on the computational experiments above, it can be concluded that this unique H-bond with the sulphur atom can indeed stabilize the enol tautomer of compound **4aa**.

4.2.3 Stability of structure 11 and 12

According to our proposed mechanistic pathway, the first step of the double addition is the nucleophilic attack on the α,β,γ,δ-conjugated system at the 1,6-position by the diphenylphosphine. After the formation of the monophosphine intermediate, the second nucleophilic attack on the β-carbon leads to the generation of compound **13** in the base-free transformation. Among the proposed possible 1,6-monophosphine structures (**11** and **12**), only compound **11** is able to proceed in the double-addition process, due to the position of the double bond (between the α- and β-carbons). In this structure, the β-carbon is still activated by the indandione moiety for the second nucleophilic addition. In compound **12**, the second addition cannot occur due to the sp^3 carbon presented at the α-position, which causes a loss of conjugation.

In our reaction, the formation of intermediate **11** bearing a conjugate double bond was observed, which ultimately allowed for dihydrophosphination. We attempted to decipher the preferential formation of **11** over **12** by comparing the relative stability of the two isomers. The calculated relative stability shows the difference in the driving force of the formation of the two isomers.

First, we performed a systematic relaxed scan along C2-C3-C4-C5 and C3-C4-C5-P dihedral angles to explore the conformational space of isomer **11**. Similarly, the conformational space of isomer **12** was examined by a relaxed scan of C1-C2-C3-C4 and C3-C4-C5-P dihedral angles. In each case, the lowest conformers were subjected to optimization at ωB97X-D/Def2SVP level of theory. Here, we only present the most stable conformer of the monosubstituted isomer **11** and **12** obtained from the extensive relaxed scans (Figure S121).

Figure S121 Relative stability of structure **11** and **12** in kcal/mol.

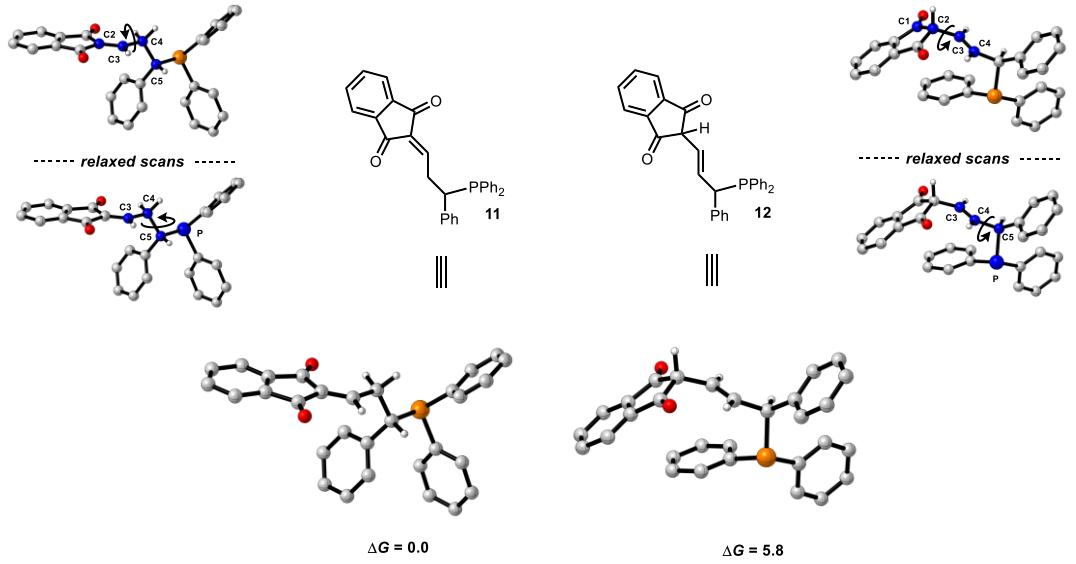

The presented conformers were found by relaxed scan. The corresponding dihedral angle (defined by atoms in blue) was varied with a step size of 10° and constrained optimization was performed for each dihedral angle at ωB97X-D/Def2SVP level.

The relative Gibbs free energy shows that isomer **11** is considerably more stable than the hypothetic isomer **12** (the formation of the latter was experimentally not observed). The notable preference for structure **11** can be ascribed to the extended conjugation between the double bond and the flat indandione scaffold. In the present case, we suspect that the formation of isomer **12** is unfavorable due to its lower stability.

4.2.4 Computed energy components of the reported structures

Table S3 Summary of energy data (given in Hartree) computed for optimized structures at the ωB97X-D/Def2SVP level of theory. Note that ***G*** contains concentration correction (0.003019 Hartree).

Structure	E_0'	G_0	E_0	G_{sol} (dcm)	G
A	-3250.6805	-3247.7069	-3248.2846	-3248.3385	-3250.1536
B	-3250.6665	-3247.6924	-3248.2687	-3248.3268	-3250.1452
C	-3250.6619	-3247.6881	-3248.2641	-3248.3250	-3250.1438
D	-3250.6695	-3247.6967	-3248.2735	-3248.3344	-3250.1506
7	-1648.8830	-1646.9892	-1647.3751	-1647.4145	-1648.5334
9	-1648.8746	-1646.9805	-1647.3663	-1647.4047	-1648.5242

4.3 Cartesian coordinates of the reported structures

Structure A

0 1

C	2.52767800	14.24560300	15.85376200
C	2.87030500	15.40031600	16.75565900
C	2.48602300	15.68673100	18.04880100
H	1.79686500	15.03020500	18.58371600
C	3.01710800	16.84357100	18.64605600
H	2.73848100	17.10144100	19.66998200
C	3.89372400	17.66820100	17.94413200
H	4.29152800	18.56312200	18.42768000
C	4.27454400	17.36872900	16.62456500
H	4.96613900	18.00710500	16.07247400
C	3.75336400	16.22410100	16.05503200
C	3.98380500	15.61564200	14.71757200
C	3.25968500	14.45694100	14.59350300
C	3.28408800	13.39912200	13.53420800
H	2.47234800	12.69318800	13.77927600
C	4.60467100	12.60667900	13.53153200
H	5.44135700	13.30862000	13.66301500
H	4.78141400	12.09532400	12.57399800
C	4.55616300	11.55537400	14.65390300
H	4.05643100	12.01606000	15.51972500
C	3.75171500	10.33859900	14.24952500
C	4.22915600	9.42594400	13.30047300
H	5.22600400	9.56285600	12.87509600
C	3.44942700	8.33877000	12.91541300
H	3.83906800	7.63162200	12.17993800
C	2.17921100	8.15217900	13.46033600
H	1.57117900	7.29703600	13.15606600
C	1.68873400	9.06528900	14.39105500
H	0.69221600	8.93387600	14.81890700
C	2.47052800	10.15164300	14.78309100
H	2.07810700	10.87851300	15.50070100
C	6.07074400	9.99865700	16.62050300
C	7.13684700	9.13366300	16.88456700
H	8.03262900	9.19040800	16.26112800
C	7.04446700	8.20211800	17.91625100
H	7.88226100	7.53070500	18.11559600
C	5.88412000	8.12165600	18.68451600
H	5.81018700	7.38705200	19.48943700
C	4.81273000	8.97287500	18.41744300
H	3.89599000	8.90479200	19.00662900
C	4.90312600	9.90851000	17.38957400
H	4.04449700	10.55110500	17.18580600
C	6.62932500	12.82531400	16.11259900
C	7.64904000	13.63694700	15.61258900
H	8.25042200	13.27383200	14.77500100
C	7.88411500	14.89178800	16.17486700
H	8.67867200	15.52374600	15.77290600
C	7.10650800	15.33712700	17.24058100
H	7.28440300	16.32259200	17.67641600
C	6.09040400	14.52730100	17.74886000
H	5.46905100	14.88037000	18.57484200

C	5.85144300	13.27673800	17.18768500
H	5.05199500	12.65591600	17.59909200
C	2.59461200	12.39865400	10.94688800
C	3.45164000	12.02886100	9.90868900
H	4.24155400	12.71598100	9.59574700
C	3.29893600	10.78799300	9.29098300
H	3.97300400	10.50089700	8.48146200
C	2.29545900	9.91743700	9.70936100
H	2.18226500	8.94304200	9.22917600
C	1.43681600	10.28605100	10.74532100
H	0.65532000	9.60315400	11.08240700
C	1.58356900	11.52293800	11.36367200
H	0.90526100	11.79760000	12.17505700
C	1.23375700	14.77761000	11.97480200
C	0.33012600	14.45674300	12.99678700
H	0.58800200	13.73793200	13.77815800
C	-0.91563700	15.07923400	13.04270300
H	-1.61188500	14.83082000	13.84616400
C	-1.26596000	16.01931700	12.07476300
H	-2.24278200	16.50619800	12.11527500
C	-0.36504100	16.34578200	11.06188800
H	-0.63206600	17.08926500	10.30813400
C	0.88391000	15.73145600	11.01365800
H	1.60540300	16.00065500	10.23826000
O	1.80402600	13.30786200	16.13194600
O	4.79482100	16.22354300	13.89273300
H	4.75796600	15.84206000	12.97752100
P	6.26611400	11.22710000	15.28146100
P	2.86096300	13.96787500	11.84085900
S	7.59527900	10.74261900	13.92108400
S	4.26553300	15.09898400	11.01605100

Structure B

0 1

C	2.41392100	14.19263100	15.62084900
C	2.68449200	15.40102000	16.47577200
C	2.13046700	15.81239700	17.67022300
H	1.32805800	15.23867400	18.13813000
C	2.63432300	16.98807300	18.25309700
H	2.21751200	17.34673000	19.19656000
C	3.65732200	17.70585100	17.63660000
H	4.02963300	18.61931300	18.10563900
C	4.21895200	17.27410200	16.42327000
H	5.02977100	17.82524200	15.94438700
C	3.71830300	16.11381300	15.86579600
C	4.11284000	15.37911800	14.63824400
C	3.32332200	14.28151800	14.45393800
C	3.38161500	13.18101700	13.43898300
H	2.51340300	12.53870000	13.66912400
C	4.66527000	12.34852900	13.57497500
H	5.53131800	13.02236100	13.66800800
H	4.85040500	11.72259400	12.69009400
C	4.56865700	11.42224400	14.80290800
H	4.03051200	11.96648200	15.59376700

C	3.79153200	10.16137200	14.49449200
C	4.34960800	9.11653500	13.74787600
H	5.39312000	9.17767600	13.42940000
C	3.58327000	8.00227100	13.41574700
H	4.03397700	7.19220100	12.83815500
C	2.24748300	7.92144200	13.80981600
H	1.64756800	7.04833400	13.54318000
C	1.68297900	8.96061200	14.54742300
H	0.63701700	8.91056300	14.85748100
C	2.45200900	10.07173200	14.89297000
H	2.00160700	10.89528200	15.45541000
C	6.08388300	9.99163300	16.87427600
C	7.18024600	9.18893800	17.20265600
H	8.09491200	9.27087100	16.61024600
C	7.09400900	8.28543900	18.25954700
H	7.95466300	7.66183300	18.51004400
C	5.91104500	8.17203600	18.98810100
H	5.84239200	7.45921800	19.81278900
C	4.81055200	8.96146500	18.65656300
H	3.87695100	8.86593400	19.21449700
C	4.89380600	9.86878600	17.60324800
H	4.01320700	10.46106400	17.34685000
C	6.53530800	12.82277900	16.30391200
C	7.57264600	13.64086100	15.85462300
H	8.23273400	13.27073200	15.06569200
C	7.75518600	14.90773200	16.40975600
H	8.56614200	15.54423300	16.04988500
C	6.90586400	15.35856500	17.41609900
H	7.04327600	16.35284200	17.84631700
C	5.86728400	14.54446900	17.87009200
H	5.18694800	14.90364800	18.64534500
C	5.68244700	13.28154500	17.31778600
H	4.86631900	12.65648300	17.68788400
C	4.38414400	14.73429800	11.14353800
C	4.18162000	16.08294200	10.83302100
H	3.16972600	16.49001500	10.90995200
C	5.25547100	16.88331600	10.44631100
H	5.08802900	17.93600100	10.21002000
C	6.53815000	16.34354200	10.36773700
H	7.37971900	16.97307600	10.07087800
C	6.74749200	14.99560800	10.66316700
H	7.74824700	14.56479800	10.59428300
C	5.67577300	14.18919600	11.04304500
H	5.85340000	13.13204200	11.24829100
C	3.01848700	12.21341000	10.71836500
C	3.50191000	12.25366300	9.40521500
H	3.89625900	13.18560900	8.99365900
C	3.48288600	11.10734400	8.61386900
H	3.86441100	11.14930500	7.59156000
C	2.97870200	9.91275300	9.12579400
H	2.96918800	9.01323900	8.50647400
C	2.48424700	9.86925100	10.42825600
H	2.08847500	8.93978900	10.84162500
C	2.49617100	11.01464700	11.22023500
H	2.10019600	10.95291100	12.23619200
O	1.65499100	13.28470600	15.88254700

O	5.13180800	15.85311000	13.94418200
H	5.27106400	15.35522100	13.12461800
P	6.26427900	11.18932500	15.50867100
P	2.94890600	13.73956300	11.72122900
S	7.65781500	10.73174300	14.19910000
S	1.24731100	14.69332700	11.65770000

Structure C

0 1

C	2.15621900	14.30916600	15.68484600
C	2.48056400	15.40856000	16.66235000
C	1.82172600	15.83336800	17.79619500
H	0.89978000	15.34472000	18.11734500
C	2.37417000	16.91075100	18.51087300
H	1.87840100	17.27524800	19.41277500
C	3.54486000	17.52448900	18.07479100
H	3.95327300	18.36685200	18.63698300
C	4.20941500	17.08027900	16.91814900
H	5.12639100	17.57582500	16.58923800
C	3.66517300	16.01152900	16.23087700
C	4.10573700	15.29908700	14.99825800
C	3.19248300	14.35525700	14.63072300
C	3.24789700	13.34899200	13.52832900
H	2.42670300	12.63943400	13.72008500
C	4.56530000	12.55949500	13.50911900
H	5.40761000	13.26340800	13.56382300
H	4.68971800	12.00751200	12.56628900
C	4.56963100	11.55514200	14.67525300
H	4.14233200	12.06741100	15.55330800
C	3.71155100	10.34446800	14.37434200
C	4.12013800	9.36409200	13.46166500
H	5.10749200	9.43509900	12.99992500
C	3.27906100	8.30008600	13.14707600
H	3.61478400	7.54236100	12.43591100
C	2.01402800	8.20432400	13.72613000
H	1.35583700	7.36965500	13.47414100
C	1.59286800	9.18270600	14.62423400
H	0.60096800	9.12433000	15.07788900
C	2.43781700	10.24385300	14.94722800
H	2.08958100	11.02097200	15.63427100
C	6.19480900	10.04509200	16.59949600
C	7.28278100	9.20373400	16.85174100
H	8.14447600	9.23452600	16.18031000
C	7.25406000	8.32607900	17.93306700
H	8.10820500	7.67263100	18.12231900
C	6.13569800	8.27534500	18.76380000
H	6.11147600	7.58243400	19.60772300
C	5.04230100	9.10185500	18.50922800
H	4.15728900	9.05504600	19.14698400
C	5.06937700	9.98386500	17.43135000
H	4.19331500	10.60549600	17.23784600
C	6.78148500	12.82325800	15.94459300
C	7.80334500	13.57555600	15.36425500
H	8.32976200	13.16976800	14.49643600

C	8.13910000	14.82498000	15.88819300
H	8.94426300	15.40393300	15.43050100
C	7.45313300	15.32755900	16.99354900
H	7.72286400	16.30083800	17.41138000
C	6.43248300	14.57546100	17.58071600
H	5.89263700	14.96279700	18.44695900
C	6.09992800	13.32843900	17.05954900
H	5.30761000	12.74802700	17.53811000
C	2.59888600	12.44618200	10.91496200
C	3.37230100	12.18091100	9.78341000
H	4.08948900	12.93415300	9.44689000
C	3.23428900	10.96746800	9.11006000
H	3.84561800	10.76598600	8.22785200
C	2.32637700	10.01399800	9.56546300
H	2.22444400	9.06088500	9.04166600
C	1.54905000	10.27583000	10.69385100
H	0.84169600	9.53050800	11.06210900
C	1.68247200	11.48684100	11.36599800
H	1.06675100	11.66775500	12.24958400
C	1.22839900	14.80772000	11.97455500
C	0.23310300	14.33751300	12.84093700
H	0.41748200	13.49953000	13.51540500
C	-1.00949600	14.96663900	12.88475300
H	-1.77373900	14.59897600	13.57258200
C	-1.27069400	16.06178100	12.06274500
H	-2.24603500	16.55238600	12.09885900
C	-0.28159300	16.53464500	11.20157800
H	-0.47790800	17.39688300	10.56071000
C	0.96486500	15.91389000	11.16053700
H	1.75509700	16.28780300	10.50468300
O	1.25450000	13.50518200	15.79491100
O	5.24513600	15.55804800	14.38572400
H	5.84794800	16.04599100	14.96090900
P	6.31134000	11.20724700	15.19294000
P	2.87174000	14.01139200	11.83879400
S	7.54442000	10.64545100	13.77577000
S	4.25058200	15.16077800	11.05973200

Structure D

0 1

C	2.37782600	14.44570500	15.75925300
C	2.96123800	15.37783900	16.75799800
C	2.61446700	15.55996700	18.09459300
H	1.82418800	14.95954700	18.54894200
C	3.30039200	16.53762700	18.81268700
H	3.05034600	16.71575300	19.86080400
C	4.30630800	17.30573400	18.20691000
H	4.82182300	18.06783800	18.79556700
C	4.66308200	17.10276200	16.87529500
H	5.45714400	17.67677100	16.39491700
C	3.97603100	16.12593200	16.16300800
C	4.17816700	15.69254600	14.74652400
C	2.98030500	14.79448900	14.39434400
C	3.14150100	13.60012700	13.44723900

H	2.35204400	12.88218800	13.72825100
C	4.49001800	12.87567300	13.55415100
H	5.29531500	13.61169200	13.68154400
H	4.73075000	12.34739200	12.62023500
C	4.47006400	11.83665300	14.69220100
H	4.01672300	12.29669400	15.58571700
C	3.66098200	10.60692400	14.33391500
C	4.13711500	9.66244000	13.41592100
H	5.11922900	9.80082900	12.95804000
C	3.37678700	8.53938500	13.10345300
H	3.76732500	7.80804800	12.39274900
C	2.12367700	8.34978700	13.68482200
H	1.53038500	7.46677400	13.43648700
C	1.63000700	9.29763800	14.57802200
H	0.64553700	9.16571800	15.03268400
C	2.39553300	10.41753800	14.90159400
H	2.00239900	11.16130500	15.60041500
C	6.09550300	10.12352700	16.44492800
C	7.17829600	9.24736400	16.56119400
H	8.03858600	9.37847700	15.90006600
C	7.14578800	8.21237200	17.49344600
H	7.99639200	7.53273500	17.57687400
C	6.02853500	8.03955100	18.30849000
H	6.00087600	7.22364800	19.03411200
C	4.94020300	8.90304500	18.18889200
H	4.05612100	8.76338300	18.81429600
C	4.97164100	9.94135000	17.26132600
H	4.10070400	10.59303900	17.17008400
C	6.61771800	12.98366500	16.20311400
C	7.51190500	13.91618900	15.67383000
H	7.96516100	13.72402700	14.69824800
C	7.82732900	15.06898500	16.39216400
H	8.52347200	15.79483300	15.96762900
C	7.26227100	15.28723300	17.64568200
H	7.51815200	16.18524100	18.21256200
C	6.36284700	14.36224500	18.17713400
H	5.91108600	14.53451900	19.15622500
C	6.03688400	13.21722000	17.45752900
H	5.34332800	12.49455800	17.89267400
C	2.59226200	12.33803800	10.94124000
C	3.51948500	11.95786100	9.96886000
H	4.28314500	12.67512200	9.65666900
C	3.45920600	10.68270200	9.40783500
H	4.18977100	10.38986100	8.65093700
C	2.46743100	9.78998700	9.80749000
H	2.41813700	8.79279100	9.36431400
C	1.53756700	10.16819200	10.77593900
H	0.76297400	9.46996800	11.09776000
C	1.60112900	11.43545500	11.34614900
H	0.86670900	11.71434500	12.10475300
C	0.99956900	14.62840500	11.77626400
C	0.09350000	14.24580400	12.77646000
H	0.39329300	13.58221300	13.59152900
C	-1.21159700	14.73539300	12.76345200
H	-1.90646300	14.43668100	13.55111800
C	-1.62479100	15.60379200	11.75430300

H	-2.64857200	15.98435900	11.74593500
C	-0.72566000	15.99313300	10.76249200
H	-1.04112100	16.68076700	9.97499100
C	0.58204700	15.51361100	10.77678700
H	1.30272300	15.83110900	10.01874300
O	1.56894400	13.57438600	15.97274900
O	5.10224400	16.00008200	14.04588900
P	6.21349500	11.48144100	15.22590500
P	2.72584800	14.00529800	11.69184800
S	7.48413800	11.14710900	13.76910400
S	3.95920100	15.20942600	10.77744300
H	2.24745900	15.50719100	13.96304500

Structure 7

0 1

C	2.08193700	14.02256400	14.12356400
C	0.71799900	14.63908700	14.14293600
C	-0.34715800	14.41018900	13.27802100
H	-0.24465100	13.70188800	12.45369200
C	-1.53123100	15.11135500	13.50443500
H	-2.38774300	14.95582800	12.84484000
C	-1.64138400	16.01716900	14.56962300
H	-2.58187800	16.55136400	14.72128000
C	-0.57015200	16.24333100	15.43369400
H	-0.63996700	16.94466200	16.26729100
C	0.60819400	15.54122800	15.20364500
C	1.89551400	15.58803000	15.96381300
C	2.81390100	14.62029900	15.28271000
C	4.05800400	14.37136000	15.71901300
H	4.36848300	14.92648800	16.61514200
C	5.03072600	13.39546200	15.14869800
H	5.96559700	13.93303000	14.91580100
H	4.64932300	12.97488700	14.20941300
C	5.34656200	12.28060600	16.16852600
H	5.81519400	12.72919000	17.05948000
C	4.12158100	11.52425800	16.63427200
C	3.19267500	11.01048000	15.72036000
H	3.32166300	11.18768900	14.65049000
C	2.09119700	10.28154900	16.16367200
H	1.37455000	9.89350400	15.43637000
C	1.90293300	10.04768300	17.52568900
H	1.03975500	9.47449800	17.87119300
C	2.82290500	10.55242900	18.44252600
H	2.68807600	10.37417600	19.51153500
C	3.92125800	11.28519200	17.99757600
H	4.64742700	11.66524800	18.72095800
C	6.88295900	9.99325400	16.87805700
C	6.03611300	8.89000500	17.05850100
H	5.24942000	8.68773400	16.32654400
C	6.17170500	8.06168700	18.16997700
H	5.49452900	7.21473400	18.29977300
C	7.17133600	8.31197000	19.10910200
H	7.28390900	7.65971700	19.97809400
C	8.03150100	9.39436300	18.93033000

H	8.82239600	9.59132300	19.65775500
C	7.88782900	10.23076100	17.82366900
H	8.57128600	11.07326900	17.69746500
C	8.10961900	12.05078700	15.29238300
C	9.05014400	11.63664200	14.33929100
H	8.82643500	10.77305500	13.70682100
C	10.26102400	12.30999400	14.18555300
H	10.98202800	11.96739400	13.44012600
C	10.54444200	13.42400000	14.97351200
H	11.48863300	13.95879600	14.84950000
C	9.61398700	13.85634000	15.91780100
H	9.82784200	14.73003100	16.53754400
C	8.40974200	13.17294800	16.07775600
H	7.70317300	13.52421400	16.83340500
O	2.47547500	13.21056500	13.31733800
O	2.14056000	16.26789600	16.93047800
P	6.56135600	11.05371600	15.40282700

Structure 9

0 1

C	2.63452600	15.43992600	15.47091800
C	2.72750500	16.03207000	14.10754500
C	3.01431300	17.34650800	13.74884200
H	3.16365000	18.10704300	14.51754300
C	3.11509600	17.64036200	12.39099800
H	3.34348000	18.65957700	12.07165200
C	2.92946700	16.64297500	11.41956300
H	3.01734300	16.90485600	10.36287100
C	2.63734700	15.33085200	11.78538000
H	2.49464100	14.54225000	11.04419600
C	2.54131100	15.04349600	13.14480700
C	2.28960600	13.72516800	13.79555300
C	2.31298400	13.94520600	15.31149200
C	3.29318200	13.09881700	16.08326400
H	3.66314900	13.57284100	16.99979500
C	3.76576400	11.90981300	15.70873900
H	3.39149600	11.43654100	14.79461000
C	4.87188400	11.20087700	16.43852700
H	5.06676300	11.72989900	17.38566700
C	4.50521400	9.75847500	16.73903200
C	4.53986400	8.76659700	15.75223000
H	4.88032300	9.01933800	14.74498200
C	4.15512900	7.45915000	16.04453300
H	4.19209500	6.69819600	15.26183300
C	3.72961900	7.12071600	17.32790400
H	3.43260100	6.09496800	17.55664100
C	3.68578700	8.10177200	18.31751100
H	3.35072000	7.84927800	19.32606800
C	4.06676300	9.40898100	18.02205700
H	4.02368200	10.17587500	18.80065000
C	7.78769900	11.13198100	16.61255400
C	9.06202400	11.61470100	16.27250800
H	9.20684600	12.14314100	15.32589800
C	10.14387000	11.44452000	17.13063600

H	11.12404100	11.83660500	16.84995900
C	9.97815000	10.77323900	18.34301700
H	10.82695100	10.63625500	19.01651800
C	8.72348000	10.27655100	18.68459900
H	8.58243300	9.74437700	19.62805400
C	7.63558200	10.45330000	17.82758400
H	6.66712100	10.04348100	18.11695200
C	6.45174700	13.17785400	15.16382800
C	6.68865100	14.06868000	16.21857300
H	6.97315400	13.68317700	17.20138800
C	6.55434300	15.44172700	16.02908600
H	6.72734200	16.12546600	16.86280100
C	6.18879300	15.94320700	14.77909900
H	6.07629800	17.01971700	14.63279400
C	5.96270100	15.06802600	13.71904900
H	5.66824000	15.45696600	12.74107200
C	6.09533800	13.69254100	13.91183400
H	5.90278900	13.00595300	13.08285800
O	2.81179500	16.01575600	16.51227700
O	2.10803300	12.68306200	13.21917400
P	6.44202800	11.34597100	15.37325000
H	1.28796300	13.78614300	15.69828300

5. X-ray measurement data

Crystallographic data of **4aa** (CCDC 1938165):

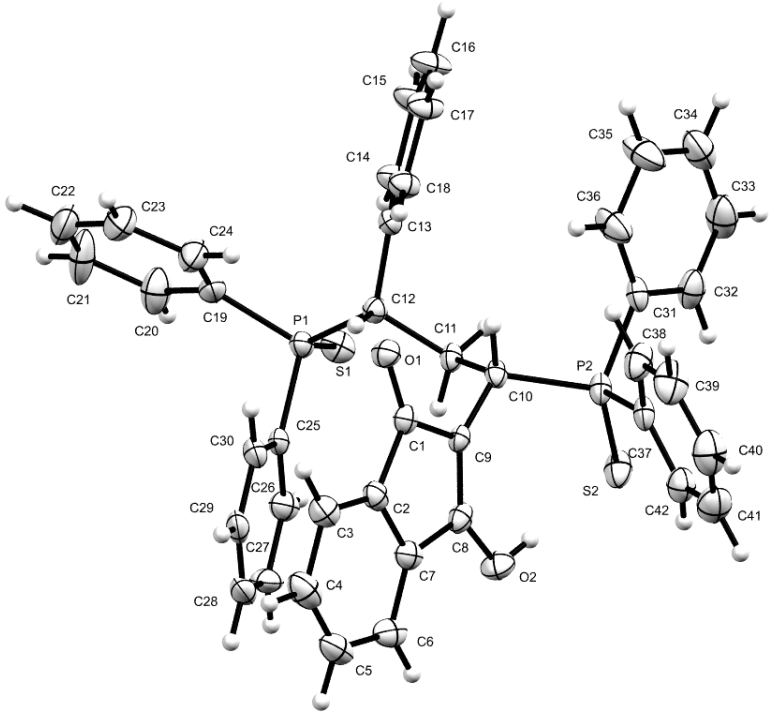

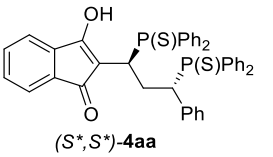

(*S*,S**)-**4aa**

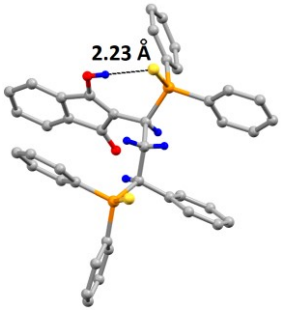

Table S4 Sample and crystal data for **4aa**.

Chemical formula	$C_{42}H_{34}O_2P_2S_2$	
Formula weight	696.75 g/mol	
Temperature	100(2) K	
Wavelength	0.71073 Å	
Crystal size	0.040 x 0.200 x 0.220 mm	
Crystal habit	yellow plate	
Crystal system	monoclinic	
Space group	P 1 21/n 1	
Unit cell dimensions	a = 8.7505(4) Å	α = 90°
	b = 20.8649(11) Å	β = 92.892(2)°
	c = 19.0714(9) Å	γ = 90°
Volume	3477.6(3) $Å^3$	
Z	4	
Density (calculated)	1.331 g/cm^3	
Absorption coefficient	0.282 mm^{-1}	
F(000)	1456	

Table S5 Data collection and structure refinement for **4aa**.

Theta range for data collection	2.35 to 27.90°
Index ranges	-11<=h<=10, -27<=k<=27, -25<=l<=25
Reflections collected	33224
Independent reflections	8304 [R(int) = 0.1190]
Coverage of independent reflections	99.7%
Absorption correction	Multi-Scan
Max. and min. transmission	0.9890 and 0.9410
Structure solution technique	direct methods
Structure solution program	XT, VERSION 2014/5
Refinement method	Full-matrix least-squares on F^2
Refinement program	SHELXL-2016/6 (Sheldrick, 2016)
Function minimized	$\Sigma\ w(F_o^2 - F_c^2)^2$
Data / restraints / parameters	8304 / 0 / 434
Goodness-of-fit on F^2	1.021
Δ/σ_{max}	0.001
Final R indices	4906 data; I>2σ(I) R1 = 0.0611, wR2 = 0.1133
	all data R1 = 0.1294, wR2 = 0.1423
Weighting scheme	$w=1/[\sigma^2(F_o^2)+(0.0371P)^2+3.5060P]$ where $P=(F_o^2+2F_c^2)/3$
Largest diff. peak and hole	0.511 and -0.510 eÅ^{-3}
R.M.S. deviation from mean	0.082 eÅ^{-3}

Crystallographic data of **9** (CCDC 1938166):

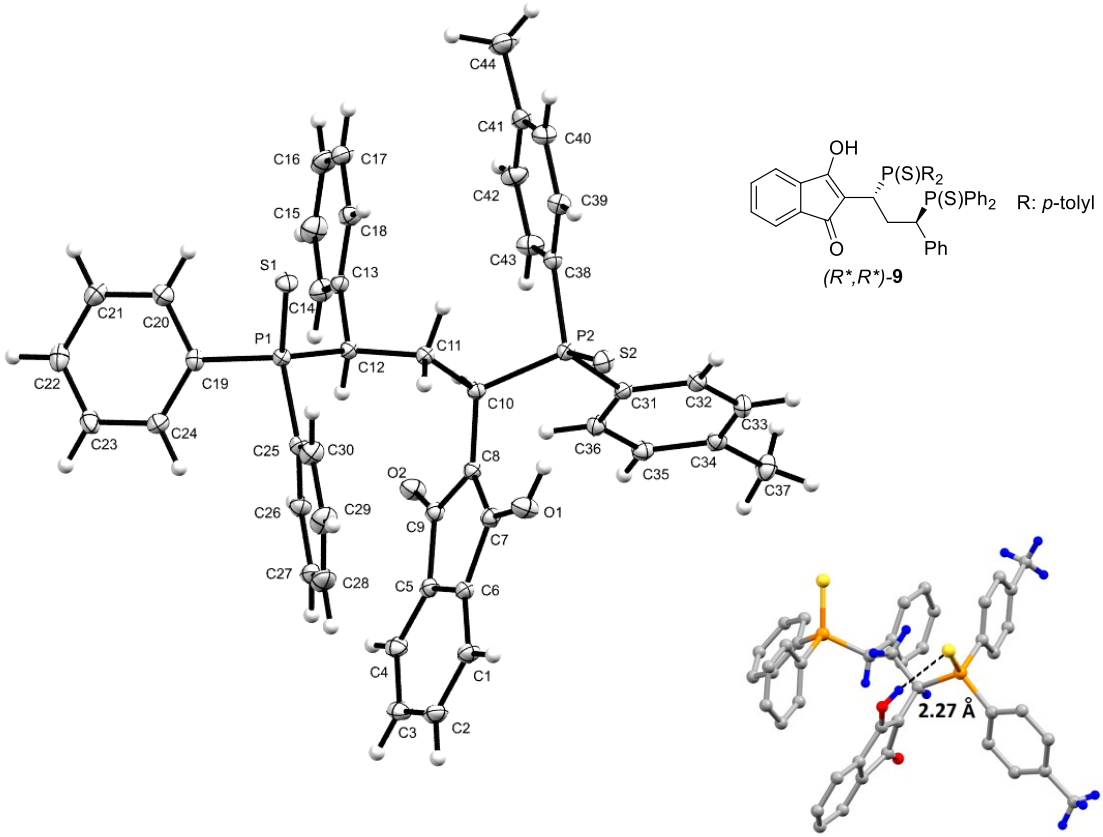

Table S6 Sample and crystal data for **9**.

Chemical formula	$C_{44}H_{38}O_2P_2S_2$	
Formula weight	724.80 g/mol	
Temperature	100(2) K	
Wavelength	0.71073 Å	
Crystal size	0.020 x 0.120 x 0.140 mm	
Crystal habit	yellow plate	
Crystal system	monoclinic	
Space group	P 1 21/c 1	
Unit cell dimensions	a = 23.0930(5) Å	α = 90°
	b = 8.8734(2) Å	β = 107.3313(9)°
	c = 18.7652(4) Å	γ = 90°
Volume	3670.66(14) $Å^3$	
Z	4	
Density (calculated)	1.312 g/cm^3	
Absorption coefficient	0.270 mm^{-1}	
F(000)	1520	

Table S7 Data collection and structure refinement for **9**.

Theta range for data collection	2.27 to 31.52°
Index ranges	-33<=h<=33, -10<=k<=13, -27<=l<=27
Reflections collected	66108
Independent reflections	12190 [R(int) = 0.0896]
Coverage of independent reflections	99.8%
Absorption correction	Multi-Scan
Max. and min. transmission	0.9950 and 0.9630
Structure solution technique	direct methods
Structure solution program	XT, VERSION 2014/5
Refinement method	Full-matrix least-squares on F^2
Refinement program	SHELXL-2017/1 (Sheldrick, 2017)
Function minimized	$\Sigma\, w(F_o^2 - F_c^2)^2$
Data / restraints / parameters	12190 / 0 / 454
Goodness-of-fit on F^2	1.023
Δ/σ_{max}	0.001
Final R indices	8365 data; I>2σ(I) R1 = 0.0502, wR2 = 0.0997
	all data R1 = 0.0890, wR2 = 0.1163
Weighting scheme	$w=1/[\sigma^2(F_o^2)+(0.0392P)^2+2.1945P]$ where $P=(F_o^2+2F_c^2)/3$
Largest diff. peak and hole	0.571 and -0.431 eÅ^{-3}
R.M.S. deviation from mean	0.081 eÅ^{-3}

Crystallographic data of *(S,R,R,S)*-**16a** (CCDC 1938163):

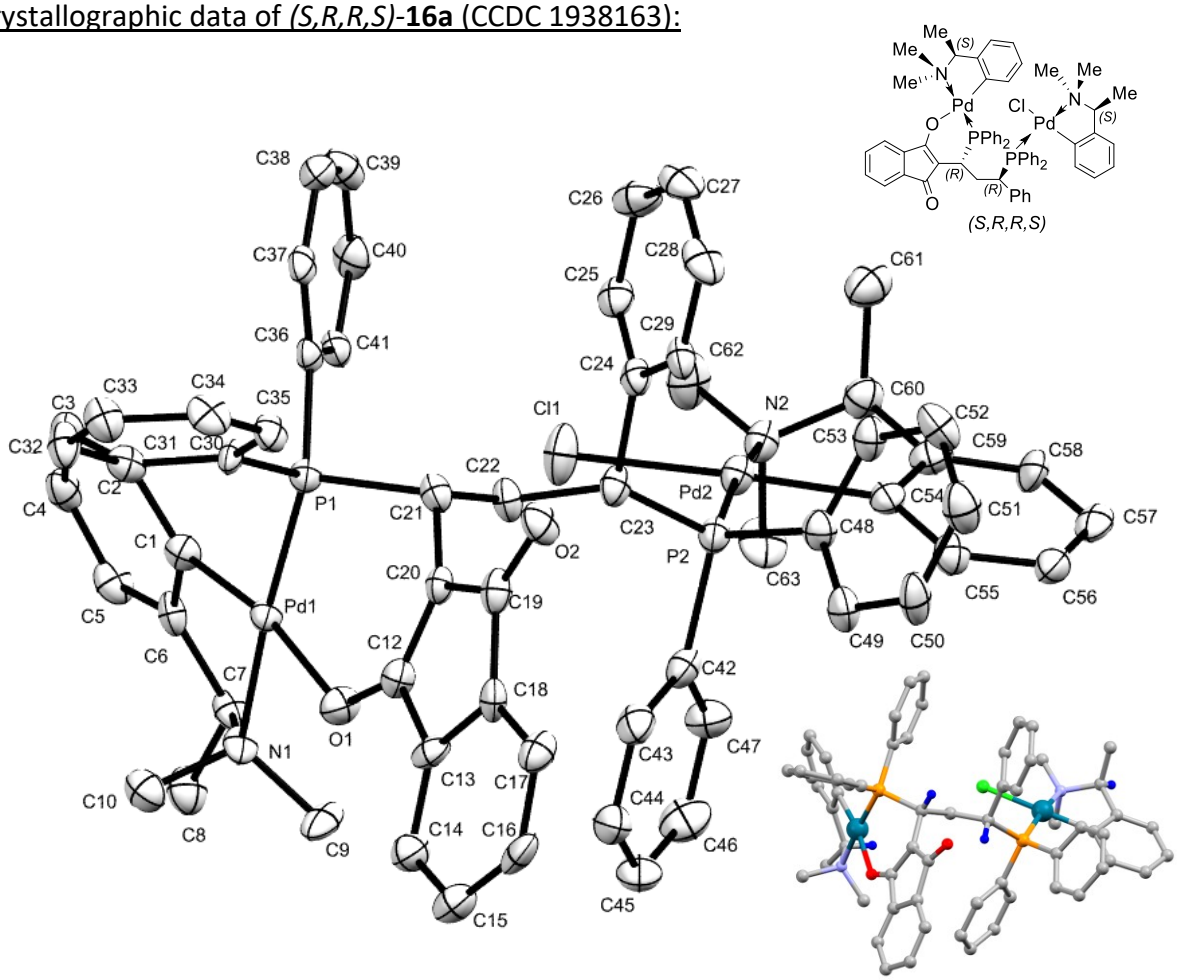

Remark: hydrogens were omitted from the ORTEP structure for clarity. For chirality, see the additional structure (blue atoms: hydrogens).

Table S8 Sample and crystal data for *(S,R,R,S)*-**16a**.

Chemical formula	$C_{62}H_{61}ClN_2O_2P_2Pd_2$	
Formula weight	1176.31 g/mol	
Temperature	100(2) K	
Wavelength	0.71073 Å	
Crystal size	0.020 x 0.100 x 0.280 mm	
Crystal habit	orange plate	
Crystal system	orthorhombic	
Space group	P 21 21 21	
Unit cell dimensions	a = 11.4070(9) Å	α = 90°
	b = 14.9513(11) Å	β = 90°
	c = 31.156(3) Å	γ = 90°
Volume	5313.6(7) $Å^3$	
Z	4	
Density (calculated)	1.470 g/cm^3	

Absorption coefficient	0.834 mm^{-1}
F(000)	2408

Table S9 Data collection and structure refinement for *(S,R,R,S)*-**16a**.

Theta range for data collection	2.21 to 31.61°
Index ranges	-16<=h<=16, -22<=k<=16, -45<=l<=26
Reflections collected	33081
Independent reflections	17602 [R(int) = 0.0694]
Coverage of independent reflections	99.7%
Absorption correction	Multi-Scan
Max. and min. transmission	0.9840 and 0.8000
Structure solution technique	direct methods
Structure solution program	XT, VERSION 2014/5
Refinement method	Full-matrix least-squares on F^2
Refinement program	SHELXL-2017/1 (Sheldrick, 2017)
Function minimized	$\Sigma\ w(F_o^2 - F_c^2)^2$
Data / restraints / parameters	17602 / 0 / 646
Goodness-of-fit on F^2	1.083
Δ/σ_{max}	0.001
Final R indices	12456 data; I>2σ(I) R1 = 0.0780, wR2 = 0.1411
	all data R1 = 0.1164, wR2 = 0.1560
Weighting scheme	$w=1/[\sigma^2(F_o^2)+(0.0150P)^2+27.7463P]$ where $P=(F_o^2+2F_c^2)/3$
Absolute structure parameter	0.028(19)
Largest diff. peak and hole	2.531 and -1.631 $eÅ^{-3}$
R.M.S. deviation from mean	0.158 $eÅ^{-3}$

Crystallographic data of *(S,R,R)*-**18** (CCDC 1938164):

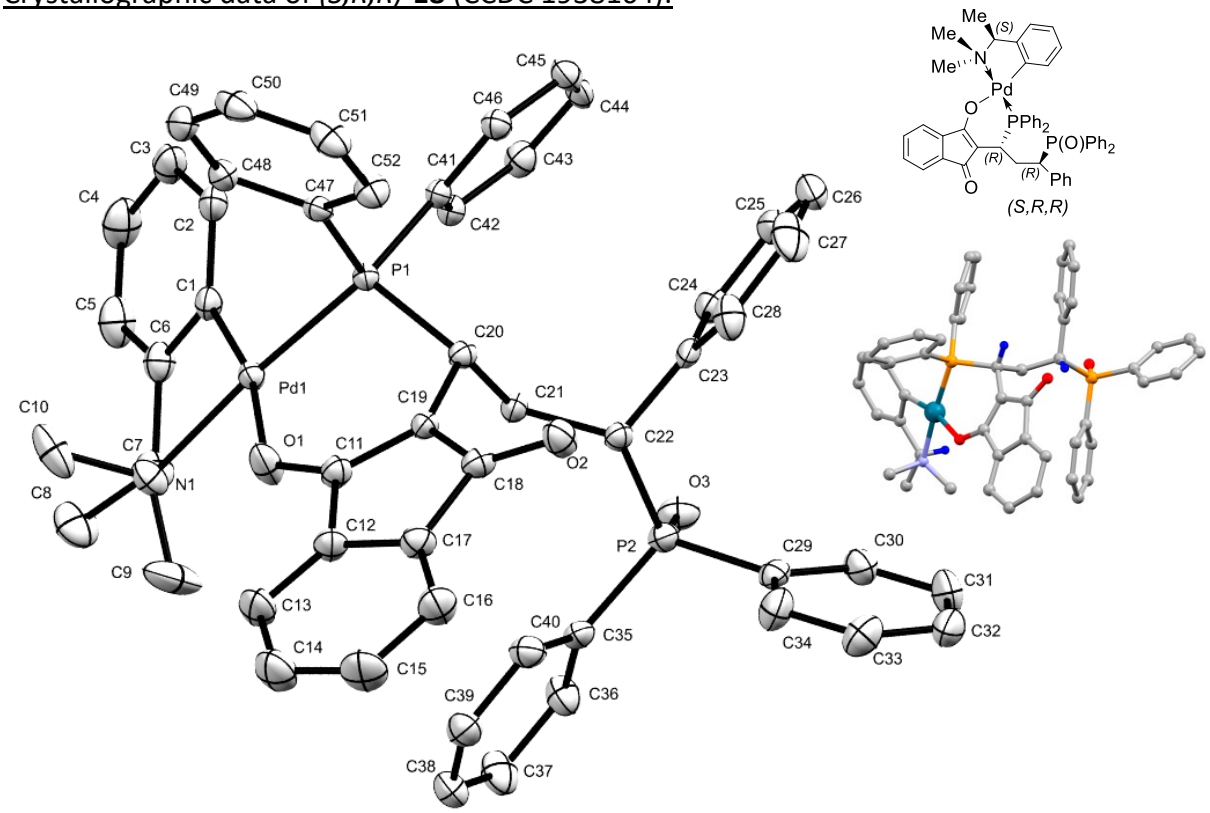

Remark: hydrogens were omitted from the ORTEP structure for clarity. For chirality, see the additional structure (blue atoms: hydrogens).

Table S10 Sample and crystal data for *(S,R,R)*-**18**.

Chemical formula	$C_{52}H_{49}NO_4P_2Pd$	
Formula weight	920.26 g/mol	
Temperature	100(2) K	
Wavelength	0.71073 Å	
Crystal size	0.080 x 0.140 x 0.200 mm	
Crystal habit	orange block	
Crystal system	orthorhombic	
Space group	P 21 21 21	
Unit cell dimensions	a = 9.8394(11) Å	α = 90°
	b = 20.038(3) Å	β = 90°
	c = 22.336(2) Å	γ = 90°
Volume	4403.8(8) $Å^3$	
Z	4	
Density (calculated)	1.388 g/cm^3	
Absorption coefficient	0.541 mm^{-1}	
F(000)	1904	

Table S11 Data collection and structure refinement for *(S,R,R)*-**18**.

Theta range for data collection	2.26 to 30.47°	
Index ranges	-13<=h<=14, -23<=k<=28, -31<=l<=31	
Reflections collected	40416	
Independent reflections	13300 [R(int) = 0.0644]	
Coverage of independent reflections	99.6%	
Absorption correction	Multi-Scan	
Max. and min. transmission	0.9580 and 0.8990	
Structure solution technique	direct methods	
Structure solution program	XT, VERSION 2014/5	
Refinement method	Full-matrix least-squares on F^2	
Refinement program	SHELXL-2017/1 (Sheldrick, 2017)	
Function minimized	$\Sigma\, w(F_o^2 - F_c^2)^2$	
Data / restraints / parameters	13300 / 1 / 552	
Goodness-of-fit on F^2	1.033	
Final R indices	10960 data; $I>2\sigma(I)$	R1 = 0.0444, wR2 = 0.0805
	all data	R1 = 0.0641, wR2 = 0.0896
Weighting scheme	$w=1/[\sigma^2(F_o^2)+(0.0302P)^2+0.7791P]$ where $P=(F_o^2+2F_c^2)/3$	
Absolute structure parameter	-0.025(13)	
Largest diff. peak and hole	0.566 and -0.869 eÅ^{-3}	
R.M.S. deviation from mean	0.087 eÅ^{-3}	

6. References

1. H. Gulyás, J. Benet-Buchholz, E. C. Escudero-Adan, Z. Freixa and P. W. N. M. van Leeuwen, *Chem. Eur. J.*, 2007, **13**, 3424-3430.
2. S. O. Grim and A. W. Yankowsky, *The Journal of Organic Chemistry*, 1977, **42**, 1236-1239.
3. N. Gül and J. H. Nelson, *Organometallics*, 2000, **19**, 91-104.
4. F.-J. Chang, R. Gurubrahamam and K. Chen, *Adv. Synth. Catal.*, 2017, **359**, 1277-1282.
5. M. Ryoka, T. Nobuki, S. Okihiro and O. Naomichi, *Chemistry Letters*, 2001, **30**, 200-201.
6. X.-Q. Hao, Y.-W. Zhao, J.-J. Yang, J.-L. Niu, J.-F. Gong and M.-P. Song, *Organometallics*, 2014, **33**, 1801-1811.
7. X.-Y. Yang, W. S. Tay, Y. Li, S. A. Pullarkat and P.-H. Leung, *Chem. Commun.*, 2016, **52**, 4211-4214.
8. Y.-R. Chen and W.-L. Duan, *Org. Lett.*, 2011, **13**, 5824-5826.
9. X.-Y. Yang, W. S. Tay, Y. Li, S. A. Pullarkat and P.-H. Leung, *Organometallics*, 2015, **34**, 5196-5201.
10. X. Wei, J. Lu and W.-L. Duan, *Synthesis*, 2016, **48**, 4155-4160.
11. X.-Y. Yang, J. H. Gan, Y. Li, S. A. Pullarkat and P.-H. Leung, *Dalton Trans.*, 2015, **44**, 1258-1263.
12. Gaussian 16, Revision A.03, M. J. Frisch, G. W. Trucks, H. B. Schlegel, G. E. Scuseria, M. A. Robb, J. R. Cheeseman, G. Scalmani, V. Barone, G. A. Petersson, H. Nakatsuji, X. Li, M. Caricato, A. V. Marenich, J. Bloino, B. G. Janesko, R. Gomperts, B. Mennucci, H. P. Hratchian, J. V. Ortiz, A. F. Izmaylov, J. L. Sonnenberg, D. Williams-Young, F. Ding, F. Lipparini, F. Egidi, J. Goings, B. Peng, A. Petrone, T. Henderson, D. Ranasinghe, V. G. Zakrzewski, J. Gao, N. Rega, G. Zheng, W. Liang, M. Hada, M. Ehara, K. Toyota, R. Fukuda, J. Hasegawa, M. Ishida, T. Nakajima, Y. Honda, O. Kitao, H. Nakai, T. Vreven, K. Throssell, J. A. Montgomery, Jr., J. E. Peralta, F. Ogliaro, M. J. Bearpark, J. J. Heyd, E. N. Brothers, K. N. Kudin, V. N. Staroverov, T. A. Keith, R. Kobayashi, J. Normand, K. Raghavachari, A. P. Rendell, J. C. Burant, S. S. Iyengar, J. Tomasi, M. Cossi, J. M. Millam, M. Klene, C. Adamo, R. Cammi, J. W. Ochterski, R. L. Martin, K. Morokuma, O. Farkas, J. B. Foresman, and D. J. Fox, Gaussian, Inc., Wallingford CT, 2016.
13. J.-D. Chai and M. Head-Gordon, *Physical Chemistry Chemical Physics*, 2008, **10**, 6615-6620.
14. A. V. Marenich, C. J. Cramer and D. G. Truhlar, *The Journal of Physical Chemistry B*, 2009, **113**, 6378-6396.
15. F. Weigend and R. Ahlrichs, *Physical Chemistry Chemical Physics*, 2005, **7**, 3297-3305.
16. C. Y. Legault, CYLview, 1.0b; Universite de Sherbrooke, 2009 (http://www.cylview.org).